Title

RAP and RAS in HMA Pilot Project on SJ 26: Material Testing, Observations, and Findings

Authors

Harvey, John
Buscheck, Jeff
Yu, Justin
et al.

Publication Date

2026

DOI

10.7922/G2N87855

TECHNICAL MEMORANDUM

RAP and RAS in HMA Pilot Project on SJ 26: Material Testing, Observations, and Findings

AUTHORS

John Harvey, Jeff Buscheck, Justin Yu, Julian Brotschi, Mohammad Rahman, Hanyu Deng, Angel Mateos, Michael Bowman, and Irwin Guada

Report No. UCPRC-TM-2023-03 | January 2026

Partnered Pavement Research Center (PPRC) Strategic Plan Element Number 4.79: RAP and RAS in HMA Pilot Project on SJ 26: Material Testing, Observations, and Findings (DRISI Task 3819)

PREPARED FOR

California Department of Transportation
Division of Research, Innovation and System Information
Office of Materials and Infrastructure

PREPARED BY

University of California Pavement Research Center
UC Davis and UC Berkeley

Caltrans

UC PRC UNIVERSITY of CALIFORNIA PAVEMENT RESEARCH CENTER | Davis Berkeley

TECHNICAL REPORT DOCUMENTATION PAGE

1. REPORT NUMBER UCPRC-TM-2023-03	**2. GOVERNMENT ASSOCIATION NUMBER**	**3. RECIPIENT'S CATALOG NUMBER**
4. TITLE AND SUBTITLE RAP and RAS in HMA Pilot Project on SJ 26: Material Testing, Observations, and Findings		**5. REPORT PUBLICATION DATE** January 2026 **6. PERFORMING ORGANIZATION CODE**
7. AUTHOR(S) John Harvey (ORCID: 0000-0002-8924-6212); Jeff Buscheck (ORCID: 0000-0002-0930-6861); Justin Yu (ORCID: 0009-0001-1068-3090); Julian Brotschi (ORCID: 0000-0002-1752-2898); Mohammad Rahman (ORCID: 0000-0001-7855-5346); Hanyu Deng (ORCID: 0000-0003-4299-0922); Angel Mateos (ORCID: 0000-0002-3614-2858); Irwin Guada (ORCID: 0000-0002-5100-2589); Michael Bowman (ORCID: 0009-0008-2708-9048)		**8. PERFORMING ORGANIZATION REPORT NUMBER** UCPRC-TM-2023-03 UCD-ITS-RR-23-92
9. PERFORMING ORGANIZATION NAME AND ADDRESS University of California Pavement Research Center Department of Civil and Environmental Engineering, UC Davis 1 Shields Avenue Davis, CA 95616		**10. WORK UNIT NUMBER** **11. CONTRACT OR GRANT NUMBER** 65A0788
12. SPONSORING AGENCY AND ADDRESS California Department of Transportation Division of Research, Innovation, and System Information P.O. Box 942873 Sacramento, CA 94273-0001		**13. TYPE OF REPORT AND PERIOD COVERED** Technical Memorandum July 2022 to October 2025 **14. SPONSORING AGENCY CODE**
15. SUPPLEMENTAL NOTES doi:10.7922/G2N87855		

16. ABSTRACT

A pilot project for the inclusion of high percentages of reclaimed asphalt pavement (RAP) and recycled asphalt shingles (RAS) in hot mix asphalt (HMA) was built on State Route 26 in San Joaquin County in September 2022. Six mixes were included in short test sections: (1) a control mix with no RAS or RAP, (2) a mix with 25% RAP and recycling agent (RA) (3) a mix with 30% RAP and RA, (4) a mix with 35% RAP and RA, (5) a mix with 40% RAP and RA, and (6) a mix with 25% RAP, 3% RAS, and RA. A seventh mix, which was a typically used mix with 12% RAP and no RA, was used for construction of the rest of the overall project. This technical memorandum presents the laboratory test results from plant mix produced for job mix formula verification and from one or two quality assurance (QA) samples, depending on the test, taken during test section construction, as well as observations of plant production and construction. None of the mixes passed the Delta Tc specification, which is not uncommon for polymer-modified binder mixes. There is FHWA guidance and past UCPRC experience with other polymer-modified Caltrans mixes that indicate Delta Tc may not be a good parameter to use with modified binders. The mixes with 40% RAP and 25% RAP/3% RAS and one of the two QA samples for the mixes with 30% and 35% RAP and RA did not meet the performance grade (PG) specification low temperature limit. All mixes passed high and intermediate temperature PG specifications, and the other QA samples passed the low temperature PG specification. The 25% RAP with RA mix and one of the two QA sublots of the 30% RAP with RA mix missed the IDEAL cracking tolerance (IDEAL-CT) index number by a small amount, and one of the sublots for the 35% and 40% mixes missed by a wider margin. Results are presented for volumetric tests, flexural and axial dynamic modulus tests, repeated load triaxial tests, flexural fatigue tests, and Hamburg Wheel-Track tests. IDEAL-CT tests were done with both reheated and medium-term oven-aged samples, and results are reported for the IDEAL-CT index and indirect tensile strength for both aging conditions.

17. KEYWORDS reclaimed asphalt pavement (RAP), recycled asphalt shingles (RAS), recycled binder ratio, hot mix asphalt (HMA), pilot project	**18. DISTRIBUTION STATEMENT** No restrictions.	
19. SECURITY CLASSIFICATION (of this report) Unclassified	**20. NUMBER OF PAGES** 149	**21. PRICE** None

UCPRC ADDITIONAL INFORMATION

1. DRAFT STAGE Final	**2. VERSION NUMBER** 1
3. UCPRC STRATEGIC PLAN ELEMENT NUMBER 4.79	**4. CALTRANS TASK NUMBER** 3819
5. CALTRANS TECHNICAL LEAD AND REVIEWER(S) Jessaneil Perez and Saeed Pourtahmasb	**6. FHWA NUMBER** CA26-3819

7. PROPOSALS FOR IMPLEMENTATION

No proposal for implementation.

8. RELATED DOCUMENTS

Harvey, J., Buscheck, J., Brotschi, J., Rahman, M., Mateos, A., and Jones, D. 2023. *RAP and RAS in HMA Pilot Project on ED 49: Material Testing, Observations, and Findings* (Technical Memorandum: UCPRC-TM-2022-04). Davis and Berkeley, CA: University of California Pavement Research Center.

Harvey, J., Buscheck, J., Brotschi, J., Yu, J., Rahman, M., Mateos, A. 2025. *RAP and RAS in HMA Pilot Project on SBD 215: Material Testing, Observations, and Findings* (Technical Memorandum: UCPRC-TM-2023-02). Davis and Berkeley, CA: University of California Pavement Research Center.

9. VERSION UPDATES

10. LABORATORY ACCREDITATION

The UCPRC laboratory is accredited by AASHTO re:source and CCRL for the laboratory testing discussed in this report.

11. SIGNATURES

J. Harvey **FIRST AUTHOR**	J.Buscheck, J. Brotschi **TECHNICAL REVIEW**	C. Fink **EDITOR**	J. Harvey **PRINCIPAL INVESTIGATOR**	J. Perez **CALTRANS TECHNICAL LEAD(S)**	S. Mafi **CALTRANS CONTRACT MANAGER**

DISCLAIMER

ACKNOWLEDGMENTS

The University of California Pavement Research Center acknowledges the following individuals and organizations who contributed to the project: Caltrans Office of Asphalt Pavement reviewers Jessaneil Perez and Saeed Pourtahmasb, DRISI project managers T. Joseph Holland and Somayeh Mafi; Construction and Materials staff in District 10; the staff of George Reed, Inc., including Phil Reader and Arthur Trillo, who produced and placed the mix; the UCPRC laboratory and field staff; and UCPRC publications manager Camille Fink.

PROJECT OBJECTIVES

This project is a continuation of PPRC Project 4.64 (Continued Development of Guidelines for Determining Binder Replacement in High RAP/RAS Content Mixes). The objective of this project, PPRC Project 4.79 (Guidance, Tests, and Specifications for High Recycled Asphalt Pavement/Recycled Asphalt Shingle Contents in Hot Mix Asphalt [HMA] and Rubberized Hot Mix Asphalt [RHMA] Mixes), is to develop guidelines for determining binder replacement rates in high RAP/RAS content mixes without the need for binder extraction and performance-related tests for use in routine mix design and construction quality control/quality assurance (QC/QA). This will be achieved through the following tasks:

- Task 1: Update the literature review to include recently completed research.
- Task 2: Complete testing of high RAP and RAP/RAS mixes to determine their performance properties.
- Task 3: Complete testing of extracted and recovered RAP, RAP/RAS including RA, and RAP/RAS/virgin binder blends to assess the effectiveness of different recycling agents.
- Task 4: Complete investigation into the use of fine aggregate matrix mix testing to assess the fatigue performance of mixes and to predict binder properties.
- Task 5: Investigate long-term aging effects of high RAP and RAP/RAS mixes using different laboratory-aging protocols.
- Task 6: Monitor field performance of high RAP and RAP/RAS mixes, and use results to evaluate laboratory-aging protocols.
- Task 7: Prepare a research report with recommendations for use of RAP and RAP/RAS as binder replacement and, if applicable, recommendations for accelerated wheel-load testing.

The results presented in this technical memorandum contribute to Tasks 2, 3, 5, and 6 by presenting the results of laboratory testing of binders and mixes for a pilot project on State Route 26 (SJ 26) in San Joaquin County, including sampling and testing for job mix formula approval, sampling and testing of plant-sampled materials during construction of the test sections, and observations from construction. This technical memorandum is being completed under PPRC Project 4.92 (Continued Support for Implementation of Performance-Related Tests and Specifications for Balanced Mix Design, Increased Recycling of Asphalt Mixes, and Integration of Mix Design and Structural Design).

TABLE OF CONTENTS

LIST OF FIGURES

LIST OF TABLES

LIST OF ABBREVIATIONS

AMPT	Asphalt mixture performance tester
APCS	Automated pavement condition survey
BMD	Balanced mix design
BBR	Bending beam rheometer
CG	Continuous grade
DM	Dynamic modulus test
DSR	Dynamic shear rheometer
FAT	Beam fatigue test
FM	Flexural modulus test
FS	Frequency sweep
FTIR	Fourier transform infrared
FTIR-ATR	Fourier transform infrared spectroscopy with attenuated total reflection
HMA	Hot mix asphalt
HWT	Hamburg Wheel-Tracking
IDEAL-CT	IDEAL cracking tolerance test
JMF	Job mix formula
LAS	Liquid antistrip
MTOA	Medium-term oven aging
NMAS	Nominal maximum aggregate size
nSSP	Non-Standard Special Provision
OLTS	Online laboratory testing system
PAV	Pressurized aging vessel
PG	Performance grade
PGI	Intermediate performance grade
QA	Quality assurance
RA	Recycling agent
RAP	Reclaimed asphalt pavement
RAS	Recycled asphalt shingles
RBR	Recycled binder ratio
RHMA	Rubberized hot mix asphalt

RLT	Repeated load triaxial test
RTFO	Rolling thin-film oven
RVE	Representative volume element
SCB	Semicircular bending test
SSD	Saturated surface dry
Superpave	SUperior PERforming Asphalt PAVEment
TCE	Trichloroethylene
TMA	Total mass of aggregate
TMM	Total mass of mix

LIST OF TEST METHODS AND SPECIFICATIONS

AASHTO M 320	Standard Specification for Performance-Graded Asphalt Binder
AASHTO M 323	Standard Specification for Superpave Volumetric Mix Design
AASHTO PP 3	Standard Practice for Preparing Hot Mix Asphalt (HMA) Specimens by Means of the Rolling Wheel Compactor
AASHTO R 28	Standard Practice for Accelerated Aging of Asphalt Binder Using a Pressurized Aging Vessel (PAV)
AASHTO R 30	Standard Practice for Mixture Conditioning of Hot Mix Asphalt (HMA)
AASHTO T 84	Standard Method of Test for Specific Gravity and Absorption of Fine Aggregate
AASHTO T 85	Standard Method of Test for Specific Gravity and Absorption of Coarse Aggregate
AASHTO T 164	Standard Method of Test for Quantitative Extraction of Asphalt Binder from Hot-Mix Asphalt (HMA)
AASHTO T 166	Standard Method of Test for Bulk Specific Gravity (Gmb) of Compacted Hot Mix-Asphalt (HMA) Using Saturated Surface-Dry Specimens
AASHTO T 209	Standard Method of Test for Theoretical Maximum Specific Gravity (Gmm) and Density of Hot-Mix Asphalt (HMA)
AASHTO T 240	Standard Method of Test for Effect of Heat and Air on a Moving Film of Asphalt Binder (Rolling Thin-Film Oven Test)
AASHTO T 308	Standard Method of Test for Determining the Asphalt Binder Content of Hot Mix-Asphalt (HMA) by the Ignition Method
AASHTO T 312	Standard Method of Test for Preparing and Determining the Density of Asphalt Mix Specimens by Means of the Superpave Gyratory Compactor
AASHTO T 313	Standard Method of Test for Determining the Flexural Creep Stiffness of Asphalt Binder Using the Bending Beam Rheometer
AASHTO T 315	Standard Method of Test for Determining the Rheological Properties of Asphalt Binder Using a Dynamic Shear Rheometer
AASHTO T 316	Standard Method of Test for Viscosity Determination of Asphalt Binder Using Rotational Viscometer
AASHTO T 321	Standard Method of Test for Determining the Fatigue Life of Compacted Asphalt Mixtures Subjected to Repeated Flexural Bending
AASHTO T 331	Bulk Specific Gravity (Gmb) and Density of Compacted Hot Mix Asphalt (HMA) Using Automatic Vacuum Sealing Method
AASHTO T 378	Standard Method of Test for Determining the Dynamic Modulus and Flow Number for Asphalt Mixtures Using the Asphalt Mixture Performance Tester (AMPT)

AASHTO TP 124	Provisional Standard Method of Test for Determining the Fracture Potential of Asphalt Mixtures Using Semicircular Bend Geometry (SCB) at Intermediate Temperature
ASTM D8225	Standard Test Method for Determination of Cracking Tolerance Index of Asphalt Mixture Using the Indirect Tensile Cracking Test at Intermediate Temperature

CONVERSION FACTORS

APPROXIMATE CONVERSIONS TO SI UNITS				
Symbol	**When You Know**	**Multiply By**	**To Find**	**Symbol**
		LENGTH		
in.	inches	25.40	millimeters	mm
ft.	feet	0.3048	meters	m
yd.	yards	0.9144	meters	m
mi.	miles	1.609	kilometers	km
		AREA		
in^2	square inches	645.2	square millimeters	mm^2
ft^2	square feet	0.09290	square meters	m^2
yd^2	square yards	0.8361	square meters	m^2
ac.	acres	0.4047	hectares	ha
mi^2	square miles	2.590	square kilometers	km^2
		VOLUME		
fl. oz.	fluid ounces	29.57	milliliters	mL
gal.	gallons	3.785	liters	L
ft^3	cubic feet	0.02832	cubic meters	m^3
yd^3	cubic yards	0.7646	cubic meters	m^3
		MASS		
oz.	ounces	28.35	grams	g
lb.	pounds	0.4536	kilograms	kg
T	short tons (2000 pounds)	0.9072	metric tons	t
		TEMPERATURE (exact degrees)		
°F	Fahrenheit	(F-32)/1.8	Celsius	°C
		FORCE and PRESSURE or STRESS		
lbf	pound-force	4.448	newtons	N
lbf/in^2	pound-force per square inch	6.895	kilopascals	kPa

APPROXIMATE CONVERSIONS FROM SI UNITS				
Symbol	**When You Know**	**Multiply By**	**To Find**	**Symbol**
		LENGTH		
mm	millimeters	0.03937	inches	in.
m	meters	3.281	feet	ft.
m	meters	1.094	yards	yd.
km	kilometers	0.6214	miles	mi.
		AREA		
mm^2	square millimeters	0.001550	square inches	in^2
m^2	square meters	10.76	square feet	ft^2
m^2	square meters	1.196	square yards	yd^2
ha	hectares	2.471	acres	ac.
km^2	square kilometers	0.3861	square miles	mi^2
		VOLUME		
mL	milliliters	0.03381	fluid ounces	fl. oz.
L	liters	0.2642	gallons	gal.
m^3	cubic meters	35.31	cubic feet	ft^3
m^3	cubic meters	1.308	cubic yards	yd^3
		MASS		
g	grams	0.03527	ounces	oz.
kg	kilograms	2.205	pounds	lb.
t	metric tons	1.102	short tons (2000 pounds)	T
		TEMPERATURE (exact degrees)		
°C	Celsius	1.8C + 32	Fahrenheit	°F
		FORCE and PRESSURE or STRESS		
N	newtons	0.2248	pound-force	lbf
kPa	kilopascals	0.1450	pound-force per square inch	lbf/in^2

*SI is the abbreviation for the International System of Units. Appropriate rounding should be made to comply with Section 4 of ASTM E380.
(Revised April 2021)

1 INTRODUCTION

1.1 Background of the Study

The California Department of Transportation (Caltrans) is interested in finding, developing, and implementing approaches to reduce life cycle cost and improve life cycle environmental performance for maintaining and rehabilitating existing pavements and constructing new ones. Two approaches under investigation that offer the potential to advance these goals for asphalt mixes are the use of increased amounts of reclaimed asphalt pavement (RAP) and the use of recycled asphalt shingles (RAS) in hot mix asphalt (HMA) materials. Caltrans is investigating the performance of high RAP content mixes, which are mixes containing more than 25% RAP binder replacement, with and without the use of recycling agents (RAs). The University of California Pavement Research Center (UCPRC) has been investigating the use of higher percentages of RAP in HMA through laboratory testing of laboratory-prepared and field-sampled materials, observations of construction, and mechanistic-empirical simulations using the performance-related test properties for the mixes.

Previous and ongoing research at the UCPRC, working with Caltrans and industry, has identified potential concerns regarding using highly aged, stiff RAP. Research is underway at the UCPRC to study the impact of different RAP sources, varying RAP content, and the addition of RAs to restore the properties of highly aged RAP on the performance-related properties of binders and mixes. Several performance-related tests have been identified to assess the performance of these mixes, including rutting, stiffness, and fatigue performance-related properties. These performance-related tests include long-established tests such as the Hamburg Wheel-Tracking (HWT) test, repeated load triaxial (RLT) test, and four-point bending beam test. Other recently developed tests, such as the IDEAL cracking tolerance (IDEAL-CT) test, are also being assessed for their potential to provide a quick and simple indicator of mix performance for mix design and quality control/quality assurance (QC/QA) purposes.

The UCPRC, Caltrans, and industry had conducted limited work on the replacement of virgin binder with binder from RAS in California mixes prior to the pilot study presented in this technical memorandum. Limited previous work by the UCPRC indicated poor results because of the lack of blending of the RAS and virgin binders due to the very heavy oxidation of the RAS source used *(1)*. This technical memorandum presents project information, materials testing data from tests performed by the UCPRC, and construction observations by the UCPRC from a pilot project on State Route 26 (SJ 26) in San Joaquin County. The project included seven mixes: (1) a control mix with no RAP or RAS constructed on September 29, 2022 (2) a mix with 15% RAP aggregate replacement used on the majority of the project outside the test sections (referred to as the “mainline” mix), sampled during construction on September 26, 2022; (3) a mix with 25% RAP aggregate replacement sampled on September 27, 2022; (4) a mix with 30% RAP aggregate replacement also sampled on September 27, 2022; (5) a mix with 35% RAP aggregate replacement sampled on September 28, 2022; (6) a mix with 40% RAP aggregate replacement sampled on September 29, 2022; and (7) a mix with 25% RAP aggregate replacement and 3% RAS aggregate replacement sampled on September 29, 2022. As is discussed further in Section 2.2, the nSSP for the high

RAP mixes for the test sections called for 25%, 30%, and 40% binder replacement rather than the aggregate replacement values achieved by the mixes.

1.2 Problem Statements

The following problem statements related to the inclusion of RAS and RAP in HMA were identified for this project:

- The degree of blending between RAP, RAP/RAS, and virgin binders could be significant, particularly for mixes using highly aged RAP, typical of Inland Valley scenarios, and RAS. Incomplete blending could alter the properties of the mix because of less available binder and partial activation of the stiff RAP and/or RAS binder. The effects of potentially not achieving full blending need to be better understood to be effectively considered in mix design procedures and performance-related testing. This problem is addressed in this pilot project and technical memorandum.
- Plant-produced mixes subjected to silo storage undergo additional blending and aging, leading to increased stiffness, improved rutting, and reduced cracking and fatigue resistance. These outcomes need to be factored into mix design procedures and performance-related testing. The issue of additional blending and aging from silo storage was not addressed in this pilot project or technical memorandum because all materials were sampled without silo storage. Silo storage is addressed in a separate UCPRC report *(2)*.
- The impact of long-term aging after placement in the field on the performance of high RAP and RAP/RAS mixes with different recycling agents needs to be fully investigated using various aging protocols. This problem was addressed with respect to both binder aging and mix aging through laboratory testing of the plant-produced mixes sampled for this project. Binder aging was addressed through performance grade (PG) testing of extracted binders from plant mix. Mix aging was addressed through use of the CT 320 provisional medium-term oven aging (MTOA) protocol.

1.3 Report Structure

This report includes the following chapters, which address the goals of this study:

- Chapter 2 details the test section layout, testing plan, material sampling, mix designs, and test method overview for the SJ 26 pilot project.
- Chapter 3 discusses the results of binder testing of the pilot project mixes, addressing Task 3 of the project objectives (complete testing of extracted and recovered RAP, RAP/RAS, and RAP/RAS/virgin binder blends to assess the effectiveness of different recycling agents).
- Chapter 4 reviews the testing of the mixes from the pilot project, including testing during the job mix formula (JMF) approval process and during construction, addressing Task 2 of the project objectives (complete testing of high RAP and RAP/RAS mixes to determine their performance properties) and setting the baseline for future testing of field mixed/field compacted specimens for Task 6 (monitor field performance of high RAP and RAP/RAS mixes, and use results to evaluate laboratory-aging protocols).

- Chapter 5 presents initial field construction observations.
- Chapter 6 presents preliminary conclusions from this pilot project.

Detailed data tables are not included in this report. All data are available through the UCPRC Online Testing Service web application or in Excel tables. Contact the report's authors for access.

1.4 Measurement Units

Although Caltrans has returned to the use of US standard measurement units, metric units have always been used by the UCPRC in the design and layout of test tracks, and for laboratory, Heavy Vehicle Simulator, and field measurements and data storage. In this technical memorandum, both US and metric units (provided in parentheses after the US units) are provided in general discussion. In keeping with convention, metric units are used in laboratory data analyses and reporting, with some US units, where appropriate, to assist the reader. A conversion table is provided on page xvi.

2 TESTING PLAN AND MATERIAL SAMPLING

2.1 Pilot Project Test Sections Overview and Pre-Overlay Observations

The test sections are within Caltrans project 10-1J2004 on SJ 26 just west of Linden, California. The project consisted of milling failed asphalt pavement surface and replacing it with 0.2 ft. (60 mm) of new HMA. The beginning and ending post miles of the seven test sections are shown in Table 2.1. The plan was for the mixes to be proportioned to meet the binder replacement rates shown in the table. During the mix design process, the mix producer had difficulty proportioning the mixes to exactly hit those binder replacement rates. The mix producer instead focused on matching them as closely as possible using two definitions of binder replacement rate, one including the recycling agent in the virgin binder and the other including it in the RAP and RAS binder. The test sections are in a generally flat area with few horizontal curves.

Table 2.1: Pilot Project Test Section Location Lane and Post Miles and Mix Types from Project Special Provisions

Pilot Project Test Sections[a]			
Type[b]	Begin Post Mile	End Post Mile	Direction and Lane Number[c]
0% RAP and RAS (Control)	9.0	9.2	EB
12%-15% RAP (Mainline)	8.0	17.8	EB/WB
25% RAP	8.0	8.2	EB
30% RAP	8.2	8.4	EB
35% RAP	8.4	8.6	EB
40% RAP	8.6	8.8	EB
25% RAP and 3% RAS	8.8	9.0	EB

[a] See Caltrans project plans for details.
[b] Percentages are by weight of aggregate with a maximum binder replacement of 15% from RAS. Percentages were specified as % binder replacement. However, the contractor used replacement by weight of RAP aggregate.
[c] EB = eastbound, WB = westbound; SJ 26 is a two-lane highway, and, therefore, all sections are in Lane 1.

The existing pavement had age-related cracking (transverse and block cracks) and load-related fatigue cracking in the wheel paths, shown in Figure 2.1, and wheel path rutting, shown in Figure 2.2. Some of the rutting had been addressed by intermittently micro milling, shown in Figure 2.3. Automated pavement condition survey (APCS) data for fatigue cracking (alligator A + B) for the postmiles of the test sections in Figure 2.4 show that the previous treatment in 2014 had reduced fatigue cracking from approximately 50% of the wheelpath, but by the time of construction in 2022, it had reached more than 10% again. The previous treatment was a 0.1 ft. (30 mm) thin overlay, which indicates that the wheelpath cracking present in 2022 was reflective cracking. Corroborating the rutting shown in Figure 2.2, the APCS data in Figure 2.5(a) shows that approximately 5% of the wheelpaths had rutting greater than 1/4 in. (6 mm) in 2022. The figure also shows that more than 10% of the wheelpath had rutting greater than 1/4 in. in 2018, but the rutting had been reduced by district maintenance forces using micromilling. Figure 2.5(b) shows that rutting was not allowed to reach 1/2 in. (12.5 mm).

Figure 2.1: Fatigue cracking in the wheel path.

Figure 2.2: Rutting outside the wheel paths, near an intersection with farming equipment traffic.

Figure 2.3: Micro milling across the wheel path.

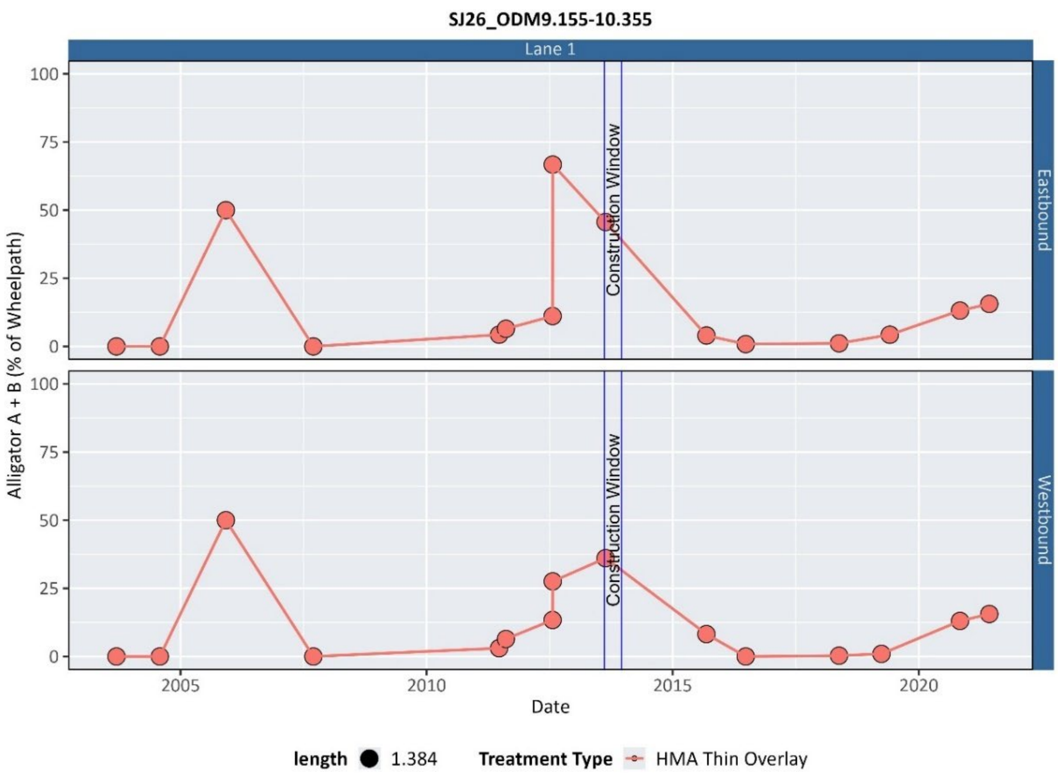

Figure 2.4: Alligator A + B cracking (percent of wheelpath) prior to section construction (test sections are in eastbound direction).

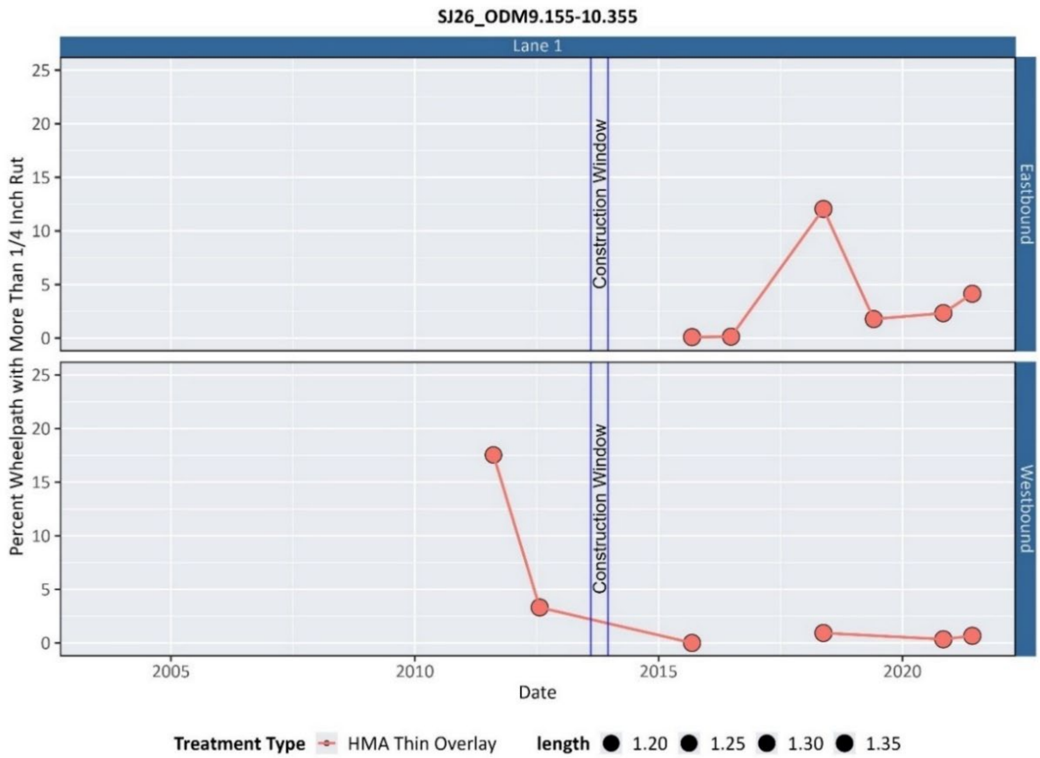

(a)

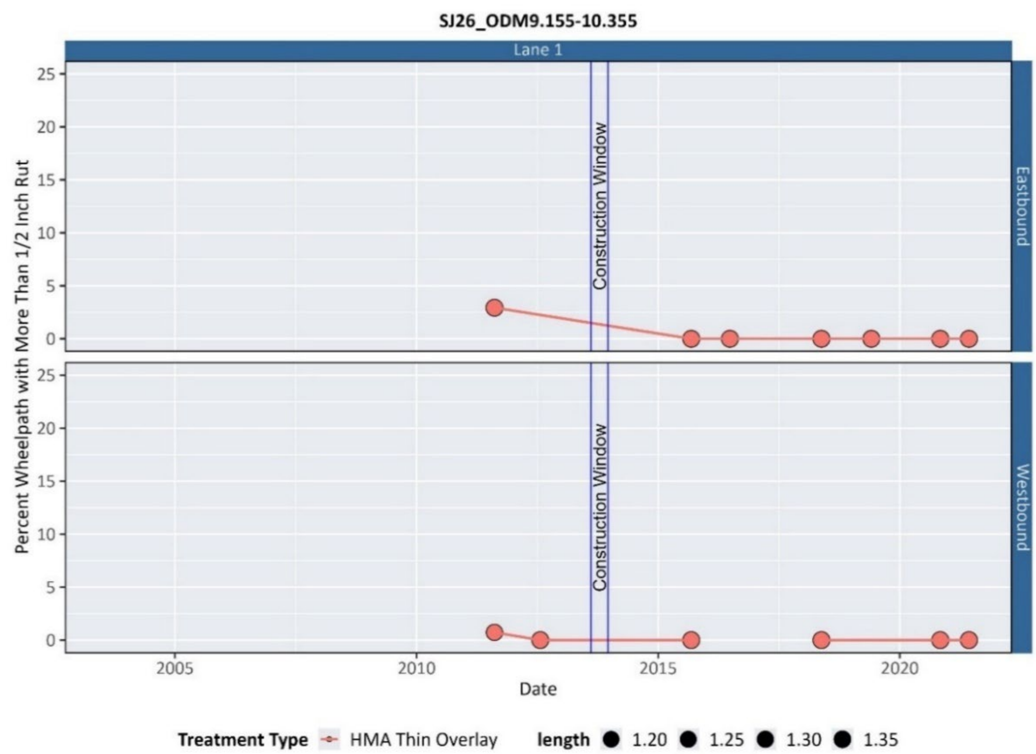

(b)

Figure 2.5: Prior to section construction, percent of wheelpaths with greater than (a) 1/4 in. (6 mm) rut on bottom and (b) 1/2 in. (12.5 mm) rut on top (test sections are in eastbound direction).

2.2 Mix Designs

All the mixes in the test sections were designed to meet Caltrans specifications for 3/4" nominal maximum aggregate size (NMAS) specifications and the Non-Standard Special Provisions (nSSPs) for the contract. The mainline mix used on the project outside of the test sections did not need to meet the nSSP requirements, shown in Figure 2.6. The nSSP mix design requirements are the same as those in the Caltrans Standard Specifications, except for the following:

- The gyratory compaction requirements (Ndesign, VMA) and gradation requirements for the mixes with high RAP and RAS were waived.
- The moisture susceptibility test dry strength has minimum and maximum values, and the wet strength has a minimum tensile strength ratio.
- The HWT test has a minimum number of cycles to a specified rut depth, and the minimum number of passes at the inflection point was waived for mixes with high RAP or RAS.
- Extracted PG-M binder grade and Delta Tc values are specified for all mixes.
- The IDEAL-CT test value of the high RAP mixes must be greater than or equal to that of the virgin mix (with no RAP).
- Flexural fatigue testing and asphalt mixture performance tester (AMPT) RLT testing are required for informational use only, with testing done by the UCPRC only.

The JMF submittals from the contractor for the seven mixes are shown in Table 2.2, along with mix codes used throughout the report (Mix J to Mix O for the control and high RAP and/or RAS mixes, and Mix P for the mainline mix). The information in the table comes from the CEM 3511/3512 forms submitted by the contractor prior to the collection of the JMF verification samples.

The nSSP for this project and the other high RAP pilot projects called for setting the RAP content based on the percentage of binder replacement (25%, 30%, 35%, and 40%). However, for this pilot project, the contractor developed the mix designs based on the percentage of aggregate replacement with RAP and then calculated the replacement binder contents, which the district approved. The contractor was not confident that the binder content of the RAP aggregates would be consistent enough to focus on controlling the plant to match the RAP binder replacement ratio, and during production, RAP is controlled based on aggregate replacement rather than binder replacement. Therefore, the specified binder replacement percentages became RAP aggregate replacement percentages of 25%, 30%, 35%, and 40%.

One aggregate source, one RAP source, and one RAS source were used by the contractor to produce the mix designs included in the pilot sections. The aggregate was a crushed granite from the Sierra Nevada mountain range. The binder grade of the virgin asphalt used in the mixes containing high RAP and/or RAS was PG 58-34M, while in the control mix with no RAP or RAS and in the 15% RAP mix, it was PG64-28M. The contractor used the softer binder and recycling agent (RA), sometimes referred to as a rejuvenating agent depending on formulation, to match the high temperature grade of the control mix.

The RAP binder content obtained from the JMF report from the contractor was 4.64% and the binder content of the RAP/RAS blend for the 28% aggregate replacement (25% RAP + 3% RAS) was 6.28%.

Table 2.3 shows that the binder contents of all of the laboratory-specimen-based mix designs are either 4.5% or 4.6%, including virgin binder and RAP and RAS binder, except for the 35% and 40% RAP mixes (Mix M and Mix N) which have binder contents of 4.0%. The lower binder contents increased the RAP binder replacement percentage relative to the RAP aggregate replacement percentage for these mixes because the percentage of RAP content was considered based on RAP aggregate content rather than RAP binder replacement. This effect can be seen in the RAP binder replacement values in the table, which are 3% to nearly 5% greater than the targets of 35% and 40%, depending on how the recycling agent is accounted for, while the RAP binder replacement rates are much closer to the targets for the 25% and 30% mixes (Mix K and Mix L). These lower binder contents are expected to result in poorer cracking performance and better rutting performance than in the other mixes. It is not certain why those two mix designs had this potentially significant difference in binder content.

All the JMF target gradations were in the middle of the Caltrans 3/4" Standard Specifications limits, summarized in Figure 2.7. The JMF submittal verification information from Caltrans for the plant-produced samples of the seven mixes is also shown in Table 2.2. This information comes from the CEM 3513 forms completed by the Caltrans district laboratory or its consultants. The verification shows that the results are within the allowable ranges, and no adjustments needed to be made to the contractor's JMFs. The binder contents were higher than those of the submitted laboratory specimen-based mix designs, with the control (Mix J), the 25% and 30% RAP mixes (Mix K and Mix L), the RAP/RAS mix (Mix O), and the mainline mix (Mix P) having binder contents of 0.1% to 0.5% more than the targets of 4.5% or 4.6%. The 35% and 40% RAP mixes (Mix M and Mix N) had binder contents 0.25% greater than the target of 4.0%.

39-2.13B(2) Type A Hot Mix Asphalt—High RAP Mix Design

The mix design for Type A HMA—High RAP must comply with the requirements shown in the following table:

Type A HMA—High RAP Mix Design Requirements

Quality characteristic	Test method	Requirement	
		HMA Virgin Mix and HMA with Up to 25% RAP BR	HMA Mix with RAS or High RAP
Air voids content (%)	AASHTO T 269[a]	$N_{initial}$ > 8.0 N_{design} = 4.0 (N_{design} = 5.0 for 1-inch aggregate) N_{max} > 2.0	Report value at N_{design} gyrations on job mix formula (JMF) submittal form
Gyration compaction (no. of gyrations)	AASHTO T 312	$N_{initial}$ = 8 N_{design} = 85.0 N_{max} = 130	$N_{initial}$ = 8 N_{design} = 85.0 N_{max} = 130
Voids in mineral aggregate (min, %)[b] Gradation: No. 4 3/8-inch 1/2-inch 3/4-inch 1-inch with NMAS = 1-inch with NMAS = 3/4-inch	MS-2 Asphalt Mixture Volumetrics	 16.5–19.5 15.5–18.5 14.5–17.5 13.5–16.5 13.5–16.5 14.5–17.5	Report value on JMF submittal form
Dust proportion	MS-2 Asphalt Mixture Volumetrics	0.6–1.3	0.6–1.3
Hamburg wheel track (min number of passes at 0.5-inch rut depth) Binder grade: PG 58 PG 64 PG 70 PG 76 or higher	California Test 389[c]	 10,000 15,000 20,000 25,000	 10,000 15,000 20,000 25,000
Hamburg wheel track (min number of passes at the inflection point) Binder grade: PG 58 PG 64 PG 70 PG 76 or higher	California Test 389[c]	 10,000 10,000 12,500 15,000	 10,000 10,000 12,500 15,000
Moisture susceptibility (min, psi, dry strength)	AASHTO T 283[c]	100	100-300
Moisture susceptibility (min, psi, wet strength)	AASHTO T 283[d]	70	70
Recovered asphalt from HMA Mix	Must comply with section 92[e]	Must comply with project specified PG binder	Must comply with project specified PG binder
Delta Tc (ºC)	ASTM D7643[e,f]	≥ -5.0	≥ -5.0
IDEAL CT	ASTM D8225	Report only	≥ the virgin mix value
I-FIT	AASHTO TP 124[g]	Report only[h]	Report only[h]
Bending Beam Fatigue (psi)	AASHTO T 321[g]	Report only[h]	Report only[h]
Repeated Load Triaxial test (psi)	AASHTO T 378[g]	Report only[h]	Report only[h]

[a]Calculate the air voids content of each specimen using AASHTO T 275, Method A, to determine bulk specific gravity. Use AASHTO T 209, Method A, to determine theoretical maximum specific gravity. Use a digital manometer and pycnometer when performing AASHTO T 209.
[b]Measure bulk specific gravity using AASHTO T 275, Method A.
[c]Test plant-produced Type A HMA.
[d]Freeze thaw required.
[e]Perform binder extraction and recovery for HMA mix with RAS under AASHTO T 164 and ASTM D5404.
[f]Delta Tc must be performed on virgin binder and extracted binder from HMA mix with RAP or RAS. For pilot project, run test at 20 hours for information only in addition to 40 hours.
[g]Contractor to provide and deliver loose mix samples to the Engineer.
[h]Email to High.RAP@dot.ca.gov.

Figure 2.6: Non-Standard Special Provision (nSSP) requirements for the mixes.

Table 2.2: Job Mix Formula Verification Results from Caltrans from Plant Samples for Final Approved Submittal

Parameter		3/4" NMAS													
		Control (Mix J)		High RAP Blend (Mix K)		High RAP Blend (Mix L)		High RAP Blend (Mix M)		High RAP Blend (Mix N)		High RAP Blend (Mix O)		Mainline Blend (Mix P)	
		0% RAP, 0% RAS		25% RAP, 0% RAS		30% RAP, 0% RAS		35% RAP, 0% RAS		40% RAP, 0% RAS		25% RAP, 3% RAS		15% RAP, 0% RAS	
		QA Verified	JMF Limits	QA Verified	JMF Limits	QA Verified	JMF Limits	QA Verified	JMF Limits	QA Verified	JMF Limits	QA Verified	JMF Limits	QA Verified	JMF Limits
Grading (% passing sieve)	1”	100	100	100	100	100	100	100	100	100	100	100	100	100	100
	3/4”	98	93-100	97	92-100	97	92-100	96	91-100	97	92-100	97	92-100	98	93-100
	1/2”	85	79-91	83	77-89	80	74-86	76	70-82	78	72-84	82	76-88	86	80-92
	3/8”	76	—	74	—	70	—	66	—	66	—	72	—	77	—
	#4	55	50-60	48	43-53	43	38-48	43	38-48	42	37-47	46	41-51	54	49-59
	#8	38	33-43	32	27-37	29	24-34	29	24-34	29	24-34	31	26-36	39	34-44
	#200	5.1	3.1-7.1	4.1	2.1-6.1	4.0	2.0-6.0	4.4	2.4-6.4	4.6	2.6-6.6	4.6	2.6-6.6	4.5	2.5-6.5
RAS content (% by weight of aggregate)		0	—	0	—	0	—	0	—	0	—	3	—	0	—
RAP content (% by weight of aggregate)		0	—	25	—	30	—	35	—	40	—	25	—	12	—
Base asphalt binder performance grade		64-28M	—	58-34M	—	58-34M	—	58-34M	—	58-34M	—	58-34M	—	64-28M	—
RA type		—	—	Tall Oil	—	Tall Oil	—	Tall Oil	—	Tall Oil	—	Tall Oil	—	—	—
RA dosage (% by weight of binder)		0	—	1.0	—	1.0	—	1.5	—	1.5	—	1.5	—	0	—
Binder content (% by weight of mix)		4.5	4.2-5.0	4.5	4.2-5.0	4.5	4.2-5.0	4.0	3.7-4.5	4.0	3.7-4.5	4.5	4.2-5.0	4.6	4.3-5.1
Recycled binder content (% binder by TWA)		0	—	1.16	—	1.39	—	1.63	—	1.87	—	1.79	—	0.56	—
Estimated binder replacement excluding RA (% of total binder)		0	—	25.8	—	31.0	—	40.9	—	46.7	—	39.8	—	12.1	—
Estimated binder replacement including RA (% of total binder)		0	—	26.8	—	32.0	—	42.4	—	48.2	—	41.3	—	12.1	—
Number of gyrations		85	85	85	85	85	85	85	85	85	85	85	85	85	85
Air-void content (%)		4.0	4.0±1.5	4.1	Report only	4.1	Report only	4.0	Report only	3.9	Report only	4.1	Report only	3.5	4.0±1.5

Parameter	3/4" NMAS													
	Control (Mix J)		High RAP Blend (Mix K)		High RAP Blend (Mix L)		High RAP Blend (Mix M)		High RAP Blend (Mix N)		High RAP Blend (Mix O)		Mainline Blend (Mix P)	
	0% RAP, 0% RAS		25% RAP, 0% RAS		30% RAP, 0% RAS		35% RAP, 0% RAS		40% RAP, 0% RAS		25% RAP, 3% RAS		15% RAP, 0% RAS	
	QA Verified	JMF Limits	QA Verified	JMF Limits	QA Verified	JMF Limits	QA Verified	JMF Limits	QA Verified	JMF Limits	QA Verified	JMF Limits	QA Verified	JMF Limits
Voids in mineral aggregate (%)	15.7	12.5-15.5	13.9	12.5-15.5	14.2	Report only	14.0	Report only	14.0	Report only	13.9	Report only	14.3	12.5-15.5
Dust proportion	1.07	0.6-1.3	1.01	0.6-1.3	0.97	0.6-1.3	1.06	0.6-1.3	1.13	0.6-1.3	1.15	0.6-1.3	1.03	0.6-1.3
Hamburg (rut depth [in] at # passes)	—	<0.5 @15,000	—	<0.5 @15,000	—	<0.5 @15,000	—	<0.5 @15,000	—	<0.5 @15,000	—	<0.5 @15,000	0.181 @ 25,000	<0.5 @15,000
Moisture susceptibility, dry strength (psi)	196	>100	—	100-300	—	100-300	—	100-300	—	100-300	—	100-300	—	>100
Moisture susceptibility, wet strength (psi)	124	>70	—	>70	—	>70	—	>70	—	>70	—	>70	—	>70

Notse: RA = recycling agent. The binder content of the RAP aggregate assumed in the calculations from the contractor's mix designs is 4.64%

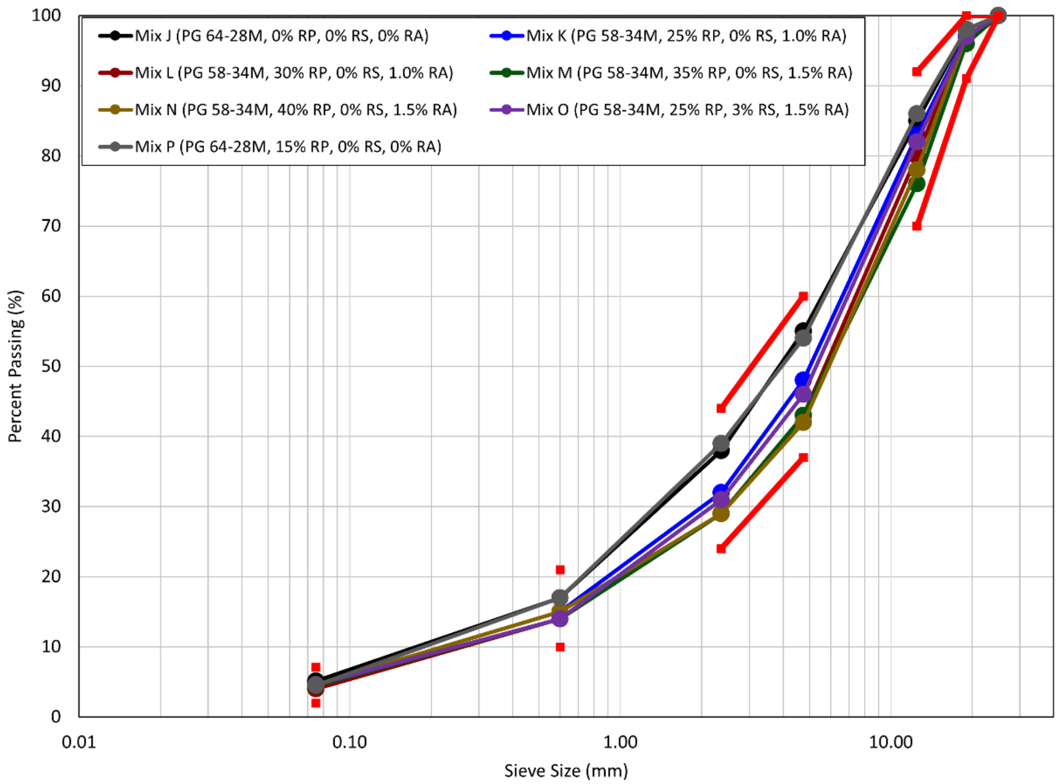

Figure 2.7: Target job mix formula gradation for all mixes on SJ 26.

The total binder content consists of the RAP binder, the virgin binder, and the recycling agent. The recycled binder ratio (RBR) is the RAP and/or RAS binder as the percentage of total binder. When RA is included in the mix, the RBR can be calculated both with and without the RA as part of the RAP/RAS component. The nSSP for the pilot project states that only the RAP binder in the total binder blend is counted as reclaimed binder, which indicates that the recycling agent used to change the properties of the RAP/virgin binder blend and that the RAP/RAS/virgin binder blend should be counted as part of the virgin binder. The nSSP also states that liquid antistrip (LAS), which was not used on this project, is not counted as part of the virgin binder.

Table 2.3 shows the percentages of virgin and RAP/RAS aggregate in the JMF laboratory mix designs, expressed as a percentage of the total mass of aggregate. For the binder, the table shows the target total binder content, the recycled asphalt binder content, and the resultant target RBR expressed as a percentage of the total binder. The inclusion of the RA with the virgin binder content, combined with the fact that the binder content of the RAP was close to the new mix design total binder contents, resulted in RBR values that are close to the percentage of virgin aggregate replaced by RAP aggregate for the 25% and 30% RAP mixes (Mix K and Mix L) and considerably higher than the percentage of virgin aggregate replaced by RAP aggregate for the 35% and 40% RAP mixes (Mix M and Mix N). For example, the addition of 40% RAP aggregate in the new mix results in 46.7% replacement of virgin asphalt binder in the new mix.

Table 2.3: Percentages of Virgin and RAP/RAS Binder and Aggregate Contents in Each Mix Design from Contractor's Job Mix Formula

Average Mix	Virgin Aggregate (% of TMA)[a]	RAP/RAS Aggregate (% of TMA)[a]	JMF Target Total AC Content (Pb, % of TMM)[b]	JMF Target Recycled AC Content (Pb, % of TMM)[b]	JMF Target RBR[c] (% of total binder)[c]
Mix J (PG 64-28M, 0% RP, 0% RS, 0% RA)	100.0	0.0	4.50	0.00	0.0
Mix P (PG 64-28M, 15% RP, 0% RS, 0% RA)	88.0	12.0	4.60	0.56	12.1
Mix K (PG 58-34M, 25% RP, 0% RS, 1.0% RA)	75.0	25.0	4.50	1.16	25.8
Mix L (PG 58-34M, 30% RP, 0% RS, 1.0% RA)	70.0	30.0	4.50	1.39	31.0
Mix M (PG 58-34M, 35% RP, 0% RS, 1.5% RA)	65.0	35.0	4.00	1.63	40.9
Mix N (PG 58-34M, 40% RP, 0% RS, 1.5% RA)	60.0	40.0	4.00	1.87	46.7
Mix O (PG 58-34M, 25% RP, 3% RS, 1.5% RA)	72.0	28.0	4.50	1.79	39.8

[a] TMA: total mass of aggregate.
[b] TMM: total mass of mix.
[c] RBR = recycled binder ratio; RA counted as part of virgin binder.

Notes: RP = RAP, RS = RAS (recycled asphalt shingles), RA = recycling agent.

2.3 Testing Plan

Laboratory testing by the UCPRC covered both binder and mix testing during both JMF approval and construction. The sampling, test methods, and testing factorials are discussed in the following sections.

2.4 Material Sampling and Handling

Sampling for JMF verification and QA was completed in coordination with asphalt plant operations and quality control groups to ensure the quality of materials and safety of all involved.

2.4.1 Plant-Produced Material Sampling for Job Mix Formula Verification Testing

One JMF submittal was verified in May 2022 by the Caltrans District 10 materials laboratory, which was used to pave a majority of the project: the conventional mix with 15% RAP (Mix P). Six JMF submittals were verified in the period from May 2022 to September 2022 by the UCPRC and the Caltrans District 10 Materials Laboratory: the control mix with no RAP or RAS (Mix J); the mixes with 25%, 30%, 35%, and 40% RAP and 0% RAS (Mix K, Mix L, Mix M, Mix N); and the mix with 25% RAP and 3% RAS (Mix O). Approximately six tons of material were produced for UCPRC testing when District 10 sampled for its testing. The seven approved JMF submittals for the SJ 26 project are shown in Table 2.4.

Table 2.4: Mix Samples for Job Mix Formula Verification Testing by Caltrans and UCPRC

Mix Type	UCPRC HMA Mix Identifier	Date Sampled	Location Sampled	Samples Taken By
3/4” Type A HMA – virgin control	4.79-Mix J-R0S0	7/15/2022, 7/25/2022	George Reed Clements, Batch Plant	UCPRC, Caltrans, and George Reed staff
3/4” Type A HMA – with 15% RAP conventional	4.79-Mix P-R15S0	5/23/2022	George Reed Clements, Batch Plant	Caltrans and George Reed Staff
3/4” Type A HMA – RAS or high RAP – 25% RAP	4.79-Mix K-R25S0	8/10/2022	George Reed Clements, Batch Plant	UCPRC, Caltrans, and George Reed staff
3/4” Type A HMA – RAS or high RAP – 30% RAP	4.79-Mix L-R30S0	8/10/2022	George Reed Clements, Batch Plant	UCPRC, Caltrans, and George Reed staff
3/4” Type A HMA – RAS or high RAP – 35% RAP	4.79-Mix M-R35S0	8/10/2022, 9/9/2022	George Reed Clements, Batch Plant	UCPRC, Caltrans, and George Reed staff
3/4” Type A HMA – RAS or high RAP – 40% RAP	4.79-Mix N-R40S0	8/10/2022, 9/9/2022	George Reed Clements, Batch Plant	UCPRC, Caltrans, and George Reed staff
3/4” Type A HMA – RAS or high RAP – 25% RAP and 3% RAS	4.79-Mix O-R25S3	8/10/2022, 9/9/2022	George Reed Clements, Batch Plant	UCPRC, Caltrans, and George Reed staff

The mixes sampled for JMF verification were produced in a batch plant in two- to six-ton increments with no silo storage or additional processing of the mix and were loaded directly into a loader bucket below the pugmill. When the loader placed the mix in a large pile for sampling, a small stockpile was formed and then flattened into a sampling pad. The pad was split into four quadrants, and mix was shoveled from each of the four quadrants into the quartermaster for reduction to 3.5-gallon buckets. Use of the quartermaster at the plant was performed in accordance with CTM 125. The 3.5-gallon buckets were sealed and immediately transported to the UCPRC’s Davis laboratory for storage and processing. The materials were labeled and stored in an outdoor, shaded area prior to laboratory processing.

2.4.2 Plant-Produced Material Sampling During Construction

Plant-produced mixes for the seven mixes were sampled at the plant during construction, as shown in Figure 2.8, Figure 2.9, and Figure 2.10. The UCPRC, Caltrans, and George Reed field staff worked very closely with one another to ensure that the mixes were properly sampled and labeled. The sampling for the production QA testing was performed similarly to the JMF process and completed over four days. During production, the boxes of mix for volumetric verification by Caltrans were collected by the contractor at the same time for all parties, and 3.5-gallon buckets were used with a quartermaster splitter following CT 125 to collect representative boxes. The materials for determining the PG of the binders for the UCPRC were collected by box, and all other UCPRC samples were collected by 3.5-gallon bucket.

Seven mixes were paved on September 26, 27, 28, and 29, 2022, with approximately 210 tons of production for each test section. The plant first shipped out Mix P (3/4” HMA with 15% RAP), and samples were taken after approximately 75 tons and 150 tons, a sampling pattern that was repeated for the other six mixes. The mix production and sampling followed the same process used for JMF sampling. The next mixes paved on September 27, 2022, were Mix K and Mix L (3/4” HMA with 25% and 30% RAP). The next mix paved on September 28, 2022, was Mix M (3/4” HMA with 35% RAP). The last three mixes paved on September 29, 2022, were Mix N (3/4” HMA with 40% RAP), Mix O (3/4” HMA with 25% RAP and 3% RAS), and Mix J (3/4” HMA with no RAP or RAS).

Figure 2.8: Sampling from hot drop and putting in buckets and boxes for QA sampling (each person is sampling from a quadrant of the pile of hot mix).

Figure 2.9: Samples from job mix formula submittal of one mix loaded into the back of a truck.

Figure 2.10: UCPRC staff preparing for QA sampling during production on September 26, 2022.

2.4.3 Storage and Reheating to Compaction

As discussed in the sampling discussion, the mixes were all sampled in sealed 3.5-gallon steel cans or cardboard boxes. The cardboard boxes for binder extraction were stored inside the UCPRC asphalt binder laboratory at temperatures between 60°F and 80°F (15°C to 27°C) for up to 60 days prior to extraction. The buckets for mix testing were stored in an outdoor, shaded receiving area at temperatures between 40°F and 95°F (4°C to 35°C).

The laboratory reheating to compaction procedure was discussed with the contractor, and the procedures labeled as "SJ 26" in Table 2.5 were agreed upon for this project. The AASHTO R30 procedure for laboratory mixed material is included as a reference. AASHTO R30 does not provide specific procedures for reheating for compaction or laboratory aging of plant-produced mix.

Table 2.5: Mix Sampling, Storage, and Reheating-to-Compaction Temperature Procedures for SJ 26 Pilot Project Materials, Compared with AASHTO R30

Activity	SJ 26	Activity	AASHTO R30
Sampling (bucket or box)	—	Components pre-heated	1–4 hours
Transport and storage (cooled)	—	Loose mixed in lab	4 minutes
Bucket/box reheating (workable at 135°C)[a]	4 hours	Conditioned at 135°C[b]	4 hours
Split to compaction mass	0.25 hours	Flipped every hour	—
Loose mix in pan to compaction temperature	1–2 hours	Loose mix in pan to compaction temperature	0.5 hours
Compact	—	Compact Superpave gyratory compactor specimens	—

[a] Material starts from room temperature.
[b] Material starts at mixing temperature (140°C or higher).

All materials for mix tests other than flexural beam testing were stored prior to being reheated and compacted as specimens within 45 days of sampling. Materials for flexural beams were stored for up to a maximum of 120 days before specimen preparation. After compaction and cutting to final dimensions, specimens for tests other than flexural beam testing were tested within 14 days. Specimens for flexural beam testing were tested within 90 days. All specimens were stored indoors at temperatures between 60°F and 80°F (15°C to 27°C).

2.4.4 Medium-Term Mix Aging

A draft standard test method for a Caltrans asphalt mixture conditioning protocol for plant-produced materials was developed in the fall of 2021 with Caltrans Materials Engineering and Testing Services (METS) and the UCPRC, following a detailed literature review and technical review. This draft Caltrans practice describes the procedure for reheating and medium-term oven aging (MTOA) of plant-produced asphalt mixture prior to compaction in the laboratory. A comparison of the draft Caltrans standard method and the AASHTO R30 standard is shown in Table 2.6.

Asphalt mixtures have varying asphalt binder contents, different combinations of additives, aggregates, RAP, RAS, and other components. Mixtures may be sampled and tested shortly after production; however, their performance may significantly change after several years of in-service aging in the field. The MTOA procedure is an accelerated approach to simulate the aging of the compacted mixture in the field after several years of service. The years of service that MTOA simulates depend on the climate region, the depth of the asphalt in the pavement, and the air permeability of the mix, which is largely dependent on compaction.

Table 2.6: Comparison of AASHTO R30 and Draft MTOA Procedure for Mix Sampling, Storage, and Reheating-to-Compaction Temperature Procedures

Activity	Pilot nSSP	Activity	AASHTO R30
Sampling (bucket or box)	—	Components pre-heated	1–4 hours
Transport and storage (cooled)	—	Loose mixed in lab	4 minutes
Bucket/box reheating (workable at 135°C or 150°C[a])	4 hours	Conditioned at 135°C[b]	4 hours
Split to compaction mass	0.25 hours	Flipped every hour	—
Rest period	1 hours	Standardize starting temperature	—
MTOA aging at 100°C	20 hours	Midterm aging	—
Loose mix in pan to compaction temperature, flipping at the midpoint	1–2 hours	Loose mix in pan to compaction temperature	0.5 hours
Compaction	—	Compact specimens	—

[a] Material starts from room temperature.
[b] Material starts at mixing temperature (140°C or higher).

The draft Caltrans MTOA test method is shown in Appendix A.

2.4.5 Binder Extraction

To determine the PG grade and the Delta T_c parameter of each JMF verification and QA sublot, binder was extracted following ASTM D8159 and ASTM D5404 procedures with the use of an automated asphalt extraction unit and rotary evaporator (Figure 2.11).

Figure 2.11: Closed loop binder extraction system.

To obtain loose mix, sufficient cardboard sample boxes were minimally reheated to 110°C and the loose mix was split down to begin processing. The automated extraction process of eight to nine wash cycles for a complete trichloroethylene (TCE) solvent extraction took approximately 90 minutes to run. Extraction was performed on a minimum of four 2,000 to 2,200 g replicates of loose mix to obtain enough recovered asphalt for AASHTO R29 PG grading and ASTM D7643 continuous grading of PG binders, with 20-hour and 40-hour pressure aging vessel long-term aging.

Following the solvent extraction process, the recovered asphalt binder and TCE solvent solution were stored in 500 mL glass jars for no more than two days prior to recovery. To remove the TCE solvent and recover the asphalt binder, a rotary evaporator was used. The recovery process took approximately 100 minutes in a heated silicone fluid bath under continuously flowing nitrogen gas to minimize oxidation. After all the TCE was removed from the recovered asphalt binder, the glass flask was turned upside down and heated to 163°C to remove and recover all binder. The sample was then transferred to a metal tin and PG grading began.

The recovered asphalt binder from loose mix produced in the asphalt plant was assumed to have undergone aging like that caused by the rolling thin-film oven (RTFO) test (AASHTO T240), and no further short-term aging was applied for PG grading. The 20-hour pressurized aging vessel (PAV) aging and then 40-hour PAV aging immediately followed, and the Delta T_c parameter was calculated per ASTM D7643 using the low temperature bending beam rheometer (BBR) results in either an Excel worksheet or a transmittal database such as StonemontQC.

2.5 Test Methods

The UCPRC completed the binder and mix tests shown in Table 2.7 on materials sampled from the plant for JMF verification. Section 2.6 provides a summary of the binder tests shown in the table, and Section 2.7 summarizes the mix tests.

Table 2.7: Job Mix Formula Verification Testing Performed by UCPRC for Pilot Project

Test Type	Test Method	Material Tested	Goal
IDEAL-CT test[a]	ASTM D8225	Laboratory-compacted plant mix	Intermediate cracking tolerance
Binder true grade and Delta T_c[b]	AASHTO R29	Binder extracted from plant-sampled mix	Post-plant PG grade
IDEAL-CT indirect tension[c]	ASTM D8225	Laboratory-compacted plant mix	Intermediate cracking tolerance index and strength
Repeated load triaxial[c]	AASHTO T378	Laboratory-compacted plant mix	Dynamic modulus (stiffness) and permanent deformation
Four-point flexural beam[c]	AASHTO T321	Laboratory-compacted plant mix	Dynamic modulus (stiffness) and fatigue life

[a]nSSP requirement.
[b]Report only in nSSP.
[c]Performance-related property; not required by nSSP.

2.6 Binder Testing

Binder testing included the following (an overview of the methods and data interpretation is discussed in the following sections):

- Performance grade (PG)
- Frequency sweep (FS) tests to evaluate binder stiffness
- Fourier transform infrared (FTIR) spectroscopy tests to track changes in binder chemistry after aging

These tests were all performed on binders extracted from the QA samples, while only PG tests were performed on the binders from the JMF verification samples.

2.6.1 Performance Grading

A dynamic shear rheometer (DSR) was used to determine the high and intermediate temperature binder PG. Short-term aging of the binders was not simulated in an RTFO because binders were extracted from mixes that were plant produced. Long-term aging of the binder was simulated in a PAV following the AASHTO R 28 method for 20 hours, and additional PAV specimens were aged 40 hours. The low temperature PGs were determined on PAV-aged binders using a BBR, following AASHTO T 313.

2.6.2 Frequency Sweep

A symmetric sigmoidal fit function was used to convert the frequency sweep data into a master curve at the reference temperature using the fit function in Equation 2.1 *(3)*. The midpoint of the temperature testing range was selected as the reference temperature (i.e., 40°C).

$$log|E^*| = \delta + \frac{\alpha}{1+e^{\beta+\gamma log \omega f_r}} \qquad \textbf{(2.1)}$$

Where:

$|E^*|$ = magnitude of complex modulus (kPa)

α = fitting parameter (the high asymptote of the master curve)

δ = fitting parameter (the lower asymptote of the master curve)

β, γ = fitting parameters (the slope of the transition region of the master curve)

ω = frequency (Hz)

f_r = reduced frequency, which is the shifted frequency at the reference temperature from the frequency at the test temperature (Hz)

Equation 2.1 can be used to generate a binder master curve by substituting the complex modulus (E^*) with the shear complex modulus (G^*). The reduced frequency can be calculated using the Arrhenius equations (Equation 2.2 and Equation 2.3), which are based on the time-temperature superposition *(1)*.

$$log f_r = log f + log \alpha_T \qquad \textbf{(2.2)}$$

$$log \alpha_T = \frac{E_a}{R(ln10)}\left(\frac{1}{T} - \frac{1}{T_r}\right) \qquad \textbf{(2.3)}$$

Where:

f = frequency sweep test loading frequency (Hz)

α_T = shift factor as a function of temperature in Kelvin (°K)

E_α = activation energy (J/mol)

T = test temperature (°K)

T_r = reference temperature (°K)

R = ideal gas constant, 8.314 J/(°K/mol)

Measured dynamic moduli can be horizontally shifted into a single master curve at the reference temperature using the above equations. The shift factor (α_T) can be determined using the solver function in Excel by minimizing the sum of squares error between the predicted and measured dynamic moduli. Figure 2.12 and Figure 2.13 show examples of the fitting procedure.

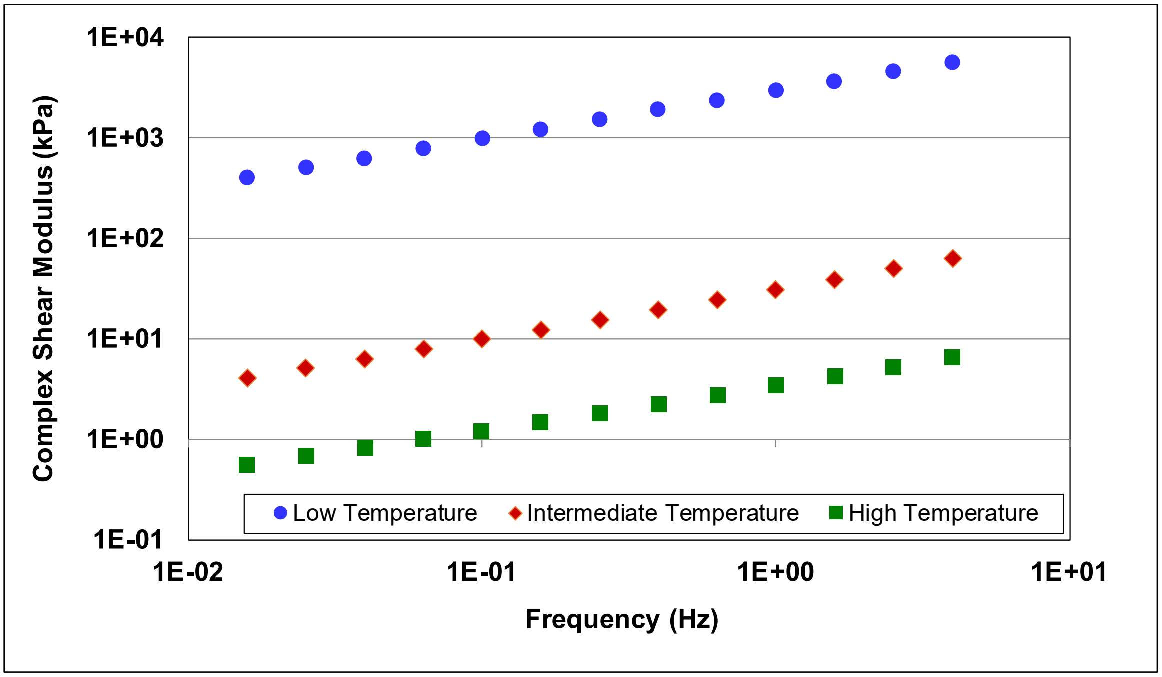

Figure 2.12: Example of modulus master curves (plotted by frequency at tested temperature).

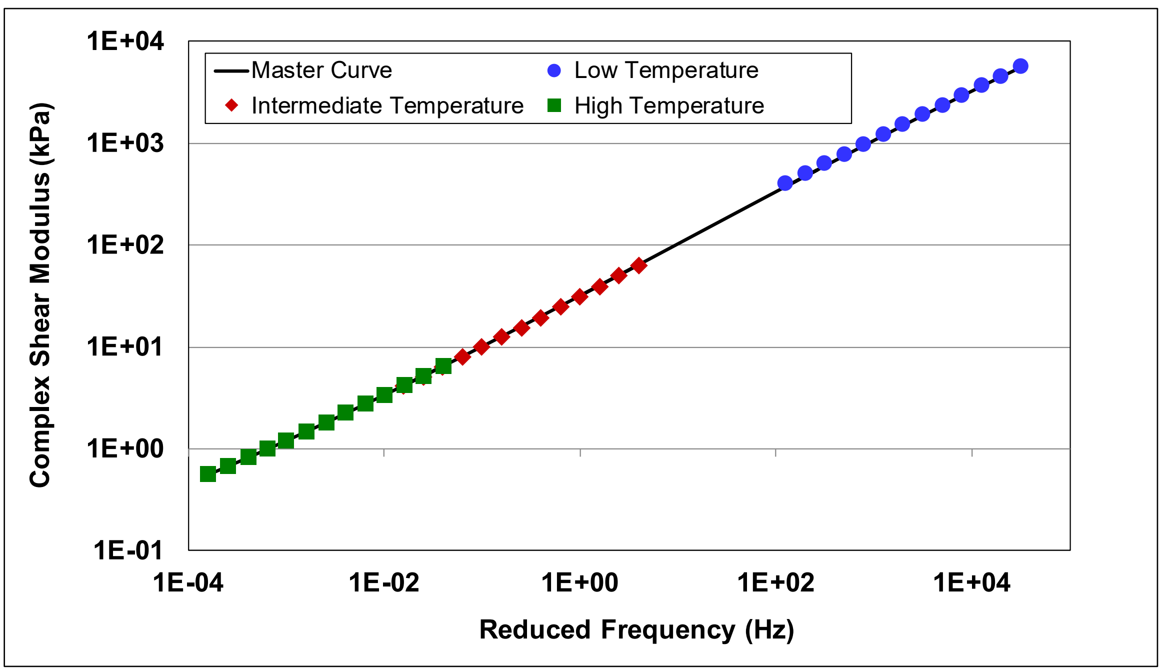

Figure 2.13: Example of modulus master curves (plotted by shifted frequency).

2.6.3 Fourier Transform Infrared Spectroscopy

Chemical component changes in the control and blended binders were evaluated using Fourier transform infrared spectroscopy with attenuated total reflection (FTIR-ATR). The spectra measured by the FTIR were recorded in a reflective mode, from 4,000 to 400 cm^{-1}, at a resolution of 4 cm^{-1}. Each measurement included 24 scans, and an average value was recorded. Nine replicate measurements were taken to ensure that representative measurements were collected for each binder sample. The carbonyl component was used to track oxidative aging, which is usually defined by the peak at 1,680 cm^{-1} *(4-7)*. The tangential integration of the component area index was calculated between the upper and lower wavenumbers (1,675 cm^{-1} and 1,750 cm^{-1}).

The spectra were normalized using the aliphatic band at 2,923 cm^{-1} to eliminate any variability introduced by the operator and any background impacts between repeat measurements. This aliphatic band structure is not affected by aging over time *(7,8)*. The chemical component area index was then integrated from the normalized spectra using Equation 2.4 *(7)*. Figure 2.14 shows an example of a spectrum and the respective component.

$$I_i = \int_{w_{l,i}}^{w_{u,i}} a(w)dw - \frac{a(w_{u,i})+a(w_{l,i})}{2} \times (w_{u,i} - w_{l,i}) \qquad \textbf{(2.4)}$$

Where:

I_i = index of area i

$w_{l,I}$ = lower wavenumber integral limit of area i

$w_{u,I}$ = upper wave number integral limit of area i

$a(w)$ = absorbance as a function of wavenumber

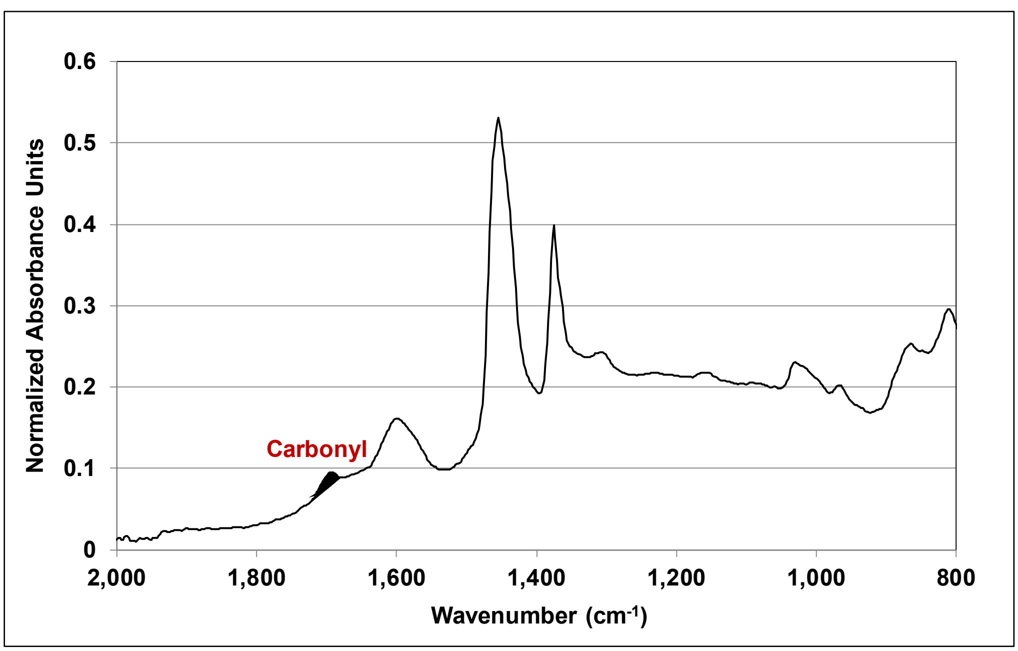

Note: Plot shows tangential integration with carbonyl areas.

Figure 2.14: Example of normalized Fourier transform infrared spectroscopy absorbance spectrum.

2.7 Mix Testing

Mix testing completed by the UCPRC included the following (an overview of the methods and data interpretation is discussed in the following sections):

- Dynamic modulus (DM, AASHTO T 378; specimens prepared in a gyratory compactor)
- Flexural modulus (FM, AASHTO T 321; specimens prepared using a rolling wheel compactor)
- Repeated load triaxial (RLT, flow number, AASHTO T 378; specimens prepared in a gyratory compactor)
- Beam fatigue (FAT, AASHTO T 321; specimens prepared using a rolling wheel compactor)
- IDEAL-CT indirect tensile strength test (IDEAL-CT, ASTM D 8225; specimens prepared in a gyratory compactor)

2.7.1 Test Specimen Air-Void Contents

The bulk densities of the IDEAL-CT specimens were determined according to AASHTO T 166 (saturated surface-dry [SSD] method). The bulk densities of the beam, AMPT, and SCB specimens were determined according to AASHTO T 331 (CoreLok). Theoretical maximum specific gravity (Gmm) was determined according to AASHTO T 209. All specimens for all tests were compacted to 7% air-voids with a 0.5% tolerance around that target.

2.7.2 Triaxial Dynamic Modulus

Triaxial dynamic modulus testing followed AASHTO T 378 using an AMPT with specimens prepared in a gyratory compactor.

Specimens were tested at 4°C, 21°C, 38°C, and 54°C and at frequencies between 25 and 0.1 Hz. Measured dynamic moduli and phase angles were horizontally shifted into a master curve at 20°C using Equation 2.2, Equation 2.3, and the Williams-Landel-Ferry shift function *(9)* in Equation 2.5.

$$log(\alpha_T) = \frac{-C_1(T-T_r)}{C_2+(T-T_r)} \quad \textbf{(2.5)}$$

Where:

α_T = shift factor as a function of temperature T

T = test temperature in Kelvin (°K)

T_r = reference temperature in Kelvin (°K)

C1 and *C2* = fitting parameters

2.7.3 Flexural Dynamic Modulus

Flexural beam frequency sweep testing followed AASHTO T 321 using a beam fatigue apparatus and beams prepared using a rolling wheel compactor. Specimens were tested at 10°C, 20°C, and 30°C and at frequencies between 15 and 0.01 Hz. A sinewave frequency was applied to produce a tensile strain of 100 µstrain on the longitudinal surface of the beam. The measured stiffnesses and phase angles were horizontally shifted into master curves at 20°C using Equation 2.2, Equation 2.3, and Equation 2.5. Flexural stiffnesses were used in the *CalME* simulations discussed in Chapter 8.

2.7.4 Fatigue Cracking Resistance

Fatigue cracking resistance testing followed AASHTO T 321 on beams prepared using a rolling wheel compactor. Beam specimens were subjected to four-point bending by applying sinusoidal loading at three different strain levels (high, intermediate, low) at a frequency of 10 Hz and temperature of 20°C. The fatigue life for each strain level was selected by multiplying the maximum stiffness value for that strain level by the number of cycles at which that stiffness value occurred.

In this study, the testing approach currently specified in AASHTO T 321 was modified to optimize the quantity and quality of the data collected. Replicate specimens were first tested at high and medium strain levels to develop an initial regression relationship between fatigue life and strain (Equation 2.6). Strain levels were selected, based on experience, to achieve fatigue lives between 10,000 and 100,000 load cycles at high strains and between 300,000 and 500,000 load cycles for medium strains. Additional specimens were then tested at lower strain levels selected based on the results of the initial linear regression relationship to achieve a fatigue life of about 1 million load repetitions. The final regression relationship was then refined to accommodate the measured stiffness at the lower strain level.

$$Ln(N) = A + B \times Ln(\varepsilon) \quad \textbf{(2.6)}$$

Where:

N = fatigue life (number of cycles)

ε = strain level (µstrain)

A and B = model parameters

Test results can also be used to generate the material fatigue response in the *CalME* simulations when used with flexural stiffness master curves to calculate estimated strains in the pavement. Flexural fatigue results can be directly compared—without *CalME* simulation—when taking into consideration that laboratory test results will generally correspond with field fatigue or reflective cracking performance for overlays thinner than about 62 mm (0.2 ft.), but may not correspond with expected field performance for thicker layers of asphalt. For thicker layers, the interaction of the pavement structure, traffic loading, temperature, and mix stiffness with the controlled-strain beam fatigue results needs to be simulated using mechanistic analysis to rank mixes for expected field performance.

2.7.5 Rutting Resistance

Permanent deformation resistance testing followed AASHTO T 378 using an AMPT with specimens prepared in a gyratory compactor. The RLT parameters assessed included flow number and the number of cycles to reach 5% permanent axial strain. Specimens were tested with no confinement under a deviator stress of 483 kPa *(10-12)*. Given that the addition of RAP tends to stiffen mixes and therefore improve rutting resistance, HWT tests were not done in addition to the RLT tests.

2.7.6 Indirect Tensile Cracking Resistance IDEAL-CT

The IDEAL-CT test uses a loading apparatus and specimen fixture as shown in Figure 2.15. A loading rate of 50 mm/min was applied until the tested specimen reached failure. An example of a test result from IDEAL-CT is shown in Figure 2.16.

Figure 2.15: Testing machine for IDEAL-CT with a specimen.

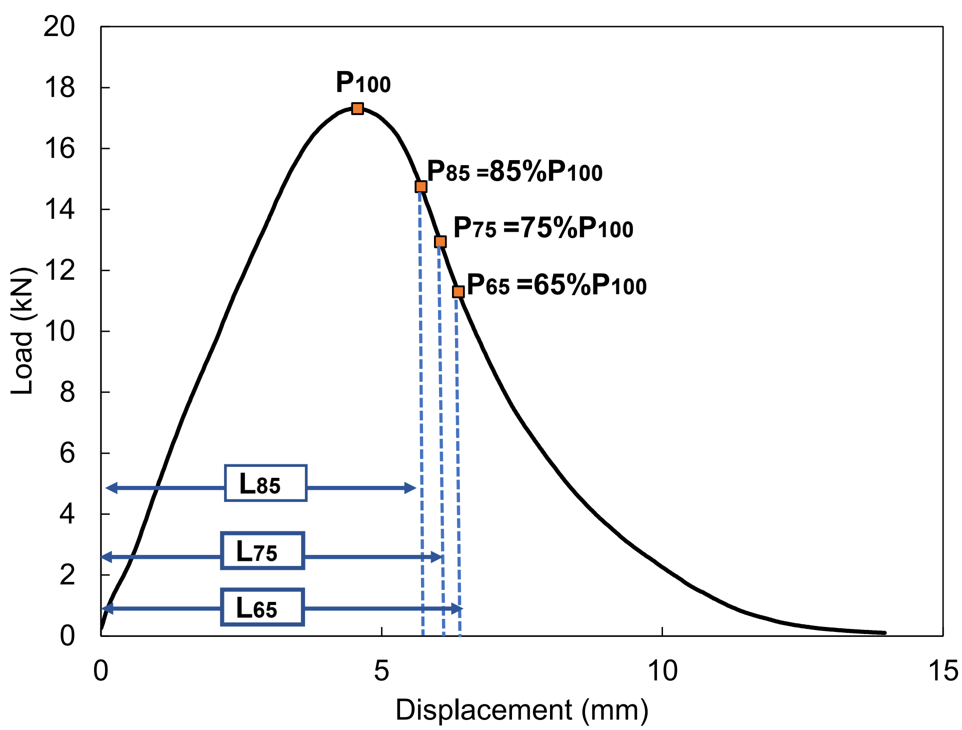

Figure 2.16: Example load-displacement curve from IDEAL-CT.

Fracture parameters obtained from IDEAL-CT are shown in Table 2.8, along with definitions. The two parameters of primary interest are the IDEAL-CT parameter, which is intended to relate to cracking and which the UCPRC has found correlates very well with flexural stiffness at 10 Hz and 20°C, and the Strength parameter, which has also been found to have a strong correlation with flexural stiffness but half the test variability of the IDEAL-CT parameter.

Table 2.8: Fracture Parameters from IDEAL-CT

Parameters	Equations
$\|m_{75}\|$: post-peak slope (N/m)	$\|m_{75}\| = \left\|\frac{P_{85} - P_{65}}{I_{85} - I_{65}}\right\|$
	Where:
	P_{85} = 85% of peak load
	P_{65} = 65% of peak load
	I_{85} = deformation at P_{85}
	I_{65} = deformation at P_{65}
l_{75} (mm)	Displacement at 75% of the peak load after the peak
G_f: failure energy (J/m^2)	$G_f = \frac{W_f}{D \times t} \times 10^6$
	Where:
	W_f = area under load-displacement curve (J)
	$t = thickness\ (mm)$
	$D = diameter\ (mm)$
CT_{index}: cracking tolerance index	$CT_{index} = \frac{t}{62} \times \frac{l_{75}}{D} \times \frac{G_f}{\|m_{75}\|} \times 10^6$
Strength	$Strength = \frac{Peak\ load}{2rt}$

2.7.7 Hamburg Wheel-Tracking Test Rutting and Moisture Resistance

Hamburg Wheel-Tracking (HWT) tests were also performed following AASHTO T 324-23. The HWT test provides information regarding both rutting resistance and moisture sensitivity by measuring the development of rutting in two gyratory compacted specimens under a steel wheel under water at 50°C (122°F). The rut depth in both specimens is tracked and the average value is reported. Moisture sensitivity is indicated when an "inflection point" is seen in the rutting versus load repetitions relationship, shown in Figure 2.17.

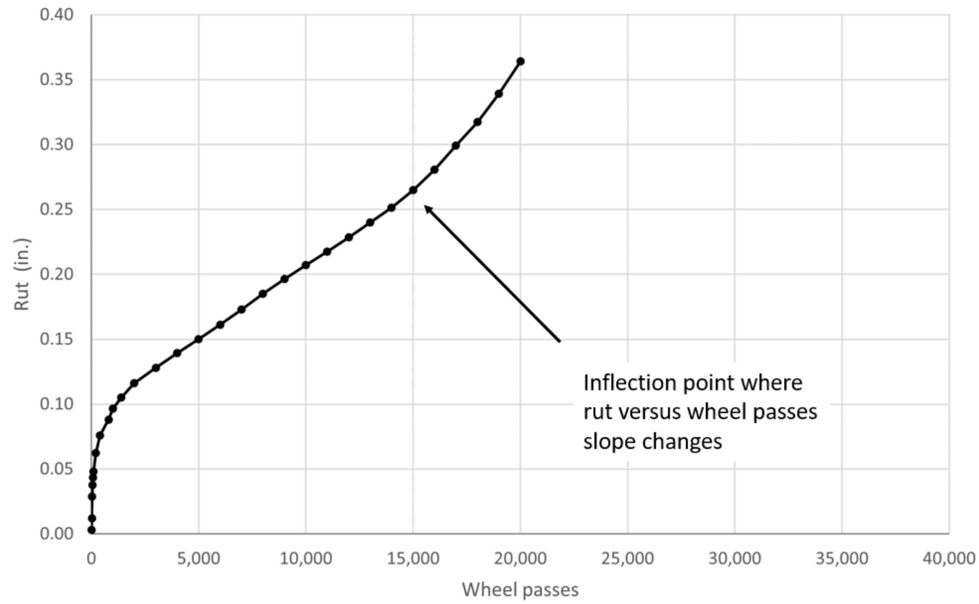

Figure 2.17: Hamburg Wheel-Tracking test result showing inflection point attributed to moisture damage.

2.7.8 Testing Done by Caltrans

Testing for volumetric properties for JMF verification and during QA was completed by Caltrans. Neither of these sets of results are included in this technical memorandum.

3 BINDER TESTING RESULTS

3.1 Introduction

This chapter discusses the binder testing results on the blended binders extracted from the seven mixes, including extracted binders from the mixes sampled during JMF verification and extracted binders from the two samples from each mix during construction QA. Summary plots are presented in the text, while more detailed, tabulated results are available in the UCPRC online laboratory testing system (OLTS). It should be noted that binder extracted from mixes results in complete blending of the virgin binder, RAP binder, and recycling agent and that this complete diffusion may not have occurred in the mix at the time of sampling.

3.2 Binder Testing Results for Job Mix Formula Verification Mix Samples

3.2.1 PG Grading

Table 3.1 summarizes the true grades of the binders at high, intermediate, and low temperatures at a non-standard 40 hours of PAV aging for the samples taken during JMF verification and during QA. JMF verification samples were only taken for Mix K (3/4" HMA with 25%), Mix L (30% RAP), Mix M (3/4" HMA with 35% RAP), Mix N (3/4" HMA with 40% RAP), Mix O (3/4" HMA with 25% RAP and 3% RAS), and Mix J (3/4" HMA with no RAP or RAS). Mix P (15% RAP) had been previously submitted for JMF verification because it is the mix that was used on the rest of the project outside of the test sections.

The continuous high temperature grade is defined as the temperature where the unaged binder's G*/sin(δ) value equals 1.00 kPa and the RTFO-aged binder's G*/sin(δ) value equals 2.20 kPa, whichever is the lower temperature. For the JMF verification and QA testing performed for the pilot project, the binder was extracted from a plant-produced mix, so there were no virgin binder test results for the blend. "Plant-produced" results are presented in place of RTFO-aged results. Intermediate temperature grading is defined as the temperature where the 20-hour PAV-aged binder G*×sin(δ) value equals the maximum allowable stiffness of 5,000 kPa, as specified in AASHTO M 320. The low temperature grading is defined as the highest of the following two temperatures using 20-hour PAV-aged binder: (1) the temperature where the creep stiffness (300 MPa) occurs or (2) the temperature where the lowest minimum allowable m-value (0.300) occurs.

The specification (Figure 2.6) calls for mixes with RAS or high RAP to comply with the project-specified PG binder. This can be interpreted as the binder must meet the project-specified grade of PG 64-28M. This would mean a binder that grades as a 70-28M would not be the same project-specified grade. However, a higher high temperature true grade indicates better rutting performance at high temperatures, which is the intent of the PG grading specification. Therefore, a second interpretation of meeting or exceeding the project-specified grade would qualify mixes that do not match the exact specification but instead meet or exceed it. Based on the second interpretation, the mixes meeting the specification are the control mix with no RAP or RAS (Mix J), the mix with 40% RAP aggregate replacement (Mix N), and the mix with 25% RAP and 3% RAS (Mix O). The mixes with 25%, 30%, and 35% RAP aggregate replacement (Mixes K, L, and M) did not meet the low temperature PG.

The JMF results in Table 3.1 and the plot of JMF results in Figure 3.1 show that Mix L (30% RAP) had the lowest high temperature true grade at 72.4°C and graded as a PG 70-22, Mix J (0% RAP) had the next lowest high temperature true grade at 72.9°C and graded as a PG 70-34, and Mixes K, M, and N (25% RAP, 35% RAP, and 40% RAP) had high temperature true grades of 73.8°C, 74.9°C, and 73.4°C and graded as a PG 70-22, PG 70-28, and PG 70-28, respectively. Mix O (25% RAP and 3% RAS) had the highest temperature true grade at 79.8°C and graded as a PG 76-28. Mix J (0% RAP), which was the control mix, used a PG 64-28M based binder and all other RAS or high RAP mixes used a PG 58 base binder with recycling agent. The RA worked to varying degrees within each mix design. The mixes with the highest binder replacement, Mix N (40% RAP) and Mix O (25% RAP and 3% RAS), both meet or exceed the binder specification of PG 64-28. The UCPRC did not evaluate the elastic recovery of the extracted binders to verify modification. The control Mix J (0% RAP) also met or exceeded the PG 64-28 specification.

As shown in the Table 3.1 JMF verification results and Figure 3.1, the control Mix J binder had the lowest average true grade low temperature of -35.5°C, followed by Mix O (25% RAP and 3% RAS), Mix N (25% RAP and 3% RAS), and Mix M (35% RAP) at -28.8°C, -28.7°C, and -28.6°C. Mix K (25% RAP) and Mix L (30% RAP) had true grade low temperatures of -27.3°C, -27.0°C, respectively, which do not meet the low temperature binder specification of -28°C by 1.0°C or less, but meet the low temperature PG when considering the precision and bias of the test method. Additional aging using 40 hours of PAV aging, shown in Figure 3.2, the ranking for the low temperature true grade with rank order lowest to highest are Mix J (0% RAP), Mix M (35% RAP), Mix N (40% RAP), Mix L (30% RAP), Mix K (25% RAP), and Mix O (25% RAP and 3% RAS).

For the intermediate temperature true grade, Table 3.1 JMF verification results and Figure 3.1 show that the results are similar, with rank order from softest to stiffest: (1) Mix J (0% RAP) at 6.1°C, (2) Mix O (25% RAP and 3% RAS) at 13.2°C, (3) Mix L (30% RAP) at 15.5°C, (4) Mix N (40% RAP) at 16.3°C, (5) Mix K (25% RAP) at 16.4°C, and (6) Mix M (35% RAP) at 17.5°C. The difference in intermediate temperature grade between all mixes with RAS or high RAP is 4.3°C. The virgin control Mix J (0% RAP) was 7.1°C softer than the softest RAS or high RAP mix and had a true grade intermediate PG of 6.1°C. Regardless, all mixes were well below the Caltrans modified binder specification of a 22°C intermediate temperature PG. Additional aging using 40 hours of PAV aging, shown in Figure 3.2, did not change the rankings much for the low temperature PG but showed more effect of the additional aging on the high RAP/RAS mix extracted binders than the control mix extracted binder.

For thin overlays, less than about 0.2 to 0.25 ft. (60 to 75 mm) thick, softer binders at intermediate temperatures will tend to provide longer fatigue and reflective cracking lives. The opposite is true as overlay or new asphalt layer thicknesses increase above about 0.2 to 0.25 ft., with stiffer binders generally providing increasingly better fatigue and reflective cracking lives as the thickness increases. These results indicate similar performance for all mixes with high RAP and/or RAS, assuming that the binders become fully blended in the mix. These results indicate slightly better intermediate performance of the virgin control mix. Additional aging using 40 hours of PAV aging, shown in Figure 3.2, did not change the rankings much for the intermediate temperature PG but showed more effect of the additional aging on the high RAP/RAS mix extracted binders than the control mix extracted binder.

The average Delta T_c results for 20-hour and 40-hour PAV-aged specimens can be seen in Table 3.1 and Figure 3.3 for the JMF samples. All results failed to meet a specification requirement of ≥-5°C. Based on a review of the FHWA technical brief about the Delta T_c binder specification parameter *(13)*, a traditional PG specification is not applicable to polymer-modified binders because it does not adequately account for the unique rheological properties imparted by polymers. These binders exhibit different aging characteristics, viscosity-temperature relationships, and creep recovery behaviors compared with neat asphalt, necessitating alternative specifications tailored to modified binder performance attributes. An appropriate Delta T_c specification value and aging level for Caltrans modified binder are not known at this time.

Control Mix J (0% RAP) had the lowest Delta T_c values and was lower than any of the mixes with high RAP/RAS, indicating that its low temperature performance is controlled more by stiffness than creep, which is considered an indication of lower performance with regard to long-term age-related low temperature and block cracking, according to the literature. The mixes with RAS or high RAP still had relatively low Delta T_c values ranging from -6.1°C to -11.2°C. Additional PAV aging to 40 hours to simulate very long-term aging performance showed that Mix L (30% RAP) had a Delta T_c value of -15.7°C and theoretically will suffer the most from the detrimental effects of very long-term aging, while all other mixes still have relatively low Delta T_c values ranging from -10.8°C to -15.0°C.

Figure 3.4 shows PG true grade temperatures normalized to those of Mix J (0% RAP) for 20-hour PAV aged samples, showing that the high RAP/RAS mixes had slightly stiffer high temperature true grades, slightly stiffer low temperature true grades, and much stiffer intermediate temperature true grades (for this thin overlay application). The degree of asphalt binder stiffness is controlled by the combination of the virgin binder, binder reclaimed from the RAP, binder reclaimed from the RAS, and RA. Assuming these are 100% blended, the RAP and RAS reclaimed binder PG is consistent, and the ratios of these products do not change outside normal production tolerances, the stiffness of the combined binder is controlled by the dosage of RA. Possibly, a higher dosage of RA could have been used as there are 15.8°C to 8.4°C of potential high temperature stiffness reductions, and the low temperature stiffness demands -1°C of softening for Mix L (30% RAP) and 0.7°C of softening for Mix K (25% RAP) to meet the PG 64-28M specification.

Figure 3.5 shows similar results, except the PG true grade temperatures are normalized to those of Mix J for 40-hour PAV aging. The results show that there is less difference between the true grades of the mixes with RAP and the mix with RAP and RAS and the control mix with no RAP or RAS after 40-hours of PAV aging than there was for the 20-hour PAV aging. This result is expected and indicates that there is more potential for aging of the control mix, when it starts without PAV aging, than when the control has been 20-hour PAV aged. All binders have a finite capacity, and, as further aging is applied, the changes in properties (in this case PG true grade temperature) with additional aging diminish.

Table 3.1. Continuous Binder Grading Results for JMF Verification Samples

Mix Sample	Sample Type	PG Grade (20-Hour)	PG Grade (40-Hour)	PG True Grade (20-Hour PAV)[a]	ΔTc (°C) (20-Hour)	PG True Grade (40-Hour PAV)	ΔTc (°C) (40-Hour)	ΔTc (°C) (Change from 20-Hour to 40-Hour)
Mix J (PG 64-28M, 0% RP, 0% RS, 0% RA)	JMF (post plant extracted)	PG 70-34	PG 70-28	72.9-35.5 (6.1)	-8.1	72.9-30.2 (8.7)	-13.4	5.3
Mix K (PG 58-34M, 25% RP, 0% RS, 1.0% RA)	JMF (post plant extracted)	PG 70-22	PG 70-22	73.8-27.3 (16.4)	-10.1	73.8-22.1 (19.6)	-12.6	2.5
Mix L (PG 58-34M, 30% RP, 0% RS, 1.0% RA)	JMF (post plant extracted)	PG 70-22	PG 70-22	72.4-27 (15.5)	-11.2	72.4-22.6 (17.7)	-15.7	4.5
Mix M (PG 58-34M, 35% RP, 0% RS, 1.5% RA)	JMF (post plant extracted)	PG 70-28	PG 70-22	74.9-28.6 (17.5)	-6.1	74.9-23.5 (21.2)	-10.8	4.7
Mix N (PG 58-34M, 40% RP, 0% RS, 1.5% RA)	JMF (post plant extracted)	PG 70-28	PG 70-22	73.4-28.7 (16.3)	-9.5	73.4-23.5 (23.2)	-10.9	1.4
Mix O (PG 58-34M, 25% RP, 3% RS, 1.5% RA)	JMF (post plant extracted)	PG 76-28	PG 76-16	79.8-28.8 (13.2)	-9.1	79.8-19.7 (21.7)	-15.0	5.9

[a] Also known as continuous grade (CG), shown as [high temperature, low temperature, (intermediate temperature)].

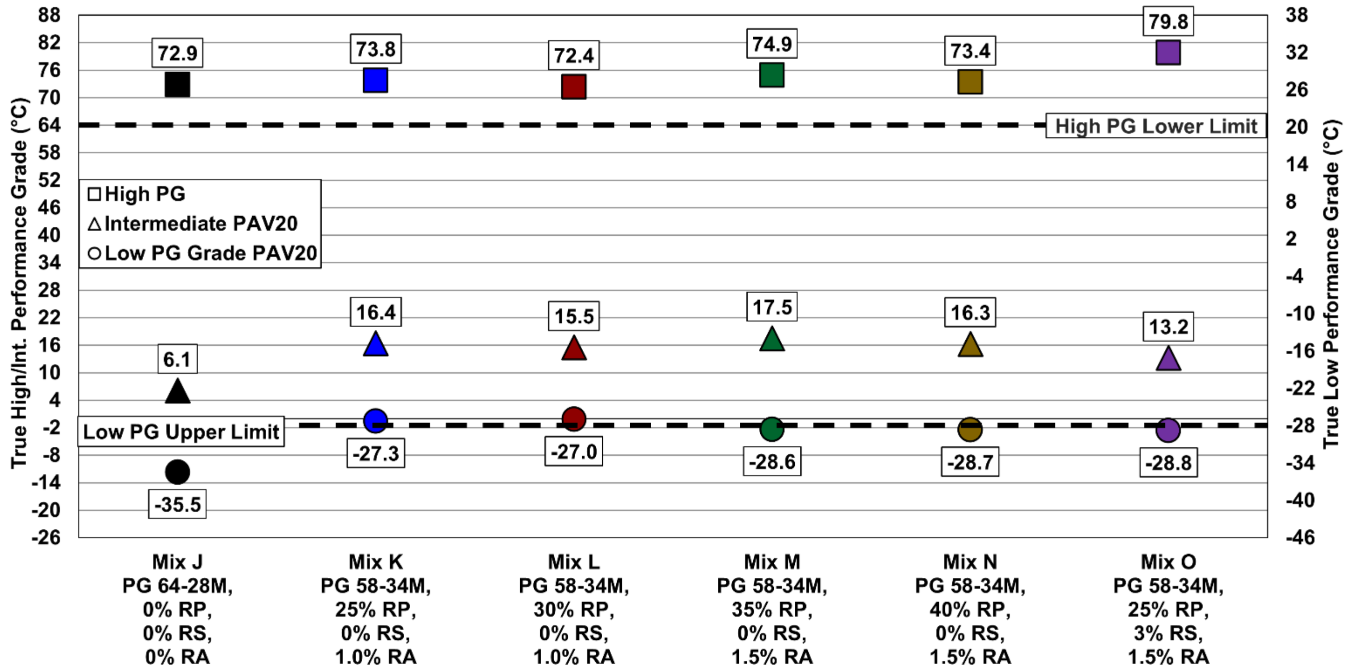

Figure 3.1: Continuous temperature binder grades for JMF verification sampled binders, 20-hour PAV.

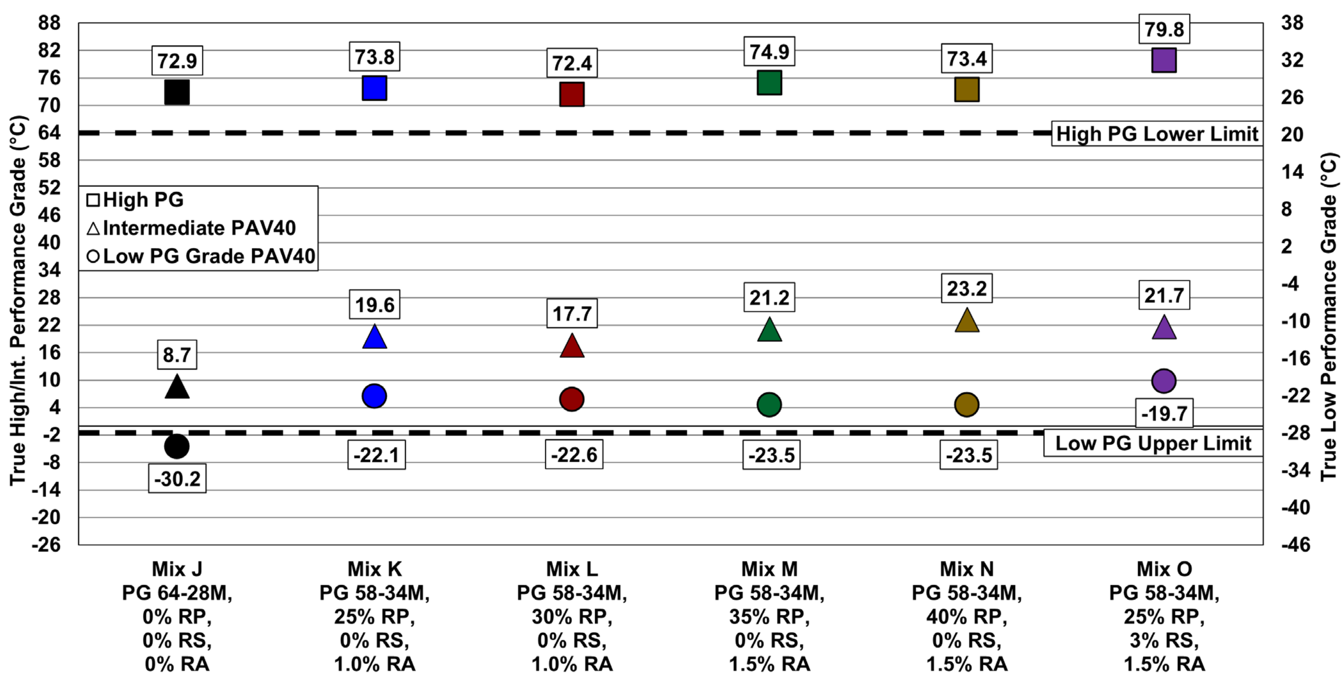

Figure 3.2: Continuous temperature binder grades for JMF verification sampled binders, 40-hour PAV.

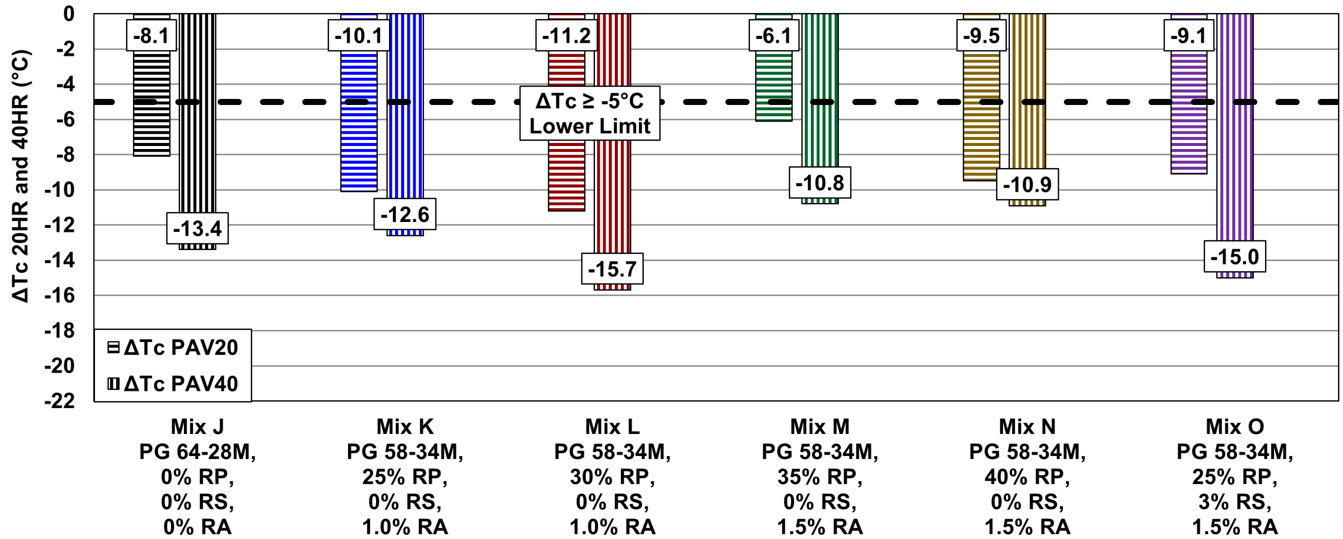

Figure 3.3: Delta Tc values for JMF samples (20-hour and 40-hour PAV specification values).

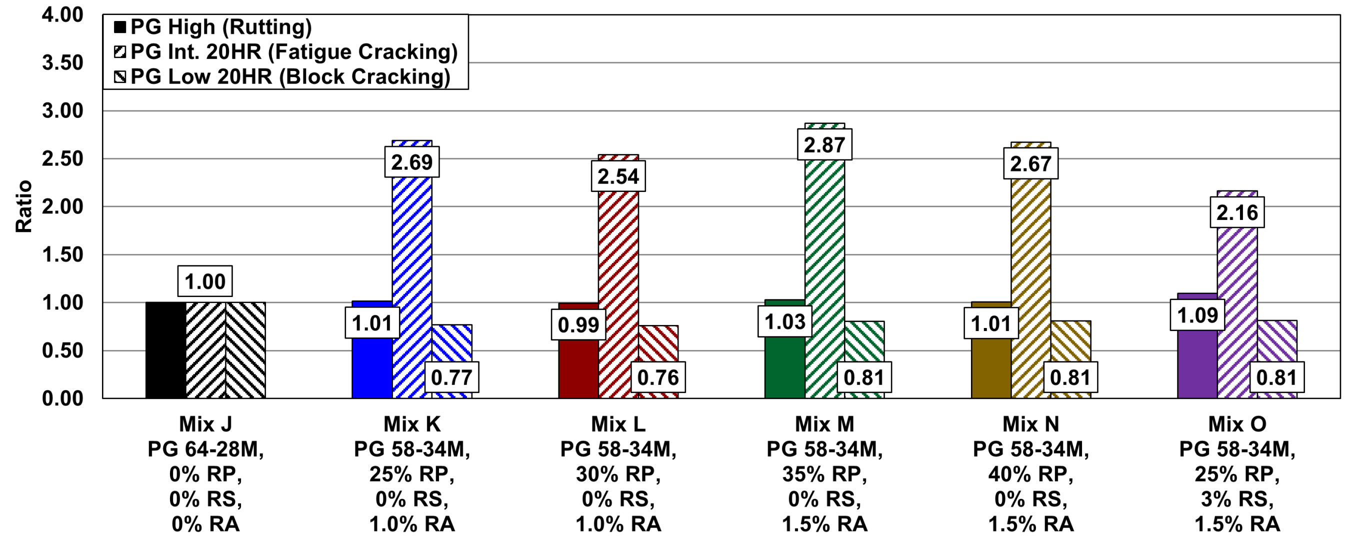

Figure 3.4: Binder grades for JMF verification sampled binders normalized to Mix J (0% RAP, 0% RAS) control mix, 20-hour PAV.

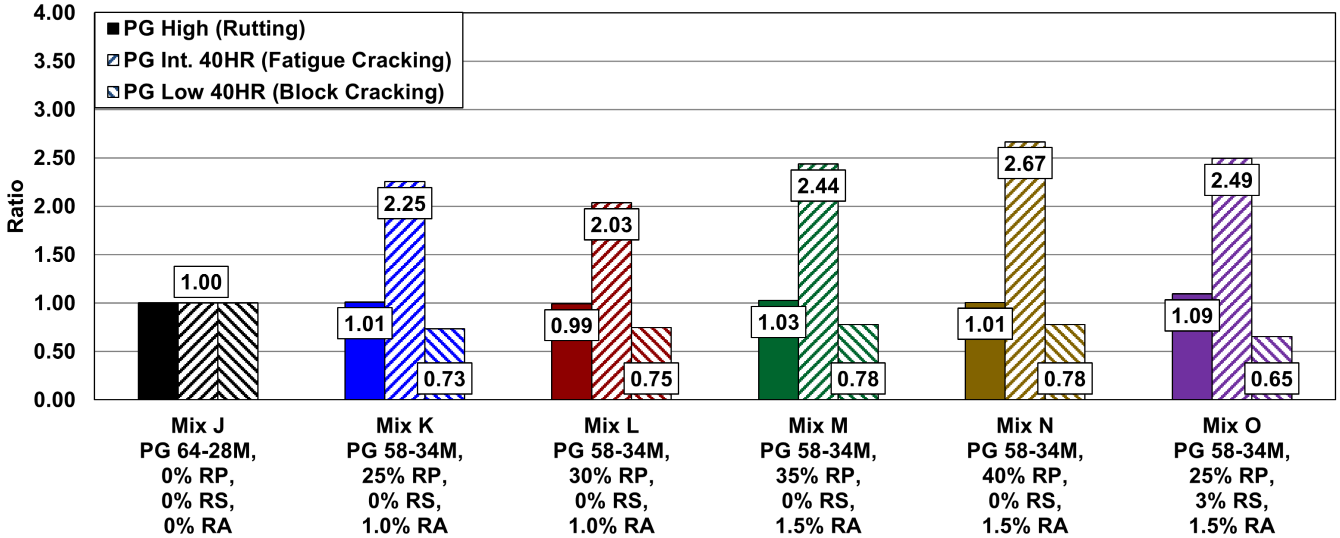

Figure 3.5: Binder grades for JMF verification sampled binders normalized to Mix J (0% RAP, 0% RAS) control mix, 40-hour PAV.

3.2.2 Frequency Sweep

Frequency sweep testing was not performed on JMF verification sampled binders.

3.2.3 Fourier Transform Infrared Spectroscopy Testing

Fourier transform infrared (FTIR) spectroscopy testing was not performed on JMF verification sampled binders.

3.3 Binder Testing Results from Quality Assurance Mix Samples

3.3.1 PG Grading

Table 3.2 and Figure 3.6 show that the true grade temperatures were consistent between the two QA samples. The one exception is the intermediate temperature for Mix L (30% RAP), which may be a testing anomaly considering that the 40-hour PAV aging results are consistent between the two sublots. Table 3.3 shows that the PG 64-28M binder used in the control mix with no RAP or RAS (Mix J) and in the mainline mix with 15% RAP (Mix P) sampled during QA met specifications for the low temperature PG (-28°C) and exceeded the 64°C specifications for the high temperature PG, classifying as a PG 70-28. All of the high RAP mixes and the RAP/RAS mix (Mixes K, L, M, N, O) met the high and intermediate temperature requirements, but both QA samples of Mix N and Mix O (40% RAP and 15% RAP/3% RAS) and one sample of Mix L and Mix M (30% RAP and 35% RAP) missed the low temperature requirements by 1.5°C to 3.1°C.

Table 3.2. Continuous Binder Grading Results for JMF Verification and QA Samples

Mix Sample	Sample Type	PG Grade (20-Hour)	PG Grade (40-Hour)	PG True Grade (20-Hour PAV)[a]	ΔTc (°C) (20-Hour)	PG True Grade (40-Hour PAV)[a]	ΔTc (°C) (40-Hour)	ΔTc (°C) (Change from 20-Hour to 40-Hour)
Mix J (PG 64-28M, 0% RP, 0% RS, 0% RA)	JMF	PG 70-34	PG 70-28	72.9-35.5 (6.1)	-8.1	72.9-30.2 (8.7)	-13.4	5.3
Mix K (PG 58-34M, 25% RP, 0% RS, 1.0% RA)	JMF	PG 70-22	PG 70-22	73.8-27.3 (16.4)	-10.1	73.8-22.1 (19.6)	-12.6	2.5
Mix L (PG 58-34M, 30% RP, 0% RS, 1.0% RA)	JMF	PG 70-22	PG 70-22	72.4-27 (15.5)	-11.2	72.4-22.6 (17.7)	-15.7	4.5
Mix M (PG 58-34M, 35% RP, 0% RS, 1.5% RA)	JMF	PG 70-28	PG 70-22	74.9-28.6 (17.5)	-6.1	74.9-23.5 (21.2)	-10.8	4.7
Mix N (PG 58-34M, 40% RP, 0% RS, 1.5% RA)	JMF	PG 70-28	PG 70-22	73.4-28.7 (16.3)	-9.5	73.4-23.5 (23.2)	-10.9	1.4
Mix O (PG 58-34M, 25% RP, 3% RS, 1.5% RA)	JMF	PG 76-28	PG 76-16	79.8-28.8 (13.2)	-9.1	79.8-19.7 (21.7)	-15.0	5.9
Mix J (PG 64-28M, 0% RP, 0% RS, 0% RA)	QA Sample 1 (SL1)	PG 70-34	PG 70-22	72.1-35.3 (4.7)	-9.8	72.1-27.8 (8.5)	-18.5	8.7
Mix J (PG 64-28M, 0% RP, 0% RS, 0% RA)	QA Sample 2 (SL2)	PG 70-34	PG 70-28	70.2-36.5 (4.1)	-9.1	70.2-31.4 (7.7)	-13.8	4.7
Mix P (PG 64-28M, 15% RP, 0% RS, 0% RA)	QA Sample 1 (SL1)	PG 70-28	PG 70-22	72.5-30.5 (8.2)	-9.4	72.5-23.3 (12.6)	-19.2	9.8
Mix K (PG 58-34M, 25% RP, 0% RS, 1.0% RA)	QA Sample 1 (SL1)	PG 70-28	PG 70-22	73.6-30.8 (13.9)	-8.1	73.6-22.7 (17.5)	-16.8	8.7
Mix K (PG 58-34M, 25% RP, 0% RS, 1.0% RA)	QA Sample 2 (SL2)	PG 70-28	PG 70-22	72.7-29.2 (15.1)	-9.5	72.7-24.6 (16.5)	-13.0	3.5
Mix L (PG 58-34M, 30% RP, 0% RS, 1.0% RA)	QA Sample 1 (SL1)	PG 70-22	PG 70-16	75.0-30.8 (15.7)	-10.3	75.0-20.7 (20.0)	-17.5	7.2
Mix L (PG 58-34M, 30% RP, 0% RS, 1.0% RA)	QA Sample 2 (SL2)	PG 76-22	PG 76-16	77.1-26.1 (17.0)	-9.9	77.1-20.8 (20.0)	-15.8	5.9
Mix M (PG 58-34M, 35% RP, 0% RS, 1.5% RA)	QA Sample 1 (SL1)	PG 76-28	PG 76-16	77.7-28.2 (17.8)	-6.7	77.7-20.5 (21.2)	-18.5	11.8
Mix M (PG 58-34M, 35% RP, 0% RS, 1.5% RA)	QA Sample 2 (SL2)	PG 76-22	PG 76-16	79.9-25.3 (19.0)	-9.5	79.9-19.0 (23.7)	-13.2	3.7
Mix N (PG 58-34M, 40% RP, 0% RS, 1.5% RA)	QA Sample 1 (SL1)	PG 76-22	PG 76-16	79.3-26.5 (20.4)	-6.8	79.3-20.1 (24.0)	-12.1	5.3

Mix Sample	Sample Type	PG Grade (20-Hour)	PG Grade (40-Hour)	PG True Grade (20-Hour PAV)[a]	ΔTc (°C) (20-Hour)	PG True Grade (40-Hour PAV)[a]	ΔTc (°C) (40-Hour)	ΔTc (°C) (Change from 20-Hour to 40-Hour)
Mix N (PG 58-34M, 40% RP, 0% RS 1.5% RA)	QA Sample 2 (SL2)	PG 70-22	PG 70-16	75.0-27.1 (19.5)	-9.0	75.0-20.9 (22.5)	-13.1	4.1
Mix O (PG 58-34M, 25% RP, 3% RS, 1.5% RA)	QA Sample 1 (SL1)	PG 82-22	PG 82-16	82.3-26.3 (15.1)	-11.5	82.3-17.4 (20.1)	-20.5	9.0
Mix O (PG 58-34M, 25% RP, 3% RS, 1.5% RA)	QA Sample 2 (SL2)	PG 82-22	PG 82-16	82.1-25.0 (18.2)	-11.8	82.1-19.7 (19.1)	-17.6	5.8

[a] Also known as continuous grade (CG), shown as [high temperature, low temperature, (intermediate temperature)].

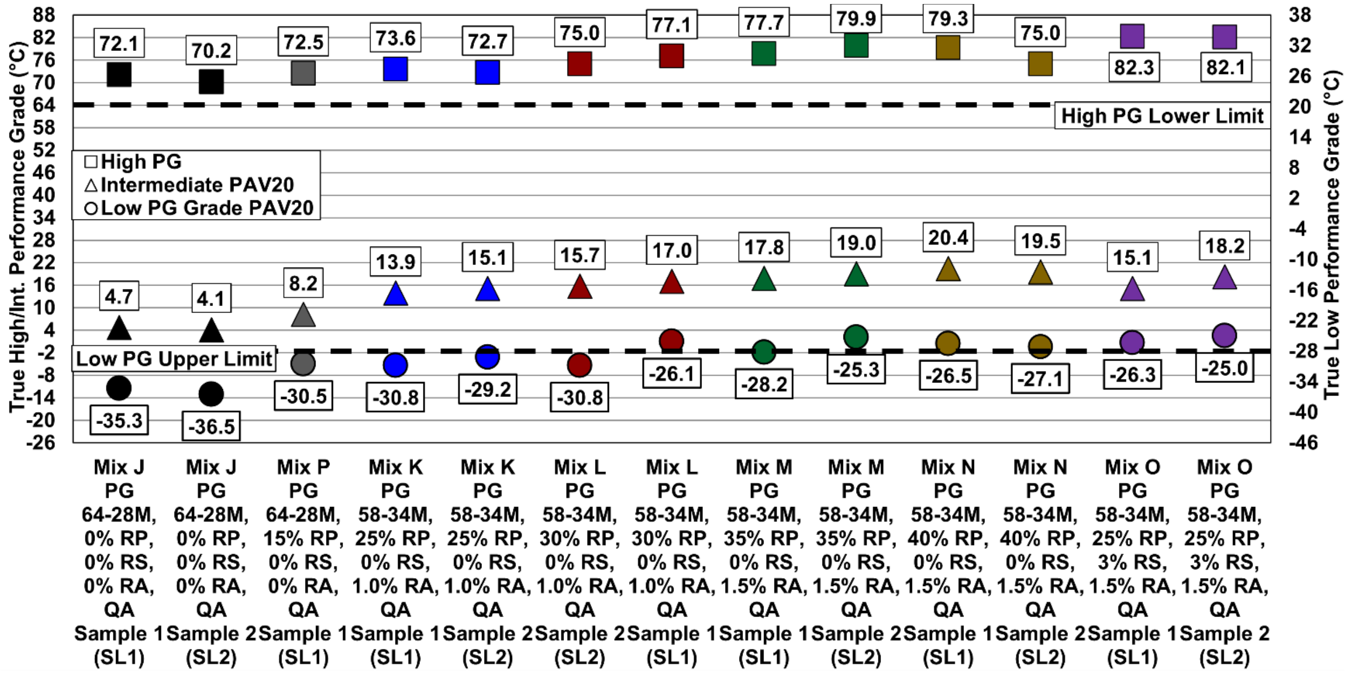

Figure 3.6: Continuous temperature binder grades for QA-sampled binders by sample, 20-hour PAV.

Table 3.3. Continuous Binder Grading Results for QA Tank Binder PG 64-28M

Binder ID	PG Grade (20-Hour)	PG Grade (40-Hour)	PG True Grade (20-Hour PAV)[a]	ΔTc (°C) (20-Hour)	PG True Grade (40-Hour PAV)[a]	ΔTc (°C) (40-Hour)	ΔTc (°C) (Change from 20-Hour to 40-Hour)
PG 64-28M Tank Binder	70-28	70-22	72.7-31.2 (6.9)	-12.4	72.7-26.6 (9.0)	-16.9	4.5

[a] Also known as continuous grade (CG), shown as [high temperature, low temperature, (intermediate temperature)].

Figure 3.7 shows the 40-hour PAV aging QA sublot results. Comparing the 20-hour and 40-hour PAV results, it can be seen that the rankings remained consistent for the low and intermediate temperature PGs that are controlled by PAV aging. It can also be seen that the change in low and intermediate true grade temperatures with additional aging was generally consistent across mixes and between QA sublots of each mix with a few cases where the effect of additional PAV aging was different between sublots (the low temperature PG for Mix O as an example).

Figure 3.8 shows average PG true grade results for the two QA samples for each mix type. The control Mix J (0% RAP, 0% RAS) binder had the lowest average true grade high temperature, followed by mainline Mix P (15% RAP), Mix L (30% RAP), Mix K (25% RAP), Mix N (40% RAP), Mix M (35% RAP), and Mix O (25% RAP, 3% RAS). The mixes with increasing RAP and RAP/RAS had higher average high binder true grade temperatures, indicating better resistance to rutting than the control Mix J, which had no RAP or RAS, and the mainline Mix P with 15% RAP and PG 64 virgin binder. The difference in high temperature grade between Mix J and Mix O is large, approximately 11°C. The standard error of

Mix L (30% RAP) between sublot 1 and 2 falls within the low temperature true grade of Mix K (25% RAP), which may be due to the previously mentioned testing anomaly.

None of the mixes or sublots met the high temperature PG specification of not exceeding a true grade of 70°C. The intention of the specification was to limit the high binder true grade temperatures of the mixes with increasing percentages of RAP and RAP/RAS to limit their stiffness at intermediate and low temperatures, though a higher high binder true grade temperature indicates better rutting performance at high temperatures. These results indicate that the recycling agent dosage may have been somewhat too low as RAP and RAP/RAS content increased in the mix. Previous pilot projects have found that selecting the correct recycling agent dose for the percent RAP content can match within one binder grade of the control mix *(14,15)*. Mix J and Mix O show a grade bump two grades higher than the control (PG 70 versus PG 82). These findings suggest that the target 1.5% RA dosage was an inadequate design for Mix O to match the high PG of Mix J. However, as noted several times, keeping the high temperature PG from increasing compared to the control results in greater rutting risk and should be unnecessary as long as the intermediate and low temperature PGs are not allowed to increase.

For the intermediate binder true grade temperatures, Table 3.1 and Figure 3.8 show that the rank order from softest to stiffest binder is Mix J, Mix P, Mix K, Mix L, Mix O, Mix M, and Mix N. The difference in intermediate temperature grade between Mix J and Mix N is significant, at approximately 17°C. A lower intermediate binder true grade temperature indicates that the mix will be softer at intermediate temperatures, which, for thin overlays such as those on this pilot project, will often produce better fatigue and reflective cracking resistance. These results indicate that Mixes P, K, L, M, N, and O with RAP and RAS may be expected to have worse age-related fatigue and reflective cracking resistance than the control Mix J when used in thin asphalt layers.

Figure 3.8 shows that the ranking for average low temperature from lowest (coldest) true grade to highest (softest to stiffest binder) is Mix J, Mix P, Mix K, Mix L, Mix N, and Mix O. These results indicate that the binders with RAP and RAS were stiffer or had less creep compliance at low temperatures than the virgin binder (Mix J) and the mainline mix (Mix P), which is undesirable for low temperature and age-related block cracking. The difference in the low temperature true grade of Mix J and Mix O was high, approximately 10°C. These results again indicate that the RA doses may have been somewhat low for the mixes with 35% and 40% RAP (Mix M and Mix N) and the mix with 25% RAP and 3% RAS (Mix O). The average 40-hour PAV continuous temperature PGs shown in Figure 3.9 indicate consistent changes in true grade temperatures across all mixes.

The Delta T_c results for 20-hour and 40-hour PAV-aged specimens are shown in Figure 3.10 for the two QA samples and averaged in Figure 3.11 for the two QA samples. The results are more generally consistent between sublots for the 20-hour PAV values than for the 40-hour PAV results. Mix M (35% RAP) and Mix N (40% RAP) had more positive Delta T_c values than the other mixes, and the average order from least to most negative is Mix N (40% RAP), Mix M (35% RAP), Mix K (25% RAP), Mix P (mainline mix, 15% RAP), Mix J (control, no RAP), Mix L (30% RAP), and Mix O

(25% RAP/3% RAS). A less negative (more positive) Delta T_c value indicates that there is less difference between the critical stiffness temperature controlling the binder true grade temperature and the critical creep compliance temperature, which denotes better resistance to block cracking after long-term aging than does a more negative Delta T_c value. In this case, the results show an inconclusive result and do not appear to have a predictive ability for these mixes. The difference between Mix N and Mix O for the standard 20-hour PAV aging is small at 3°C, and approximately 7°C for the severe 40-hour PAV aging.

The binder test results from the QA samples showed that every mix performed worse than the minimum specified value of -5.0. As noted previously, research has shown that polymer-modified asphalt binder, such as the kind used during this pilot, tend to have highly negative Delta T_c performance but better age-related cracking performance than unmodified binders with better Delta T_c values.

Figure 3.12 summarizes the binder true grade temperatures normalized to the control Mix J. The results show that compared to the control mix, each mix had higher high binder true grade temperatures, indicating better rutting performance; higher intermediate binder true grade temperatures, indicating worse age-related cracking performance and worse fatigue and reflective cracking performance for thin overlays; and higher low binder true grade temperatures, indicating worse resistance to low temperature cracking. These results again indicate the drawbacks of attempting to limit intermediate and low temperature stiffness by limiting specified high temperature stiffness values. In future high RAP and RAP/RAS pilot experiments, recycling agent dosage design should set the target based on the control intermediate and low temperature PG, or at least one of those two values. Figure 3.13 summarizes the binder true grade temperatures for 40-hour PAV aging, affecting the intermediate and low temperature results, normalized to the control Mix J. The results indicate similar trends between mixes as for the 20-hour PAV results. The additional aging of 40-hour PAV made the low temperature true grade ratios compared with control Mix J worse than the 20-hour aging did, and the 40-hour intermediate true grade ratios compared with Mix J are better than the 20-hour PAV ratios.

Figure 3.14 compares the true grade temperatures of each mix blended with the PG 64-28M binder (two sublots of control Mix J and the one sublot of mainline Mix P) to the true grade temperatures of the PG 64-28M tank binder. The three QA mixes and the tank binder sample all graded one PG higher for high temperature while meeting the target low temperature PG. Based on the QA results of the PG 64-28M tank binder (Table 3.3), the binder provided by the supplier graded as a PG 70-28M. Despite the increased high temperature performance, all mixes met the minimum PG requirements at the intermediate and low temperatures. If both the intermediate and low temperature performance meet the specification target, the UCPRC recommends acceptance of the high temperature PG. Since the virgin binder already exceeded the specified high temperature PG, it is not clear how trying to get the high RAP/RAS mixes to meet the high temperature specified PG would work. Figure 3.15 shows similar results for the 40-hour PAV aging compared with the 20-hour PAV aging.

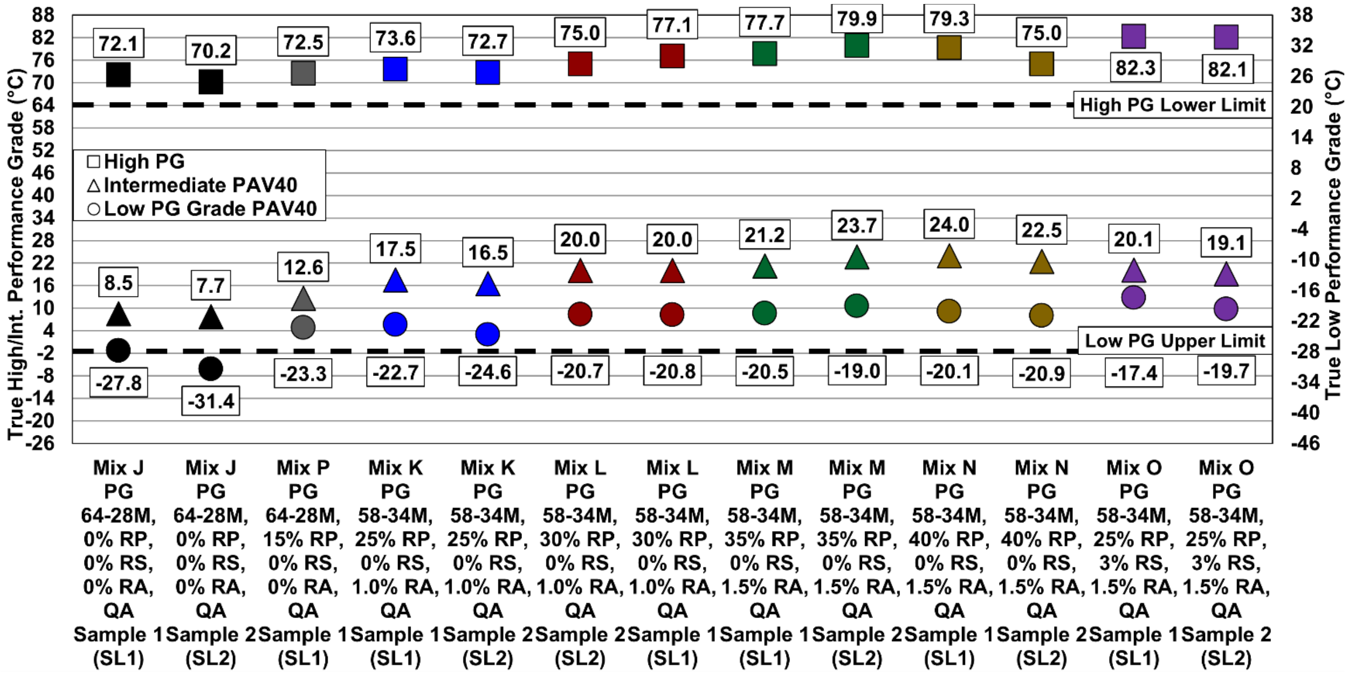

Figure 3.7: Continuous temperature binder grades for QA-sampled binders by sample, 40-hour PAV.

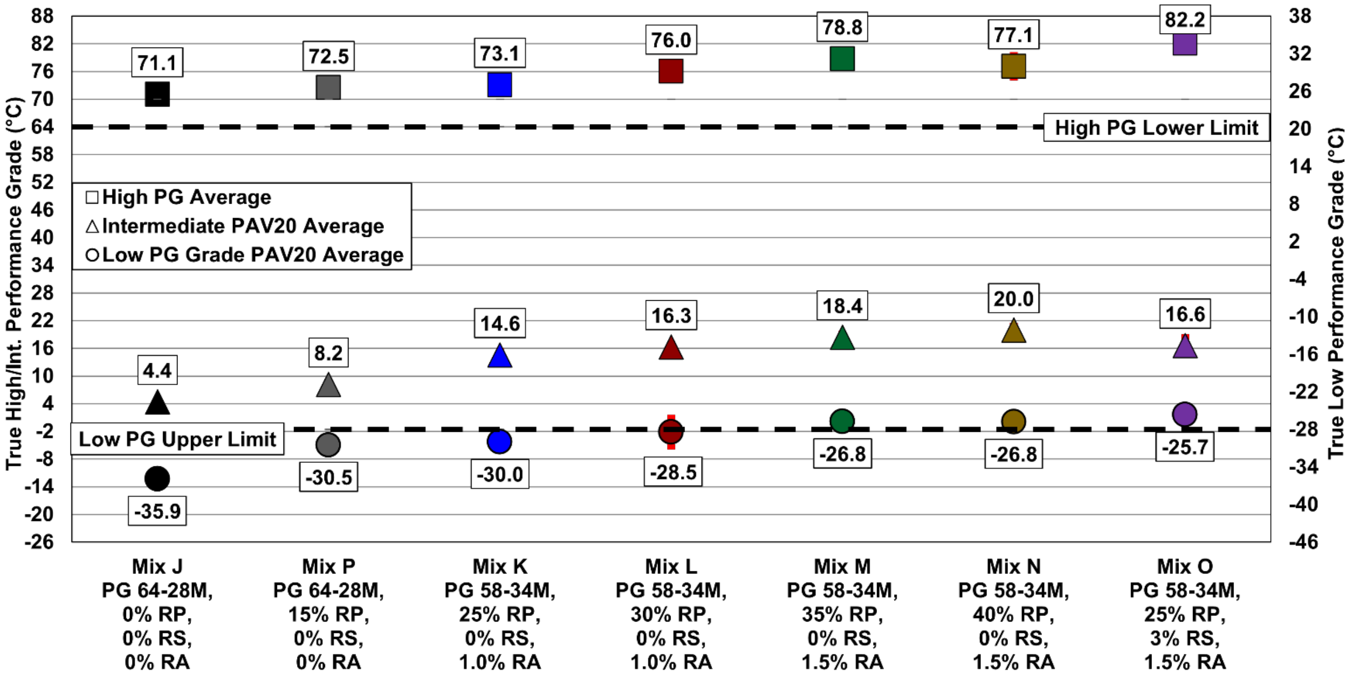

Figure 3.8: Average continuous temperature binder grades for QA-sampled binders, 20-hour PAV.

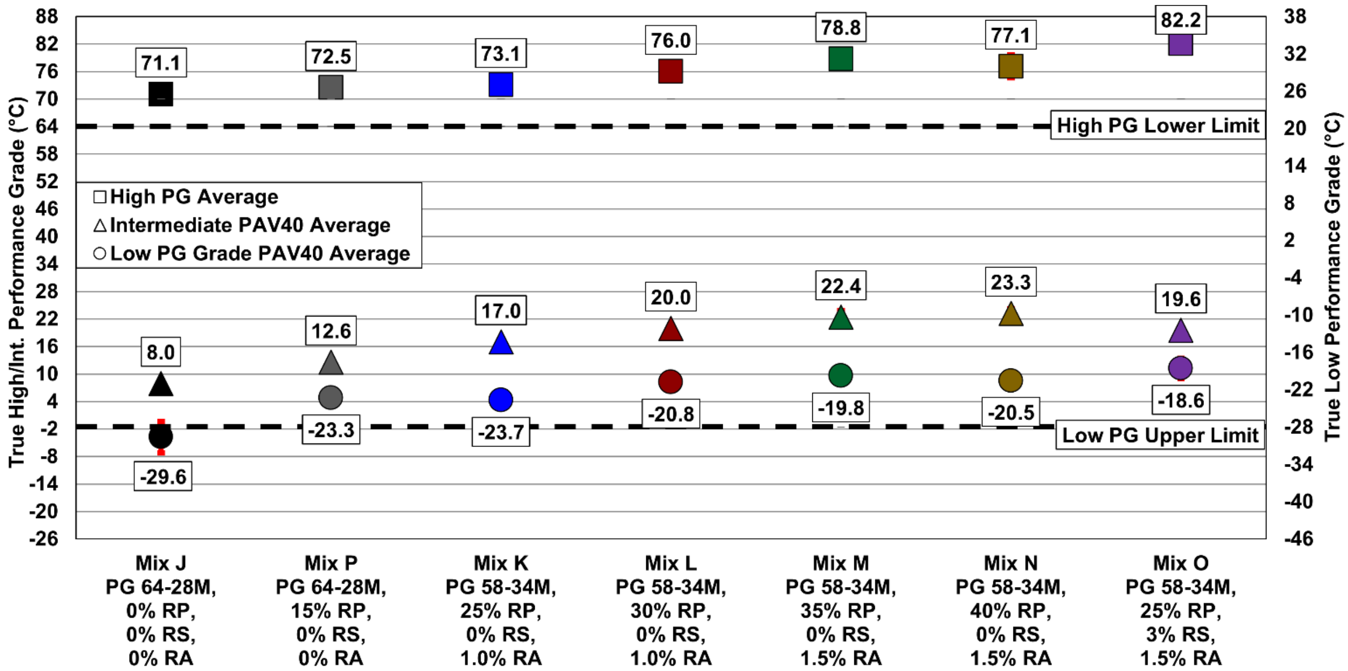

Figure 3.9: Average continuous temperature binder grades for QA-sampled binders, 40-hour PAV.

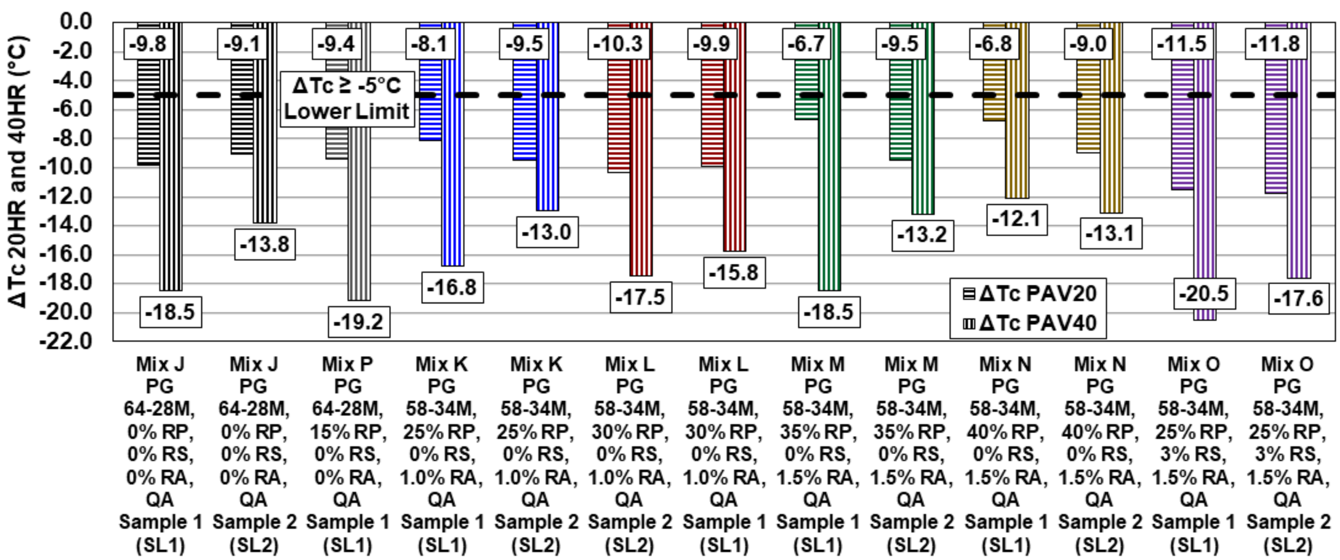

Figure 3.10: Delta T_c values by sample for both QA samples (20-hour PAV and 40-hour PAV specification values).

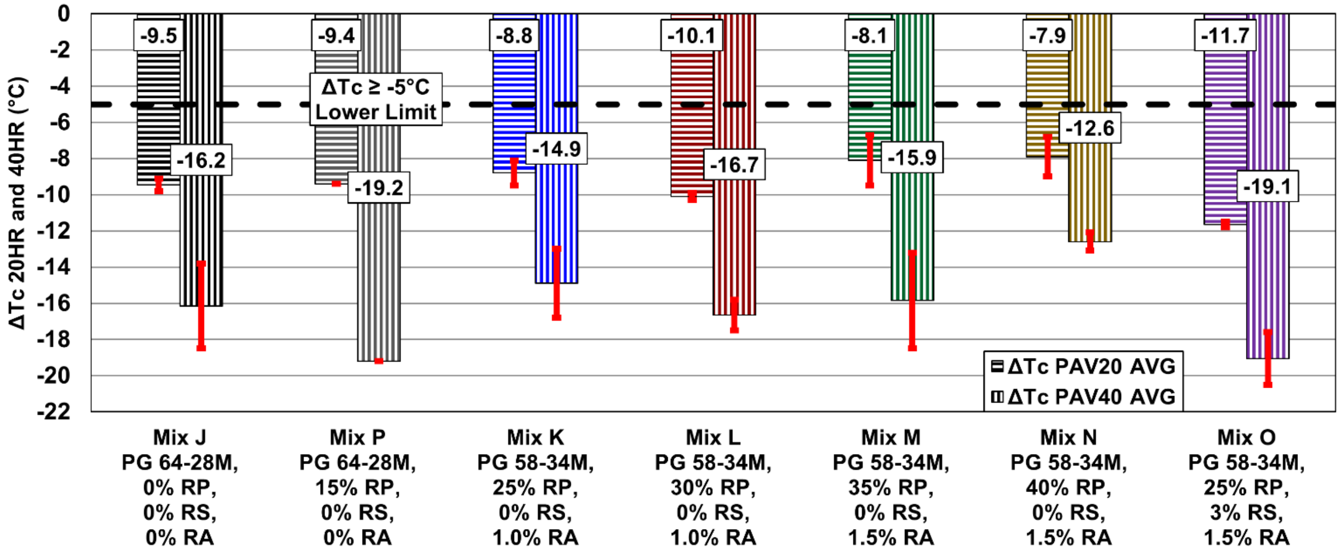

Figure 3.11: Average Delta T_c values for QA samples (20-hour PAV and 40-hour PAV specification values).

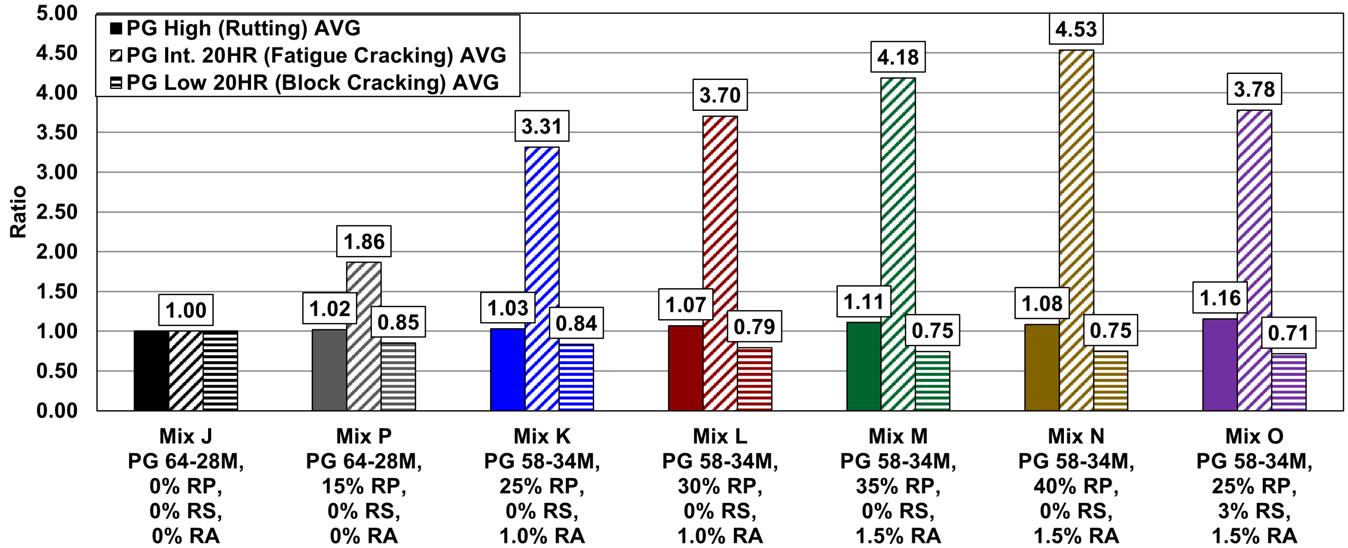

Figure 3.12: Average binder true grades for QA-sampled binders normalized to control Mix J (0% RAP, 0% RAS), 20-hour PAV.

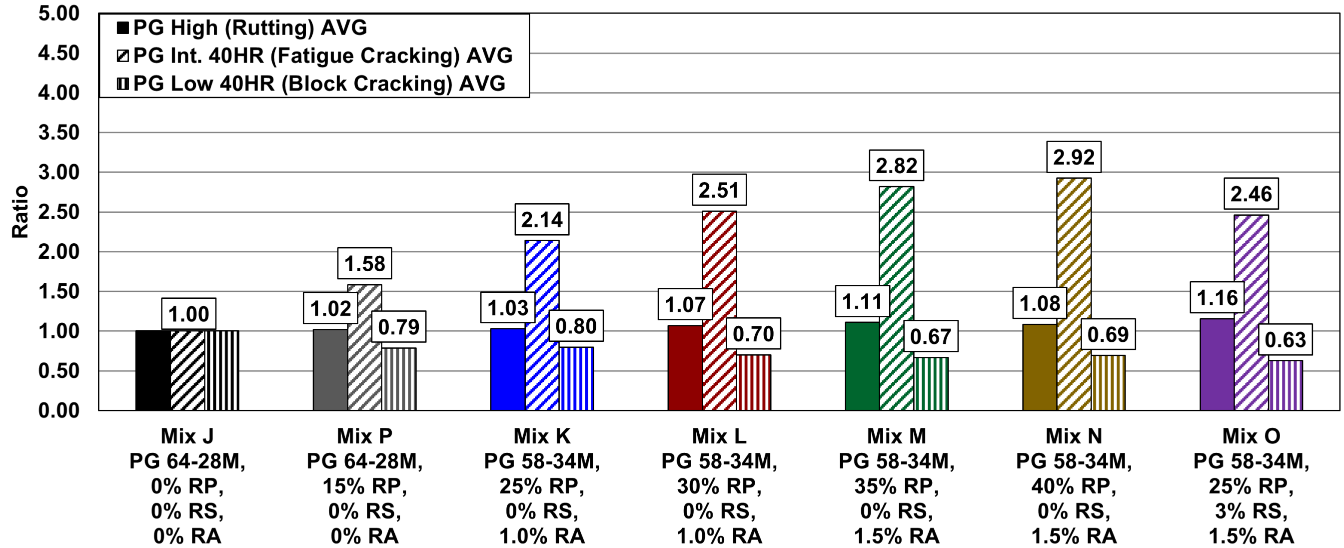

Figure 3.13: Average binder true grades for QA-sampled binders normalized to control Mix J (0% RAP, 0% RAS), 40-hour PAV.

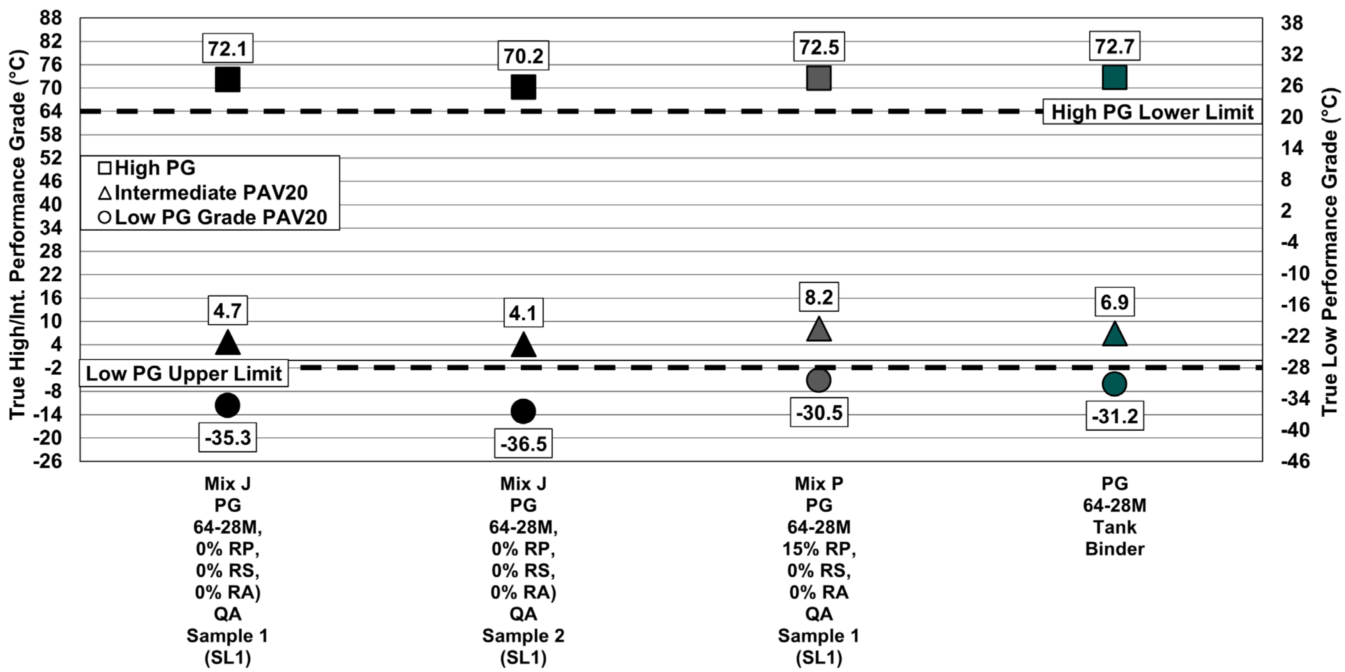

Figure 3.14: Binder grades for QA-sampled binders of Mix J (SL1), Mix J (SL2), Mix P (SL1), and PG 64-28M tank binder, 20-hour PAV.

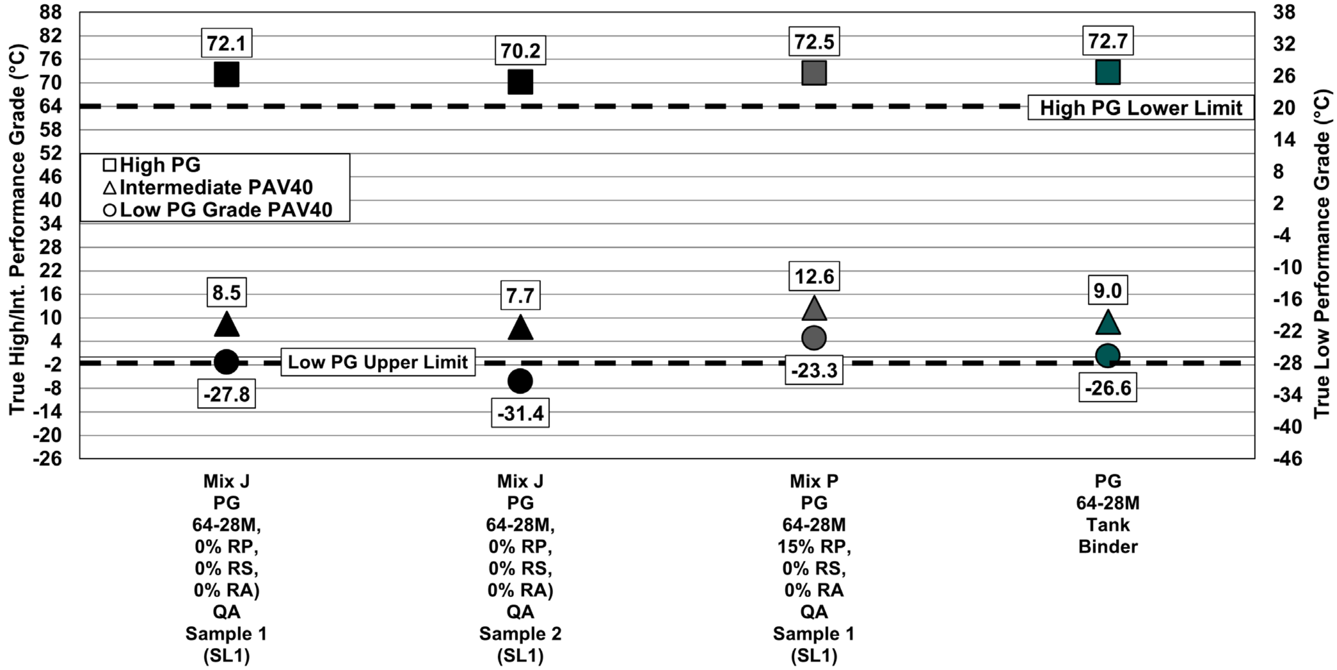

Figure 3.15: Binder grades for QA-sampled binders of Mix J (SL1), Mix J (SL2), Mix P (SL1), and PG 64-28M tank binder, 40-hour PAV.

3.3.2 Frequency Sweep

The average binder dynamic stiffness master curves from the first sublot of the QA-sampled materials are shown in Figure 3.16. The results are averages of two replicate tests. The results show that all the high RAP/RAS mix binders (Mixes K, L, M, N, O) were stiffer than the control mix with no RAP or RAS (Mix J) and the mainline mix with 15% RAP (Mix P). The extracted binders from three of the mixes—those with 25%, 30%, and 35% RAP (Mixes K, L, M)—had nearly identical master curves, stiffer than the control and mainline mix binders. The binder from the mix with 25% RAP and 3% RAS (Mix O) was slightly stiffer than Mixes K, L, and M at low reduced frequencies (slow loading) and high temperatures, and closer to those three at high reduced frequencies (faster loading) and low temperatures. The binder with 40% RAP (Mix N) showed the highest stiffness compared with other mixes at both low and high reduced frequencies.

Figure 3.17 shows binder stiffness versus reduced frequency for all RAP/RAS mixes normalized to the first sublot of control mix (Mix J) QA-sampled binder. As noted previously, Mix N, with 40% RAP and RA, showed much greater stiffness at all reduced frequencies. Therefore, Mix N is expected to show better rutting resistance than the control but poorer age-related and low temperature cracking performance. Mix O, with 25% RAP and 3% RAS, is expected to show better rutting performance but similar age-related and low temperature cracking resistance compared to the other high RAP mixes (Mixes K, L, M). The mainline mix with 15% RAP and no RA (Mix P) showed normalized binder dynamic modulus values that matched the control mix (Mix J) for most of the reduced frequencies, indicating similar performance compared with Mix J at all frequency levels.

Figure 3.18 shows a Black Space diagram (stiffness versus phase angle) with stiffness at a reduced temperature of 15°C and a reduced frequency of 8 (10^{-4}) Hz for three aging conditions: (1) plant mixed, (2) 20-hour PAV aged, and (3) 40-hour PAV aged. Imposed on the plot are the Glover-Rowe thresholds that have been identified to correlate with an increased risk of long-term aging-related block cracking *(16)*. The results show that the binder from the control mix (Mix J) and mix with 15% RAP (Mix P) have the least chance of block cracking, as indicated by the 40-hour PAV results for binders extracted from both mixes (Mixes J and P) plotting in the transition zone. The Glover-Rowe values observed after 40-hour PAV aging for all other mixes are in the block cracking zone (Figure 3.18), and for the 20-hour PAV aging, they are in the transition zone. The amount of recycling agent (1.0% to 1.5% by total weight of binder) added for the high RAP/RAS mixes may have been insufficient to match the age-related cracking resistance of the control mix or of the mainline mix.

The control mix (Mix J) with no RAP and the mainline mix (Mix P) with 15% RAP both use the same PG 64-28M virgin binder. It is interesting to note that although the mainline mix with RAP is stiffer compared with the control mix, as expected, its phase angles are higher than those of the control mix, which is unexpected. This finding indicates that the RAP binder may have had higher phase angles, indicating a greater ability to relax stress, which provides greater resistance to age-related cracking.

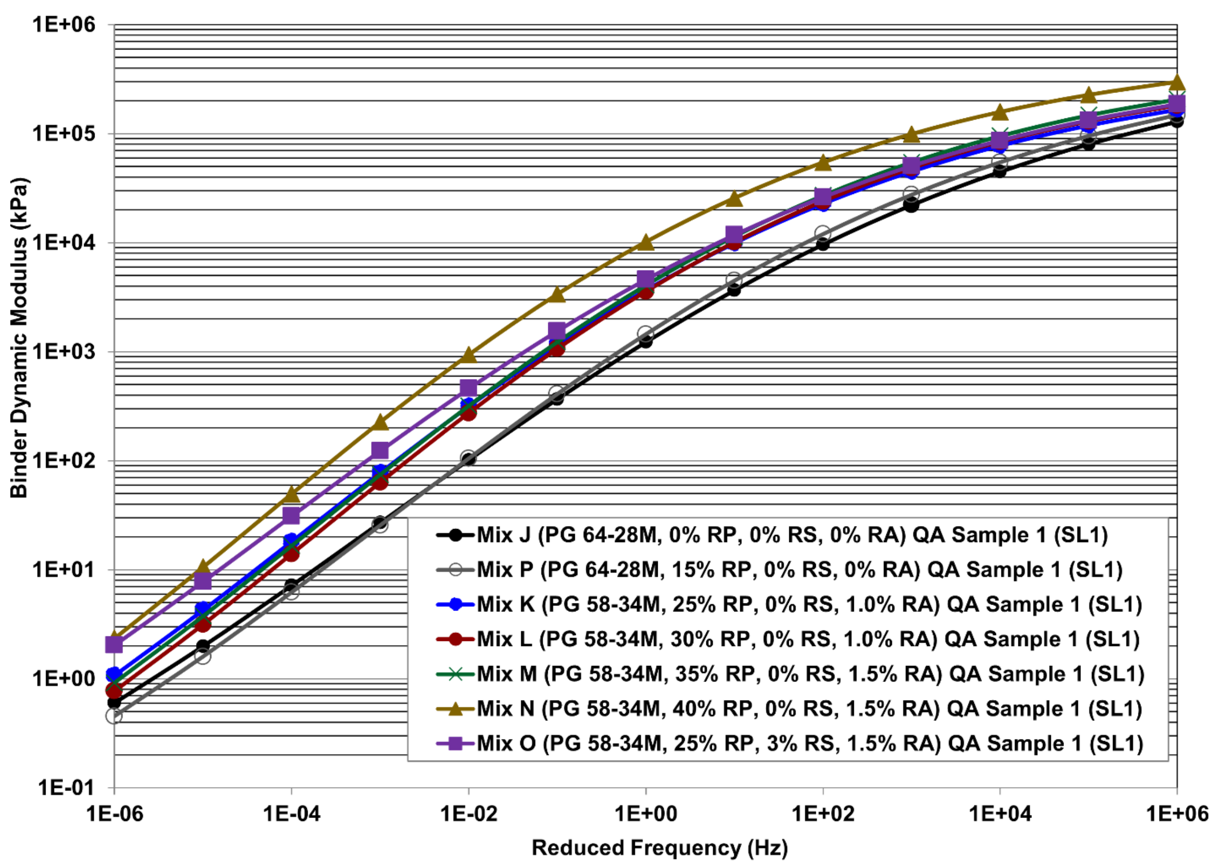

Figure 3.16: Frequency sweep master curves for plant-extracted first sublot (SL1) of QA-sampled binders.

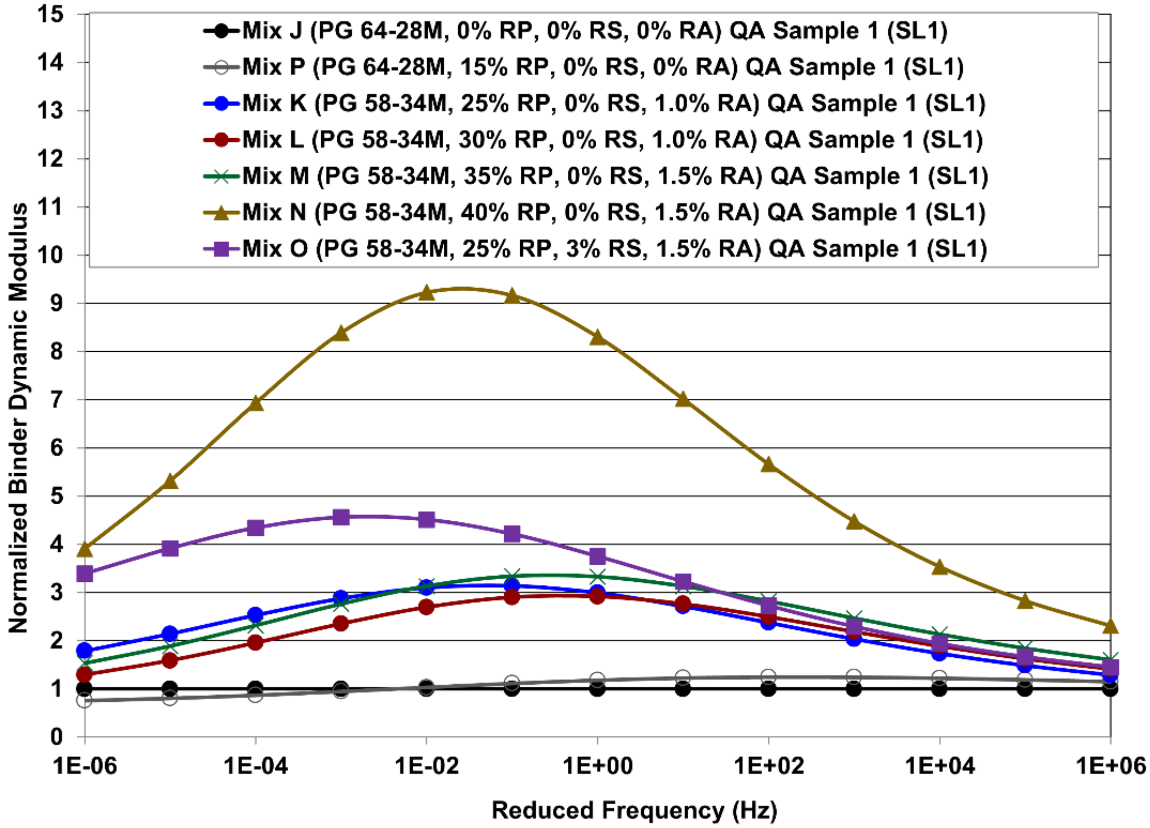

Figure 3.17: Frequency sweep master curves for plant-extracted first sublot (SL1) of QA-sampled binders normalized to Mix J (PG 64-28M, 0% RP, 0% RS, 0% RA).

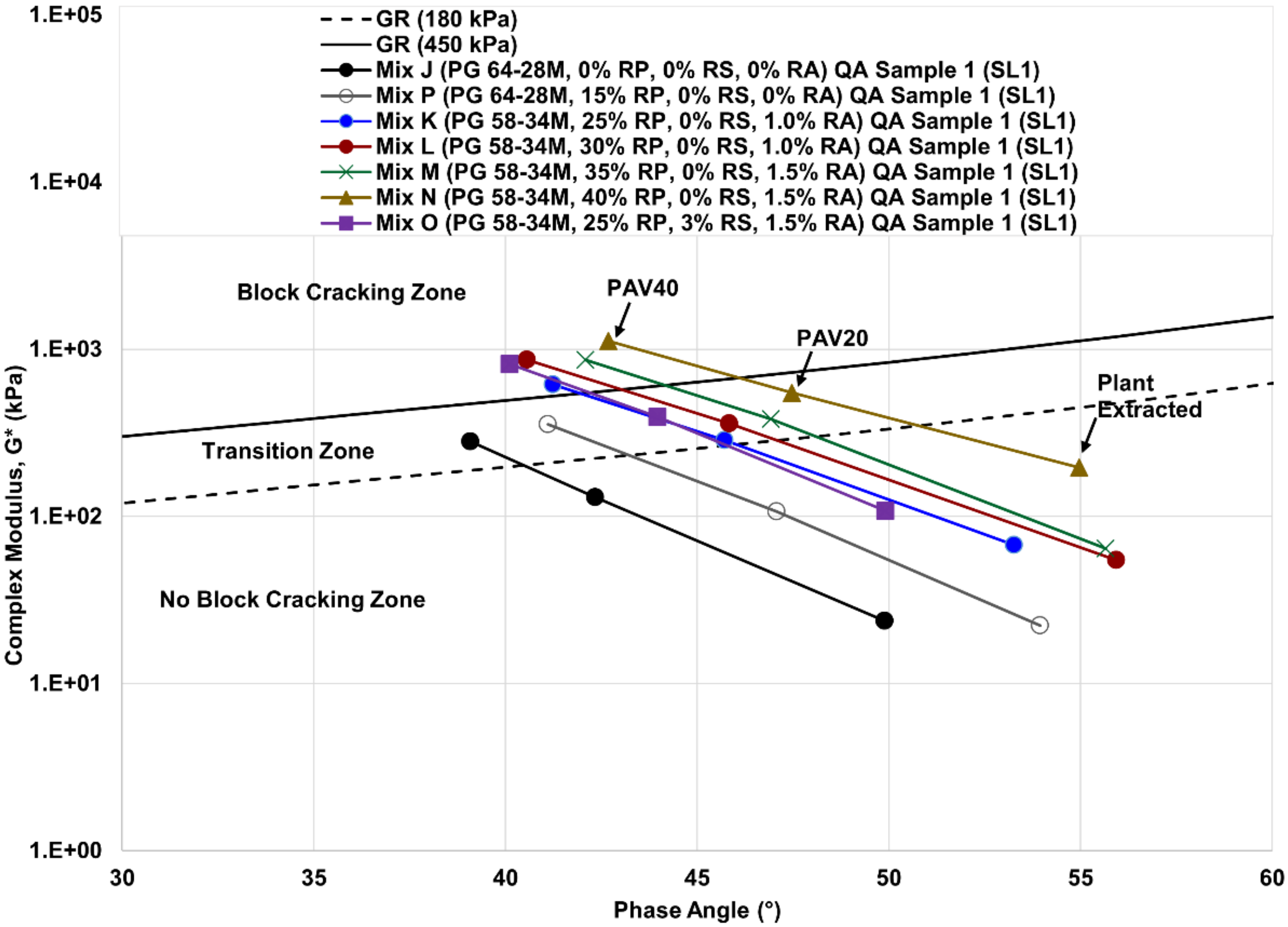

Notes: Plant-extracted: extracted and recovered binder from plant-produced mixes; PAV20: 20 hours of PAV aging of extracted and recovered binder from plant-produced mixes; PAV40: 40 hours of PAV aging of extracted and recovered binder from plant-produced mixes.

Figure 3.18: Black space plot for first sublot (SL1) of QA-sampled binders with Glover-Rowe (GR) criteria.

3.3.3 Fourier Transform Infrared Spectroscopy Testing

The QA-sampled binders were tested with Fourier transform infrared (FTIR) spectroscopy after plant mixing and 20-hour and 40-hour PAV aging. Figure 3.19 plots the carbonyl indices of the binders for these three conditions for both QA samples. The results show that the control mix, Mix J, had the least carbonyl (aging products) after plant mixing, followed by mainline Mix P, then the four high RAP mixes (Mixes K, L, O, and M), and then the mix with RAP and RAS (Mix N). The carbonyl contents increased with 20-hour PAV aging, and the results had same ranking for carbonyl content. After 40-hour PAV aging, the carbonyl indexes increased further and the ranking of carbonyl content from least to most changed slightly to Mix J, Mix P, Mix O, Mix L, Mix M, Mix K, and Mix N.

Figure 3.20 plots the sulfoxide indices for the mixes. The sulfoxide contents of the high RAP/RAS mixes and the mainline mix were nearly all less than those of the control mix, indicating less of this aging product. Sulfoxide contents have been found to not be good indicators of age-related performance-related binder and mix test results, such as PG, and the Glover-Rowe analysis of age-related cracking risk. This observation is based on the sulfoxide and binder performance-related test results in this technical memorandum and those of the previous high RAP/RAS pilot projects (ED 49 and SBD 215) *(14,15)*.

Figure 3.21 plots the carbonyl index normalized against the control Mix J. After plant mixing, Mixes K, L, M, N, and O each show about twice the apparent carbonyl index compared to Mix J, while the mainline Mix P shows about 50% more carbonyl than Mix J. The change in the 20-hour carbonyl index relative to Mix J suggests that as the asphalt binder becomes more aged, the carbonyl index increases approximately proportionately to the increasing RAP and RAS contents *(17*). For the change in 40-hour carbonyl index relative to Mix J, this ratio drops further, ranging from 8% to 30% more carbonyl for the mainline and high RAP/RAS mixes. The changes in relative aging from post-plant binder extraction to 20-hour PAV aging and to 40-hour PAV aging may indicate that the amount of carbonyl chains decreases as aging increases. This observation suggests the asphalt binder may reach an aging limit such that carbonyl chains become increasingly functionally identical to the control mix. Mix J and Mix P support this observation, as both mixes share the same virgin binder and share an 8% difference in carbonyl indices after 40-hour PAV. Figure 3.22 shows the sulfoxide indices normalized to control Mix J. The sulfoxide indices are generally similar to those of the control mix.

Previous research by the UCPRC (*4*) and by other organizations (primarily Glover and others at Texas A&M University *[17]*) before that show that carbonyl content is a good indicator of the changes in binder performance indicators with different amounts of aging for rutting at high temperatures and for stiffness related to different types of cracking at lower temperatures. This outcome can be seen for the seven mixes included in this project that were QA-sampled during paving. The results show a strong correlation between carbonyl index and the Glover-Rowe criteria (Figure 3.23) and stiffness at 64°C and 10 Hz (Figure 3.24). However, poor correlation was found between the carbonyl index and the crossover modulus (Figure 3.25), which is the opposite of the good correlations found in the previous ED 49 and SBD 215 high RAP/RAS pilot projects. The crossover modulus is the stiffness at which the phase angle is 45 degrees, with decreasing crossover modulus, indicating less ability to relax stresses under thermal contraction.

The results of binder testing suggest that the target design RA contents and their effects on extracted binders from the JMF testing generally matched those achieved during construction as measured on the QA samples. These findings suggest that those targets could have been increased somewhat to better match the control mix.

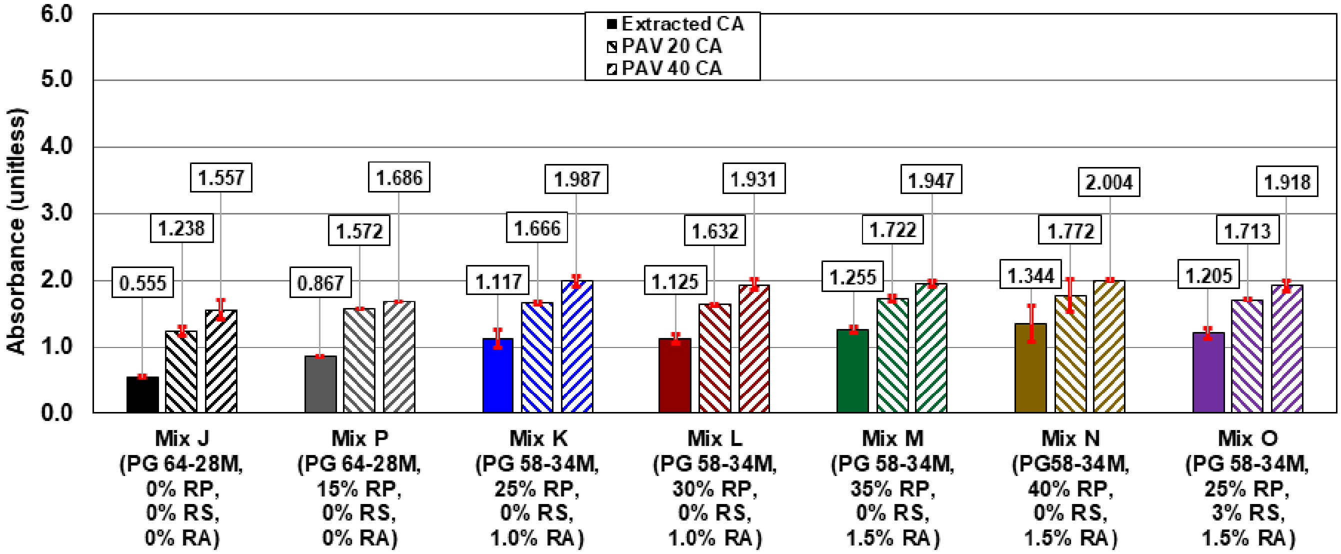

Figure 3.19: Average carbonyl area index changes after aging for QA-sampled binders between sublots.

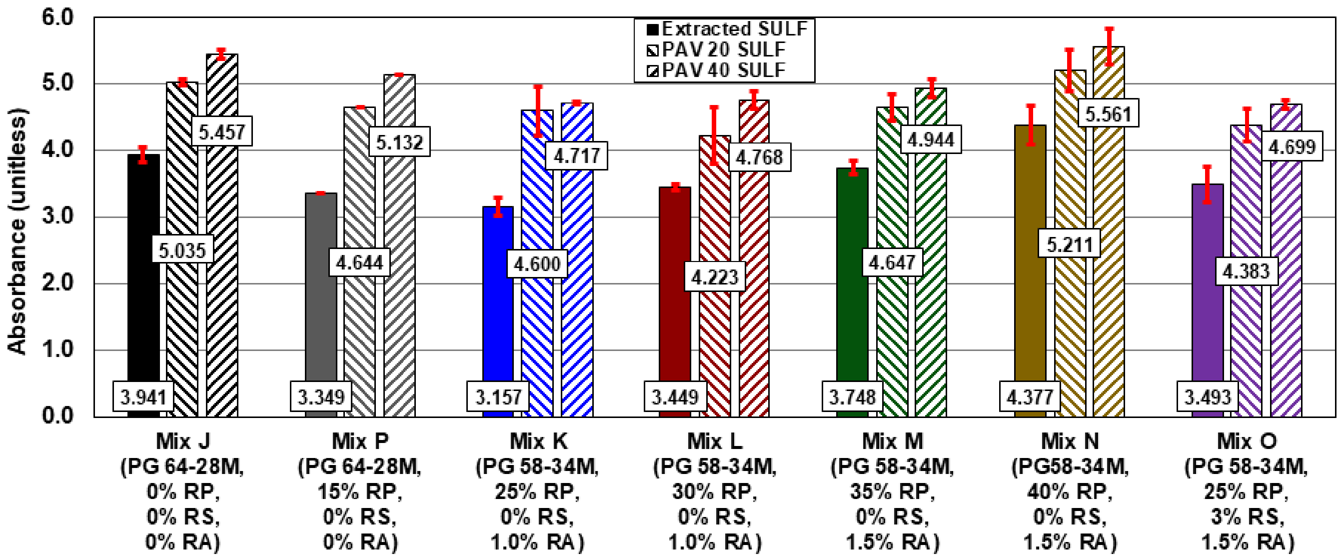

Figure 3.20: Average sulfoxide area index changes after aging for QA-sampled binders between sublots.

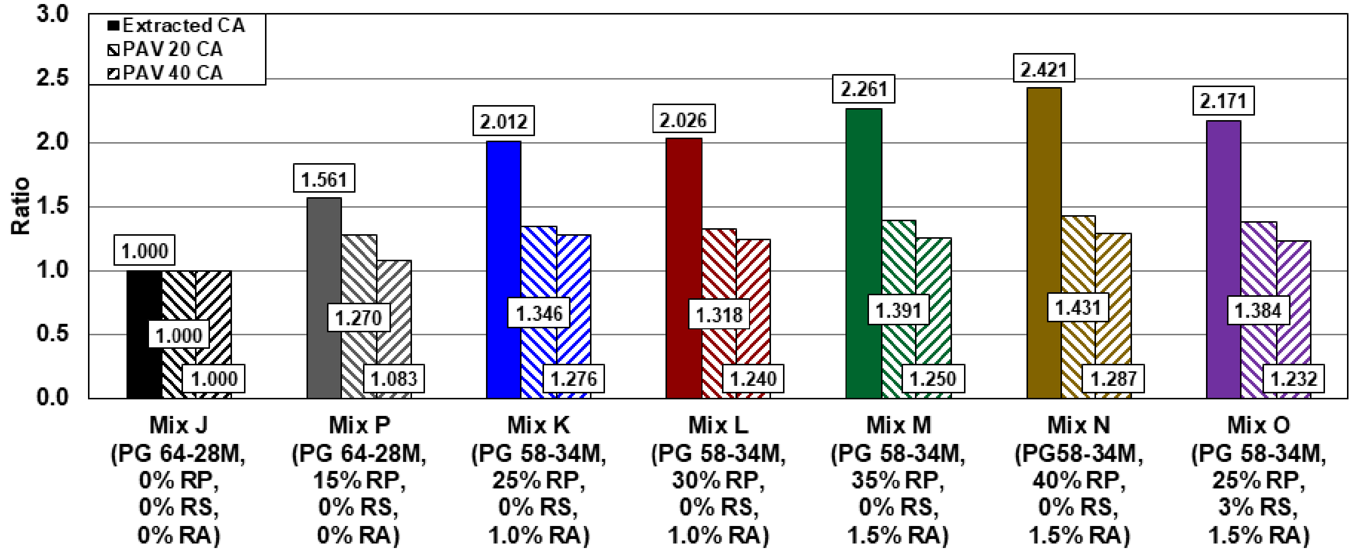

Figure 3.21: Carbonyl area index changes after aging for QA-sampled binders, normalized to Mix J.

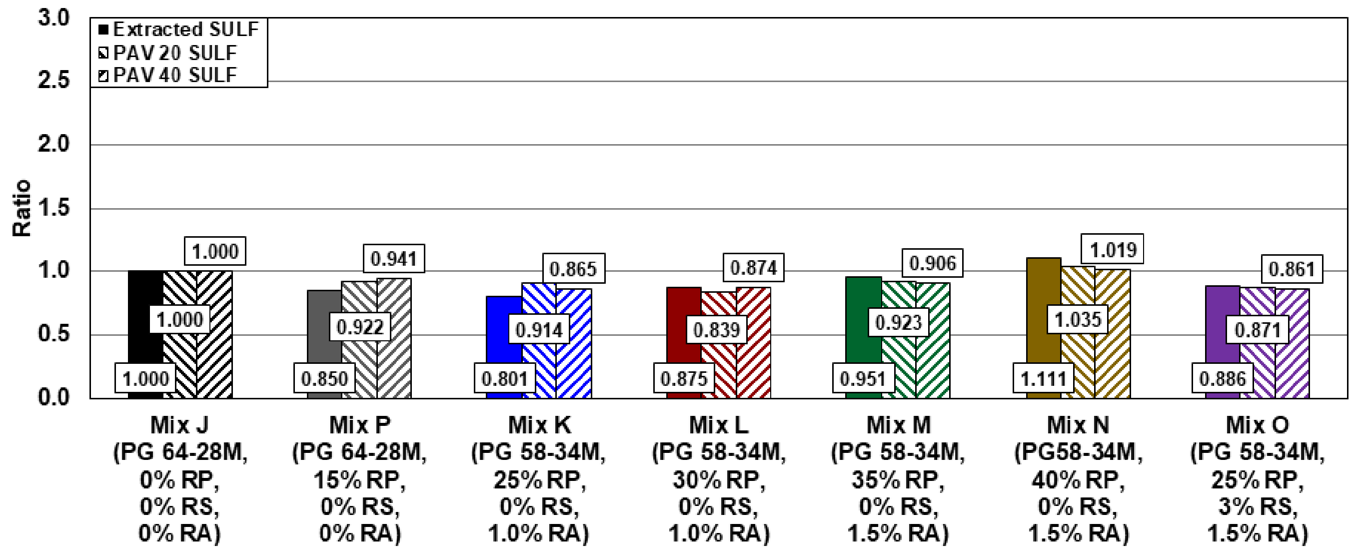

Figure 3.22: Sulfoxide area index changes after aging for QA-sampled binders, normalized to Mix J.

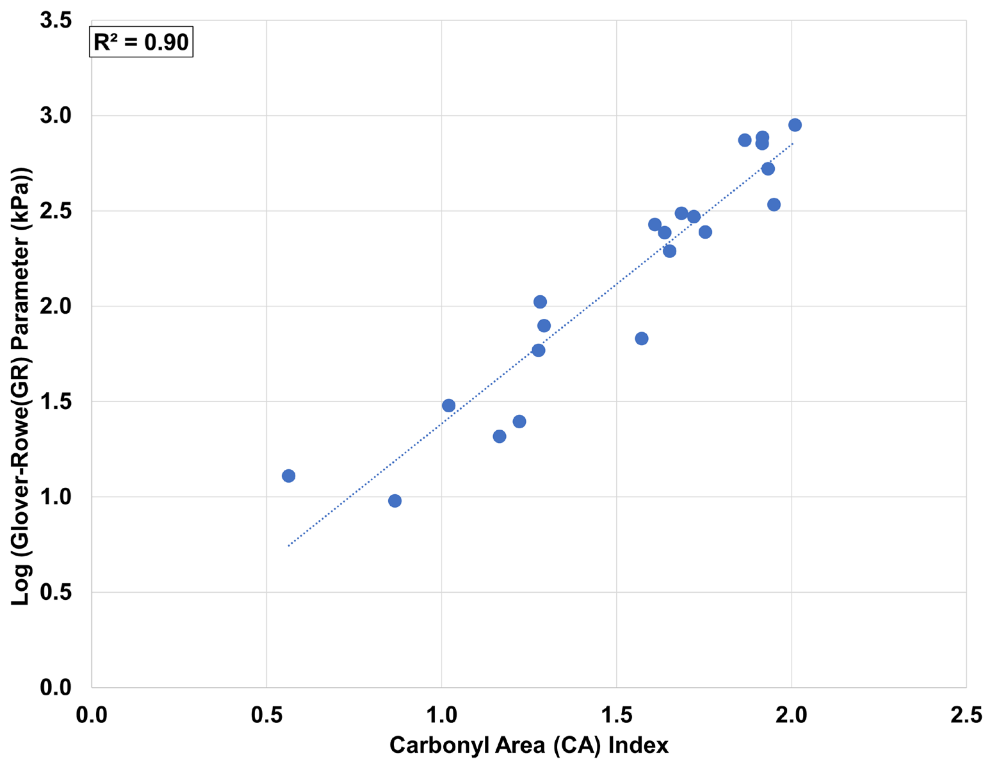

Figure 3.23: Carbonyl area versus Glover-Rowe parameter for first sublot (SL1) of QA-sampled binders at all aging conditions.

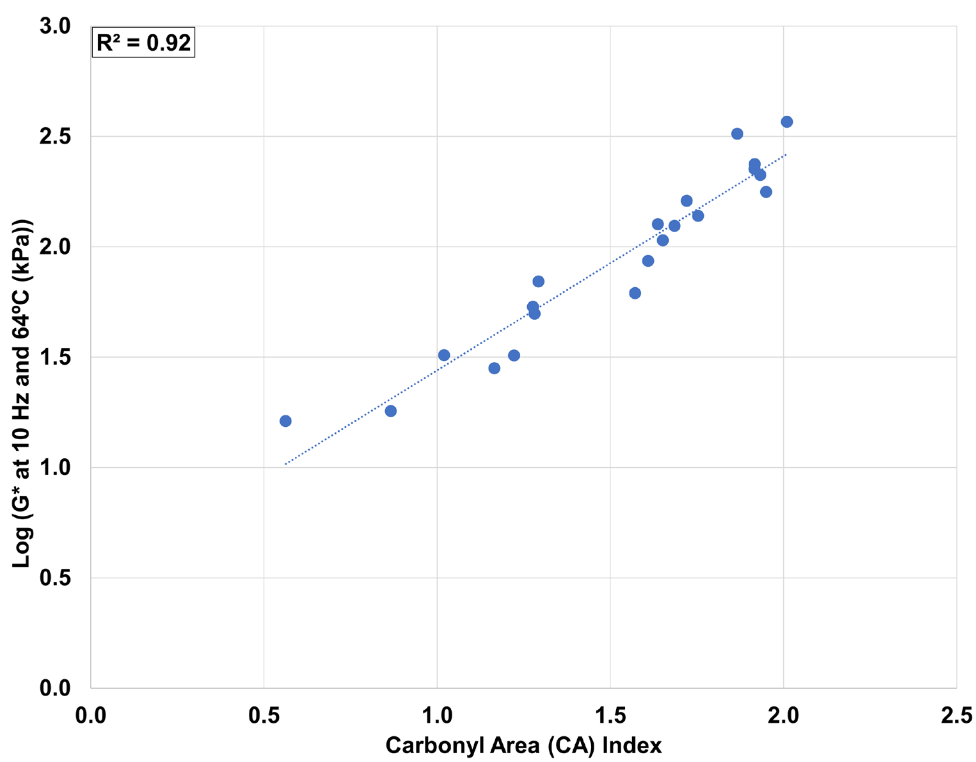

Figure 3.24: Carbonyl area versus G* at 10 Hz and 64°C for first sublot (SL1) of QA-sampled binders at all aging conditions.

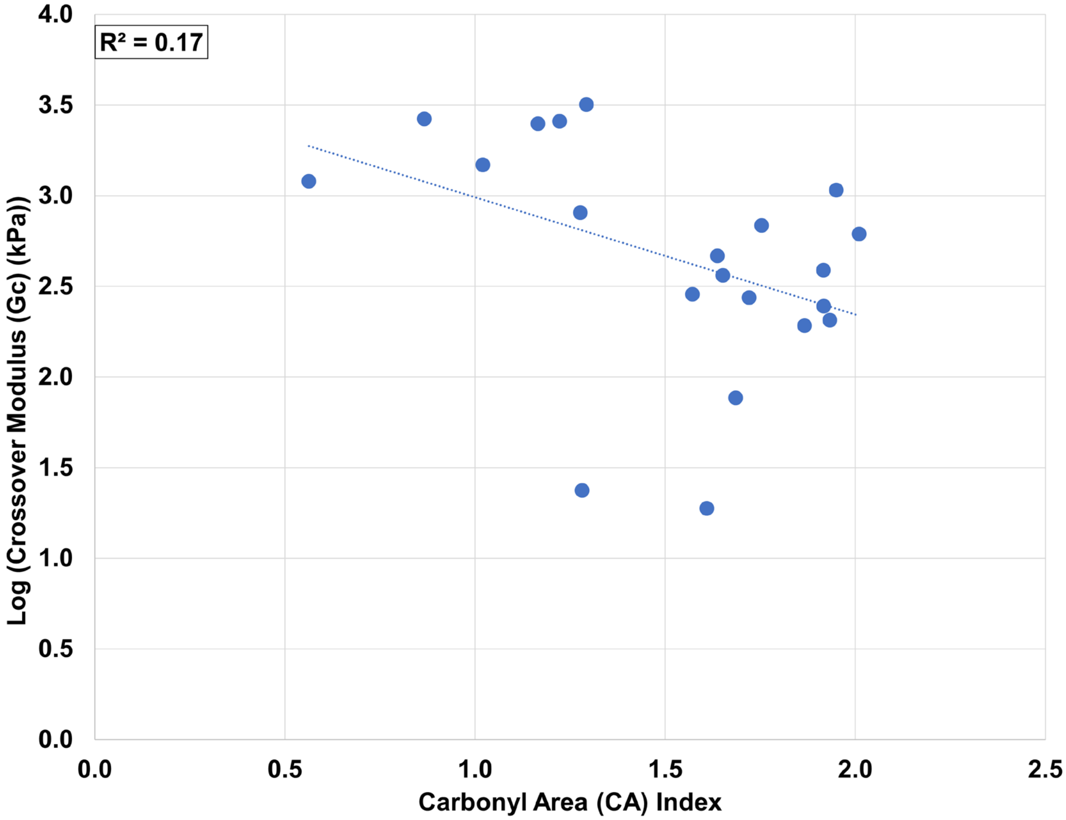

Figure 3.25: Carbonyl area versus crossover modulus for first sublot (SL1) of QA-sampled binders at all aging conditions.

4 MIX TESTING RESULTS

This chapter discusses mix testing results for plant-produced JMF verification and QA-sampled mixes. Mix designs and test method details are discussed in Chapter 2 and are not repeated in this chapter.

4.1 Mix Test Variability

4.1.1 Overview

It is desirable for pavement materials tests to be sensitive to material variables in the same way that material performance in the field is sensitive to the same variables and for the repeatability of the tests to be high (in other words, the test variance is low). A few asphalt concrete mix distresses are related to monotonic loading conditions, particularly fracture from low temperature cracking or long-term aged asphalt at intermediate temperatures (as tested by fracture). The variability of monotonic tests is generally consistent regardless of the test value once operator and equipment inconsistencies are controlled.

The distresses of rutting and fatigue are caused by phenomena related to repeated loading. Assessments of mix properties for rutting and fatigue are generally considered to require a repeated load test to obtain the best mix characterization for permanent deformation (rutting) and damage or cracking under repeated traffic loading (fatigue) *(18,19),* though stiffness information from monotonic tests provides information about fatigue cracking when combined with structural analysis and information from monotonic shear strength tests may provide information about rutting. The variability of repeated load tests is high when considered in terms of the standard deviation of the test. However, the sensitivity of repeated load tests to mix variables such as tensile strain (fatigue) or shear stress (rutting), binder stiffness and type, air-void content, and aggregate gradation is very high, sufficiently similar to mix sensitivity in the field to predict rutting and fatigue performance when used with a mechanistic-empirical simulation framework *(20)*. It has been shown that repeated load tests can discern the differences in expected performance between different mixes (or compaction levels, loading times, or temperatures) because the sensitivity of the tests to these variables is high (i.e., the change in the mean test result when a mix variable changes is greater than the variability for a given set of mix variables) *(21)*. It has also been found that the variability of repeated load tests is not constant; rather, it increases as the number of repetitions to failure increases, such that the coefficient of variation (standard deviation of repetitions to a given damage state or failure divided by mean repetitions) is approximately a constant.

The calculated variability of repeated load test results can be reduced and changed to a relatively constant variability, as opposed to a constant coefficient of variation, by changing the definition of the test result parameter from the number of repetitions to reach the failure state to instead the stress or strain state that results in a given number of repetitions to the failure state. This change has been done in Caltrans performance-related specifications for the flexural fatigue test, where the specification parameter has been changed from the repetitions at a given tensile strain to instead the tensile strain that results in 1 million cycles to failure. The test method is the same, except that the strains are selected to produce approximately 1 million repetitions to failure at the lowest strain used for a given mix. This change has also reduced the time necessary to complete testing for a mix.

Methods of minimizing variability of test results for all types of asphalt concrete performance-related tests include consistent materials handling to achieve uniform aging, consistent air-voids, consistent specimen dimensions, calibrated equipment, and certified testing staff. Once these sources of variability are controlled, inherent test variability is typically influenced by considerations of representative volume element (RVE) for the composite material (ratio of largest particle size to least specimen dimension) and the sensitivity of the results to the location of the critical stress state relative to the random locations of larger aggregate particles in the specimen.

Within-sample variability values are shown for the following tests performed on this pilot project during both JMF approval (where applicable) and QA testing:

- Mix stiffness at 20°C and 10 Hz (flexural and axial tests)
- Repeated load triaxial (RLT) tests (confined and unconfined)
- Four-point beam repetitions to failure at a given strain (lowest strain used)
- IDEAL-CT parameter and strength

The variability data shown for each test is within-sample, meaning that the JMF sample and the two QA samples are each treated as different samples. Test variability for all tests will be assessed once all the pilot projects are completed.

4.1.2 Variability of Test Results on This Pilot Project

The average within-sample variabilities of the flexural and triaxial dynamic moduli at 10 Hz and 20°C from the frequency sweep tests are shown in Table 4.1. The average within-sample variabilities of the unconfined and confined RLT test results are shown in Table 4.2 for the flow number parameter and in Table 4.3 for the repetitions to 3% permanent strain parameters. The average within-sample variabilities of the flexural fatigue beam test results are shown in Table 4.4. The average within-sample variabilities of the indirect tension (IDEAL-CT) test results are shown in Table 4.5. The within-sample test variabilities found in this project are within the ranges of those found in other projects. As noted previously, the variability of each of these tests will continue to be assessed in future pilot projects and other test programs.

Table 4.1: Variability of Within-Sample Stiffness (MPa) and Coefficient of Variation for Dynamic Modulus at 20°C/21°C and 10 Hz

Test	Replicate Tests	Average Std Dev (MPa)	Minimum Coefficient of Variation[a]	Maximum Coefficient of Variation[a]	Average Coefficient of Variation[a]
Flexural dynamic modulus at 10 Hz, 20°C	3	103	0.01	0.08	0.03
Triaxial dynamic modulus at 10 Hz, 21°C	3	386	0.02	0.13	0.07

[a] Coefficient of variation = std dev/mean.

Table 4.2: Variability of Within-Sample Rutting Resistance (Repetitions To Flow Number) and Coefficient of Variation for Repeated Load Triaxial Test

Test	Replicate Tests	Average Std Dev (repetitions)	Minimum Coefficient of Variation[a]	Maximum Coefficient of Variation[a]	Average Coefficient of Variation[a]
Unconfined flow number at 45°C	3	3,428	0.18	0.52	0.37
Confined flow number at 45°C	3	2,688	0.03	0.46	0.19
Unconfined flow number at 55°C	3	476	0.03	0.40	0.26
Confined flow number at 55°C	3	2,396	0.06	0.33	0.16
Unconfined flow number at 50°C	3-6	1,568	0.22	0.62	0.33

[a] Coefficient of variation = std dev/mean.

Table 4.3: Variability of Within-Sample Rutting Resistance (Repetitions to 3% Permanent Deformation) and Coefficient of Variation for Repeated Load Triaxial Test

Test	Replicate Tests	Average Std Dev (repetitions)	Minimum Coefficient of Variation[a]	Maximum Coefficient of Variation[a]	Average Coefficient of Variation[a]
Unconfined repetition at 45°C	3	3,192	0.03	0.54	0.26
Confined repetition at 45°C	3	0	0.00[b]	0.00[b]	0.00
Unconfined repetition at 55°C	3	792	0.10	0.67	0.30
Confined repetition at 55°C	3	104	0.00[b]	0.05[b]	0.01
Unconfined repetition at 50°C	3-6	2,099	0.03	0.75	0.29

[a] Coefficient of variation = std dev/mean.
[b] Low coefficient of variation because most specimens did not reach failure

Table 4.4: Variability of Within-Sample Tensile Strain at 1 Million Repetitions to Failure and Coefficient of Variation for Flexural Fatigue Test

Test	Replicate Tests	Average Std Dev (repetitions to failure)	Minimum Coefficient of Variation[a]	Maximum Coefficient of Variation[a]	Average Coefficient of Variation[a]
Repetitions to failure at 400-1000 με	3-6 at each strain level	835,682	0.20	0.84	0.62

[a] Coefficient of variation = std dev/mean.

Table 4.5: Variability of Within-Sample IDEAL-CT Number and Strength

Test	Replicate Tests	Average Standard Deviation (parameter or psi)	Minimum Coefficient of Variation[a]	Maximum Coefficient of Variation[a]	Average Coefficient of Variation[a]
IDEAL-CT number	5 or more	12.5	0.10	0.47	0.24
IDEAL-CT strength (psi)	5 or more	8.2	0.03	0.12	0.07

[a] Coefficient of variation = std dev/mean.

4.2 Testing of Mixes Prior to Construction for Job Mix Formula Verification

4.2.1 Indirect Tensile Cracking Resistance: IDEAL-CT Test

Table 4.6 and Figure 4.1 show the IDEAL-CT results in terms of IDEAL-CT number and indirect tensile strength (Strength). Table 4.6 also shows more details of the information from the test and the variability of that information. It has been proposed that a larger IDEAL-CT number indicates better cracking resistance under monotonic indirect tensile loading. Research by the UCPRC indicates that the IDEAL-CT number has a strong correlation with flexural stiffness and a weak correlation with fatigue cracking resistance at a given strain *(22)*. The JMF mix designs were re-submitted for Mix J (0% RAP) due to out-of-specification Ndesign air-void results, and for Mix M (35% RAP), Mix N (40% RAP), and Mix O (25% RAP and 3% RAS) due to out-of-specification IDEAL-CT results compared with the second Mix J virgin control submittal.

The results show that the second JMF verification sample for Mix N had the largest IDEAL-CT number, followed by Mix M, Mix O, Mix K, Mix L, and then control Mix J, with all of the accepted high RAP/RAS mixes exceeding Mix J, per specification. A smaller post-peak slope should indicate greater fracture toughness and less brittleness, which showed an inverse ranking for the post-peak slope compared with the IDEAL-CT number for the seven mixes, with the exception of Mix N, which was between Mix J and Mix L.

The IDEAL-CT results for the job mix verification samples show that Mixes K, L, M, N, and O met the specification of an IDEAL-CT number greater than that of Mix J in the first or second design submittals. The mainline Mix P (15% RAP with no recycling agent) was used on a majority of the project but was not subjected the high RAP/RAS nSSP and, therefore, was not tested during JMF review. Figure 4.1 also shows the IDEAL-CT Strength value (maximum stress) for the six JMF verification sample mixes. Previous UCPRC research has shown that Strength has a relatively strong correlation with flexural stiffness and largely controls the IDEAL-CT number as well (*22*). The results showed that the Strength values were very similar for each of the mixes except for the control Mix J, which had a Strength, and therefore a stiffness, that was about 30% less than that of the high RAP/RAS mixes. These results correspond to binder test and flexural and triaxial dynamic modulus results that show generally similar stiffnesses for most of the high RAP/RAS mixes at intermediate temperatures and loading frequencies, and greater stiffness than the control Mix J.

Figure 4.2 shows the fracture energy and post-peak slope results for the IDEAL-CT test. The fracture energies were all higher for the high RAP/RAS mixes compared with the control Mix J, corresponding to the greater Strength results, and ranked the mixes the same as the IDEAL-CT value results. The post-peak slopes are all greater for the high RAP/RAS mixes compared with the control Mix J. It appears that the high post-peak slope values helped the mixes meet the IDEAL-CT number specification.

Table 4.6: IDEAL-CT Results for Job Mix Formula Verification Samples

Mix ID	Cracking Tolerance (CT Index)	Standard Deviation Cracking Tolerance (CT Index)	Strength (psi)	Standard Deviation Strength (psi)	Fracture Energy (Gf)	Standard Deviation Fracture Energy (Gf)	Post-Peak Slope (m)	Standard Deviation Post-Peak Slope (m)
Mix J (PG 64-28M, 0% RP, 0% RS, 0% RA) JMF Submittal #1	66.2	11.9	81.8	2.9	4272.4	375.0	-1.9	0.2
Mix J (PG 64-28M, 0% RP, 0% RS, 0% RA) JMF Submittal #2	50.4*	7.7	84.3	2.7	4055.9	245.3	-2.1	0.2
Mix K (PG 58-34M, 25% RP, 0% RS, 1.0% RA) JMF Submittal #1	52.1	8.5	118.7	4.4	6093.7	393.5	-3.3	0.4
Mix L (PG 58-34M, 30% RP, 0% RS, 1.0% RA) JMF Submittal #1	52.0	10.5	119.8	10.1	6117.7	548.1	-3.2	0.4
Mix M (PG 58-34M, 35% RP, 0% RS, 1.5% RA) JMF Submittal #1	30.4	5.9	140.8	10.7	6182.9	691.5	-4.9	0.6
Mix M (PG 58-34M, 35% RP, 0% RS, 1.5% RA) JMF Submittal #2	59.6	23.3	119.3	9.8	6262.2	576.0	-3.2	0.8
Mix N (PG 58-34M, 40% RP, 0% RS, 1.5% RA) JMF Submittal #1	33.9	9.5	141.9	13.0	6382.1	529.0	-4.8	1.1
Mix N (PG 58-34M, 40% RP, 0% RS, 1.5% RA) JMF Submittal #2	84.6	25.7	108.1	8.9	6478.4	583.5	-2.5	0.6
Mix O (PG 58-34M, 25% RP, 3% RS, 1.5% RA) JMF Submittal #1	42.5	11.2	136.1	10.5	6487.7	533.0	-4.1	0.9
Mix O (PG 58-34M, 25% RP, 3% RS, 1.5% RA) JMF Submittal #2	52.5	15.9	123.5	13.9	6186.2	527.1	-3.4	0.8

Note: CT Index of 50.4 was established as the 0% RAP (virgin control) specification limit.

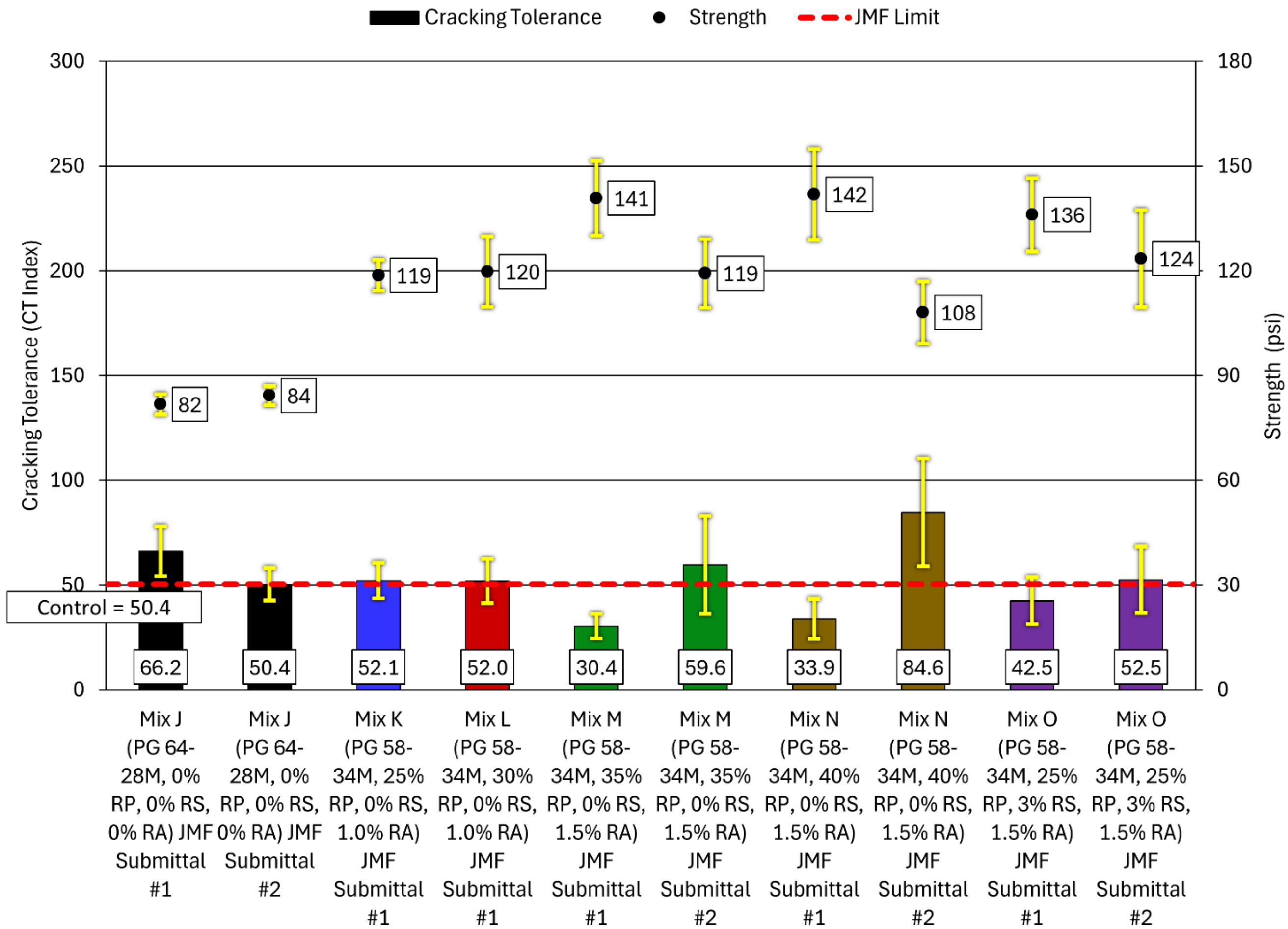

Figure 4.1: IDEAL-CT test results for mixes sampled for job mix formula verification (cracking tolerance index and indirect tensile strength).

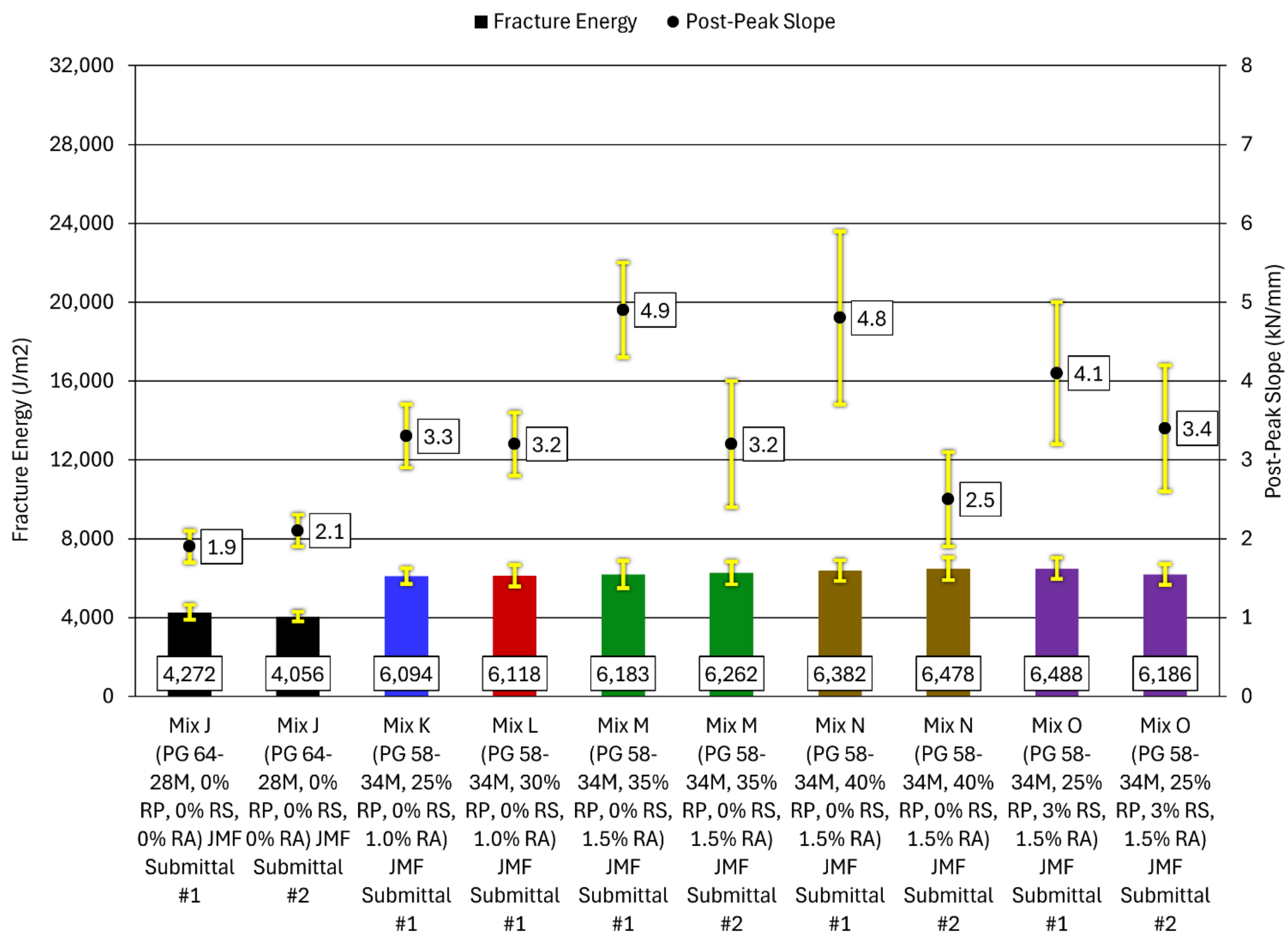

Figure 4.2: IDEAL-CT test results for mixes sampled for job mix formula verification (fracture energy and post-peak slope).

4.3 Testing of Mixes Sampled During Construction for Quality Assurance

4.3.1 Mix Design Properties: Air-Voids, Ndesign and Asphalt Binder Content

Overall, the design approach was to optimize the IDEAL-CT value with a 4.0% Ndesign air-void target. Further mix optimization could have been performed by increasing the total binder contents and decreasing the air-voids at Ndesign. Assuming this did not create a rutting problem or over-soften the mix stiffness, it would result in more flexible mix designs and likely higher CT values to further exceed the specification. Further exceeding the CT specification would reduce the risk of out-of-specification test results in production. As seen later in this chapter, some of the production sublots did not meet the 50.4 IDEAL-CT value minimum established based on the test results for control Mix J.

Table 4.7 shows the average total binder contents from QA sampling, which are compared with the design total binder contents, and the laboratory air-void contents at Ndesign. Table 4.8 shows the same information for the two sublots for each mix. The QA binder contents were up to 0.4% different from the design binder contents, all on the high side except for the first sublot of Mix N, where the measured binder content was lower than the already low design binder content, and were all within the specification allowed limits except for the first sublot of Mix N.

Figure 4.3 compares the binder content by total mass of mix for each sublot against the measured Ndesign air-void content. Figure 4.4 compares the results between the UCPRC and Caltrans. Figure 4.5 compares the total binder content by total mass of mix between the UCPRC and Caltrans, bracketed by the target binder design limits.

The measured asphalt binder content from Caltrans was higher than the one measured by the UCPRC for Mixes P, K, L, and N, and lower for Mix J (the control) and Mix M as can be seen in Figure 4.6. The Ndesign air-void content was consistently lower from Caltrans compared with the UCPRC for all measured mixes. These results may have occurred due to differences in testing procedures from ASTM D8159 (run by the UCPRC) versus AASHTO T312 (run by Caltrans) as well as operator differences for the tests (AASHTO R40, R83, and T312). Despite the differences in test results, no discernible trend from each of the mixes can be noted by these parameters within these figures from either the UCPRC or Caltrans, and the binder content and Ndesign air-void content parameters appear to not be correlated with each other for the relatively narrow ranges of both in these results. Note that only one quality sample was taken for Mix P.

Figure 4.7 plots all plant mix gradations on the same graph. All mixes appear to meet the target gradation specification limits, except for the mainline, Mix P, which was coarser than the design limits for the sand sizes (#8 to #50 sieves; 2.36 mm to 0.15 mm).

Table 4.7: Average Mix Design Properties: Asphalt Binder Content and Air-Voids at Ndesign (85 gyrations) by Mix Design

Samples	Total Binder Content (TMM, %)[a]	Design Binder Content (TMM, %)	Air-Voids at Ndesign (%)
Mix J (PG 64-28M, 0% RP, 0% RS, 0% RA)	4.7	4.5	2.3
Mix P (PG 64-28M, 15% RP, 0% RS, 0% RA)	4.7	4.6	4.9
Mix K (PG 58-34M, 25% RP, 0% RS, 1.0% RA)	4.8	4.5	4.1
Mix L (PG 58-34M, 30% RP, 0% RS, 1.0% RA)	4.8	4.5	4.2
Mix M (PG 58-34M, 35% RP, 0% RS, 1.5% RA)	4.7	4.0	4.0
Mix N (PG 58-34M, 40% RP, 0% RS, 1.5% RA)	4.1	4.0	4.2
Mix O (PG 58-34M, 25% RP, 3% RS, 1.5% RA)	4.8	4.5	3.2

[a] TMM: total mass of mix.

Table 4.8: Mix Design Properties: Asphalt Binder Content and Air-Voids at Ndesign (85 gyrations) by Sublot

Samples	Total Binder Content (TMM, %)[a]	Design Binder Content (TMM, %)	Air-Voids at Ndesign (%)
Mix J (PG 64-28M, 0% RP, 0% RS, 0% RA) QA Sample 1 (SL1)	4.67	4.50	2.49
Mix J (PG 64-28M, 0% RP, 0% RS, 0% RA) QA Sample 2 (SL2)	4.64	4.50	2.02
Mix P (PG 64-28M, 15% RP, 0% RS, 0% RA) QA Sample 1 (SL1)	4.67	4.60	4.86
Mix K (PG 58-34M, 25% RP, 0% RS, 1.0% RA) QA Sample 1 (SL1)	4.90	4.50	4.02
Mix K (PG 58-34M, 25% RP, 0% RS, 1.0% RA) QA Sample 2 (SL2)	4.63	4.50	4.12
Mix L (PG 58-34M, 30% RP, 0% RS, 1.0% RA) QA Sample 1 (SL1)	4.68	4.50	4.06
Mix L (PG 58-34M, 30% RP, 0% RS, 1.0% RA) QA Sample 2 (SL2)	4.83	4.50	4.35
Mix M (PG 58-34M, 35% RP, 0% RS, 1.5% RA) QA Sample 1 (SL1)	4.87	4.00	3.61
Mix M (PG 58-34M, 35% RP, 0% RS, 1.5% RA) QA Sample 2 (SL2)	4.45	4.00	4.32
Mix N (PG 58-34M, 40% RP, 0% RS, 1.5% RA) QA Sample 1 (SL1)	4.23	4.00	4.33
Mix N (PG 58-34M, 40% RP, 0% RS, 1.5% RA) QA Sample 2 (SL2)	3.91	4.00	4.14
Mix O (PG 58-34M, 25% RP, 3% RS, 1.5% RA) QA Sample 1 (SL1)	4.98	4.50	3.88
Mix O (PG 58-34M, 25% RP, 3% RS, 1.5% RA) QA Sample 2 (SL2)	4.53	4.50	2.53

[a] TMM: total mass of mix.

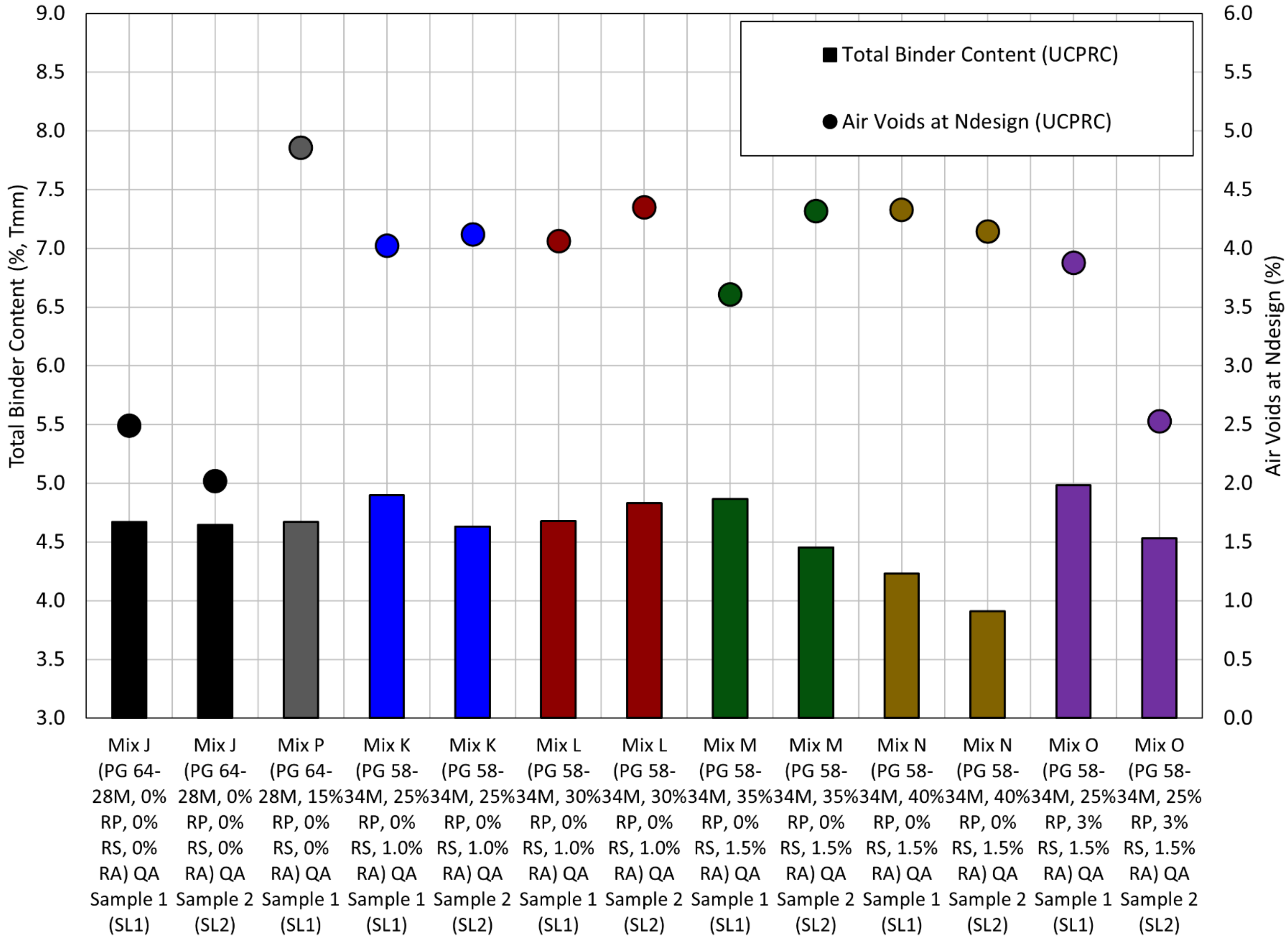

Figure 4.3: UCPRC volumetric test results for QA Sample 1 (SL1) and Sample 2 (SL2) (binder content and air-voids at 85 gyrations).

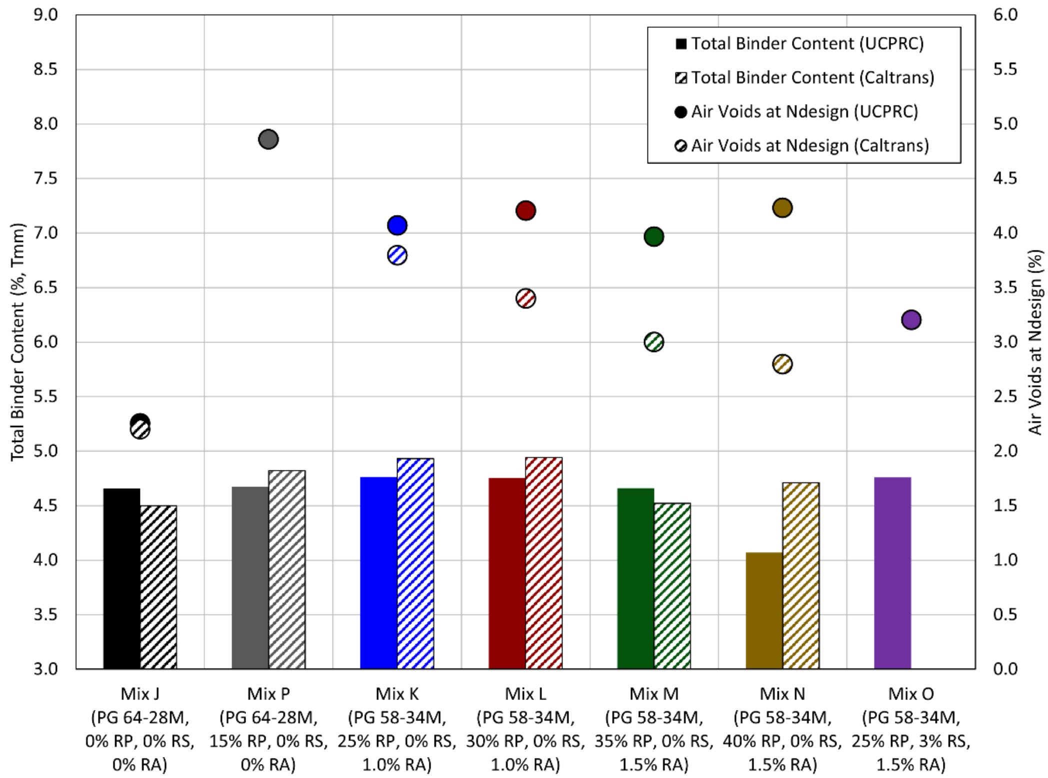

Figure 4.4: UCPRC and Caltrans volumetric test results for QA sample (binder content and air-voids at 85 gyrations).

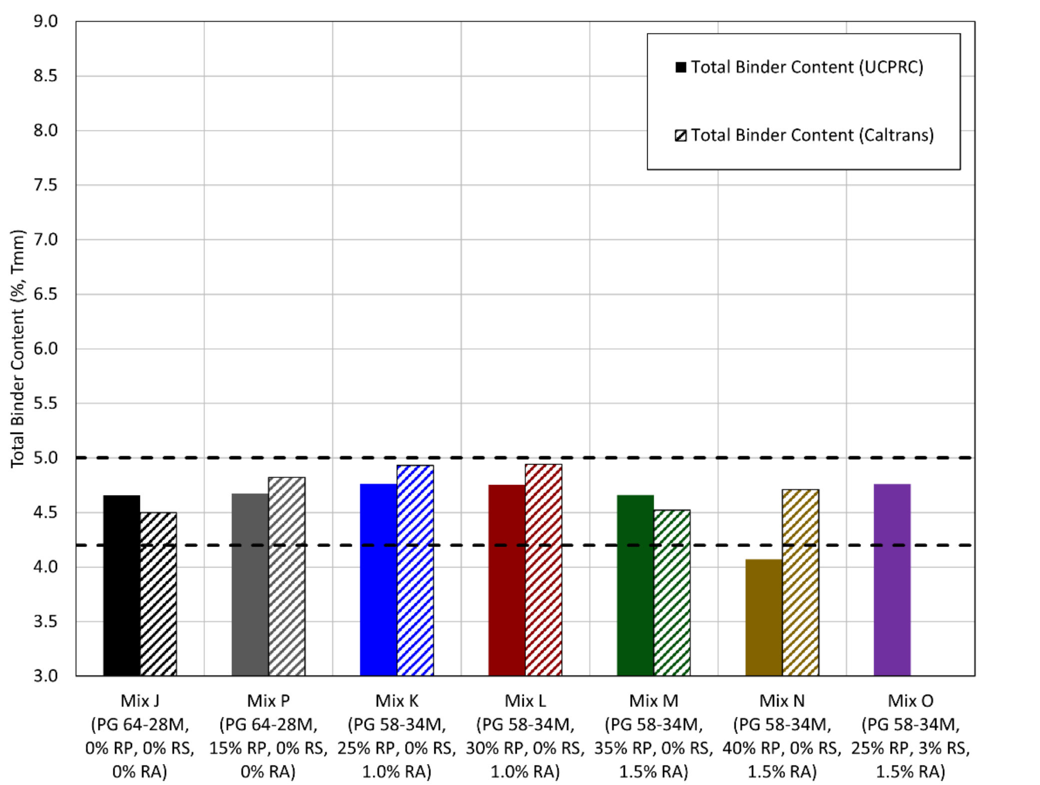

Figure 4.5: UCPRC and Caltrans volumetric test results for QA sample (binder content).

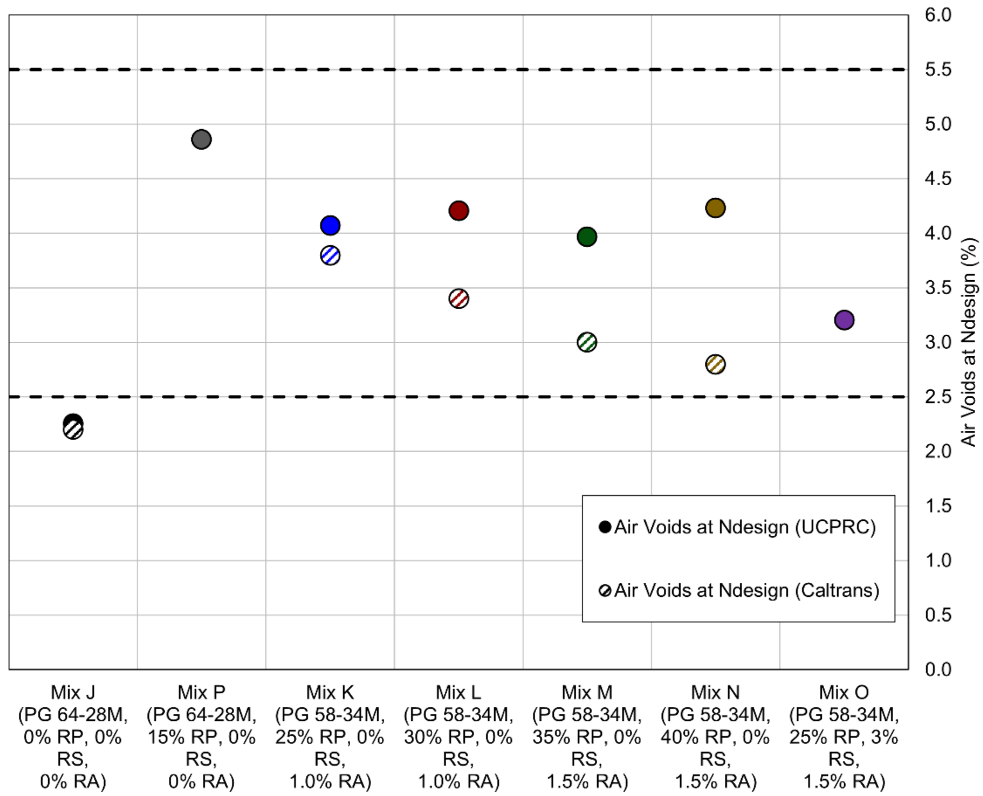

Figure 4.6: UCPRC and Caltrans volumetric test results for QA sample (air-voids at 85 gyrations).

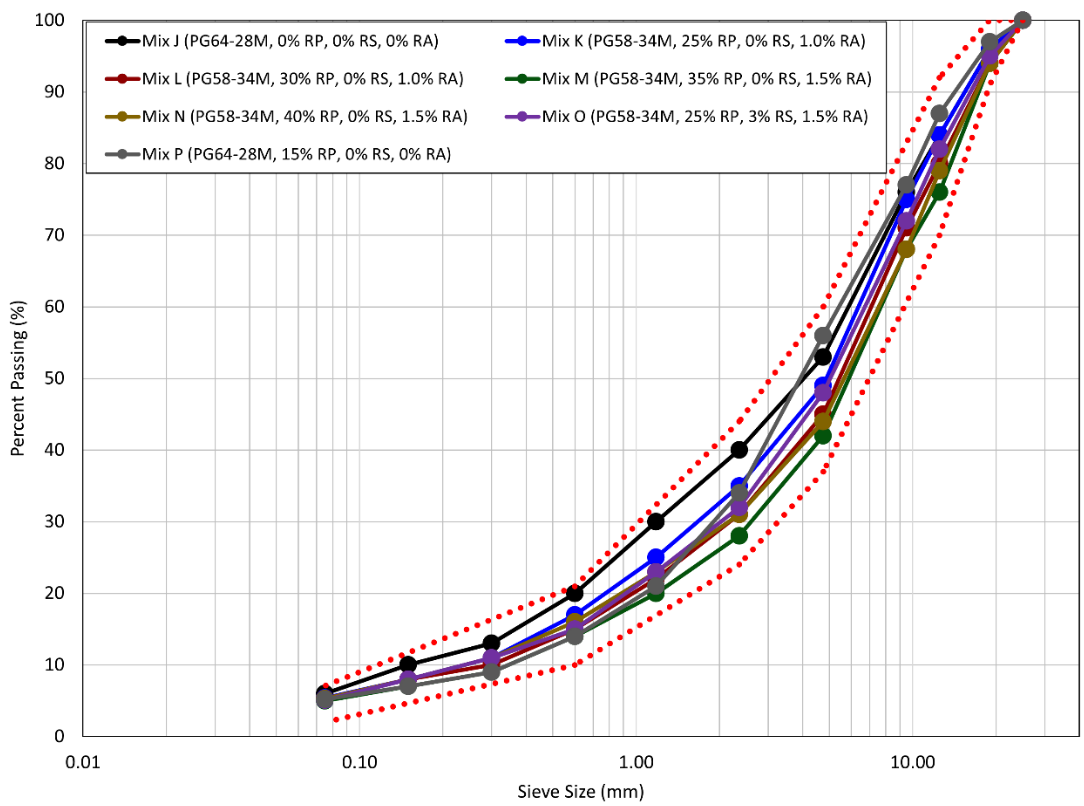

Figure 4.7: Caltrans sieve analysis test results for QA sample (percent passing for all mixes).

4.3.2 Reclaimed Asphalt Pavement Recycled Binder Ratio

The RAP recycled binder ratio (RBR) is the percentage of the combined RAP and RAS binder content over total binder content. The total binder content consists of the RAP binder, RAS binder, the virgin binder, and the recycling agent, and the Caltrans calculation includes the RA as part of the virgin binder. If it is included in the mix design, the LAS additive is typically metered into the asphalt binder at the plant, but the nSSP for these pilot projects excludes it from consideration as part of the virgin binder and does not explicitly call for it to be included with the RA when calculating RBR (LAS was not used in the mixes for this project). The RBR percentage, as well as the percentage of RAP aggregates in the total mix, were shown in Table 2.5 for the JMF mix design calculated per the nSSP. The graphical representation of the percentages of virgin and RAP and RAS binder in the total binder for each QA sublot is shown in Figure 4.8 and the virgin and RAP and RAS aggregate in the total aggregate in Figure 4.9. Figure 4.8 also shows the total binder content between the sublots from UCPRC binder extractions.

An alternative way to look at the binder is to consider the RA, and LAS if it is part of the mix, as part of the non-virgin binder portion of the total mix binder content and only the virgin binder as part of the virgin binder portion of the RBR, shown in Table 4.9. This way of looking at the total binder components is shown graphically in Figure 4.10. The table and figure show that an increasingly substantial part of the binder is RA as the RAP and RAS content increases. The RA dosage is determined based on meeting blended binder properties. The RA dosage will also depend on the stiffnesses of the RAP and RAS binders and some other chemical properties as well. In addition to, or instead of, using RA to meet binder and mix properties, different PG grades of asphalt and/or different asphalt sources can also be used for the same purpose. The most effective solution can be engineered by the mix producer. The RBR was close to the specified target, regardless of whether RA was counted with the virgin binder or the recycled portion, except for Mix N (40% RAP), where the RBR was higher than the target.

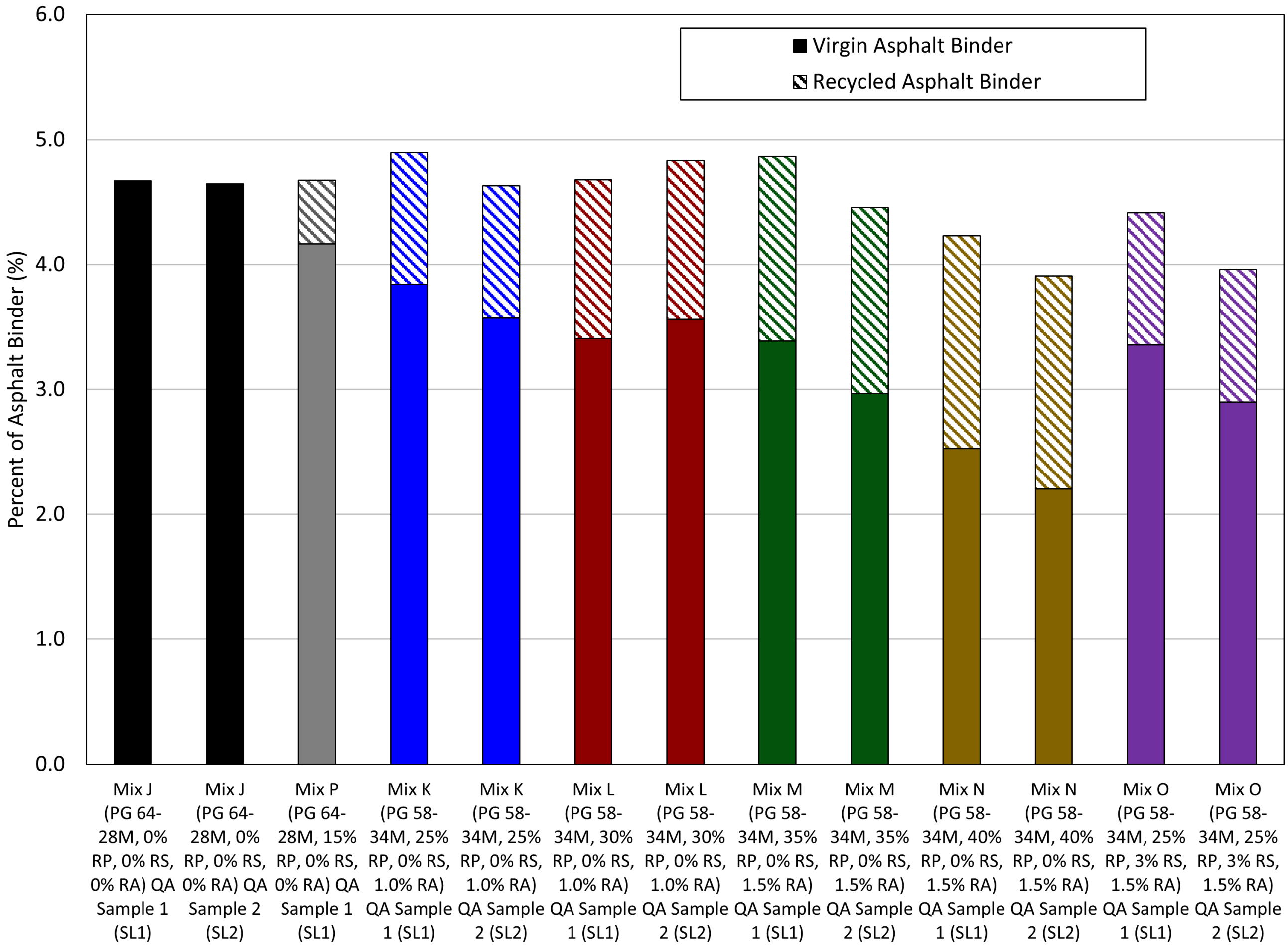

Note: Recycling agent (RA) is assumed to be part of virgin asphalt binder, and liquid antistrip is not counted.

Figure 4.8: Percent of asphalt binder of QA Sample 1 and Sample 2 (virgin and recycled asphalt binder only).

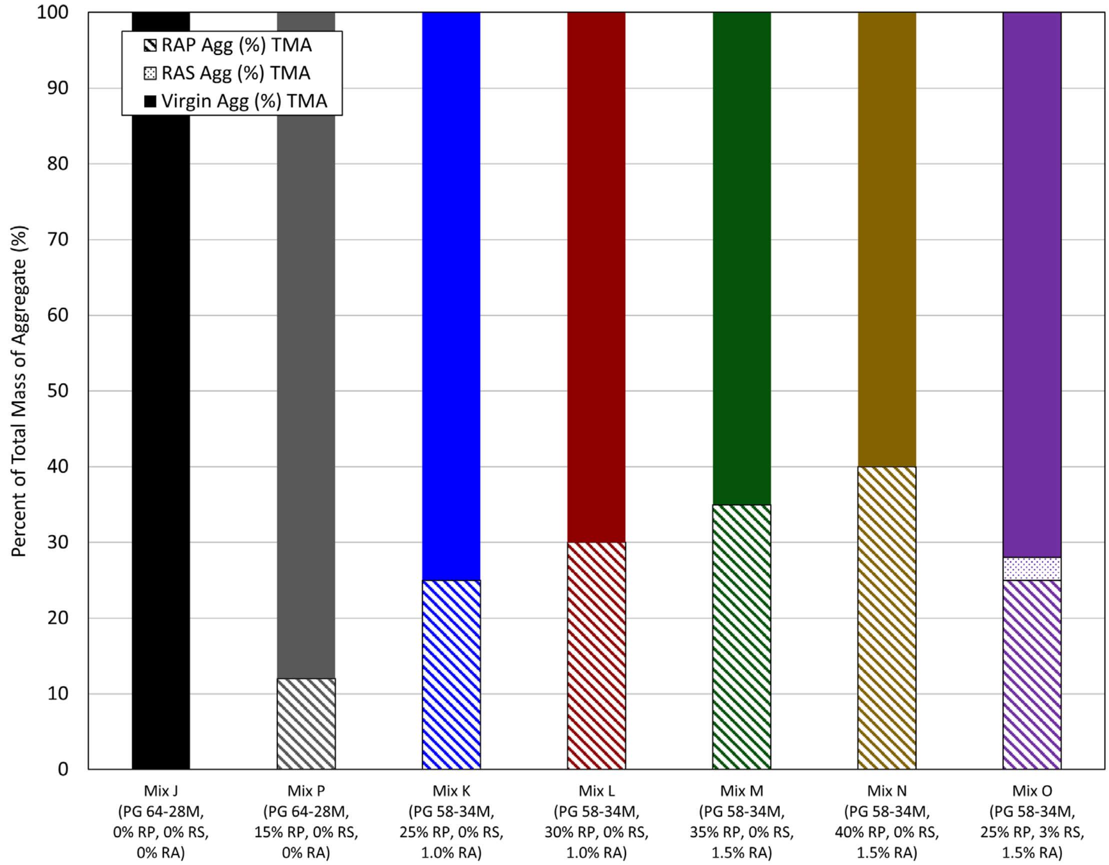

Figure 4.9: Total mass of aggregate of combined QA samples (virgin, RAP, and RAS aggregates).

Table 4.9: Virgin and RAP Components of Mix Comparing nSSP Calculation of Recycled Binder Ratio with Alternative Calculation

Samples	Virgin Aggregate (% TMA)	RAP and RAS Aggregate (% TMA)	AC Content (Pb, % TMM) (UCPRC result)	JMF Target AC Content (% TMM)	JMF Target Recycled AC Content (Pb, % TMM)	JMF Target RBR (% of binder)[a]	Actual RBR (% of binder)[a]	Recycling Agent (% of binder)	Actual RBR (% of binder)[b]
Mix J (PG 64-28M, 0% RP, 0% RS, 0% RA) QA Sample 1 (SL1)	100	0	4.67	4.5	0.00	0.0	0.0	0.0	0.0
Mix J (PG 64-28M, 0% RP, 0% RS, 0% RA) QA Sample 2 (SL2)	100	0	4.64	4.5	0.00	0.0	0.0	0.0	0.0
Mix P (PG 64-28M, 15% RP, 0% RS, 0% RA) QA Sample 1 (SL1)	88	12	4.67	4.6	0.56	12.1	11.9	0.0	11.9
Mix K (PG 58-34M, 25% RP, 0% RS, 1.0% RA) QA Sample 1 (SL1)	75	25	4.90	4.5	1.16	25.8	23.6	1.0	24.6
Mix K (PG 58-34M, 25% RP, 0% RS, 1.0% RA) QA Sample 2 (SL2)	75	25	4.63	4.5	1.16	25.8	25.1	1.0	26.1
Mix L (PG 58-34M, 30% RP, 0% RS, 1.0% RA) QA Sample 1 (SL1)	70	30	4.68	4.5	1.39	31.0	29.8	1.0	30.8
Mix L (PG 58-34M, 30% RP, 0% RS, 1.0% RA) QA Sample 2 (SL2)	70	30	4.83	4.5	1.39	31.0	28.8	1.0	29.8
Mix M (PG 58-34M, 35% RP, 0% RS, 1.5% RA) QA Sample 1 (SL1)	65	35	4.87	4.0	1.63	40.9	33.3	1.5	34.8
Mix M (PG 58-34M, 35% RP, 0% RS, 1.5% RA) QA Sample 2 (SL2)	65	35	4.45	4.0	1.63	40.9	36.5	1.5	38.0
Mix N (PG 58-34M, 40% RP, 0% RS, 1.5% RA) QA Sample 1 (SL1)	60	40	4.23	4.0	1.87	46.7	44.1	1.5	45.6
Mix N (PG 58-34M, 40% RP, 0% RS, 1.5% RA) QA Sample 2 (SL2)	60	40	3.91	4.0	1.87	46.7	47.8	1.5	49.3
Mix O (PG 58-34M, 25% RP, 3% RS, 1.5% RA) QA Sample 1 (SL1)	72	28	4.98	4.5	1.79	39.8	35.8	1.5	37.3
Mix O (PG 58-34M, 25% RP, 3% RS, 1.5% RA) QA Sample 2 (SL2)	72	28	4.53	4.5	1.79	39.8	39.5	1.5	41.0

[a] Recycling agent counted as part of virgin binder, per nSSP.
[b] Recycling agent counted as non-virgin part of total binder.

Notes: TMA = total mass of aggregate , RAS = recycled asphalt shingles, RAP = reclaimed asphalt pavement, AC = asphalt cement, TMM = total mass of mix, JMF = job mix formula, RBR = recycled binder ratio.

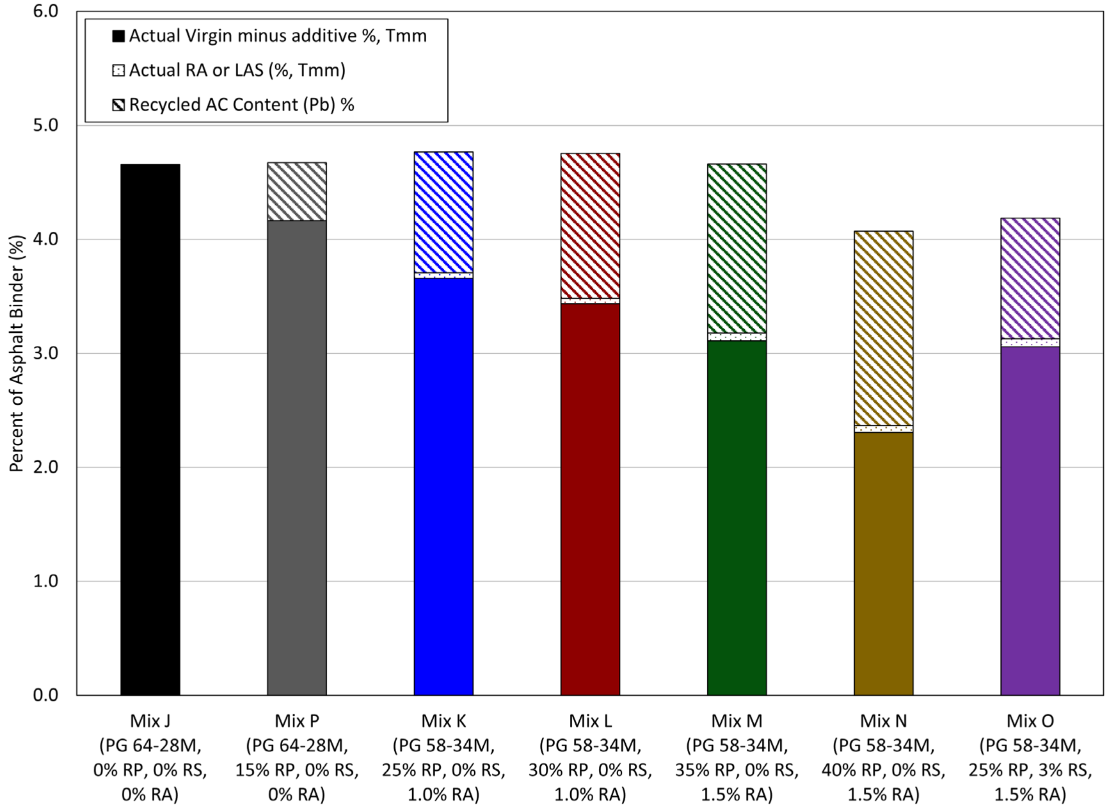

Figure 4.10: Percent of asphalt binder of QA Sample 1 (SL1) (virgin binder, RAP binder, and recycling agent).

4.3.3 Mix Stiffness: Triaxial and Flexural Dynamic Modulus

Flexural Dynamic Modulus Frequency Sweep Results

The flexural dynamic modulus curves from the first QA sample are shown in Figure 4.11. The QA sample mix stiffness results generally replicate those from binder testing and the JMF IDEAL-CT Strength results. As suggested in the binder JMF mix testing, the mixes have the greatest differentiation of stiffnesses at reduced frequencies of approximately 1 Hz, with decreasing differentiation at frequencies less than and greater than 1 Hz. Control Mix J is the softest, followed by mainline Mix P in increasing stiffness, with increasing stiffness generally correlating with increased RAP or RAP/RAS content in the order of Mix K, Mix L, Mix O, Mix M, and Mix N. The high stiffness of Mix N is likely partially attributable to its overall lower total binder content. This rank order holds across all frequency ranges.

The relative stiffnesses are shown in Figure 4.12, normalized to the first QA sample for the control Mix J, which was the softest mix, and normalized to the mainline Mix P in Figure 4.13. The normalized results show that the stiffnesses of the mixes with increasing percentages of RAP and RAS are greater than those of the control mix with no RAS or RAP (Mix J), particularly at 1 Hz (related to intermediate temperatures). These greater stiffnesses at intermediate frequencies and temperatures typically result in shorter fatigue and reflective cracking lives in thin overlays and are beneficial for the same distresses in thicker overlays. The key tool to adjusting this stiffness, assuming consistent aggregate durability and gradation, is adjusting the RA dose to offset the stiffening effect of varying recycled binder ratios. The 1% to 1.5% range of recycling agent used in the high RAP/RAS mixes could potentially be increased up to several percentage points to match the mix performance of the 0% or 15% RAP mixes.

Figure 4.14 shows the Black Space diagram from flexural dynamic stiffness testing for the first QA sample for all mixes. Mix J has a higher phase angle at slower frequencies (when lower stiffnesses are occurring), indicating greater propensity for viscous flow and less elastic recovery at those frequencies, which are contributors to increased rutting but potentially beneficial for fatigue and reflective cracking lives at higher temperatures and slower speeds for a thin overlay. Mixes N, M, and O, containing high percentages of RAP and RAS, have the lowest phase angles at the same slow frequencies and high temperatures, with high RAP Mix K and Mix L and mainline Mix P falling between Mix J and Mixes N, M, and O. The lower phase angles of Mix N are likely due in part to its low binder content.

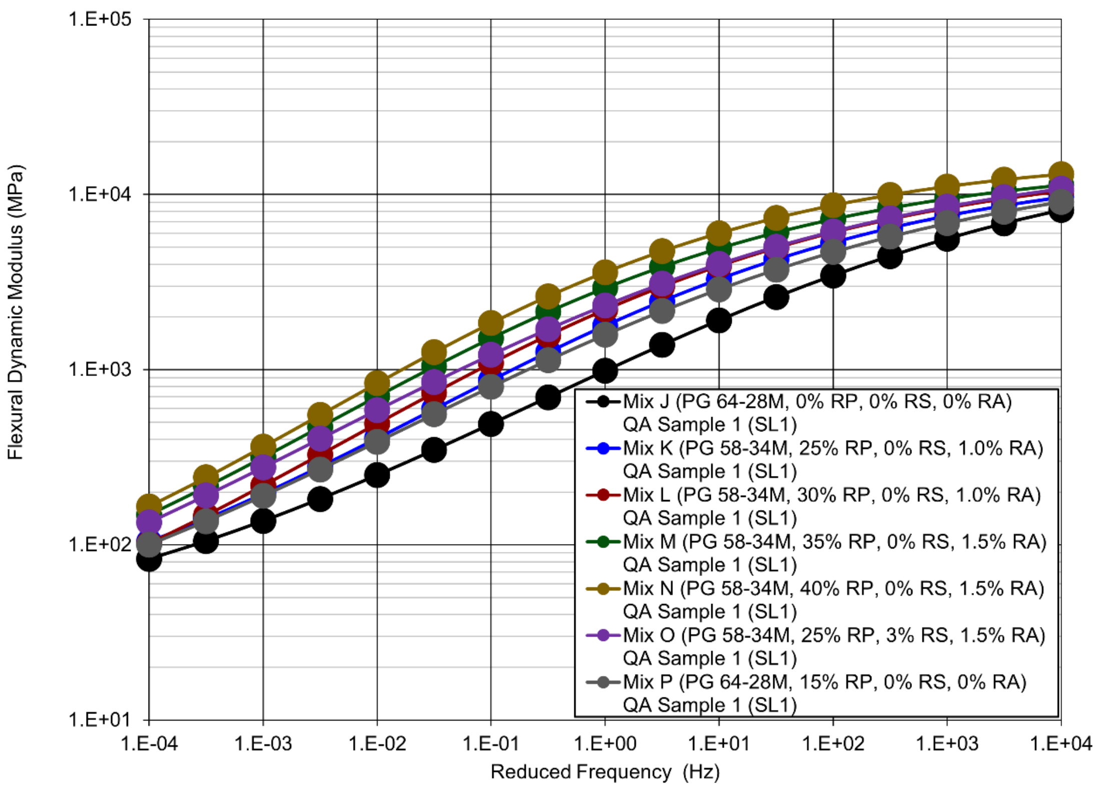

Figure 4.11: Flexural dynamic modulus master curves for QA-sampled mixes.

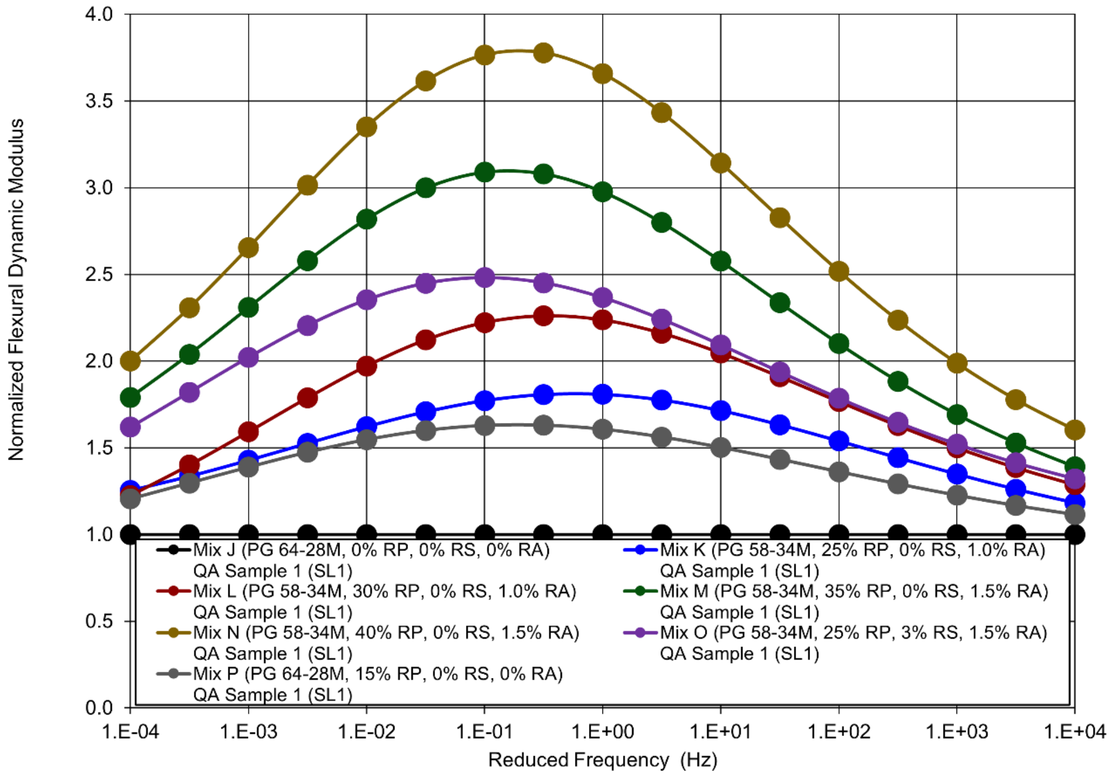

Figure 4.12: Flexural dynamic modulus master curves for QA-sampled mixes normalized to Mix J.

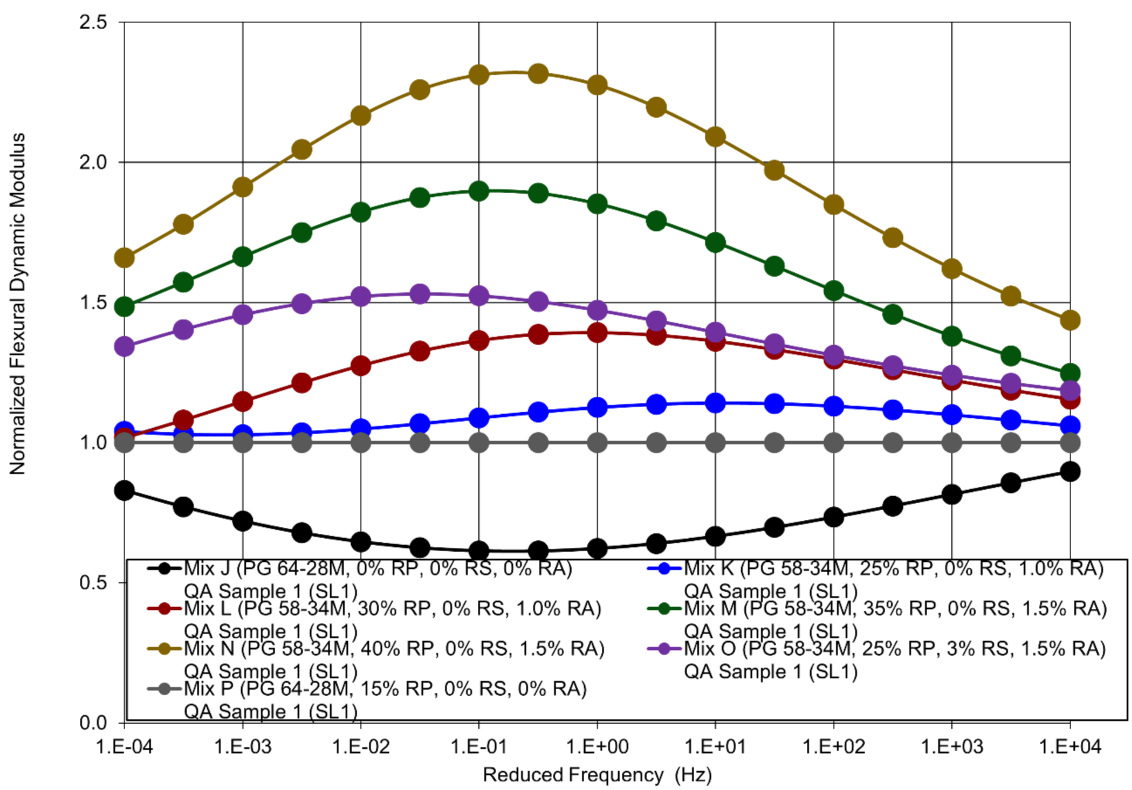

Figure 4.13: Flexural dynamic modulus master curves for QA-sampled mixes normalized to Mix P.

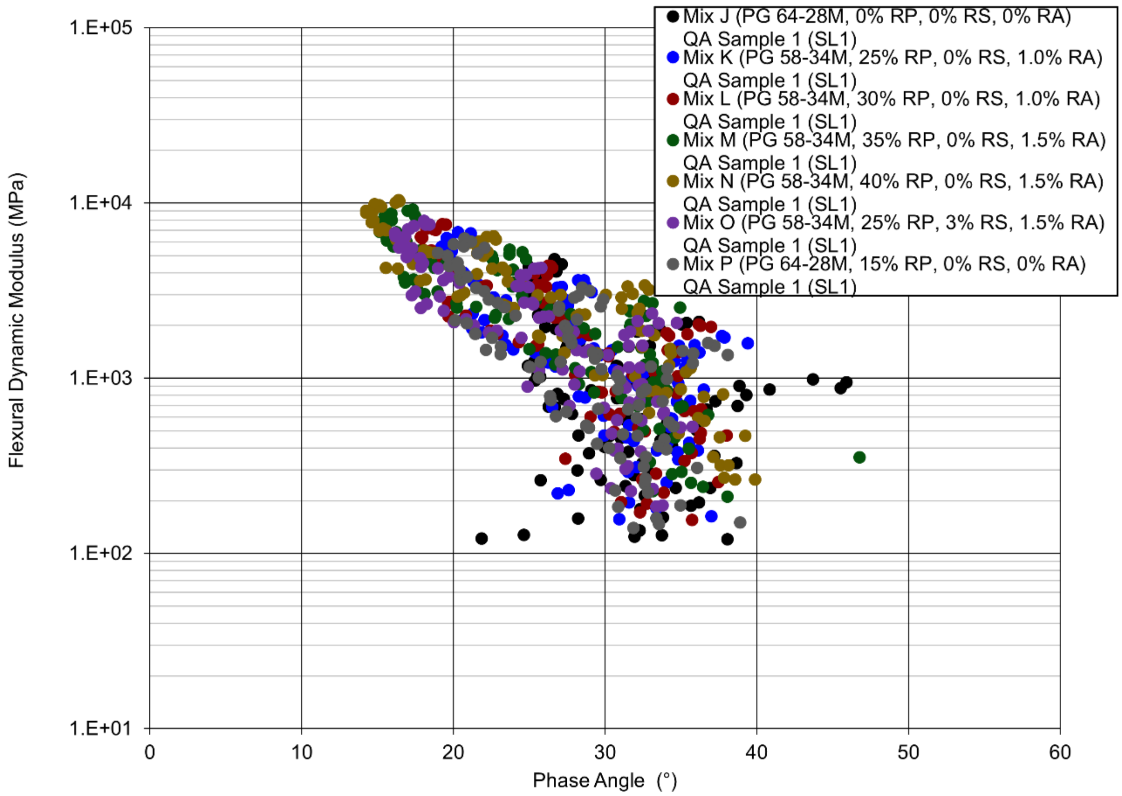

Figure 4.14: Black Space diagram for flexural dynamic modulus master curves for QA-sampled mixes.

Triaxial Dynamic Modulus Frequency Sweep Results

Figure 4.15 shows the master mix stiffness curves for the QA samples for all mixes. Figure 4.16 shows the master stiffness curves for all mixes normalized to that of control Mix J, and Figure 4.17 shows them normalized to mainline Mix P. The Black Space diagram for the six mix binders is shown in Figure 4.18. The results are generally consistent with those from the mix flexural and binder frequency sweeps, as expected, except for the stiffnesses at very slow frequencies for all mixes, which do not decrease relative to Mix J as occurred with the flexural and binder stiffness tests. As expected, the stiffnesses from the triaxial frequency sweeps shown in these figures are not always the same as those from the flexural sweeps shown previously, and the triaxial stiffnesses are somewhat greater at some frequencies.

Overall, based on the normalized axial dynamic modulus, the mixes with high RAP/RAS had intermediate stiffnesses (1 Hz and 20°C) that ranged from approximately 1.6 to 2.9 times higher than the control Mix J and 1.25 to 2.0 times higher than those of mainline Mix P at the same frequency and temperature. The stiffness differences for the high RAP/RAS mixes compared to Mix J and Mix P tended to increase with increasing RAP/RAS content. The axial Black Space plot shows less scatter than the flexural one. It is interesting to note that while the stiffness range for the dynamic modulus curve is slightly higher than that of the flexural curve, as expected due to the different stress states, the phase angles are considerably lower for the axial curves than for the flexural curves. For both parameters, the axial stress state, dominated by compressive stresses with some shear, would be expected to engage the high stiffness and no phase angle aggregate, compared with the flexural stress state, consisting of tension and compression, which would be expected to engage more of the lower stiffness and viscoelastic binder.

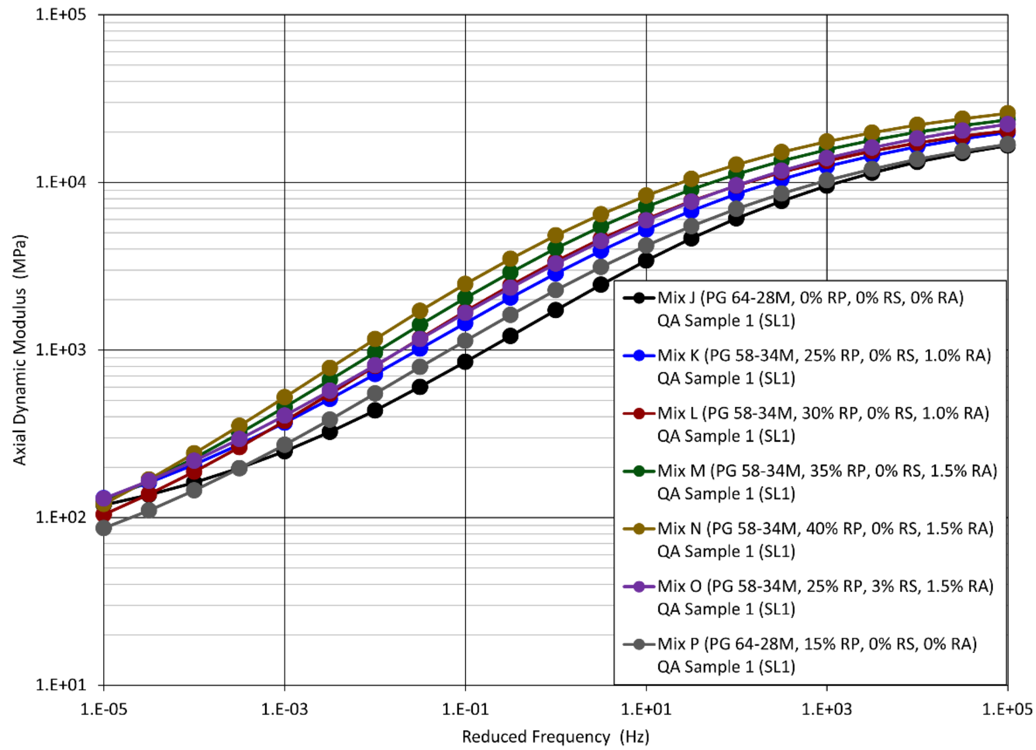

Figure 4.15: Axial dynamic modulus master curves for QA Sample 1 (SL1).

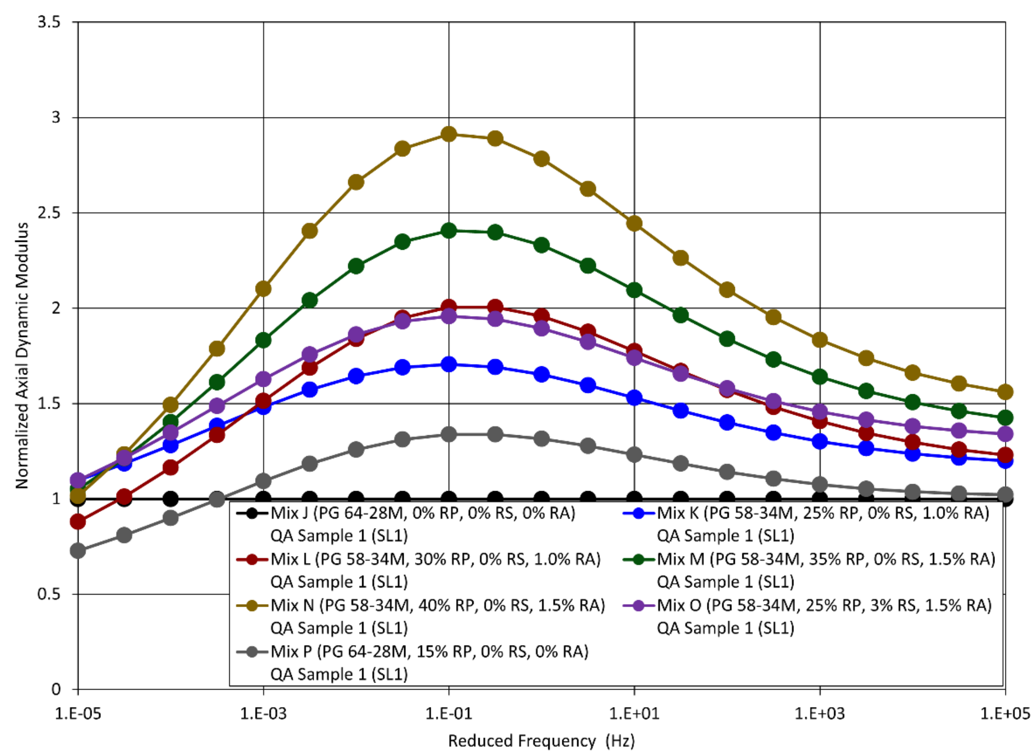

Figure 4.16: Axial dynamic modulus master curves for QA Sample 1 (SL1), normalized to Mix J.

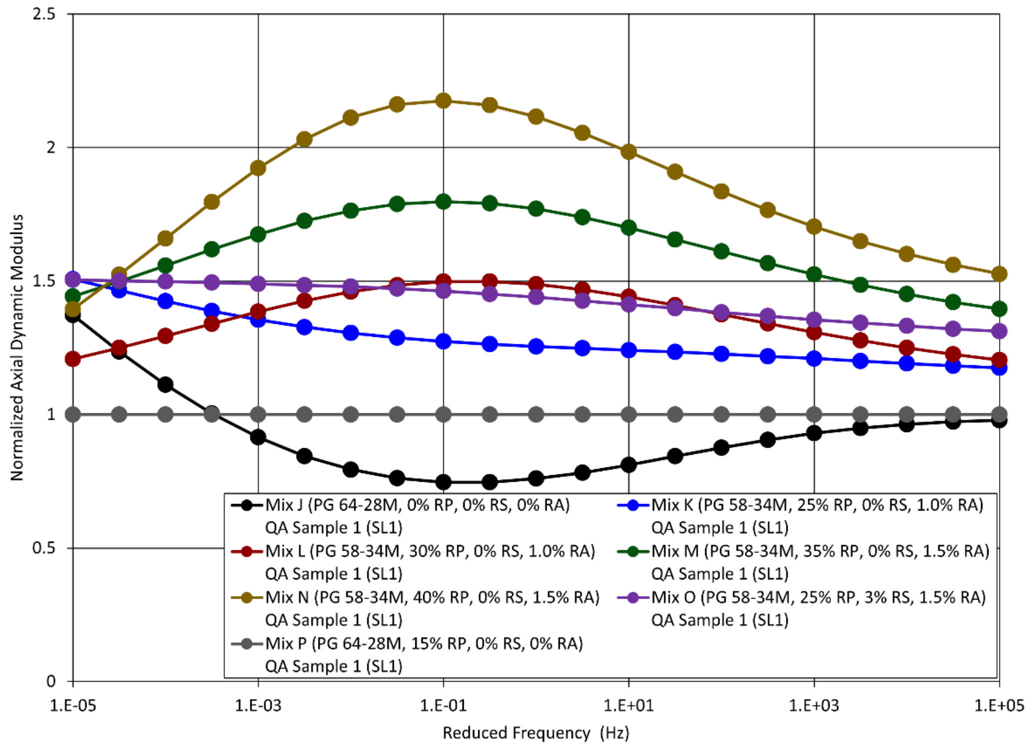

Figure 4.17: Axial dynamic modulus master curves for QA Sample 1 (SL1), normalized to Mix P.

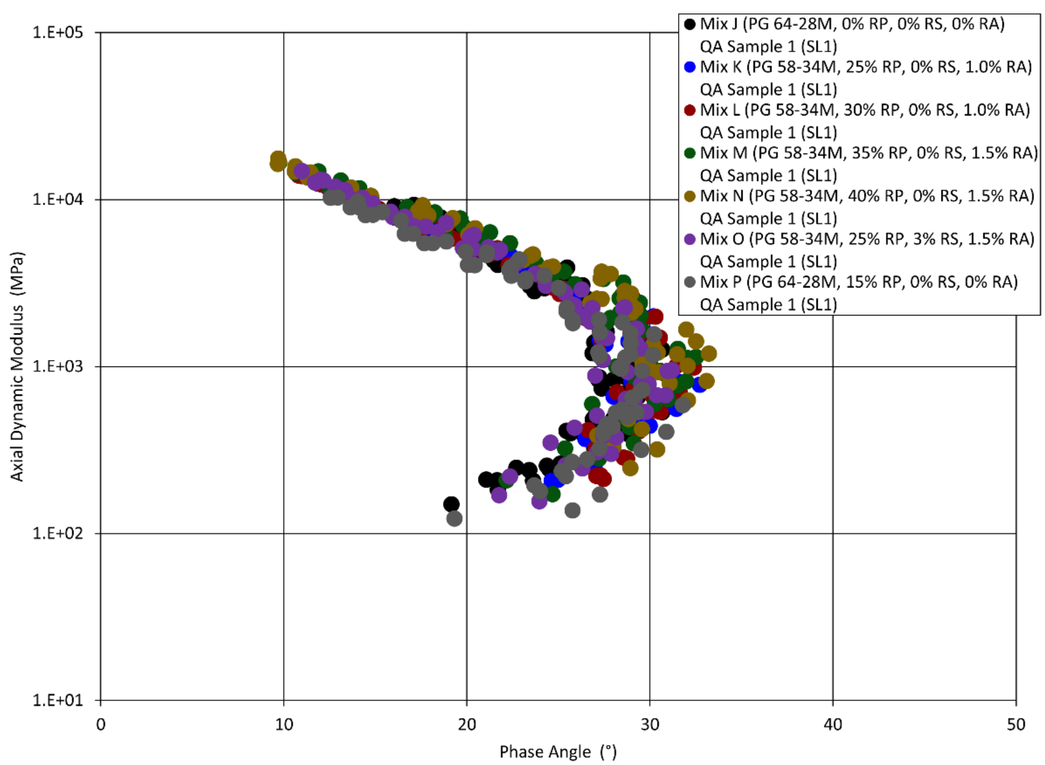

Figure 4.18: Black Space diagram for axial dynamic modulus master curves for QA Sample 1 (SL1).

4.3.4 Qualitative Assessment of Binder Blending from Comparison Binder and Mix Stiffness Rankings

As noted in the problem statement, the degree of blending of the virgin binder, RAP and/or RAS binder, and RA—which in the mix increases as a function of time at elevated temperatures—is an important question. If there is insufficient blending, the use of RAs and softer virgin binders may result in a mix that is prone to rutting and has insufficient binder content for fatigue and fracture resistance. Binder extraction and testing results in complete blending of the three binder components. Mix testing produces results that reflect the actual amount of blending that has occurred after mixing, sampling, and reheating, and also laboratory aging, if it is included in the specimen preparation. Mix testing results are also subject to the variable influences of aggregates at different temperatures and frequencies of loading for axial stiffnesses. In contrast with the axial stiffnesses, for the flexural stiffness there is less aggregate influence at low temperatures and high frequencies.

A qualitative assessment of the degree of binder blending can be made through comparison of binder stiffness testing rankings with mix stiffness testing rankings. Comparisons of the rankings of binder and mix stiffness results at three frequencies at the reference temperature (20°C) are shown in Table 4.10. The effects of aggregate on stiffness are generally least at low temperatures and high frequencies. However, because of the different temperature susceptibilities of virgin and blended binders, assessment of blending only at those conditions may not give a complete picture. The differences in mix stiffness were greatest at intermediate frequencies near 1 Hz at the reference temperature, as seen in the plots of normalized stiffness (Figure 4.12, Figure 4.13, Figure 4.16, Figure 4.17). If the rankings are similar, it is an indication that there are no major differences in binder blending.

Table 4.10: Ranking of Extracted Binder and Mix Stiffnesses from Quality Assurance Testing

QA Binder Testing Shear Stiffness Ranking (stiffest to softest)[a]	Reduced Frequency at 20°C (Hz)	QA Mix Testing Flexural Stiffness Ranking (stiffest to softest)[b]	QA Mix Testing Triaxial Stiffness Ranking (stiffest to softest)[c]
N (stiffest) M/O/L/K, P J (softest)	10^4	N (stiffest) M, O/L, K, P, J (softest)	N (stiffest) M, O, L, K, P J (softest)
N (stiffest) O/M, K/L, P J (softest)	10	N (stiffest) M, O, L, K, P J (softest)	N (stiffest) M, L, O, K, P J (softest)
N (stiffest) O, K, M, L, J P (softest)	10^{-2}	N (stiffest) M, O, L, K, P J (softest)	N (stiffest) M, O/L, K, P J (softest)

[a] Based on data from Figure 3.17.
[b] Based on data from Figure 4.12.
[c] Based on data from Figure 4.16.

Notes: Mix J (0% RAP, 0% RAS), Mix P (15% RAP, 0% RAS), Mix K (25% RAP, 0% RAS), Mix L (30% RAP, 0% RAS), Mix M (35% RAP, 0% RAS), Mix N (40% RAP, 0% RAS), Mix O (25% RAP, 3% RAS).

Overall, the rankings are generally similar between the binder tests and the two types of mix tests across all three frequencies. Mix N with 40% RAP is always the stiffest by far, and the control Mix J with no RAP or RAS is always the softest in eight of the nine comparisons (Mix P is softer for 10^{-2} Hz for the binder testing), with the mainline Mix P being the next softest. Mix K and Mix L, with 25% and 30% RAP, are nearly always the next two stiffest, followed by Mix M with 35% RAP and Mix O with 25% RAP and 3% RAS. The consistent ranking between binder and mix tests indicates that there was generally good blending. The results at the high frequency, corresponding to low temperatures, showed a general reversal of the ranking of Mix M and Mix O. In the binder testing with complete blending, Mix O is stiffer at two frequencies and similar at one frequency to Mix M, while in the mix testing, Mix M is consistently stiffer than Mix O. The significantly higher stiffness results for all the mixes with high RAP/RAS are likely indications of low RA dosages along with nearly complete binder blending within the asphalt mixes.

4.3.5 Rutting Resistance: Repeated Load Triaxial Test (Unconfined and Confined)

Repeated load triaxial (RLT) test results for both QA sublots are shown in terms of repetitions to 3% permanent axial strain and repetitions to flow number for unconfined testing at 50°C (122°F) in Figure 4.19. The flow condition was originally postulated to relate to a critical level of densification under traffic at which permanent deformation accelerates *(23)* but has also been postulated and observed to often be related to internal cracking *(24)*, which is not a phenomenon expected to be related to rutting in the field. On the other hand, the permanent axial deformation versus load repetitions in the RLT has been shown to generally correlate with repeated shear at constant height test results, which in turn are well correlated with field rutting performance *(25)*.

The control mix with no RAP (Mix J) and the mix with 25% RAP (Mix K) had the lowest resistance to permanent deformation, while the 35% and 40% RAP mixes (Mixes M and N) consistently had the highest resistance, including much higher resistance than the mainline mix with 15% RAP (Mix P).

There was high variability between sublots for Mix M and Mix N. The high rutting resistance for the second sublot of Mix M and both sublots of Mix N is likely partially attributable to their lower total binder contents, which were shown in Figure 4.3. The flow number results generally followed the same trends as the repetitions to 3% permanent axial strain, though with a smaller range of differences. The second sublot of Mix N had a low flow number but relatively high resistance to permanent deformation.

RLT test results for the first QA sublot are shown in terms of repetitions to 3% permanent axial strain and repetitions to flow number for confined testing at 45°C (113°F) in Figure 4.20. The results show that none of the mixes reached 3% permanent axial strain. The 40% RAP mix (Mix N) had the highest flow number, which is assumed to indicate low rutting resistance, though that assessment of the flow number does not match the permanent deformation results. The mixes other than Mix N had generally similar flow numbers, with the control mix with no RAP and the 25% RAP mix having the lowest flow numbers.

RLT test results for the first QA sublot are shown in terms of repetitions to 3% permanent axial strain and repetitions to flow number for confined testing at 55°C (131°F) in Figure 4.21. The results show that none of the mixes reached 3% permanent axial strain except for the control mix with no RAP (Mix J). The 40% RAP mix (Mix N) again had the highest flow number (best resistance to permanent deformation), while the control mix and the 25% RAP mix with RA (Mix K) had the lowest flow numbers.

RLT test results for both QA sublots are shown in terms of permanent deformation versus test cycles for unconfined testing at 50°C (122°F) in Figure 4.22. They are shown for QA SL1 for confined conditions at 45°C (113°F) and 55°C (131°F) in Figure 4.23 and Figure 4.24, respectively. The results are generally consistent, with the control mix with no RAP (Mix J) having the worst (highest) permanent deformation and the first sublot of the 40% RAP mix (Mix N) and the 35% RAP mix (Mix M) having the lowest or among the lowest permanent deformations. The 25% RAP/3% RAS mix with recycling agent (Mix O) had the second or third highest permanent deformations under all testing conditions.

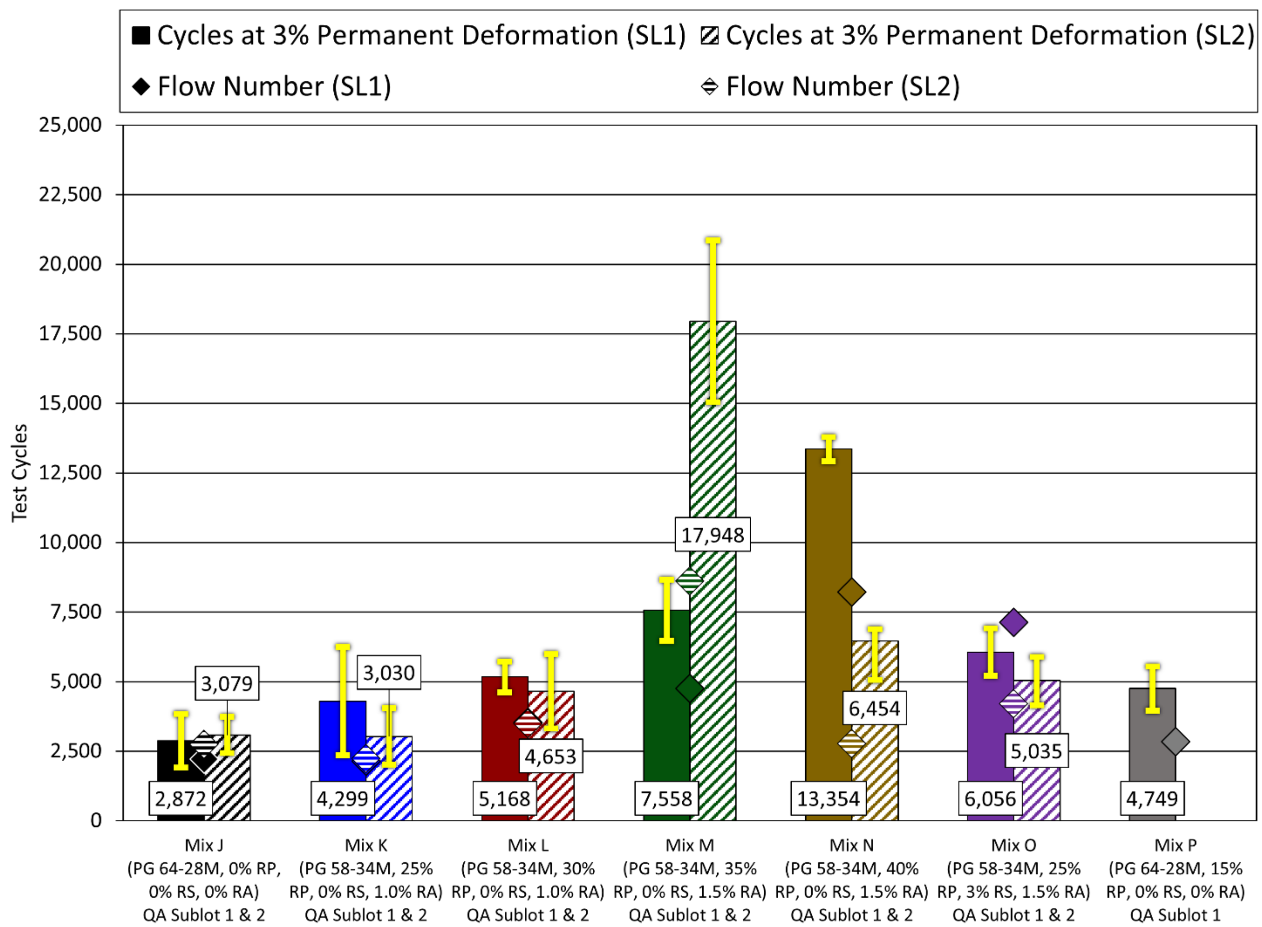

Figure 4.19: Unconfined repeated load triaxial results for both QA SL1 and SL2 of sampled mixes at 50°C (test cycles at 3% permanent deformation and flow number).

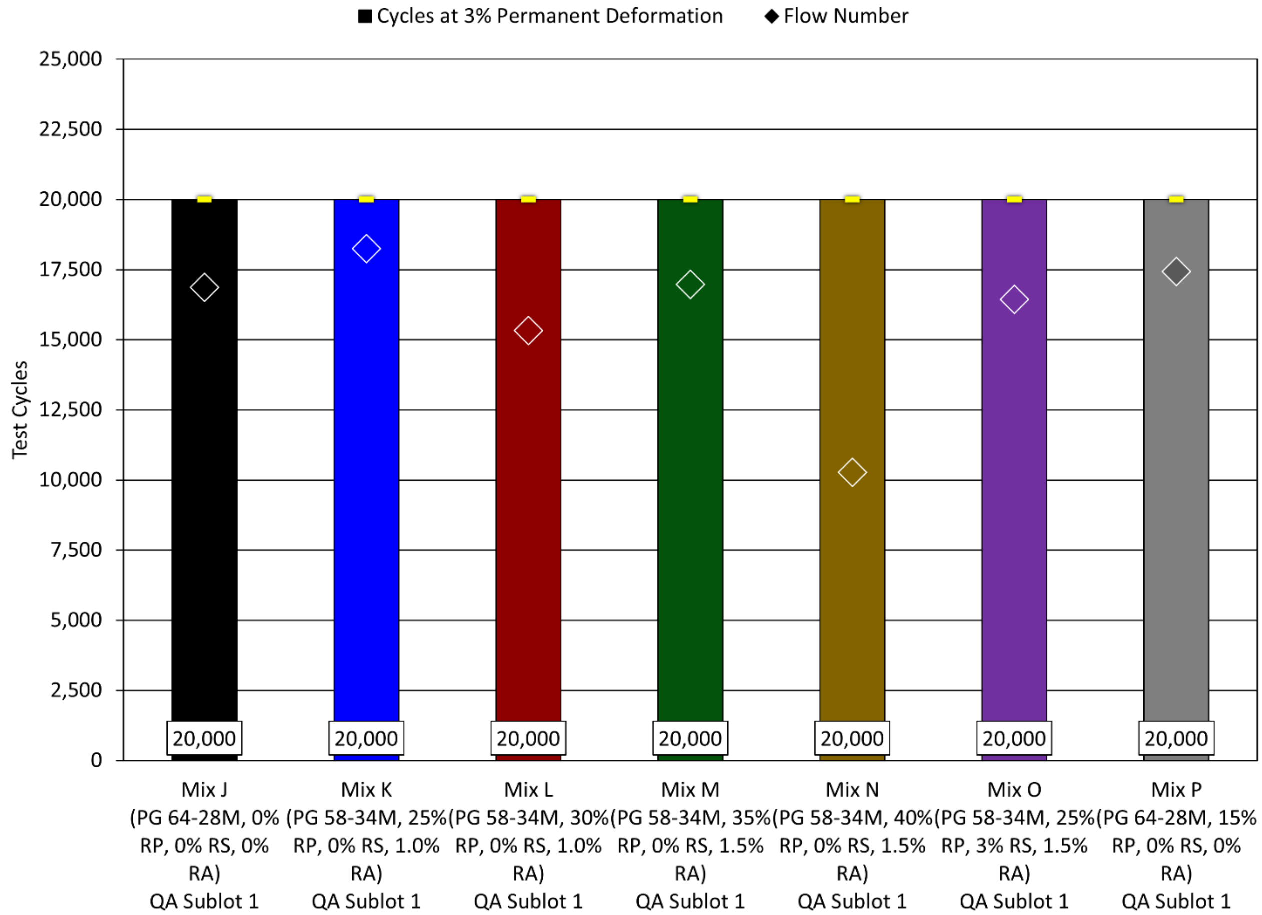

Figure 4.20: Confined repeated load triaxial results for QA SL1 sampled mixes at 45°C (test cycles at 3% permanent deformation and flow number).

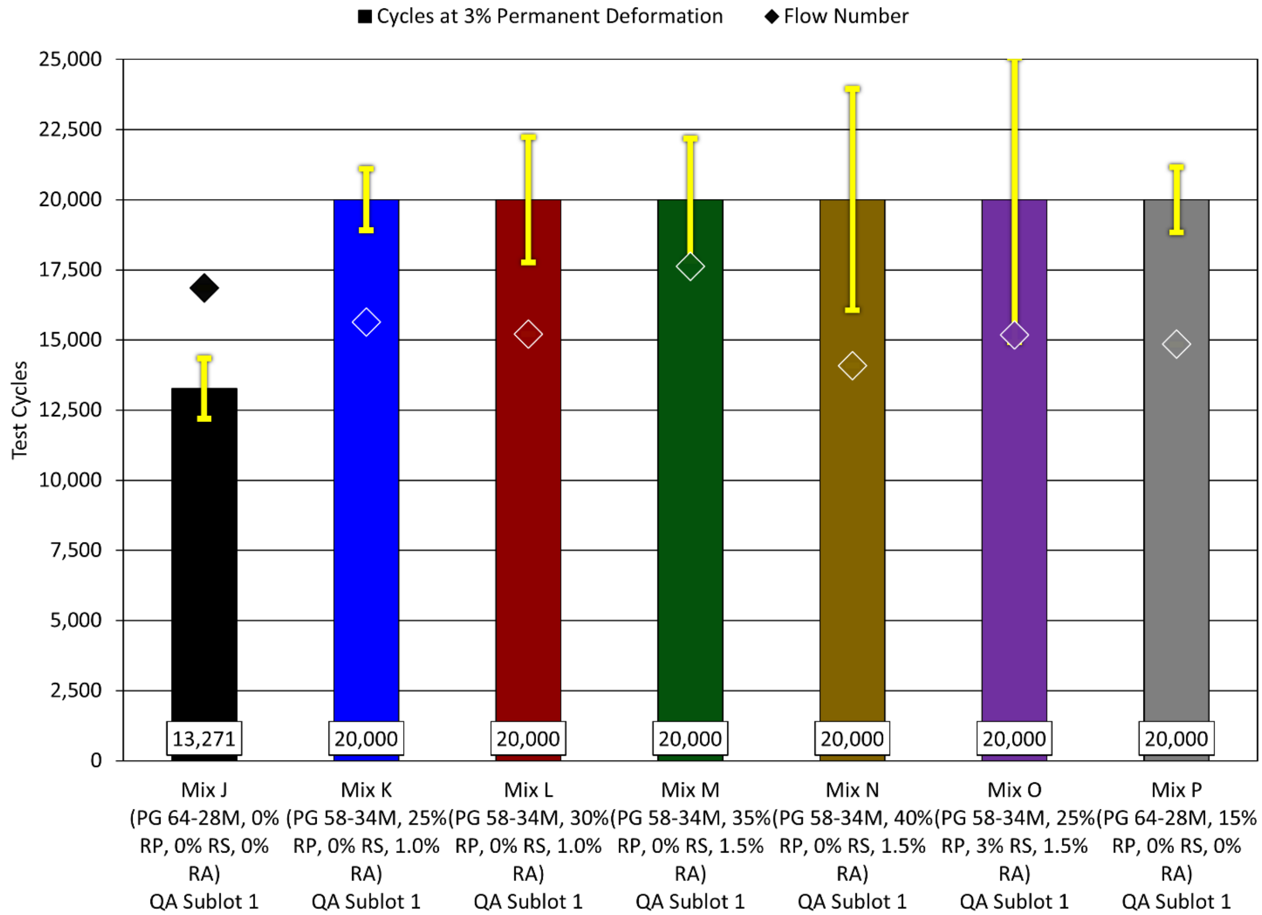

Figure 4.21: Confined repeated load triaxial results for QA SL1 sampled mixes at 55°C (test cycles at 3% permeant deformation and flow number).

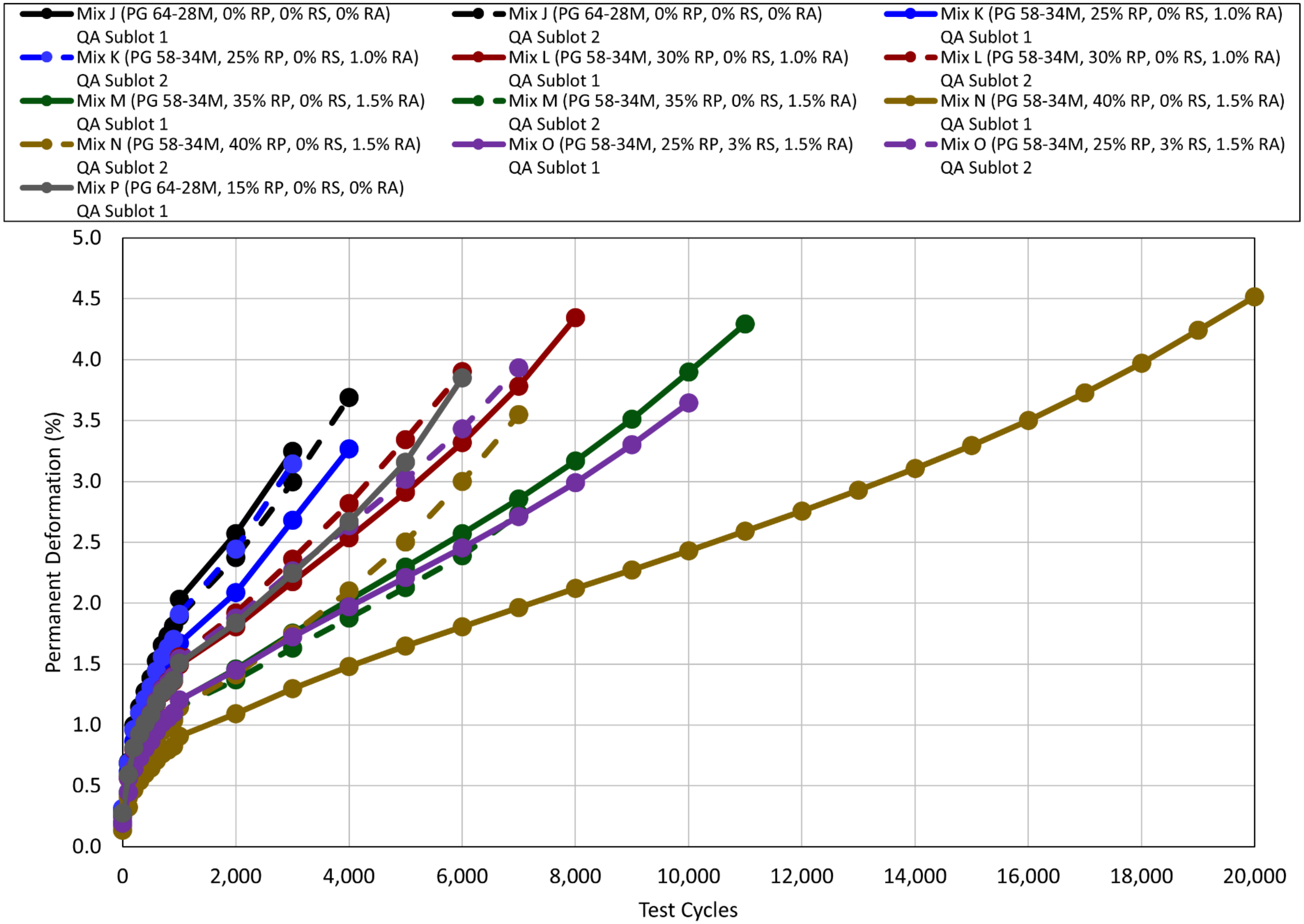

Figure 4.22: Unconfined repeated load triaxial results for QA SL1 and SL2 sampled mixes at 50°C (test cycles and permanent deformation).

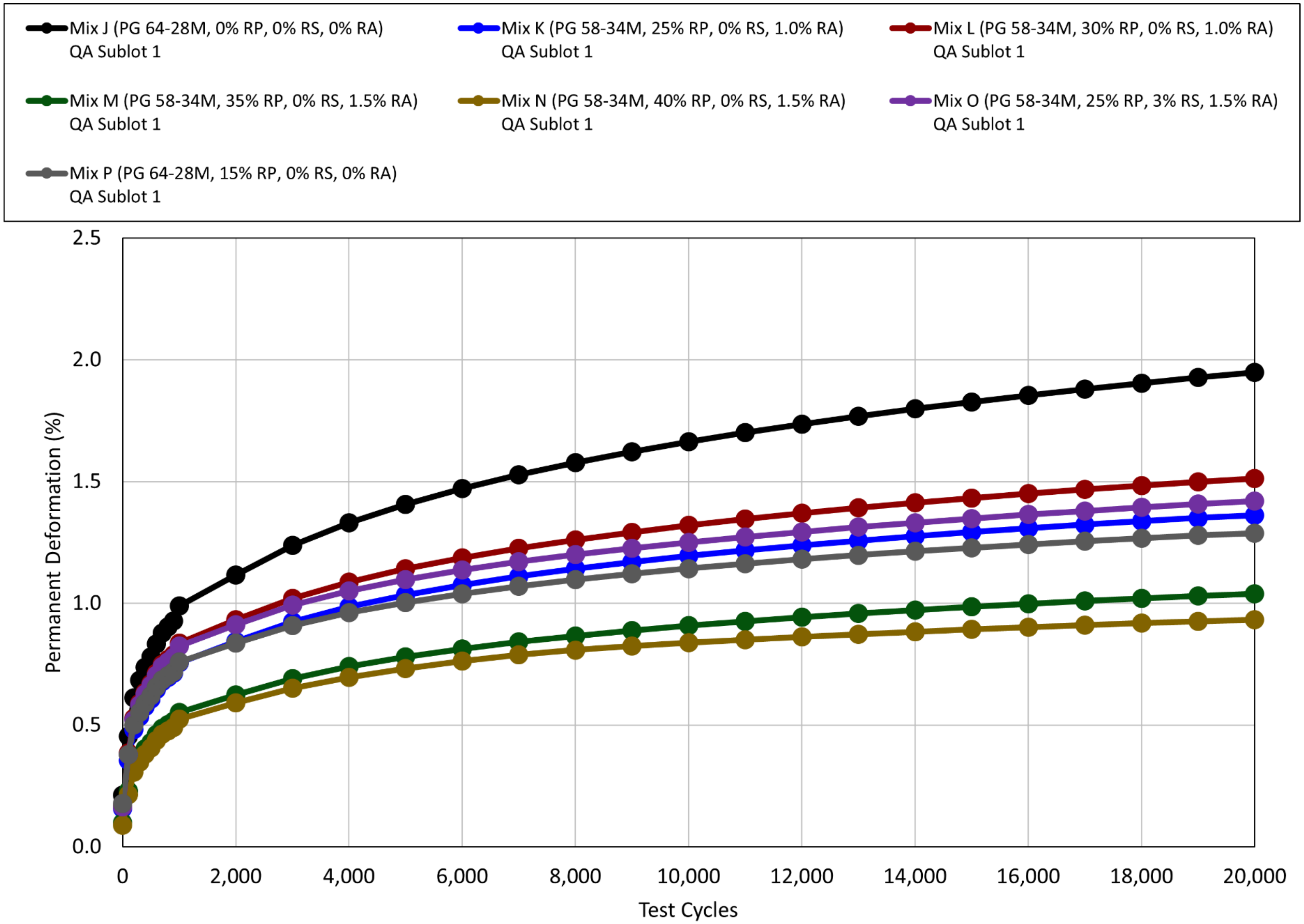

Figure 4.23: Confined repeated load triaxial results for QA SL1 sampled mixes at 45°C (test cycles and permanent deformation).

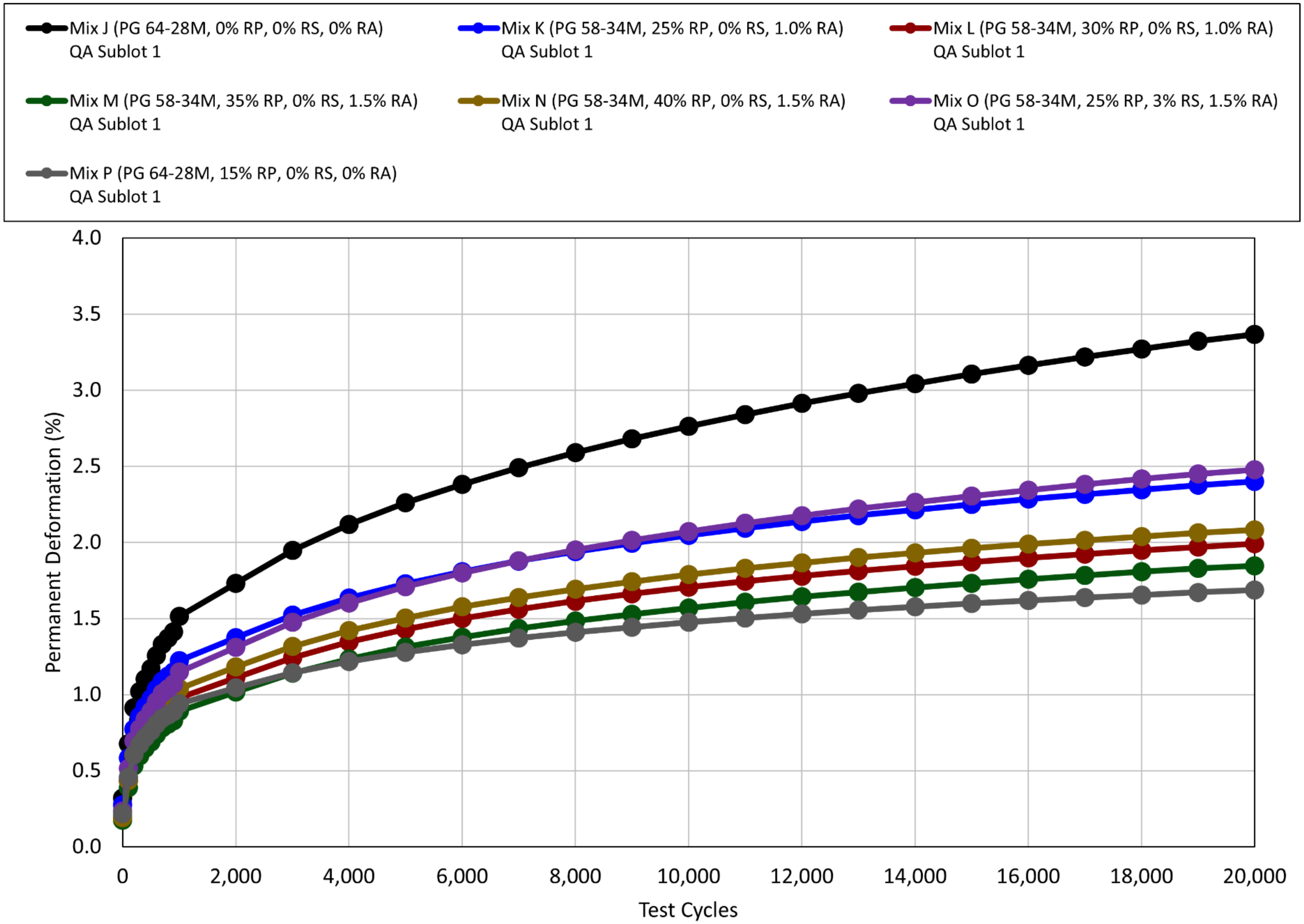

Figure 4.24: Confined repeated load triaxial results for QA SL1 sampled mixes at 55°C (test cycles and permanent deformation).

4.3.6 Fatigue/Reflective Cracking Resistance: Four-Point Beam Test

Figure 4.25 shows flexural fatigue test results for the first QA sample for each of the seven mixes in terms of Wöhler curve trend lines (log of tensile strain versus log of fatigue life). For the range of tensile strain levels used in testing (primarily 400 to 1000 με), the fatigue results are approximately the opposite of the RLT results for permanent deformation, with the 40% RAP mix that also had lower binder content (Mix N) having the worst performance and the control mix with no RAP (Mix J) having the best performance. These strain levels were selected for each mix to survive approximately 1 million and 250,000 cycles to failure, with the strains meeting these criteria differing between mixes. The 35% RAP mix (Mix M) and the 25% RAP/3% RAS mix (Mix O) generally had the next worst fatigue performance, depending on the strain level. The mainline mix (Mix P) with 15% RAP and no recycling agent and the 30% RAP mix with RA (Mix L) were among the top three performing mixes.

The regressions from Wöhler curves have generally been found over many decades of research and practice to provide reasonable estimates when extrapolated in the approximate range of 200 to 700 με, except for polymer and rubber modified mixes that tend to have much longer fatigue lives than extrapolation would indicate at strains smaller than 200 με. Figure 4.26 shows the same fatigue test data points and the regression lines for the Wöhler curve through the combined QA sample data sets for each mix extrapolated to the 200 to 800 με range. These results indicate that the 40% RAP mix (Mix N) had the highest sensitivity of fatigue life to tensile strain but remained among the worst performers even at very low extrapolated strain levels. The rankings of the mixes at low strain levels, which would be expected in thicker asphalt pavement and overlays, remain similar to the rankings at the higher strains. Higher strains would be expected in thinner overlays.

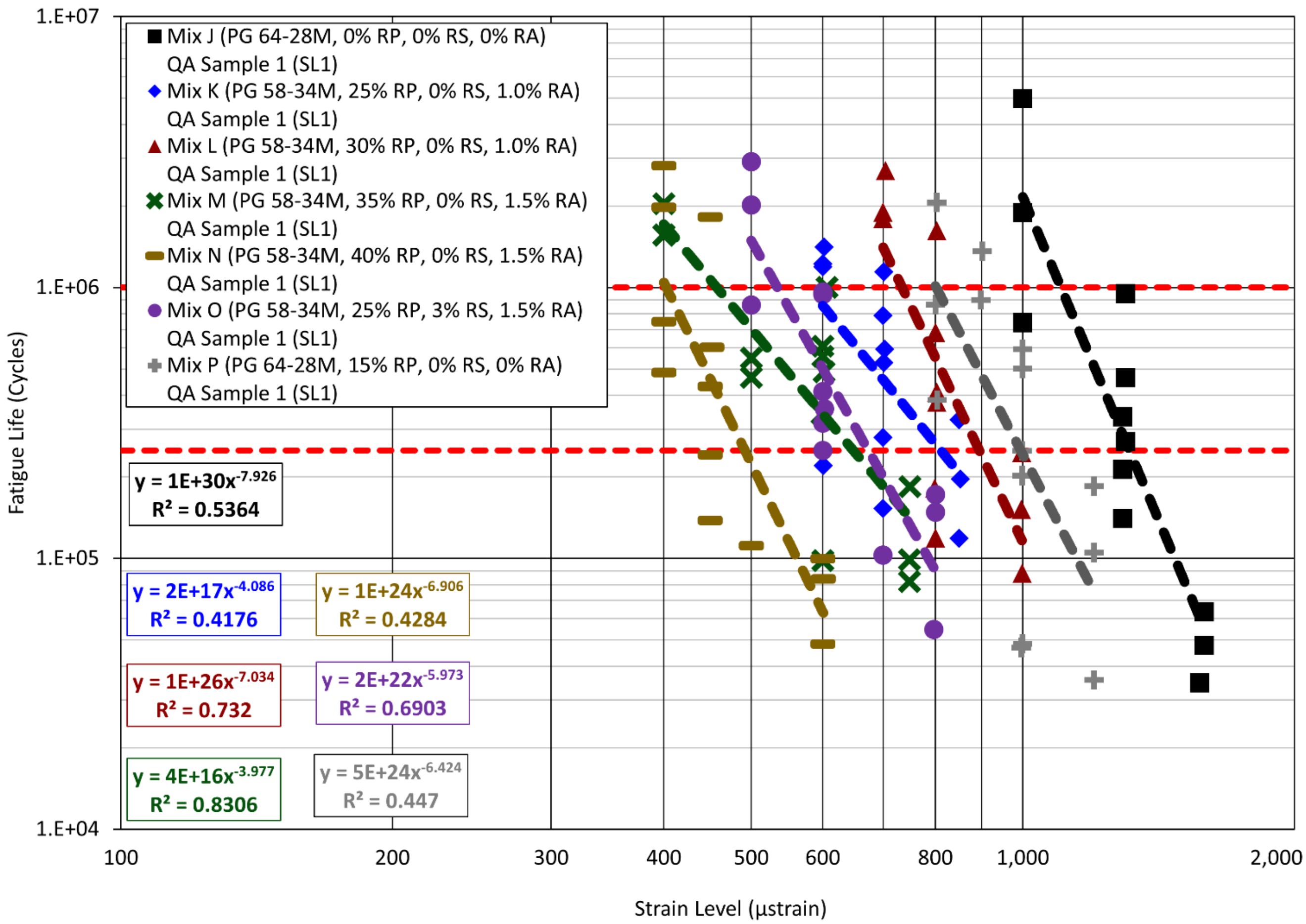

Figure 4.25: Flexural fatigue results for QA-sampled mixes (Wöhler curve).

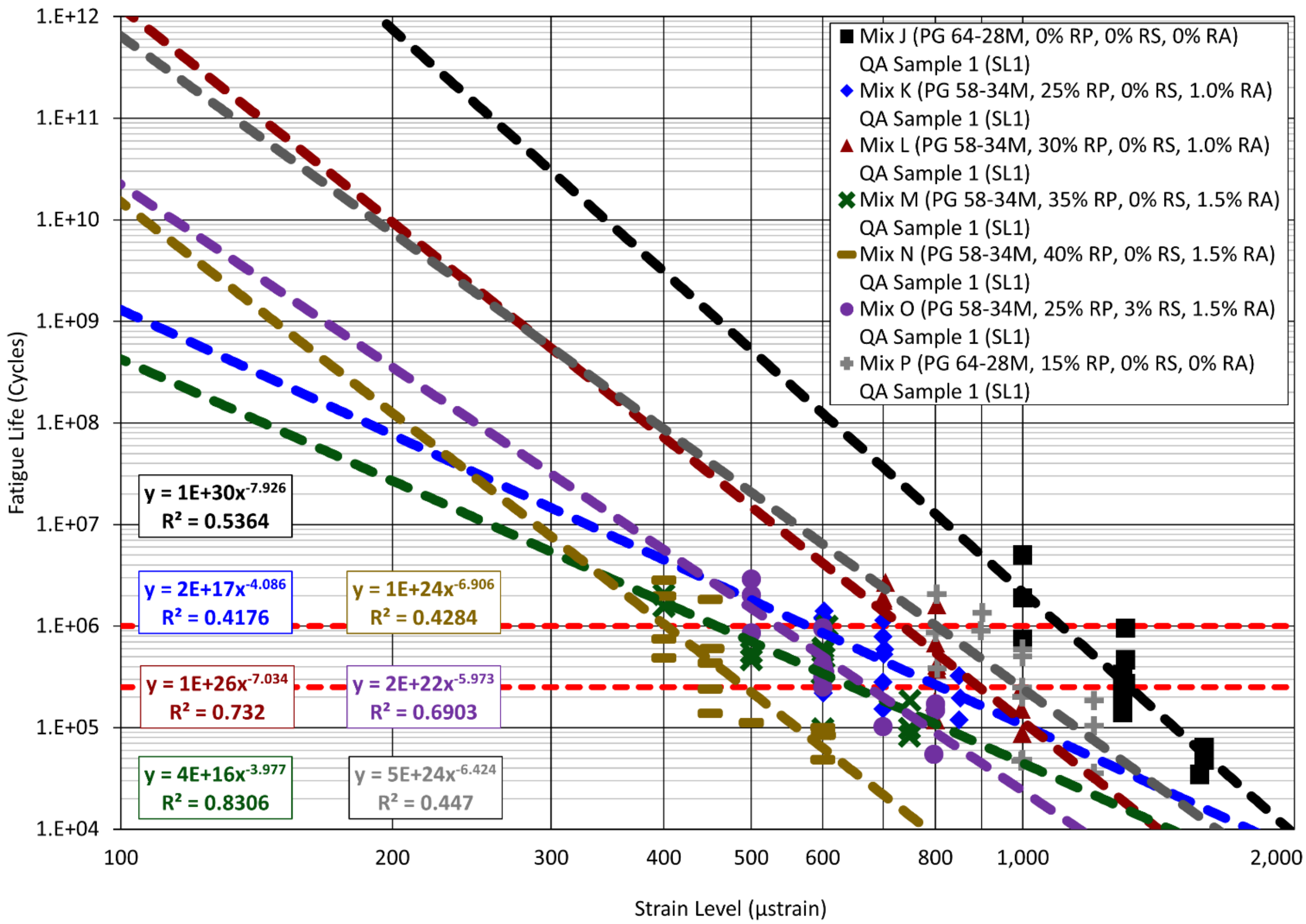

Figure 4.26: Extrapolation of flexural fatigue regression results for QA-sampled mixes (Wöhler curve).

Figure 4.27 and Figure 4.28 show the fitted Wöhler curves of the logs of fatigue life versus strain of all the mixes for strain levels of 200 to 800 µε, normalized to the control mix with no RAP (Mix J) and the mainline mix with 15% RAP (Mix P), respectively. As can be seen in Figure 4.27, all mixes had 90% to 99% less fatigue life than the control mix.

It is interesting to note that the two mixes with the best fatigue performance, the control mix and the mainline mix, used a PG 64-28M binder, while the high RAP and the RAP/RAS mixes used a PG 58-34M binder. It is not known if the fatigue performance of the PG 58-34M virgin binder is worse than that of the PG 64-28M. In general, a softer binder such as the PG 58-34M should have better performance in the laboratory fatigue test at a given strain level than the stiffer PG 64-28M. It is known that binders from different crude oil sources have better or worse fatigue life performance regardless of stiffness. However, these two virgin binders are from the same refiner and would not be expected to have significantly different fatigue properties, which suggests that the differences in fatigue performance are due to the mix designs and the high RAP and RAS content.

The more likely explanation is that polymer-modified binders tend to have better fatigue performance than conventional binders. It would be expected that the RAP and RAS do not have much polymer-modified asphalt material in them because Caltrans uses a small percentage of polymer-modified mixes and local governments use very few, and that the inclusion of more RAP will reduce the amount of binder in the mix that is polymer modified. It can be seen in Figure 4.25 that the ranking of the fatigue lives almost exactly follows the amount of virgin binder replacement, with the most replacement by RAP having the shortest fatigue life, Mix N (40% RAP) and the rest of the mixes having successively better performance as the RAP content diminishes.

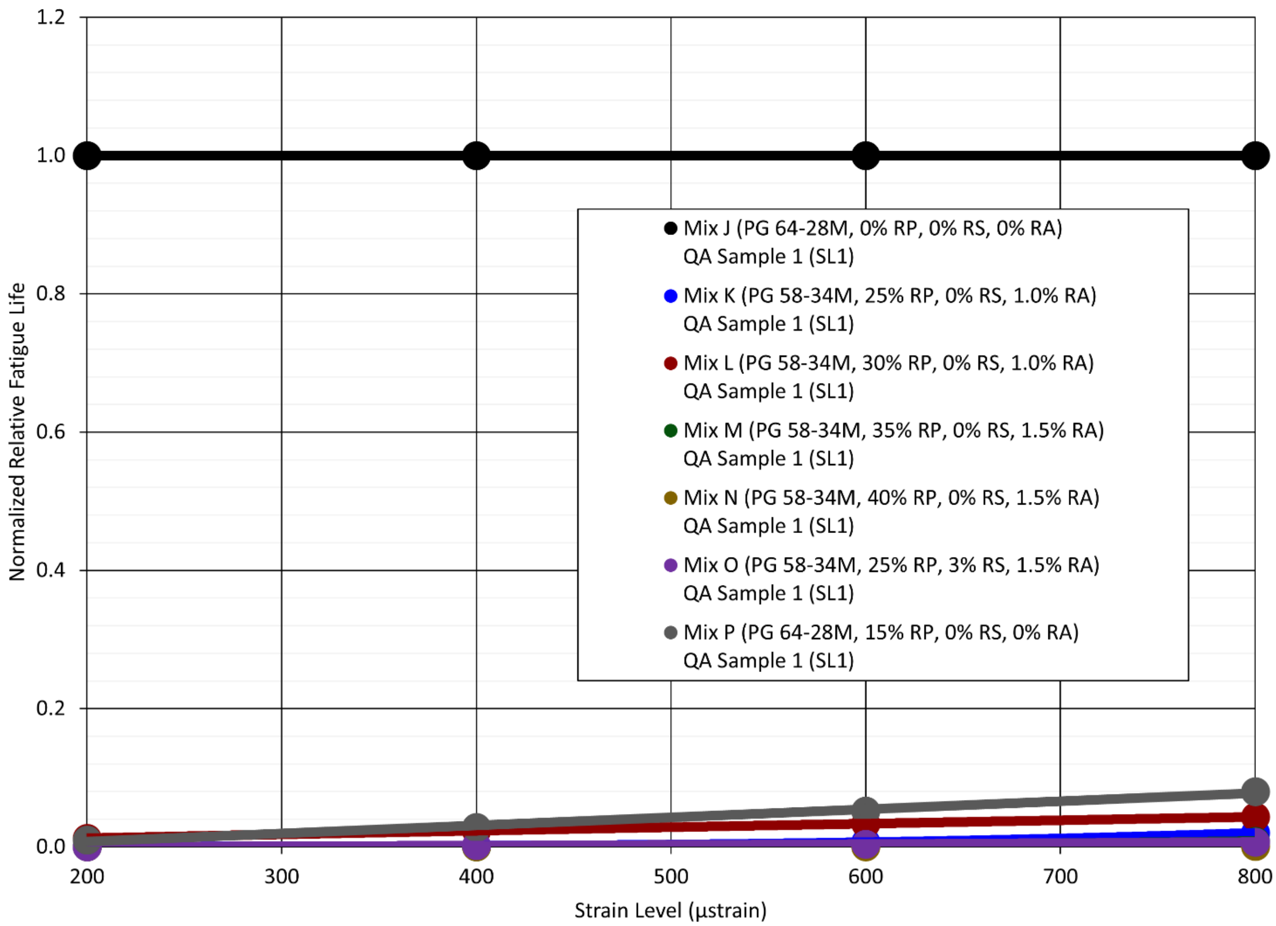

Figure 4.27: Flexural fatigue results for all QA-sampled mixes from Wöhler curve regression, normalized to Mix J.

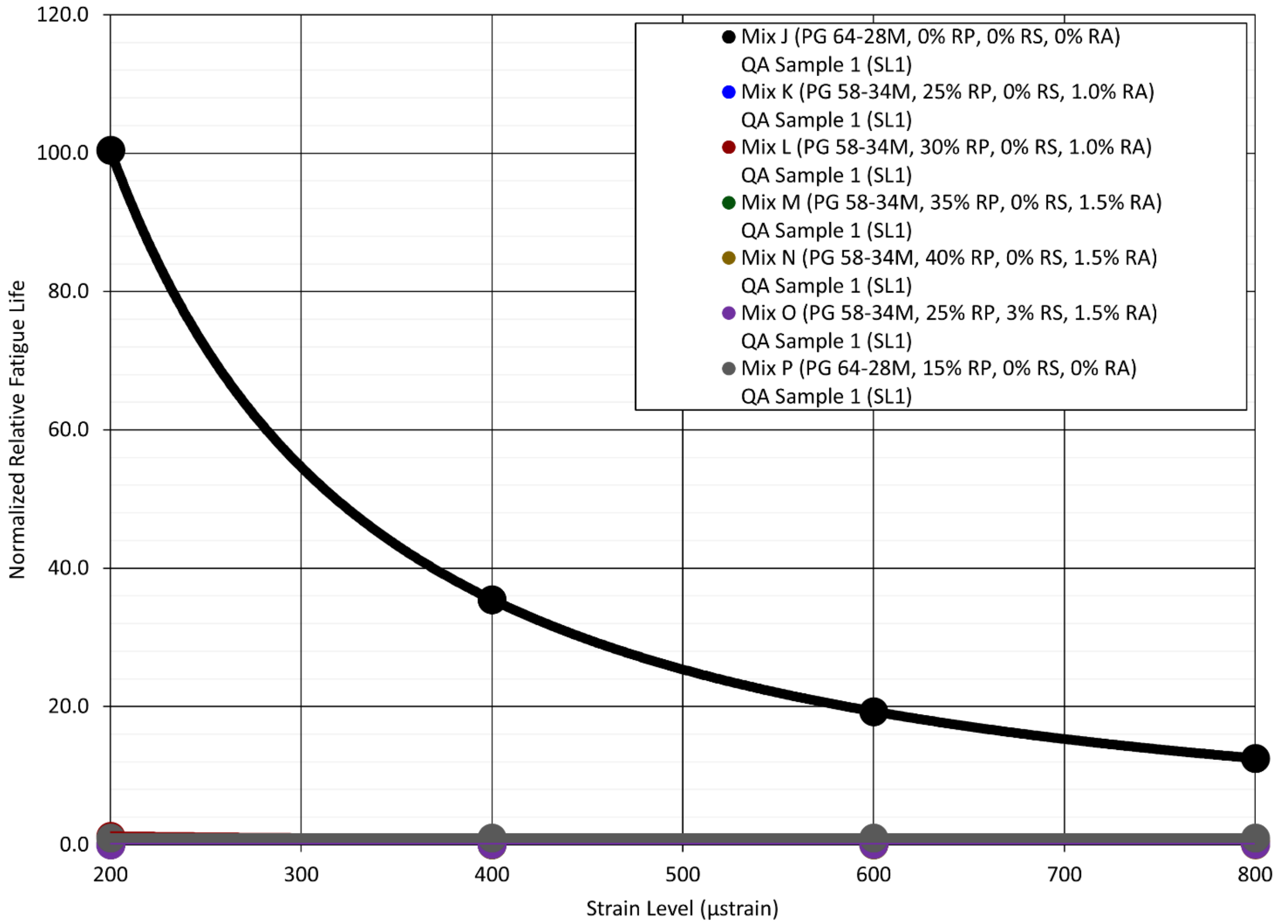

Figure 4.28: Flexural fatigue results for all QA-sampled mixes from Wöhler curve regression, normalized to Mix P (15% RAP).

4.3.7 Indirect Tensile Cracking Resistance: IDEAL-CT Test

IDEAL-CT testing was performed on both QA sublots of materials. The results shown are for samples stored, transported, and reheated in sealed steel buckets. For this pilot project, samples were also collected into cardboard boxes for comparison with the samples collected in buckets. Plots are shown in this section comparing the results for samples collected in boxes versus those collected in metal buckets. Table 4.11 and Table 4.12 show the IDEAL-CT tests results for the bucket sampled and reheated materials for Sample 1 and Sample 2, respectively. IDEAL-CT results for the bucket sampled and MTOA conditioned samples are shown in Appendix B. The tables include comparison of reheated IDEAL-CT results and results after MTOA, following Caltrans provisional reheating and aging protocol CT 320.

Figure 4.29 shows the IDEAL-CT results in terms of the IDEAL-CT number and peak indirect tensile strength for both QA samples after reheating. The results indicate that the ranges of age-related cracking tolerance, measured by the IDEAL-CT cracking tolerance (CT #), were similar for all the mixes after reheating. The differences between sublots of the same mix were a similar magnitude as the differences between the mixes. One of the sublots for each the mixes with 30%, 35% and 40% RAP and both sublots for the 25% RAP mix did not meet the specification limit of a minimum value of 51.7, as shown in the figure. On the other hand, it can be seen in the figure that the strength value was sensitive to the RAP in the mix and generally followed the percentage of RAP in the mix, with the lowest strength value for the control mix with no RAP (Mix J) and the highest strengths for the mixes with 35% and 40% RAP (Mix M and Mix N).

It is interesting to note that IDEAL-CT cracking tolerance values are very similar while the strengths are quite different. Strength values have been shown to have a high correlation with stiffness, and higher stiffness mixes tend to have lower fatigue values at a given tensile strain. These strength results inversely match the fatigue results shown in the previous section, which follows the expected trend of increased stiffness—in this case, based on the surrogate property of strength, causing shorter fatigue lives. That trend is followed here, but in other sets of mixes that have been tested by the UCPRC it is not always followed because there are some binders with poorer or better fatigue performance at given strain, even when they have the same stiffness. It is also interesting to note that the IDEAL-CT cracking tolerance value did not show sensitivity to the replacement of polymer-modified virgin binder with the RAP binder, which is expected to have a low percentage of polymer-modified binder in it.

Figure 4.30 shows the results for fracture energy and post-peak slope for the reheated samples of both QA sublots. Fracture energy shows a strong sensitivity to increased RAP content and the corresponding reduction in polymer-modified binder in the binder blend. Post-peak slope also shows strong sensitivity. Both values are used in calculation of the IDEAL-CT cracking tolerance value, with lower post-peak strengths and higher fracture energies contributing to higher cracking tolerance values. It appears that the two effects may have canceled each other out in the calculation of the cracking tolerance value for these mixes.

Table 4.11: IDEAL-CT Results of Reheated vs MTOA-aged Bucket Samples for SL1 Samples

Mix ID	Reheat Cracking Tolerance (CT Index)	Greater Than JMF Target? (CT # = 50.4)	MTOA-Aged Cracking Tolerance (CT Index)	Change After MTOA (%)	Reheat Strength (psi)	MTOA-Aged Strength (psi)	Change After MTOA (%)
Mix J (PG 64-28M, 0% RP, 0% RS, 0% RA) QA Sample 1 (SL1)	62.5	Yes	33.7	-46	73	89	22
Mix K (PG 58-34M, 25% RP, 0% RS, 1.0% RA) QA Sample 1 (SL1)	49.7	No	39.6	-20	108	128	19
Mix L (PG 58-34M, 30% RP, 0% RS, 1.0% RA) QA Sample 1 (SL1)	68.2	Yes	51.3	-25	119	127	7
Mix M (PG 58-34M, 35% RP, 0% RS, 1.5% RA) QA Sample 1 (SL1)	64	Yes	36.2	-43	127	136	7
Mix N (PG 58-34M, 40% RP, 0% RS, 1.5% RA) QA Sample 1 (SL1)	40.5	No	27	-33	138	167	21
Mix O (PG 58-34M, 25% RP, 3% RS, 1.5% RA) QA Sample 1 (SL1)	56.3	Yes	36	-36	105	127	21
Mix P (PG 64-28M, 15% RP, 0% RS, 0% RA) QA Sample 1 (SL1)	52.6	Yes	37.5	-29	99	108	9
			Average:	-33		**Average:**	15
			Standard Deviation:	9		**Standard Deviation:**	7

Table 4.12: IDEAL-CT Results of Reheated vs MTOA-aged Bucket Samples for SL2 Samples

Mix ID	Reheat Cracking Tolerance (CT Index)	Greater Than JMF Target? (CT = 50.4)	MTOA-Aged Cracking Tolerance (CT Index)	Cracking Tolerance Change After MTOA (%)	Reheat Strength (psi)	MTOA-Aged Strength (psi)	Strength Change After MTOA (%)
Mix J (PG64-28M, 0% RP, 0% RS, 0% RA) QA Sample 1 (SL2)	71.6	Yes	36	-50	69	82	19
Mix K (PG58-34M, 25% RP, 0% RS, 1.0% RA) QA Sample 1 (SL2)	49.3	No	35.1	-29	113	129	14
Mix L (PG58-34M, 30% RP, 0% RS, 1.0% RA) QA Sample 1 (SL2)	50.2	No	48.7	-3	117	124	6
Mix M (PG58-34M, 35% RP, 0% RS, 1.5% RA) QA Sample 1 (SL2)	43.5	No	24.7	-43	137	157	15
Mix N (PG58-34M, 40% RP, 0% RS, 1.5% RA) QA Sample 1 (SL2)	56	Yes	39.1	-30	132	137	4
Mix O (PG58-34M, 25% RP, 3% RS, 1.5% RA) QA Sample 1 (SL2)	76.9	Yes	47.4	-38	102	128	25
			Average:	-32		**Average:**	14
			Standard Deviation:	16		**Standard Deviation:**	8

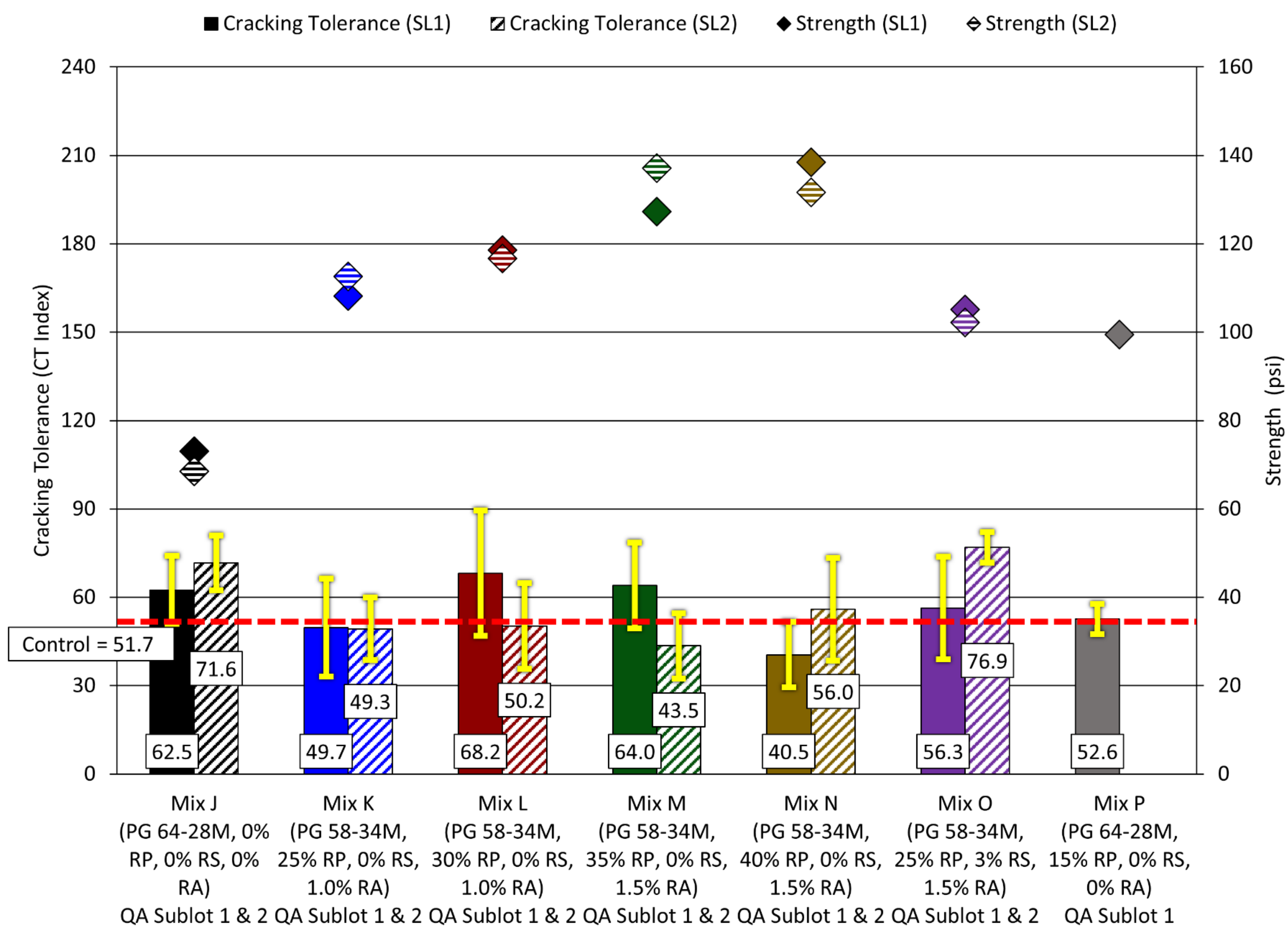

Figure 4.29: IDEAL-CT results for sublot 1 and sublot 2 QA reheated bucket mixes (cracking tolerance index and indirect tensile strength).

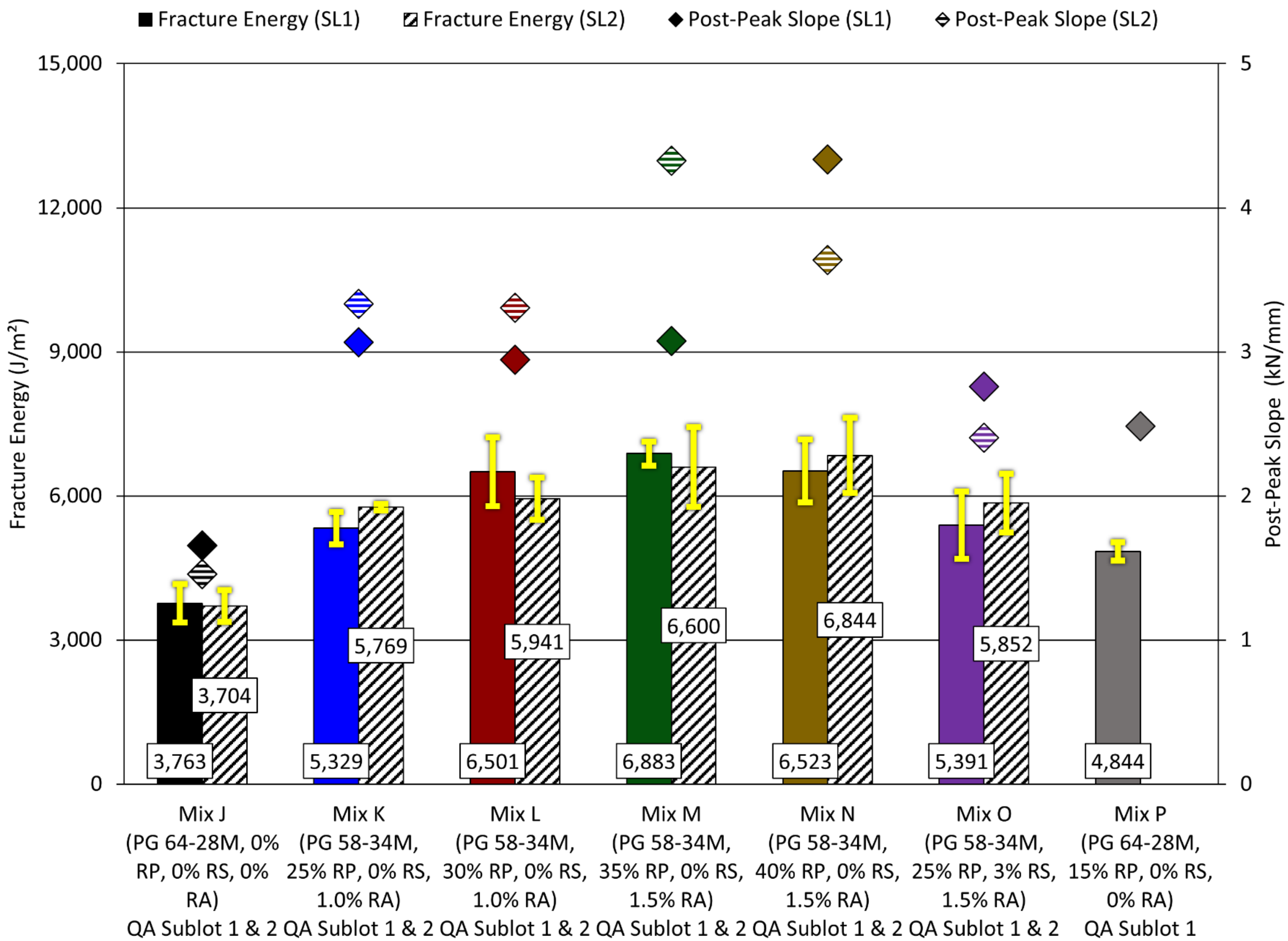

Figure 4.30: IDEAL-CT results for sublot 1 and sublot 2 QA reheated bucket mixes (fracture energy and post-peak slope).

Figure 4.31 shows the IDEAL-CT results in terms of the IDEAL-CT number and peak indirect tensile strength for both QA samples after MTOA. The results show that the MTOA conditioning decreases the IDEAL-CT cracking tolerance value and increases the strength. It was shown in Table 4.11 and Table 4.12 that reduced the cracking tolerance values and increased strengths caused by MTOA were consistent on average across all mixes for the two sublets, with a cracking tolerance reduction of 32% to 33% and strength increase of 14% and 15% for the two sublots, respectively. There was no consistent trend between how much RAP was in the mix and how much the MTOA reduced the cracking tolerance value and increased the strength value. Figure 4.32 shows the results for the fracture energy and the post-peak strength. Fracture energy increased slightly after MTOA consistently across all mixes, while post-peak slopes decreased after MTOA with greater sensitivity to the oven aging than post-peak slope and greater variability between sublots.

Figure 4.33 and Figure 4.34 show the IDEAL-CT load-displacement curves for the first and second QA sublot mixes after reheating and MTOA, respectively. MTOA generally can be seen to cause an increase in peak strength and steepening of the post-peak displacement curves for all mixes. Variability can be seen between the two sublots for the reheated mixes, and variability can also be seen in the response to MTOA between the first and second QA sublots of each mix.

Figure 4.35 shows a comparison of the IDEAL-CT cracking tolerance value for box and bucket sampled mixes, and Figure 4.36 shows the same comparison for the IDEAL-CT indirect tensile strength value. It can be seen in Figure 4.35 that there is a general trend of equality between the two sampling methods for the cracking tolerance value, likely reflecting the generally higher variability of that parameter. Figure 4.36 shows a strong trend between the two sampling methods, indicating that the sampling method had essentially no effect on the results.

Figure 4.37 shows a comparison of the IDEAL-CT cracking tolerance value for reheated and MTOA-conditioned mixes, and Figure 4.38 shows the same comparison for the IDEAL-CT indirect tensile strength value. The generally high variability of the cracking tolerance value parameter can again be seen in Figure 4.37. It can also be seen from the intercept of the linear trend line that the cracking tolerance value caused a consistent shift in the cracking tolerance value and that the MTOA caused a greater increase of the value for mixes with higher initial reheated values. Figure 4.38 shows a strong trend between the reheated and MTOA-conditioned mixes for the indirect tensile strength, indicating that MTOA caused a generally uniform increase in the strength of approximately 9 psi, regardless of the initial strength.

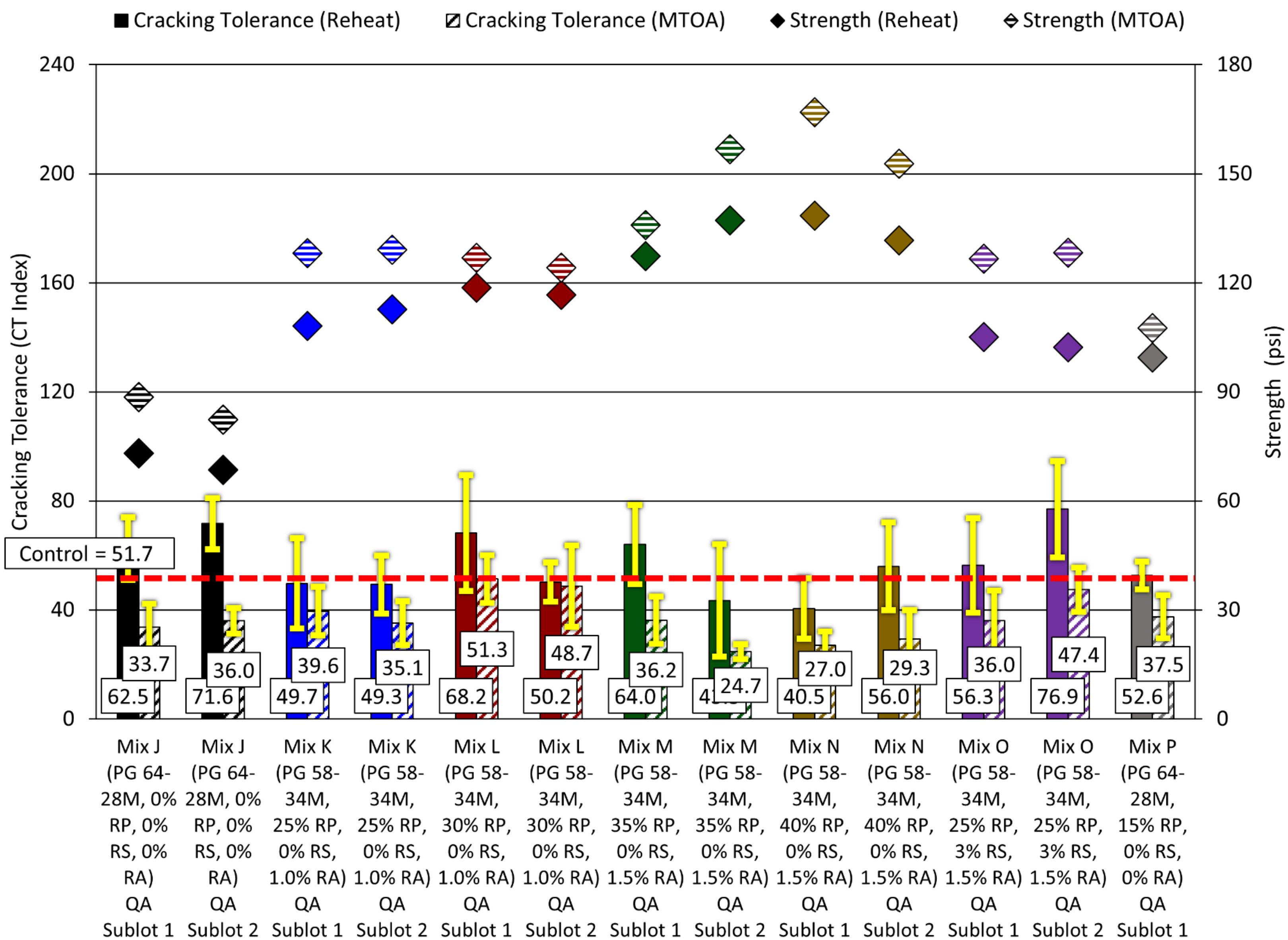

Figure 4.31: IDEAL-CT results for QA SL1 and SL2 bucket mixes for reheated and MTOA conditioning (cracking tolerance index and indirect tensile strength).

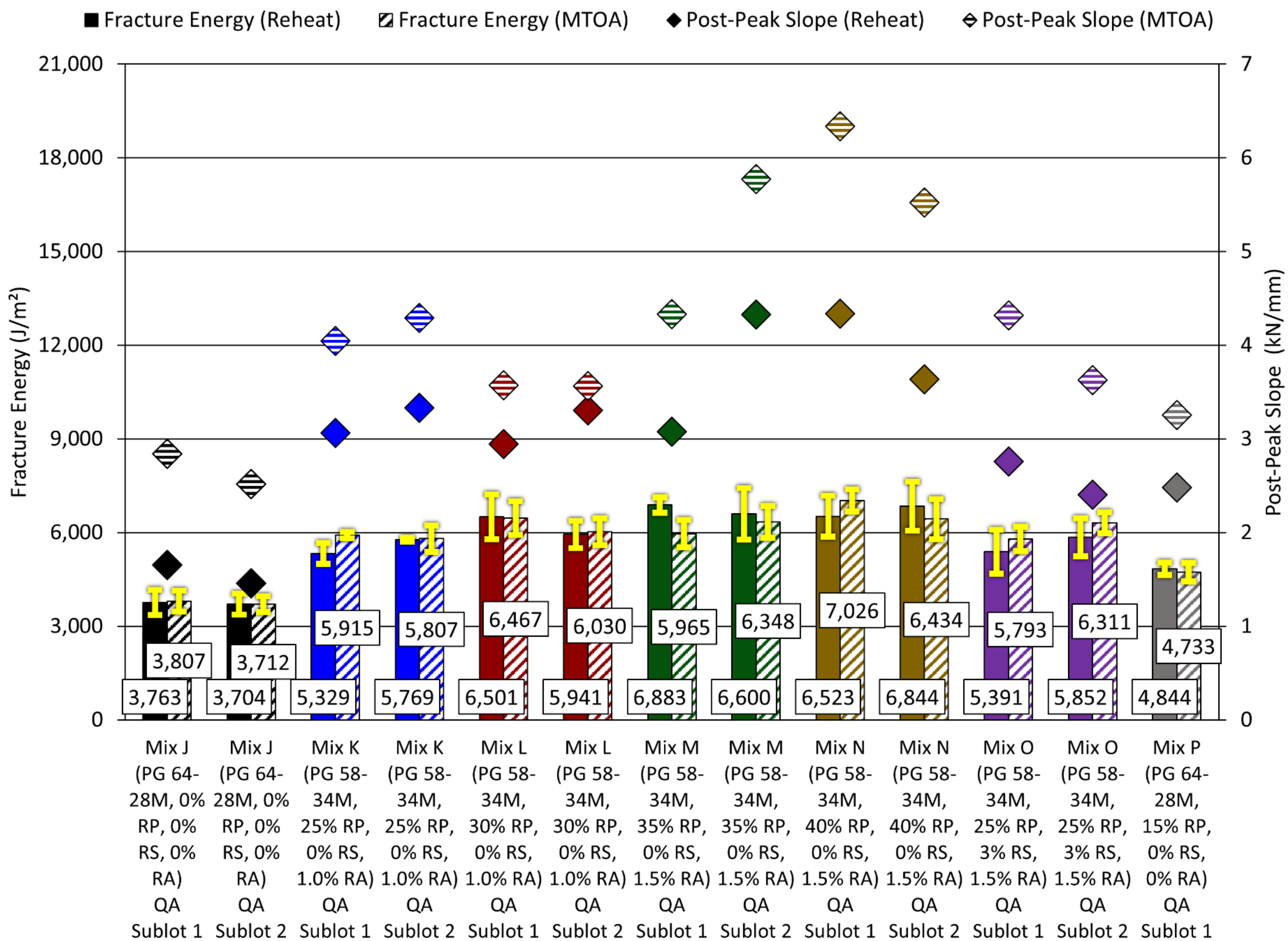

Figure 4.32: IDEAL-CT results for QA SL1 and SL2 bucket mixes for reheated and MTOA conditioning (fracture energy and post-peak slope).

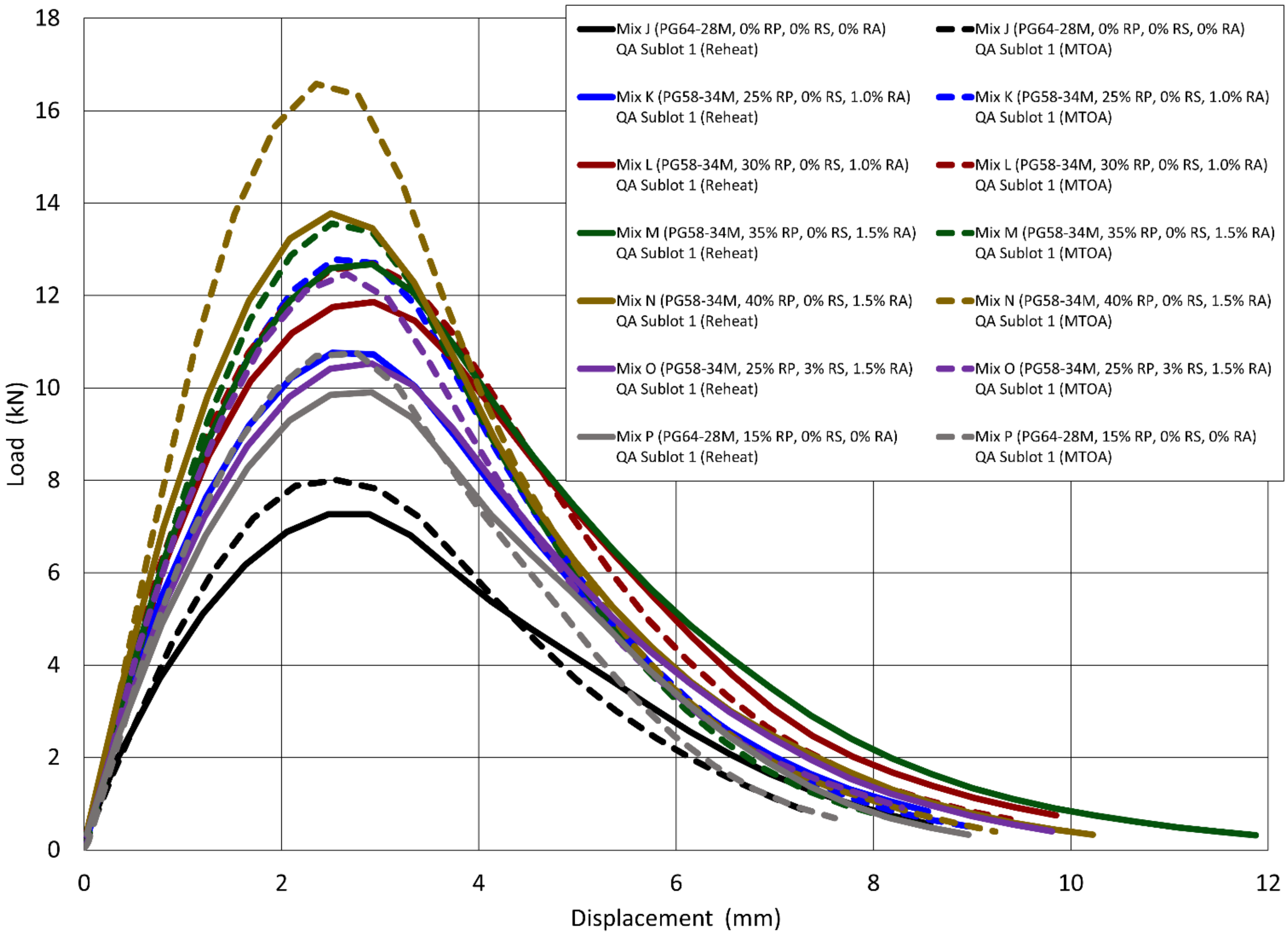

Figure 4.33: IDEAL-CT results for QA SL1 box mixes for reheated and MTOA conditioning (load-displacement graph).

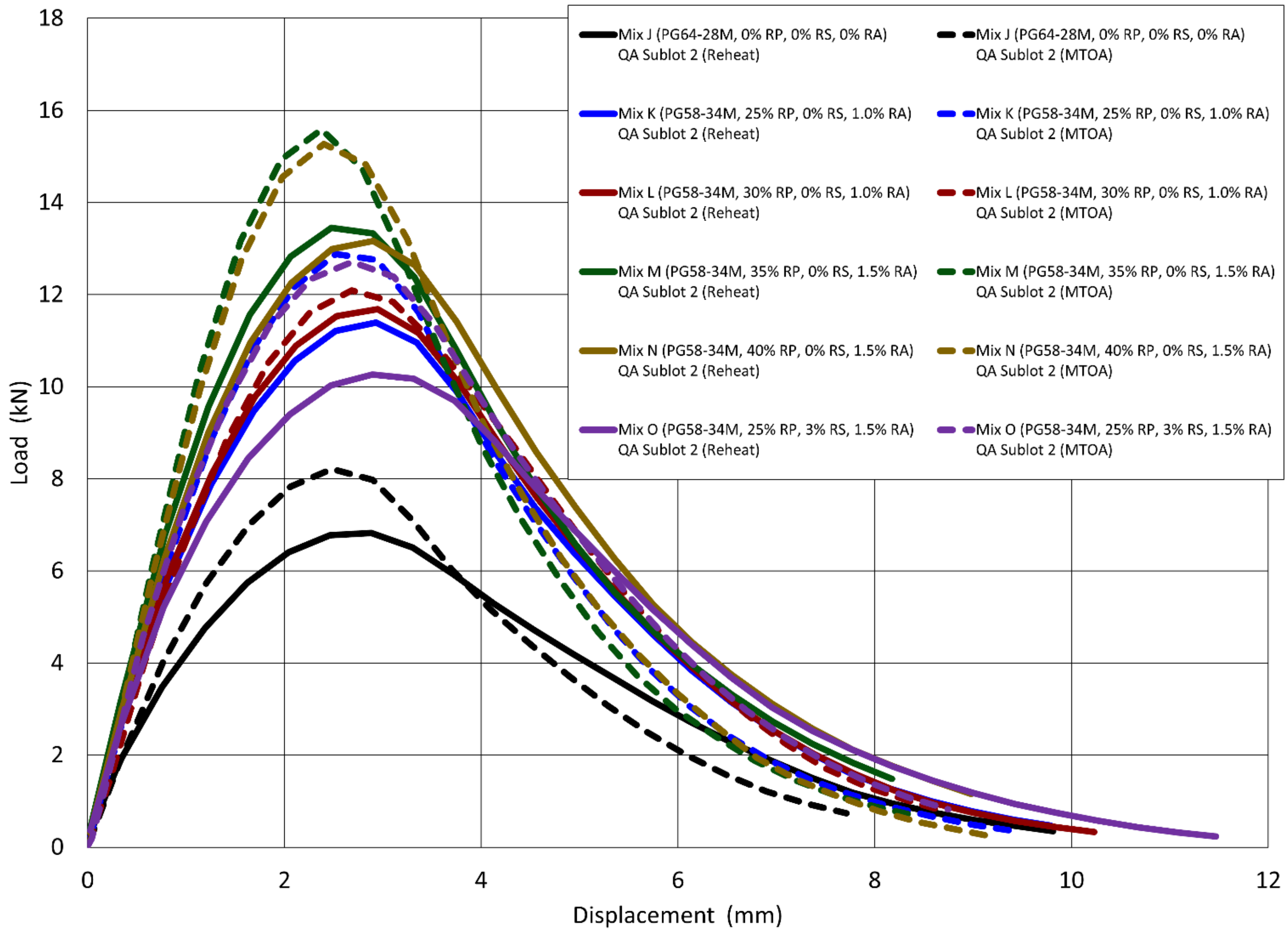

Figure 4.34: IDEAL-CT results for QA SL2 box mixes for reheated and MTOA conditioning (load-displacement graph).

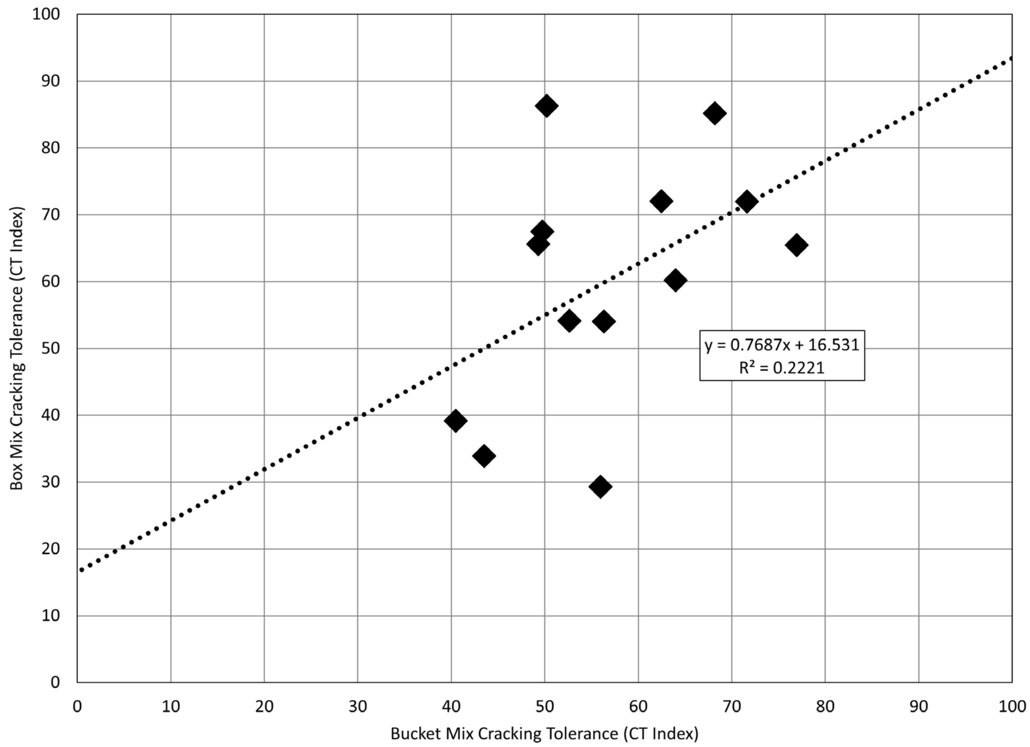

Figure 4.35: Comparison of IDEAL-CT cracking tolerance value for box versus bucket sampled mix for SL1 and SL2.

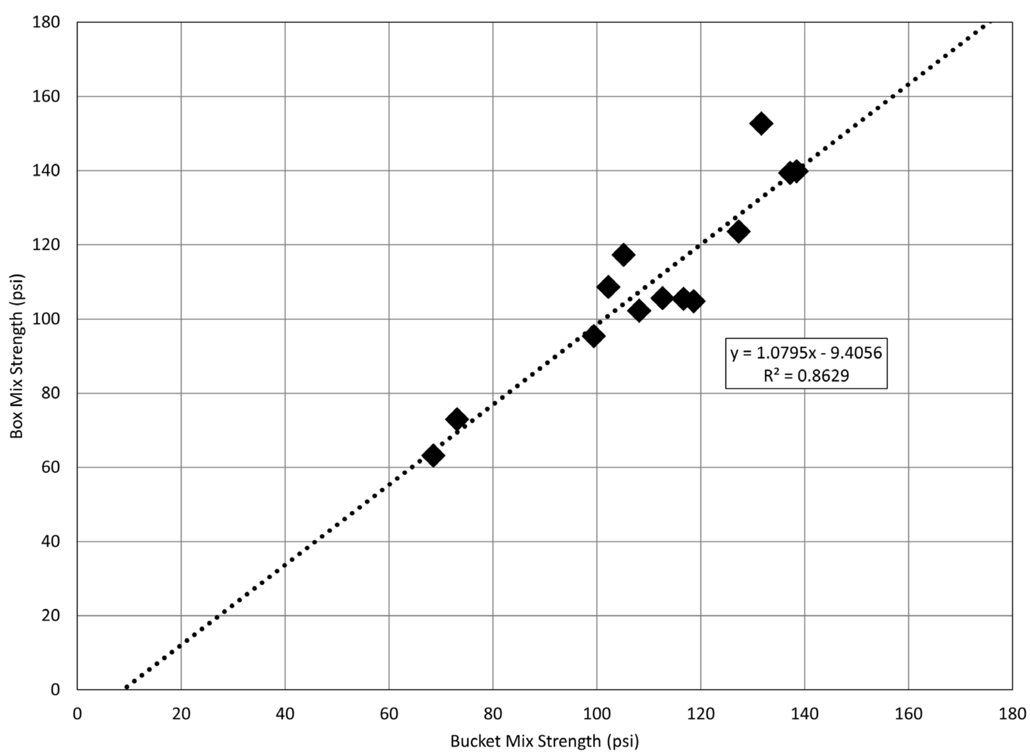

Figure 4.36: Comparison of IDEAL-CT indirect tensile strength for box versus bucket sampled mix for SL1 and SL2.

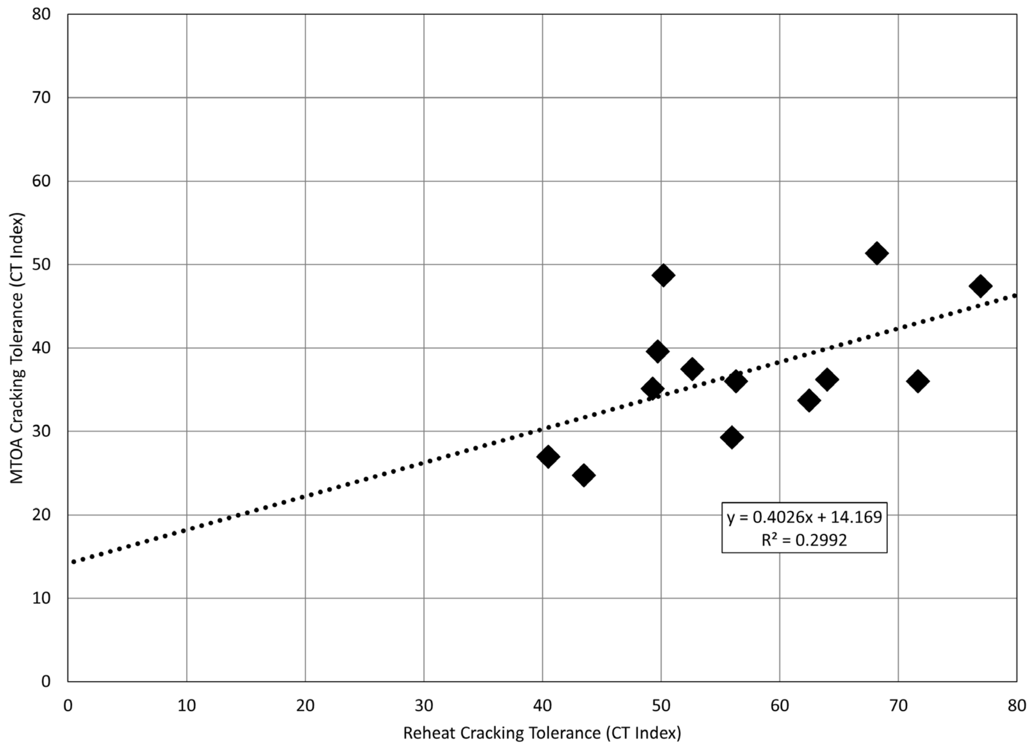

Figure 4.37: Comparison of IDEAL-CT cracking tolerance value for reheated versus MTOA-conditioned mix for SL1 and SL2.

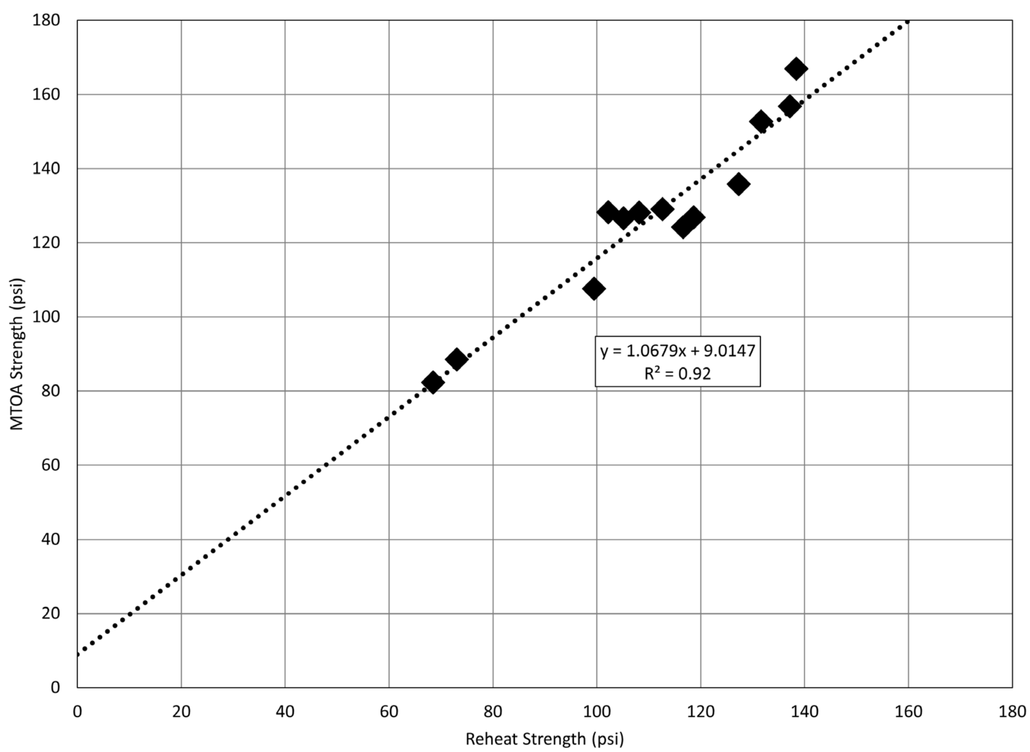

Figure 4.38: Comparison of IDEAL-CT indirect tensile strength for reheated versus MTOA-conditioned mix for SL1 and SL2.

4.3.8 Hamburg Wheel-Tracking Test

Table 4.13 and Table 4.14 show the Hamburg Wheel-Tracking (HWT) test results in terms of rut depth at the specified 15,000 passes for the first and second QA sublots, SL1 and SL2, respectively. It can be seen in the two tables and in Figure 4.39 that the mainline 15% RAP and all the high RAP and/or RAS mixes all easily met the specified maximum allowable rut depth of 0.5 in. (12.5 mm), with results all less than 0.17 in. However, the control mix with no RAP had a final rut depth approximately two to three times greater than the other mixes, which were all similar to each other. It can also be seen that the variability between the two QA sublots was small. The stripping-inflection point was not included in the analysis. However, Figure 4.40 and Figure 4.41 show that the control mix with no RAP (Mix J) has a clear increase in the rate of rut depth development between 10,000 and 15,000 wheel passes for both QA sublots.

Table 4.13: Hamburg Wheel-Tracking Test Results for QA Sample 1 (SL1) at 15,000 Cycles

Mix ID	Wheel 1 Rut Depth (in.)	Wheel 2 Rut Depth (in.)	Rut Depth Wheel 1 and 2 (in.)	Standard Deviation Rut Depth (in.)
Mix J (PG 64-28M, 0% RP, 0% RS, 0% RA) QA Sample 1 (SL1)	0.105	0.148	0.127	0.022
Mix K (PG 58-34M, 25% RP, 0% RS, 1.0% RA) QA Sample 1 (SL1)	0.064	0.057	0.060	0.004
Mix L (PG 58-34M, 30% RP, 0% RS, 1.0% RA) QA Sample 1 (SL1)	0.052	0.051	0.051	0.001
Mix M (PG 58-34M, 35% RP, 0% RS, 1.5% RA) QA Sample 1 (SL1)	0.062	0.060	0.061	0.001
Mix N (PG 58-34M, 40% RP, 0% RS, 1.5% RA) QA Sample 1 (SL1)	0.039	0.041	0.040	0.001
Mix O (PG 58-34M, 25% RP, 3% RS, 1.5% RA) QA Sample 1 (SL1)	0.083	0.072	0.077	0.006
Mix P (PG 64-28M, 15% RP, 0% RS, 0% RA) QA Sample 1 (SL1)	0.059	0.063	0.061	0.002

Table 4.14: Hamburg Wheel-Tracking Test Results for QA Sample 2 (SL2) at 15,000 Cycles

Mix ID	Wheel 1 Rut Depth (in.)	Wheel 2 Rut Depth (in.)	Rut Depth Wheel 1 and 2 (in.)	Std Deviation Rut Depth (in.)
Mix J (PG 64-28M, 0% RP, 0% RS, 0% RA) QA Sample 2 (SL2)	0.143	0.161	0.152	0.009
Mix K (PG 58-34M, 25% RP, 0% RS, 1.0% RA) QA Sample 2 (SL2)	0.040	0.049	0.044	0.005
Mix L (PG 58-34M, 30% RP, 0% RS, 1.0% RA) QA Sample 2 (SL2)	0.051	0.065	0.058	0.007
Mix M (PG 58-34M, 35% RP, 0% RS, 1.5% RA) QA Sample 2 (SL2)	0.046	0.033	0.039	0.006
Mix N (PG 58-34M, 40% RP, 0% RS, 1.5% RA) QA Sample 2 (SL2)	0.059	0.051	0.055	0.004

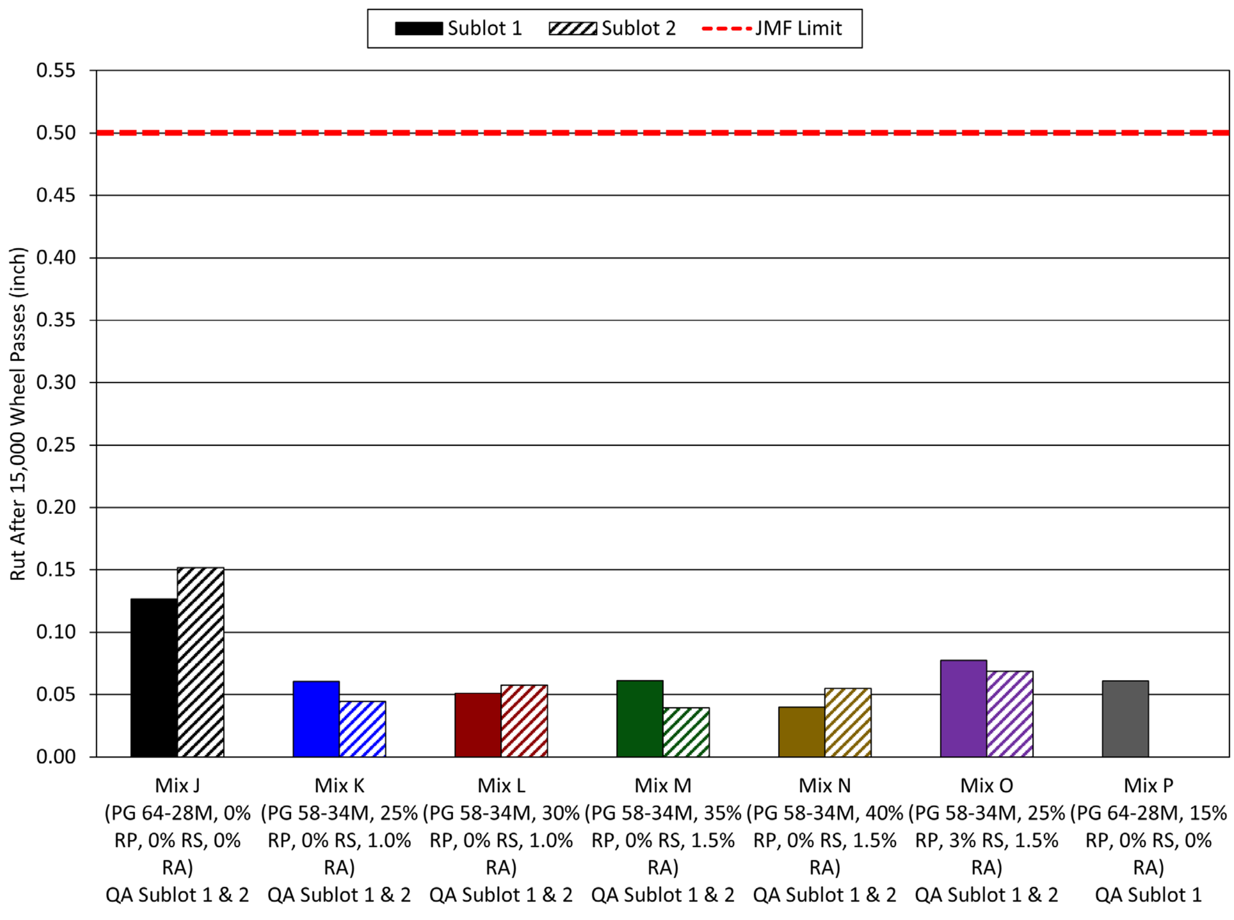

Figure 4.39: HWT test results for QA SL1 and SL2 (rutting after 15,000 wheel passes, average of both specimens).

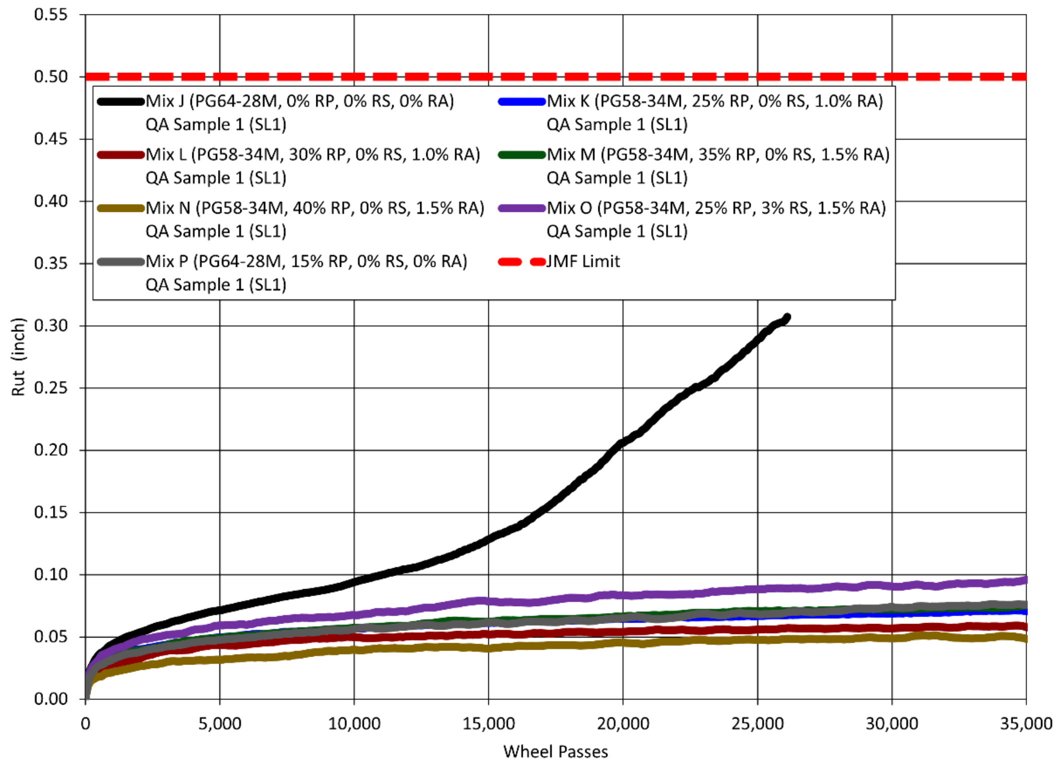

Figure 4.40: HWT test results for QA Sample 1 (SL1) (wheel passes and rut depth).

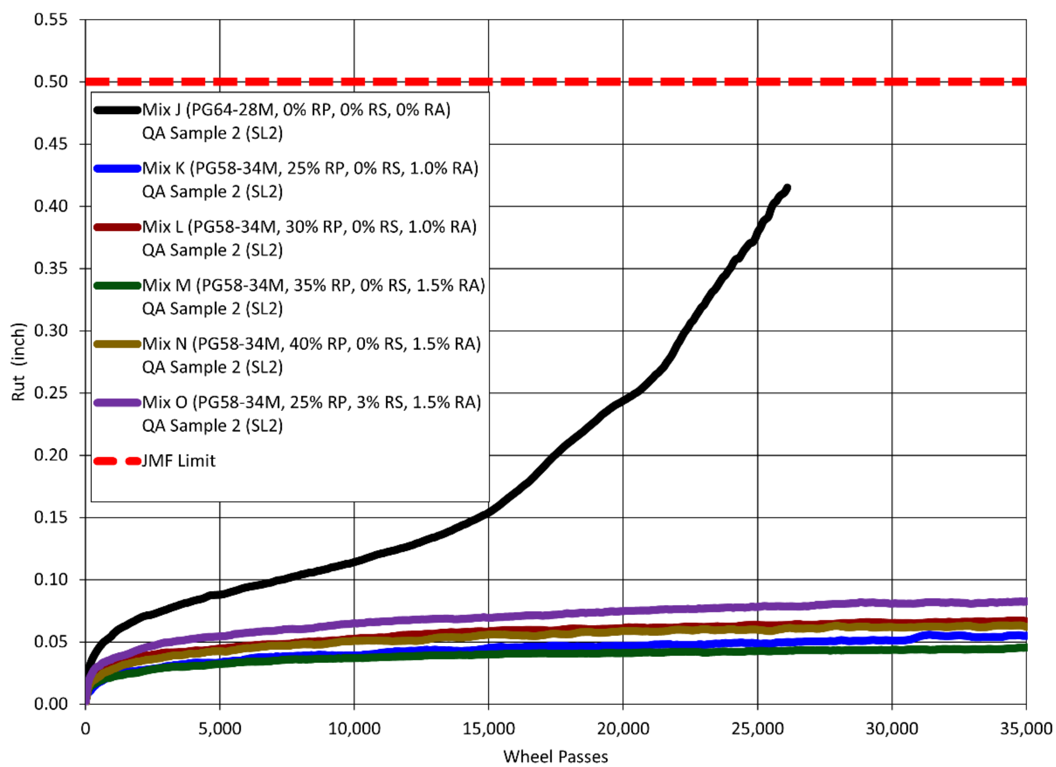

Figure 4.41: HWT test results for QA Sample 2 (SL2) (wheel passes and rut depth).

4.3.9 Performance-Related Test Correlations

Comparisons were made between potential balanced mix design (BMD) material specification tests and performance-related tests used for materials characterization for mechanistic-empirical design for the seven mixes included in the SJ 26 pilot project. The following conclusions can be drawn from the results:

- Figure 4.42 shows that axial stiffness (MPa) from the AMPT device and flexural stiffness (MPa) from the four-point bending beam device have a very strong correlation ($R^2 = 0.99$). There is a consistent shift in the results, with the axial stiffness being about 30% stiffer than the flexural stiffness over all mixes. The differences between the two stiffnesses were larger at higher temperatures and slower frequencies of loading as a percentage than at lower temperatures and faster frequencies. This finding is likely reflecting the fact that the stress state for the axial stiffness is primarily compression and shear. Shear and compression in the axial stiffness test engage the aggregate structure more than the stress state for the flexural stiffness, which is primarily tension but also includes compression.
- Figure 4.43 shows that the IDEAL-CT cracking tolerance value (CT #) and flexural stiffness (MPa) have almost no correlation, and CT tends to go down as flexural stiffness goes up ($R^2 = 0.14$ and $R^2 = 0.27$ for the two QA sublots).
- Figure 4.44 shows that the indirect tensile strength (psi) and flexural stiffness (MPa) have a strong correlation ($R^2 = 0.92$ and $R^2 = 0.95$ for the two QA sublots). Strength could potentially be a surrogate test for flexural stiffness and function as both a BMD test and relate BMD mix specifications to mechanistic-empirical material design input.
- Figure 4.45 shows that the indirect tensile strength (psi) and the cracking tolerance value (CT) from the IDEAL-CT test have a weak and negative degree of correlation ($R^2 = 0.38$, including mixes with and without MTOA).
- Figure 4.46 compares the intermediate performance grade (PGI) temperature for the binder extracted from plant-produced mix versus axial and flexural stiffness. The mix stiffness values are for 20°C and 10 Hz. It can be seen that there is a strong correlation between the binder stiffness and the two mix stiffnesses. The ability to adjust desired intermediate PG stiffness can be achieved through virgin binder variations (within a PG grade), the RA dosage, other additives such as LAS and lime, combined aggregate gradation, and manufacturing methods (e.g., production temperatures and silo time).
- Figure 4.47 shows that the IDEAL-CT cracking tolerance value and the PGI for the binder extracted from plant-produced mix have almost no correlation ($R^2 = 0.08$ and $R^2 = 0.20$ for the two QA sublots).
- Figure 4.48 shows that the IDEAL-CT indirect tensile strength and the PGI for the binder extracted from plant-produced mix have a strong correlation ($R^2 = 0.92$ and $R^2 = 0.81$ for the two QA sublots).

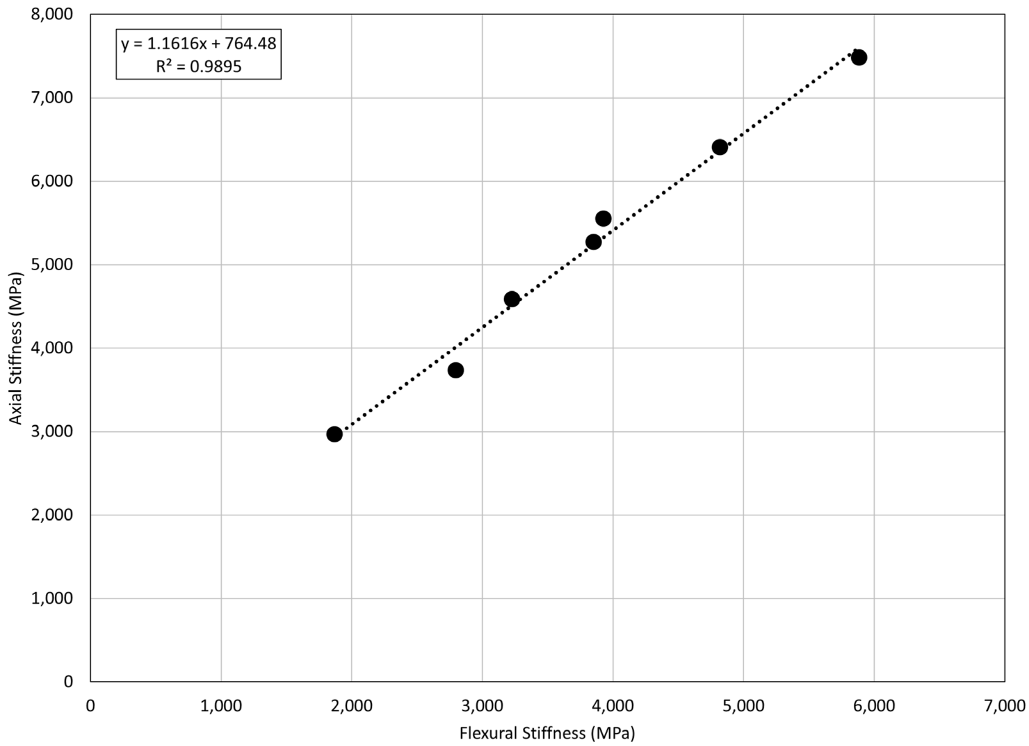

Figure 4.42: Comparison of flexural (four-point beam) and axial (AMPT) dynamic stiffness at 20°C and 10 Hz for combined QA samples.

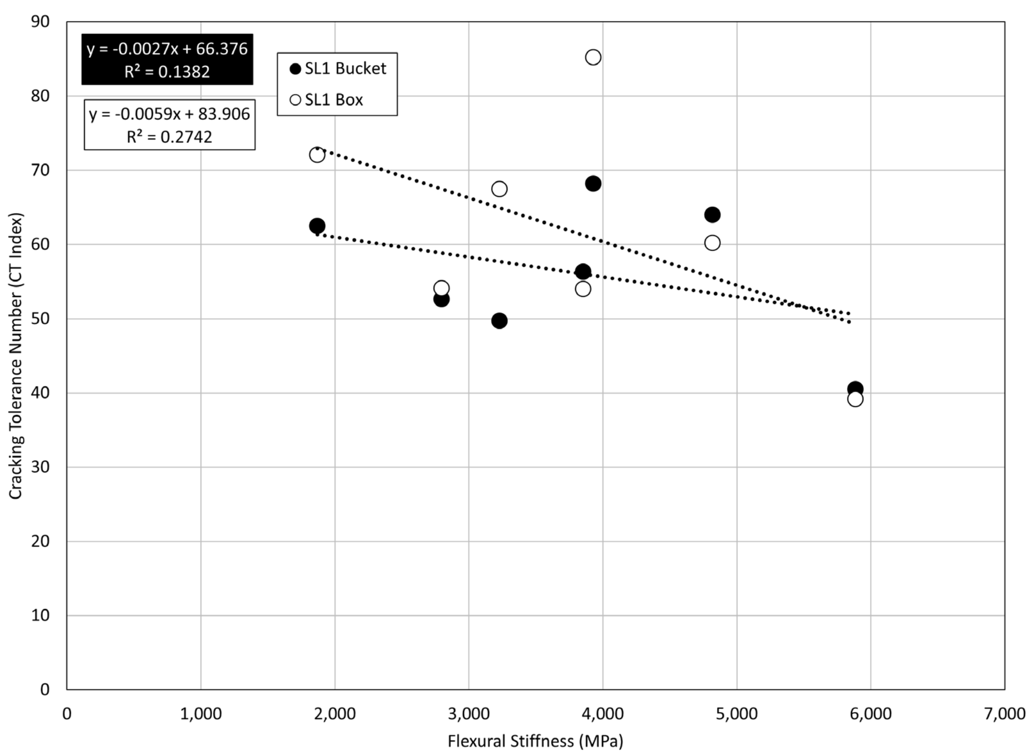

Figure 4.43: Comparison of flexural stiffness at 20°C and 10 Hz with IDEAL-CT cracking tolerance value for combined QA samples.

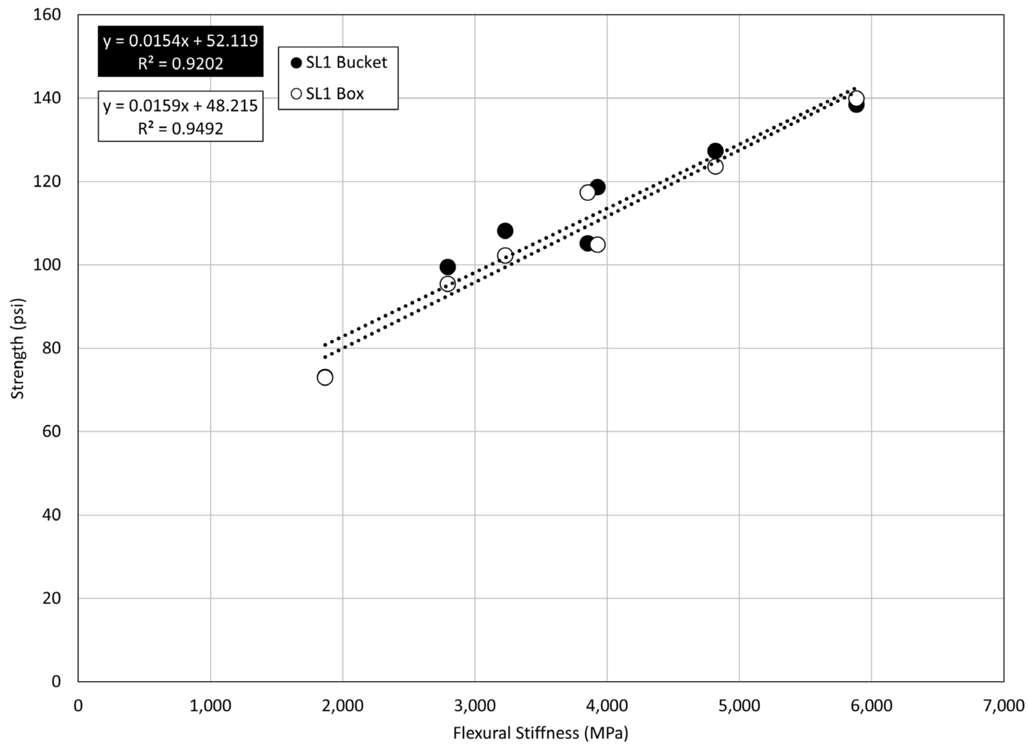

Figure 4.44: Comparison of flexural stiffness at 20°C and 10 Hz with IDEAL-CT indirect tensile strength for combined QA samples.

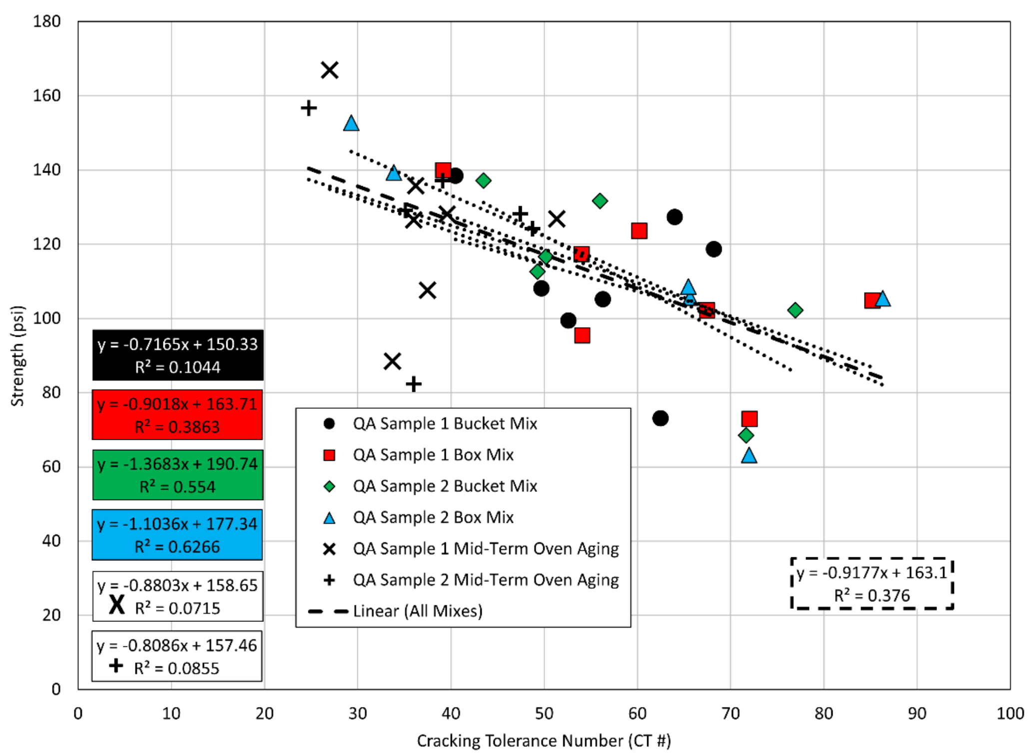

Figure 4.45: Comparison of IDEAL-CT cracking tolerance value and indirect tensile strength for combined QA samples.

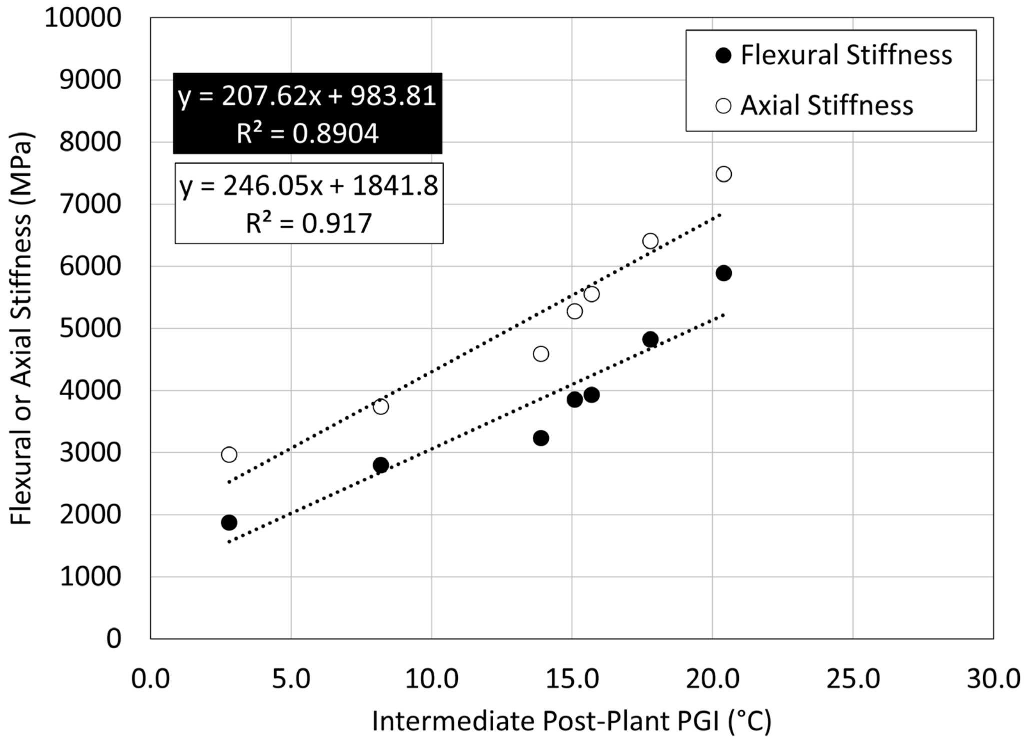

Figure 4.46: Comparison of post-plant-extracted PG binder intermediate performance grade (PGI) temperature with flexural and axial stiffness at 20°C and 10 Hz for QA SL1.

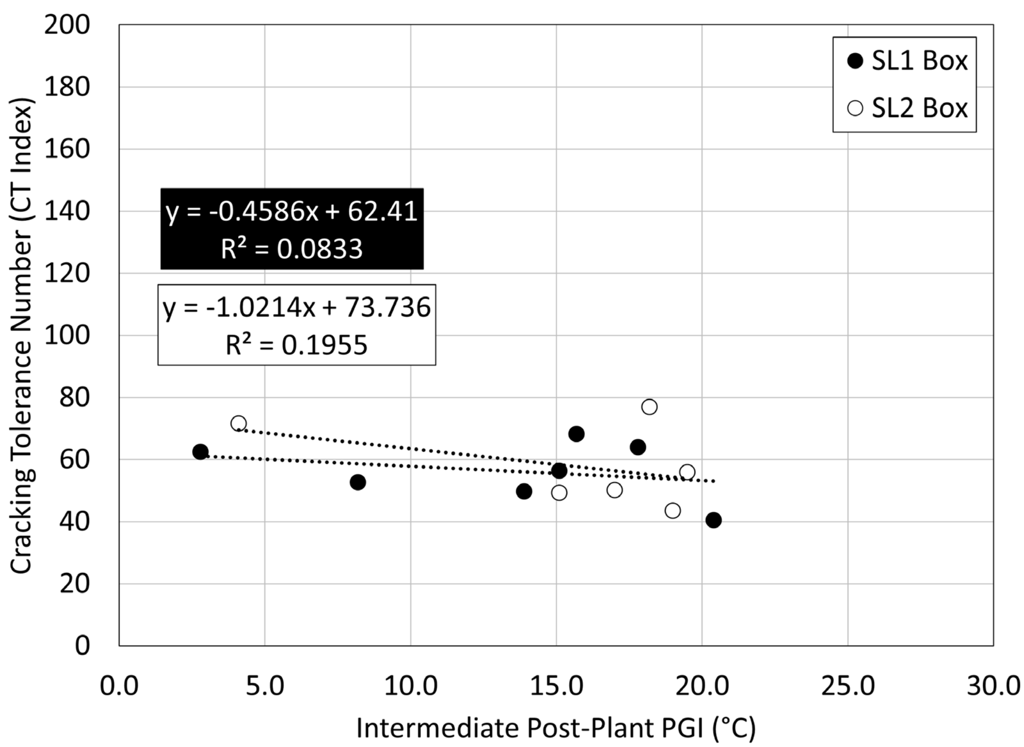

Figure 4.47: Comparison of post-plant-extracted PG binder intermediate performance grade (PGI) temperature with IDEAL-CT cracking tolerance value for QA SL1 and SL2.

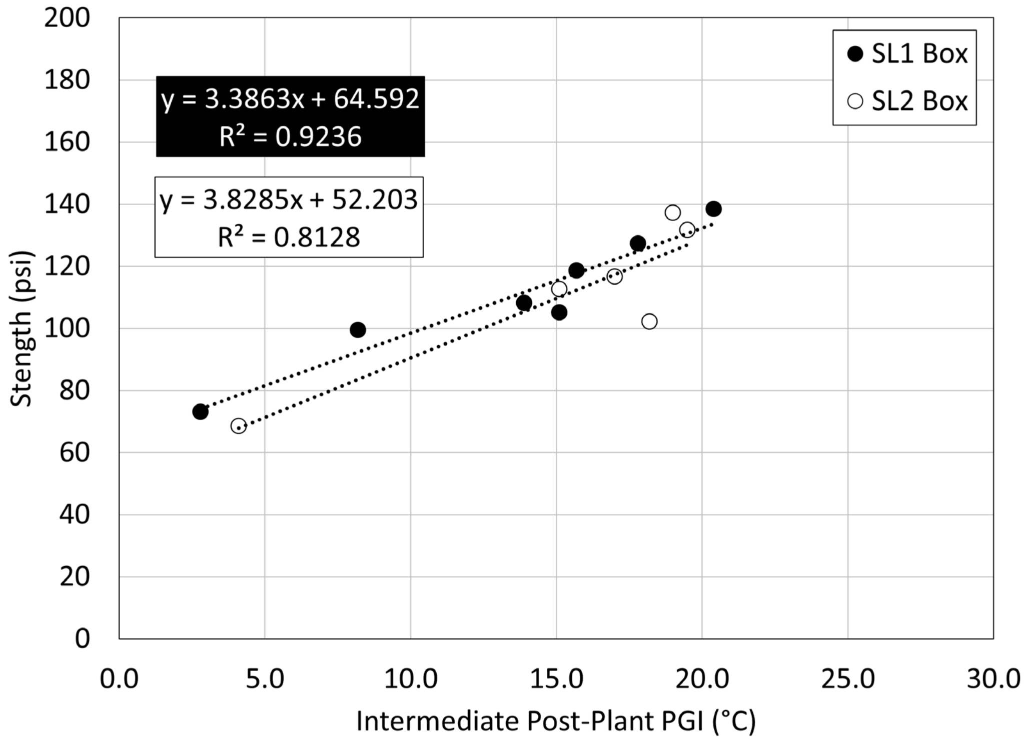

Figure 4.48: Comparison of post-plant-extracted PG binder intermediate performance grade (PGI) temperature and IDEAL-CT indirect tensile strength for QA SL1 and SL2.

5 OBSERVATIONS FROM CONSTRUCTION

5.1 Overlay Construction

5.1.1 Plant Operation Observations

There were no problems at the mixing plant that were out of the ordinary for a paving project of this type (Figure 5.1). Figure 5.2 shows the aggregate drying drum superheating virgin aggregates for the 40% RAP mix.

Figure 5.1: George Reed Clements asphalt batch plant.

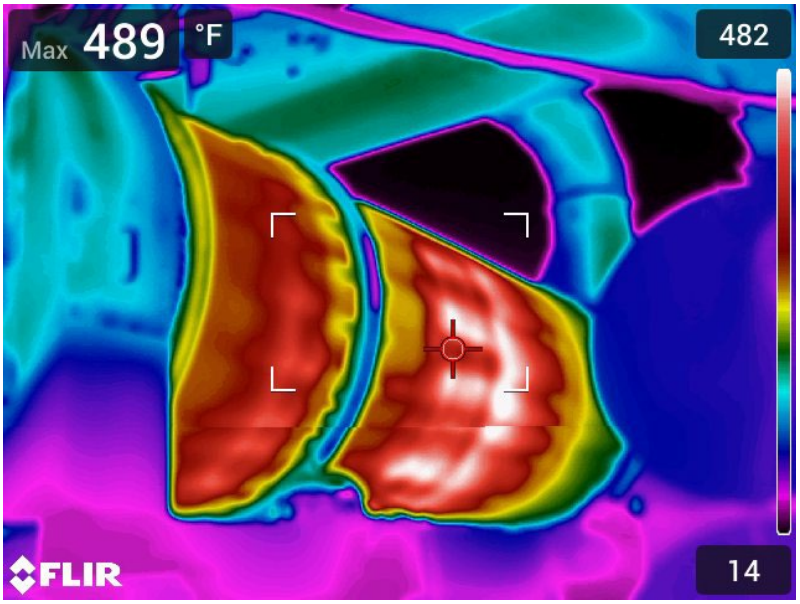

Figure 5.2: Thermal image of mixing drum.

5.1.2 Paving Operation Observations

The design thickness of the overlay was 0.2 ft. Prior to paving, 0.2 ft. of existing HMA material was removed, swept, and tacked. Figure 5.3 shows the windrow pickup machine used on the project. Figure 5.4 shows the paving machine used on the project. Figure 5.5 shows the initial breakdown of the paved mat. Figure 5.6 shows the thermal imagery of the paved mat during breakdown. The mix temperature at laydown was 270°F to 290°F. Figure 5.7 shows the intermediate rolling of the mat. The material "locked up" quickly, and paving crews indicated no problems with compaction. Three double-wheel steel drum rollers were used and no pneumatic tire rollers were used. Figure 5.8 shows the thermal imagery of the paved mat during intermediate rolling. This pattern was performed at 210°F to 250°F. Figure 5.9 shows the thermal imagery of additional intermediate rolling on the high RAP and RAS section. Figure 5.10 shows thermal imagery at the start of finish rolling of the pavement mat. Figure 5.11 shows the finished paved mat of the nSSP high RAP and RAS test sections. The thermal imagery indicates that mat temperatures were uniform, as would be expected with use of the material transfer vehicle. The mat had good surface characteristics and showed no signs of segregation, shown in the figures.

Figure 5.3: Windrow pick up using a material transfer vehicle.

Figure 5.4: Mix laydown using a paving machine.

Figure 5.5: Breakdown compaction of the mat on the high RAP and RAS sections.

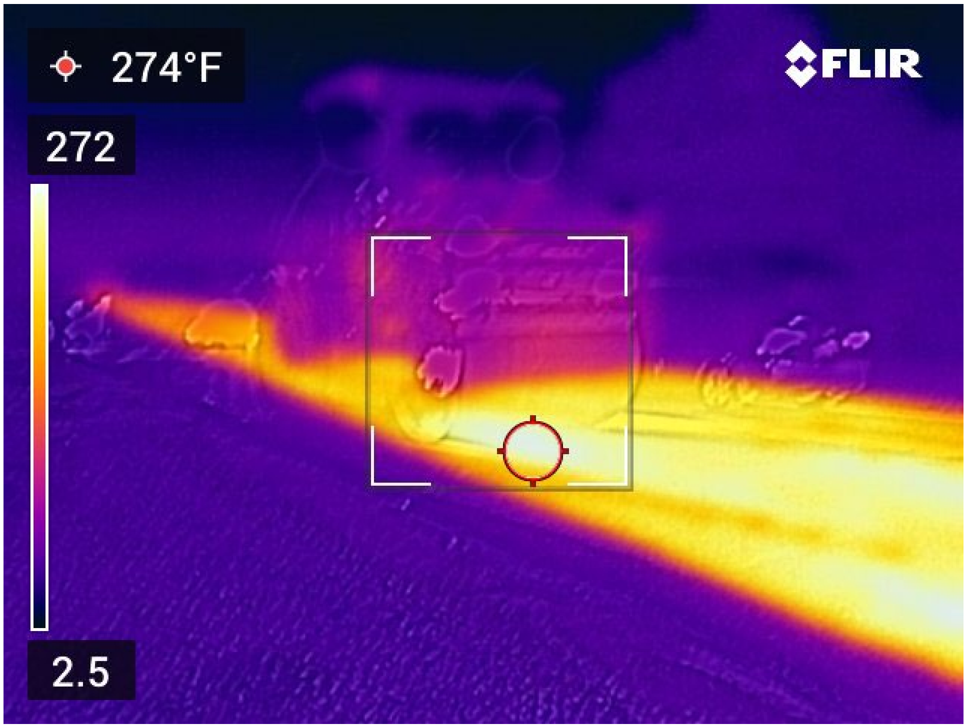

Figure 5.6: Thermal image of breakdown compaction of the mat on the high RAP and RAS sections.

Figure 5.7: Intermediate compaction of the mat on the high RAP and RAS sections.

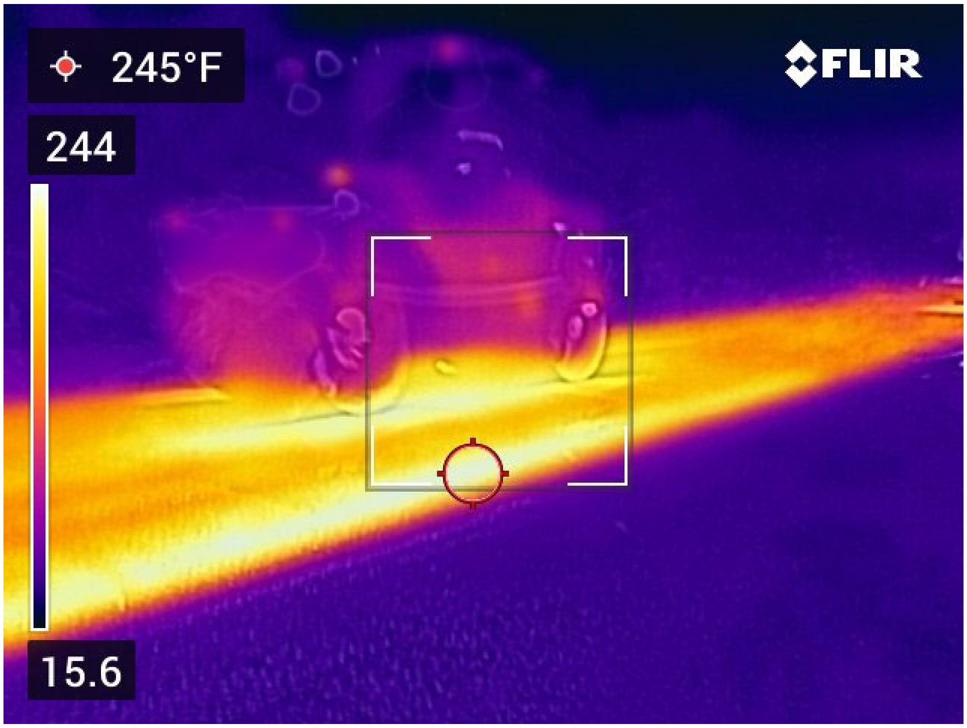

Figure 5.8: Thermal image of intermediate compaction of the mat on the high RAP and RAS sections.

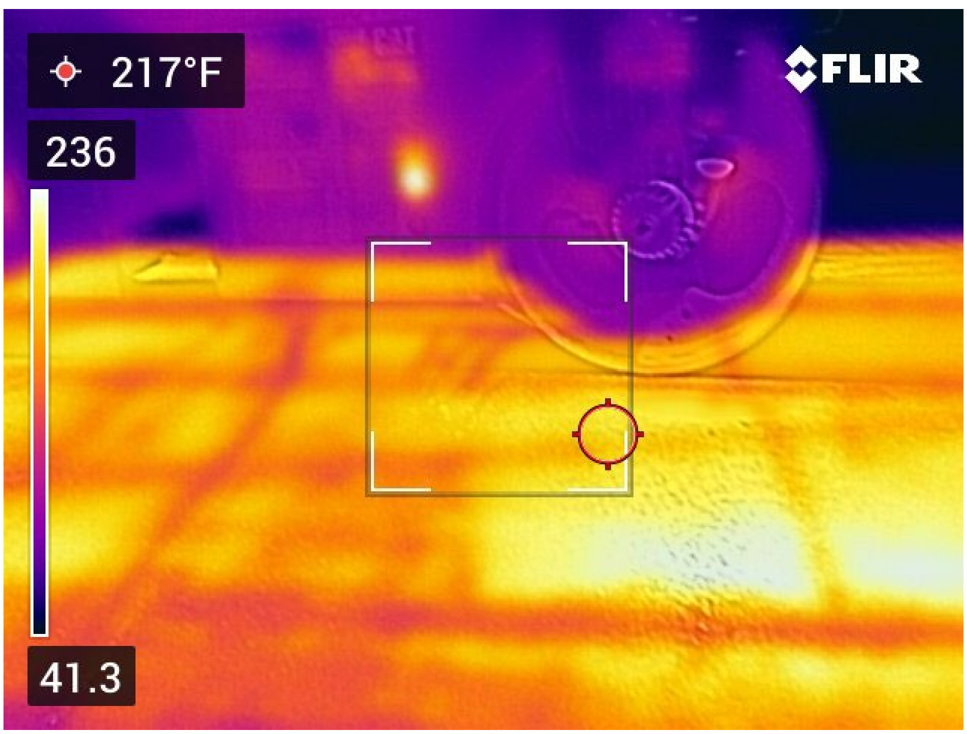

Figure 5.9: Thermal image of additional intermediate compaction of the mat on the high RAP and RAS sections.

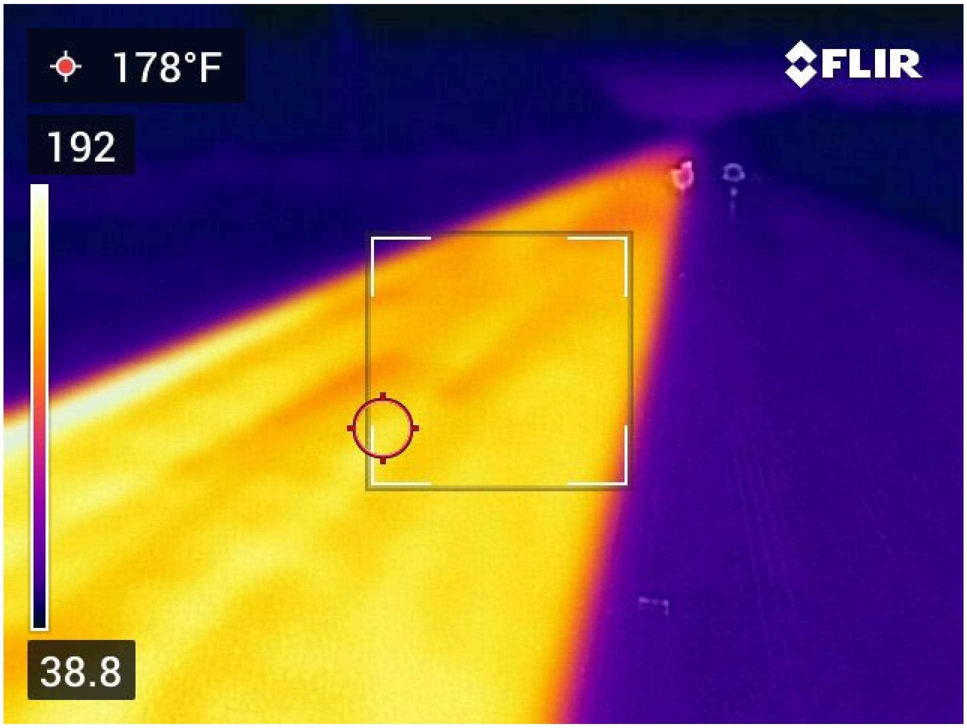

Figure 5.10: Thermal image of mat prior to final rolling and compaction on the high RAP and RAS sections.

Figure 5.11: Finish compaction of the mat on the nSSP high RAP and RAS sections.

6 CONCLUSIONS AND RECOMMENDATIONS FROM THE SJ 26 PILOT PROJECT

6.1 Conclusions

The following conclusions are drawn from the data collected during JMF verification and QA testing for the seven mixes included in the SJ 26 high RAP/RAS pilot project. For reference, the seven mixes can be summarized as follows:

- Mix J, containing 0% RAP and 0% RAS (used as a control mix for this project, though mixes without RAP are not typically used on Caltrans projects)
- Mix P, containing 15% RAP and 0% RAS (mix used on the rest of the paving project outside the test sections and typical of Caltrans HMA mixes in terms of use of RAP and RAS)
- Mix K, containing 25% RAP by aggregate replacement and 0% RAS with RA
- Mix L, containing 30% RAP by aggregate replacement and 0% RAS with RA
- Mix M, containing 35% RAP by aggregate replacement and 0% RAS with RA
- Mix N, containing 40% RAP by aggregate replacement and 0% RAS with RA
- Mix O, containing 25% RAP and 3% RAS by aggregate replacement with RA

Although the specification was written in terms of RAP and RAS binder replacement, the contractor and general practice in California is based on RAP aggregate replacement.

6.1.1 Mix Designs and Performance-Related Properties of the Seven Mixes

The following are conclusions of the results from the submitted mix designs based on laboratory-prepared specimens and resulting plant-sampled mixes during JMF approval:

- It was found when observing construction that the batch plant liquid additive weight pot limited the maximum RA contents by mass of binder to 2.0% to 3.0% for all mixes. However, none of the mix designs had more than 1.5% RA.
- The mix designs based on laboratory-prepared specimens for the control and the high RAP/RAS mixes were similar in terms of total binder content at 4.5%, except for the mix designs for the 35% and 40% RAP mixes (Mix M and Mix N), which had design binder contents of 4.0% and which is considerably lower. The binder content of the mainline mix (Mix P) with 12% RAP (specified at 15%) was 4.6%. The binder content of the RAP source used in all mixes with RAP was 4.64% and the binder content of the 25% RAP/3% RAS blend used for Mix O was 6.28%. The low binder contents and high RAP contents for those mixes reduced the amount of polymer-modified binder in those mixes because only the virgin binder is polymer modified, and increased the RAP binder replacement rates to 3% to 5% more than the 35% and 40% targets, which would be expected to have an adverse effect on age-related and fatigue cracking performance.

- Caltrans JMF volumetric verification data for the plant-sampled mixes showed the following:
  - Aggregate gradations all met specifications and were in the middle of the specification limits.
  - Binder contents were higher than those of the submitted laboratory specimen-based mix designs, with the control mix (Mix J), 25% and 30% RAP mixes (Mix K and Mix L), RAP/RAS mix (Mix O), and mainline mix (Mix P) having binder contents of 0.1% to 0.5% more than the targets of 4.5% or 4.6%. The 35% and 40% RAP mixes (Mix M and Mix N) had binder contents 0.25% greater than the targets of 4.0%.

The following are conclusions based on the results from the performance-related binder and mix tests:

- UCPRC JMF volumetric verification data for the extracted binders from the plant-sampled mixes showed the following:
  - The mixes meeting or exceeding the PG 64-28M specification for the extracted binder were the control mix with no RAP or RAS (Mix J), the mix with 40% RAP aggregate replacement (Mix N), and the mix with 25% RAP and 3% RAS (Mix O). The mixes with 25%, 30% and 35% RAP aggregate replacement (Mixes K, L and M) met the high and intermediate specifications but did not meet the low temperature PG by a very small amount (0.7°C, 1.0°C and 0.3°C, respectively). With rounding to the nearest 1°C, Mix M passes. Use of more RA would have likely improved the low temperature PG for those mixes.
  - All results failed to meet the Delta T_c specification requirement of ≥-5°C. Research by others and the previous ED 49 pilot have shown that the Delta T_c parameter often does not provide reasonable results for polymer-modified binders. The control mix with no RAP or RAS (Mix J) had the "worst" Delta T_c according to the specification, likely because it had the highest percentage (100%) of polymer-modified binder.
- UCPRC JMF volumetric verification data for the mixes from the plant-sampled mixes showed the following:
  - The higher-than-target binder contents for the JMF submittal plant-produced mixes resulted in all the mixes meeting the IDEAL-CT cracking tolerance value requirement to meet or exceed the value from the control mix with no RAP or RAS.
- UCPRC binder testing for extracted binder from the two QA samples showed the following:
  - The JMF and QA sample binder testing results showed similar trends.
  - The true grade temperatures were somewhat inconsistent between the two QA samples. The control mix with no RAP or RAS (Mix J) and the mainline mix with 12% RAP (specified at 15%) and no RA (Mix P) met or exceeded the PG 64-28M specification requirements. All of the high RAP mixes and the RAP/RAS mix (Mixes K, L, M, N, O) met the high and intermediate temperature requirements but both QA samples of Mix N (40% RAP) and Mix O (25%RAP/3%RAS) and one sample of Mix L (30% RAP) and Mix M (35% RAP) missed the low temperature requirements by 1.5°C to 3.1°C.

- Frequency sweep results for the first QA sublot showed that the dynamic moduli of the 40% RAP mix (Mix N) was considerably stiffer than the other mixes as was the RAP/RAS mix (Mix N) at higher temperatures and slower loading frequencies. The rest of the high RAP mixes (Mixes K, L, M) were stiffer than the control mix with no RAP (Mix J) and the mainline mix with 12% RAP and no recycling agent (Mix P). Mix J and Mix P had similar stiffnesses.
- The high RAP mixes and the RAP/RAS mixes were in the "transition zone" for age-related block cracking with 20 hours of PAV aging, while the control and mainline mixes were not.
- Carbonyl content was found to be a good predictor of binder stiffness, the Glover-Rowe parameter related to block cracking, and the crossover modulus related to low temperature creep with aging.

- UCPRC mix testing for both QA samples showed the following:
  - The extracted binders are fully diffused by the extraction process, while in the mix there may be less than complete diffusion. Qualitative comparison of binder and mix stiffness ranking results indicates that there was good diffusion of the RAP binder with the virgin binder, except for the mix with RAP and RAS (Mix O) where the rankings indicated less than complete blending.
  - The performance-related properties of the QA-sampled mixes were similar to those of the corresponding JMF verification samples.
  - The mix stiffnesses generally follow a pattern consistent with the amount of RAP or RAP/RAS in the mix compared with the control mix with no RAP or RAS (Mix J). The greatest differences from the control mix were at intermediate temperatures and loading frequencies. The mix with 40% RAP (Mix N) was approximately 2.5 to 3 times stiffer than the control mix, followed in order of decreasing stiffness by the 35% RAP mix (Mix M), the 30% RAP and 25% RAP/3% RAS mixes (Mix L and Mix O), the 25% RAP mix (Mix K), and the mainline mix with 12% RAP.
  - The RLT rutting test results under confined conditions at 45°C and unconfined conditions at 50°C generally ranked the mixes in opposite order of their stiffnesses, with the control mix, with no RAP or RAS (Mix J), having the greatest potential for rutting and Mix N, with 40% RAP, having the least potential. The results under confined conditions at 55°C also showed the control mix having the greatest rutting potential but showed the mainline mix (Mix P) having the least rutting potential along with the 30%, 35% and 40% RAP mixes (Mixes L, M, N) and then the 25% RAP mix and the RAP/RAS mixes (Mix K and Mix O).
  - The flexural fatigue results are approximately the opposite of the RLT results for permanent deformation, with the 40% RAP mix that also had lower binder content (Mix N) having the worst performance and the control mix with no RAP (Mix J) having the best performance. The ranking of the fatigue lives almost exactly follows the amount of virgin binder replacement, with the most replacement by RAP having the shortest fatigue life, Mix N (40% RAP) and the rest of the mixes having successively better performance as the

RAP content diminishes. This finding is likely attributable to the higher stiffnesses of the mixes at intermediate temperatures with increasing RAP and the fact that the RAP binder likely has very low polymer content and is increasingly replacing the polymer-modified virgin binder as the RAP binder content increases.

- The IDEAL-CT cracking tolerance value results showed fairly high variability between QA sublots, and this parameter consistently shows high variability even within sublots. The cracking tolerance values did not meet the specification limit by a small margin of 51.7 for both sublots of the 25% RAP mix (Mix K) and one sublot of the 30% RAP mix (Mix L), and one of the sublots of the 35 and 40% RAP mixes (Mix M and Mix N) did not meet the cracking tolerance specification by a wider margin. Both sublots of the RAP/RAS mix passed as did the mainline mix.
- The IDEAL-CT strength results showed strong correlation with the mix flexural and axial dynamic moduli at intermediate temperatures, with increasing strength as the amount of RAP in the mix increased.
- MTOA decreased IDEAL-CT cracking tolerance values and increased strengths, as expected, with the changes consistent between QA sublots on average across all mixes. However, there was no consistent trend between the amount of RAP in the mix and how much the MTOA reduced the cracking tolerance value and increased the strength value.
- HWT testing results showed that all mixes passed the specification for PG 64-28M mixes. The results indicated nearly identical results for all mixes except the control mix with no RAP or RAS (Mix J) which had 2.5 to 3 times more rut depth at 15,000 wheel passes and also showed a potential moisture-induced increase in the rate of rutting starting at about 10,000 wheel passes.

6.1.2 The Seven Mixes and Their Specifications

The following are conclusions based on experience in this pilot project and review of the specifications:

- The mixes submitted for JMF verification and tested as part of QA did not consistently meet the two performance-related specifications: IDEAL-CT values that were greater than or equal to those of the control Mix J (no RAP or RAS) and Delta T_c values that were greater than -5.
- The contractor used a combination of PG grade selection for the base binder and RA to produce mixes that successfully met the specifications. The asphalt batch plant was limited to 132 oz. of recycling agent in the batch, which restricted use of higher RA dosages (2% to 3% of binder content), and none of the mixes had target RA contents greater than 1.5%. Use of more RA with increasing RAP contents would likely have brought the high RAP and RAP/RAS mix stiffnesses closer to those of the control mix and resulted in more consistently meeting the IDEAL-CT cracking tolerance value specification.
- It is uncertain how setting the specification for the IDEAL-CT value based on test results for a control mix that has no RAP or RAS can be carried forward into future specifications, due to practical considerations. For this project the control and mainline mixes had similar

stiffnesses. However, the control mix (Mix J) with no RAP or RAS had rutting testing results (RLT and HWT) that indicated a greater susceptibility to rutting than the mainline mix and the high RAP and RAP/RAS mixes. The use of Mix J has some benefits for thin overlays with regard to cracking but may increase risks of rutting at early ages after construction. There are also practical considerations for use of this approach in routine practice.

- All the mixes with RAP or RAP/RAS had better high temperature results from binder and mix testing than the control Mix J. This indicates that the practice of requiring the same high temperature blended binder properties as a method of avoiding binder or mix testing at intermediate and low temperatures does not guarantee better performance at those temperatures while also potentially sacrificing rutting resistance at high temperatures.
- Carbonyl content was found to be a good predictor of binder stiffness, the Glover-Rowe parameter related to block cracking, and the crossover modulus related to low temperature creep with aging.

6.1.3 Construction of the Test Sections

The following are conclusions from observations during construction, including at the mixing plant and at the test sections during paving:

- There were no problems with mixing or compaction of any of the mixes.
- The surfaces appeared to be similar for all mixes.

6.2 Preliminary Recommendations

The following recommendations are based on the previously presented conclusions:

- Use of the high temperature grade to control intermediate and low temperature properties of blended binders should be reconsidered. This approach to specification may increase the risk of rutting without obtaining better cracking resistance.
- Valuable information was gathered in this pilot project, and additional pilot projects for high RAP and RAS, with higher mix tonnages, should be built and monitored to gain additional information regarding production variability and resulting mixes and simplified performance tests. Current mix types containing less than 15% RAP or mixes containing 15% to 25% RAP with a stepped-down virgin binder grade should be used as the control since they represent current practice.
- The potential performance-related tests should continue to be assessed for efficiency, variability, sensitivity to important variables, and practicality. There is strong evidence from this pilot project and other projects that IDEAL-CT strength is a very good surrogate for mix stiffness at intermediate temperatures, which provides a link to inputs used for pavement structural design with *CalME*. The RLT and HWT results showed similar trends.
- The testing for stiffness, fatigue, and fracture properties included use of the protocol for conventional laboratory MTOA of loose mix following Caltrans provisional procedure CT 320. It is recommended that MTOA continue to be included in the testing for future pilot projects.

REFERENCES

1. Alavi, M. Z., Jones, D., He, Y., Chavez, P., and Liang, Y. 2017. Investigation of the Effect of Reclaimed Asphalt Pavement and Reclaimed Asphalt Shingles on the Performance Properties of Asphalt Binders: Phase 1 Laboratory Testing (Research Report: UCPRC-RR-2016-06). Davis and Berkeley, CA: University of California Pavement Research Center. https://escholarship.org/uc/item/5jq4m661.
2. Elkashef, M., Harvey, J., Jiao, L., and Jones, D. 2023. *Impact of Silo Storage on the Performance of Plant-Produced Mixes Containing High Content of Reclaimed Asphalt Pavement or Reclaimed Asphalt Shingles* (Research Report: UCPRC-RR-2022-04). Davis and Berkeley, CA: University of California Pavement Research Center. https://doi.org/10.7922/G24J0CFF.
3. Pellinen, T.K., Witczak, M.W., and Bonaquist, R.F. 2004. "Asphalt Mix Master Curve Construction Using Sigmoidal Fitting Function with Non-Linear Least Squares Optimization." In *Recent Advances in Materials Characterization and Modeling of Pavement Systems,* edited by Tutumluer, E., Najjar, Y.M., and Masad, E., 83–101. Reston, VA: American Society of Civil Engineers.
4. Liang, Y., Wu, R., Harvey, J.T., Jones, D., and Alavi, M.Z. 2019. "Investigation into the Oxidative Aging of Asphalt Binders." *Transportation Research Record* 2673, no. 6: 368–378. https://doi.org/10.1177/0361198119843096.
5. Morian, N., Hajj, E., and Sebaaly, P. 2013. "Significance of Mixture Parameters on Binder Aging in Hot-Mix-Asphalt Mixtures." *Transportation Research Record* 2370, no. 1: 116–127. https://doi.org/10.3141/2370-15.
6. Mohammad, L.N., Cooper, S.B., and Elseifi, M.A. 2011. "Characterization of HMA Mixes Containing High Reclaimed Asphalt Pavement Content with Crumb Rubber Additives." *Journal of Materials in Civil Engineering* 23, no. 11: 1560–1568. https://doi.org/10.1061/(ASCE)MT.1943-5533.0000359.
7. Hofko, B., Alavi, M.Z., Grothe, H., Jones, D., and Harvey, J. 2017. "Repeatability and Sensitivity of FTIR ATR Spectral Analysis Methods for Bituminous Binders." *Materials and Structures* 50, no. 187: 1–15. https://doi.org/10.1617/s11527-017-1059-x.
8. Lamontagne. J., Dumas, P., Mouillet, V., and Kister, J. 2001. "Comparison by Fourier Transform Infrared (FTIR) Spectroscopy of Different Aging Techniques: Application to Road Bitumen." *Fuel* 80, no. 4: 483–488. https://doi.org/10.1016/S0016-2361(00)00121-6.
9. Williams, M.L., Landel, R.F., and Ferry, J.D. 1955. "The Temperature Dependence of Relaxation Mechanisms in Amorphous Polymers and Other Glass-Forming Liquids." *Journal of the American Chemical Society* 77, no. 14: 3701–3707. https://doi.org/10.1021/ja01619a008.
10. Harvey, J., Liu, A., Zhou, J., Signore, J., Coleri, E., and He, Y. 2014. *Superpave Implementation Phase II: Comparison of Performance-Related Test Results* (Research Report: UCPRC-RR-2015-01). Davis and Berkeley, CA: University of California Pavement Research Center. https://escholarship.org/uc/item/7vg1c54z.

11. He, Y. 2016. “Interaction Between New and Age-Hardened Binders in Asphalt Mixes Containing High Quantities of Reclaimed Asphalt Pavement and Reclaimed Asphalt Shingles.” PhD diss., University of California, Davis. https://proquest.com/openview/fe86c3c2d3a5736f49466890cde58750/1?pq-origsite=gscholar&cbl=18750&diss=y.

12. Pang, C. 2019. “Development of Shift Factors Between Repeated Load Triaxial and Repeated Simple Shear Test Results.” MS thesis, University of California Davis. https://proquest.com/openview/c275721ae6bac8151fbf30c6d64f0106/1?pqorigsite=gscholar&cbl=51922&diss=y.

13. Federal Highway Administration. 2021. *Delta T_c Binder Specification Parameter.* Washington, DC: Federal Highway Administration. Accessed April 12, 2025. https://www.fhwa.dot.gov/pavement/asphalt/HIF_Delta_Binder_Spec_TchBrf.pdf.

14. Harvey, J., Buscheck, J., Brotschi, J., Rahman, M., Mateos, A., and Jones, D. 2023. *RAP and RAS in HMA Pilot Project on ED 49: Material Testing, Observations, and Findings* (Technical Memorandum: UCPRC-TM-2022-04). Davis and Berkeley, CA: University of California Pavement Research Center. https://doi.org/10.7922/G2X065DD.

15. Harvey, J., Buscheck, J., Brotschi, J., Yu, J., Rahman, M., Mateos, A. 2025. *RAP and RAS in HMA Pilot Project on SBD 215: Material Testing, Observations, and Findings* (Technical Memorandum: UCPRC-TM-2023-02). Davis and Berkeley, CA: University of California Pavement Research Center. https://doi.org/10.7922/G2Z036JS.

16. Rowe, G. 2011. Prepared discussion response to “Evaluation of the Relationship Between Asphalt Binder Properties and Non-Load Related Cracking” by Anderson, R.M., King, G.N., Hanson, D.I., and Blankenship, P.B. *Journal of the Association of Asphalt Paving Technologists* 80: 615–664.

17. Liu, M., Lunsford, K.M., Davison, R.R., Glover, C.J., and Bullin, J.A. 1996. “The Kinetics of Carbonyl Formation in Asphalt.” *AIChe Journal* 42, no. 4: 1069–1076. https://doi.org/10.1002/aic.690420417.

18. Tayebali, A., Deacon, J., Coplantz, J., Harvey, J., and Monismith, C. 1994. *Fatigue Response of Asphalt-Aggregate Mixes; Part 1: Test Method Selection* (SHRP-A-404). Washington, DC: Transportation Research Board. https://onlinepubs.trb.org/onlinepubs/shrp/shrp-a-404.pdf.

19. Sousa, J., Leahy, R., Harvey, J., and Monismith, C. 1994. *Permanent Deformation Response of Asphalt Aggregate Mixes; Part 1: Test Method Selection* (SHRP-A-415). Washington, DC: Transportation Research Board. https://onlinepubs.trb.org/onlinepubs/shrp/SHRP-A-415.pdf.

20. Ullidtz, P., Harvey, J., Tsai, B.W. and Monismith, C. 2008. “Calibration of Mechanistic Empirical Models for Flexible Pavements Using the WesTrack Experiment.” *Journal of the Association of Asphalt Paving Technologists* 77: 591–630.

21. Harvey, J., Guada, I., and Long, F. 2000. “Effects of Material Properties, Specimen Geometry, and Specimen Preparation Variables on Asphalt Concrete Tests for Rutting.” *Journal of the Association of Asphalt Paving Technologists* 69: 236–280.

22. Jiao, L., Harvey, J., Wu, R. Elkashef, M., Jones, D., and Liang, Y. Forthcoming. *Preliminary Study on Developing a Surrogate Performance-Related Test for Fatigue Cracking of Asphalt Pavements* (Research Report: UCPRC-RR-2021-02). Davis and Berkeley, CA: University of California Pavement Research Center. https://doi.org/10.7922/G2TM78D9.
23. Witczak, M.W., Kaloush, K., Pellinen, T., El-Basyouny, M., and Von Quintus, H. 2002. *Simple Performance Test for Superpave Mix Design* (NCHRP Report 465). Washington, DC: Transportation Research Board.
24. Zhang, Y., Luo, R., and Lytton, R.L. 2012. "Characterizing Permanent Deformation and Fracture of Asphalt Mixtures by Using Compressive Dynamic Modulus Tests." *Journal of Materials in Civil Engineering* 24, no. 7: 898–906.
25. Harvey, J., Weissman, S., and Monismith, C. 2009. "Rutting Characterization of Asphalt Concrete Using Simple Shear Tests." In *Modeling of Asphalt Concrete*, edited by Y. Richard Kim, 269–316. Reston, VA: American Society of Civil Engineers.

APPENDIX A PROVISIONAL REHEATING MEDIUM-TERM OVEN AGING PROTOCOL

The test method shown in this appendix substantially corresponds to the subsequent Caltrans Test Method 320. It does not reflect requirements in CT 320 regarding time that the mix can spend at room temperature and the need to cover the samples.[1]

[1] The Provisional Method of Test for Laboratory Conditioning of Dense-Graded Asphalt Mixtures (Expires 01/07/2026) document is available at https://dot.ca.gov/-/media/dot-media/programs/engineering/documents/californiatestmethods-ctm/ct-320-jan2025-a11y.pdf.

California Test 320
January 7, 2025

STATE OF CALIFORNIA—CALIFORNIA STATE TRANSPORTATION AGENCY

DEPARTMENT OF TRANSPORTATION
DIVISION OF ENGINEERING SERVICES
Transportation Laboratory
5900 Folsom Blvd.
Sacramento, California 95819-4612

PROVISIONAL METHOD OF TEST FOR LABORATORY CONDITIONING OF DENSE-GRADED ASPHALT MIXTURES

EXPIRES 01/07/2026

A. SCOPE

This provisional test method describes the procedure for laboratory conditioning of dense-graded asphalt mixture prior to compaction in the laboratory. The loose mixture from this test method is used to estimate the volumetric properties, cracking, rutting, and moisture damage resistance of the asphalt mixture soon after production and/or after in-service aging in the field.

B. REFERENCES

AASHTO R 47	Reducing Samples of Asphalt Mixtures to Testing Size
AASHTO R 30	Standard Practice for Short-Term Laboratory Conditioning of Asphalt Mixtures
AASHTO T 209	Standard Method of Test for Theoretical Maximum Specific Gravity (G_{mm}) and Density of Asphalt Mixtures
AASHTO T 312	Standard Method of Test for Preparing and Determining the Density of Asphalt Mixture Specimens by Means of the Superpave Gyratory Compactor
CT 125	Method of Test for Sampling Highway Materials and Products Used in the Roadway Pavement Structure Sections

C. SIGNIFICANCE AND USE

Asphalt mixtures have varying asphalt binder contents, different combinations of additives, aggregates, reclaimed asphalt pavement (RAP), reclaimed asphalt shingles (RAS), and other components. Mixtures may be prepared in the laboratory or may be produced in the plants. Mixtures may also be sampled and tested shortly after production; however, their performance may significantly change after several years of in-service aging in the field.

The short-term oven conditioning (STOC) for laboratory prepared mix is designed to allow for binder absorption during the mixture design and to simulate the plant-mixing effects on the mixture. The mid-term oven aging (MTOA) test is designed to simulate the field aging of mixtures in an accelerated manner. It specifically applies to cracking tests, as the cracking performance of mixtures is more sensitive to long-term aging. The rapid mid-term oven aging (RMTOA) is an accelerated alternative to the MTOA, offering a quicker turnaround time during production. This is a provisional test method to be used on selected pilot projects only.

D. APPARATUS

1. Pan – Shallow metal pan for heating 1-2 in. of the sample size of uncompacted asphalt mixtures. The pan must be large enough to hold the sample test size.
2. Boxes – Sample containers must be cardboard boxes 8 in. x 8 in. x 4 in. or 8-1/2 in. x 8-1/2 in. x 4-1/2 in.
3. Oven – Forced-draft oven, thermostatically controlled, capable of maintaining any desired temperature setting from room temperature to 176 ± 3°C (348 ± 5°F).
4. Spatula – Metal spatula or spoon suitable for stirring heated loose asphalt mixtures.

E. LABORATORY CONDITIONING PROCEDURES

E.1. REHEATING OF PLANT PRODUCED MIXTURES

The reheating procedure applies only to plant produced loose mixtures that have been sampled in accordance with CT 125.

Preheat oven for a minimum of 2 hours prior to conditioning so that when the oven is fully loaded and the air is on, the oven will equilibrate at 135 ± 3°C (275 ± 5°F) or to the mixture’s compaction temperature ± 3°C (± 5°F), whichever is lower. Keep boxes folded closed during reheat to avoid excessive oxidation.

1. **In-box fresh sample**: Place boxes of the mixture in a preheated oven. Reheat the mixture for 1 hour. Mixtures in boxes will be considered as fresh if the mixture is workable enough to be split.
2. **In-box cold sample**: Place boxes of the mixture in a preheated oven. Reheat the mixture for 2 hours. Continue reheating for an additional 1 hour if the mixture is not sufficiently workable.
3. If the boxes have not been combined in the field, combine them in accordance with California Test 125.

4. Split the boxes of mixture to individual sample sizes in accordance with AASHTO R 47.

Note 1: The reheating process must only be applied to boxes that can be split immediately after reheating.

Note 2: Separate an appropriate amount of loose mix to measure the maximum specific gravity (G_{mm}) using AASHTO T 209. The oven conditioning of samples used for G_{mm} measurement must be consistent with the oven conditioning of samples used for compaction of specimens.

5. Place the test sample in a pan, and spread it to an even thickness equal to approximately 1-2 in.
6. Keep the pan with the mixture at controlled room temperature 25 ± 6°C (77 ± 10 °F) for a minimum of 1 hour and not to exceed 72 hours. Samples left out for longer than 3 hours must be covered with aluminum foil or any suitable cover and kept out of direct sunlight to avoid excessive oxidation.

E.2. SHORT-TERM OVEN CONDITIONING (STOC) OF LABORATORY PREPARED MIXTURES

The Short-Term Oven Conditioning (STOC) procedure applies only to laboratory-prepared loose mixtures. STOC should be used to determine volumetric properties and conduct mechanical tests during mix design stage.

Preheat oven for a minimum of 2 hours prior to conditioning so that when the oven is fully loaded and the air is on, the oven will equilibrate at a temperature of 135 ± 3°C (275 ± 4.5°F) or to the mixture's mixing temperature ± 3°C (± 5°F), whichever is lower.

1. Place the uncovered pan with the mixture in a pre-heated oven for 4 h ± 5 min.
2. At the end of 4 h ± 5 min, remove the samples from the oven. Keep the pan with the mixture at controlled room temperature (77±9°F) for a minimum of 1 hour and not to exceed 72 hours. Samples left out for longer than 3 hours must be covered with aluminum foil or any suitable cover and kept out of direct sunlight to avoid excessive oxidation.

E.3. MID-TERM OVEN AGING (MTOA)

The Mid-Term Oven Aging (MTOA) procedure applies to both lab-prepared and plant produced loose mixtures. MTOA should be used only for mixtures that will be compacted for cracking tests during mix design, and mix design verification.

Note 3: For mix design verification, MTOA applies only to plant-produced loose mixtures.

Preheat oven for a minimum of 2 hours prior to conditioning so that when the oven is fully loaded and the air is on, the oven will equilibrate at 100 ± 3°C (212 ± 4.5°F).

1. Place the uncovered pan with the mixture in a pre-heated oven for 20 h ± 30 min.
2. At the end of 20 h ± 30 min, remove the samples from the oven. Keep the pan with the mixture at controlled room temperature (77±9°F) for a minimum of 1 hour and not to exceed 72 hours. Samples left out for longer than 3 hours must be covered with aluminum foil or any suitable cover and kept out of direct sunlight to avoid excessive oxidation.

E.4. RAPID MID-TERM OVEN AGING (RMTOA)

The Rapid Mid-Term Oven Aging (RMTOA) procedure applies only to plant produced loose mixtures. RMTOA should be used for mixtures that will be compacted for cracking tests during production.

Note 4: RMTOA may also be used during mix design verification to establish a correlation between MTOA and RMTOA.

Refer to the Safety Manual for your Laboratory.

Preheat oven for a minimum of 2 hours prior to conditioning so that when the oven is fully loaded and the air is on, the oven will equilibrate at 135 ± 3°C (275 ± 4.5°F).

1. Place the uncovered pan with the mixture in a pre-heated oven for 3 h ± 5 min.
2. At the end of 3 h ± 5 min, remove the samples from the oven. Keep the pan with the mixture at controlled room temperature (77±9°F) for a minimum of 1 hour and not to exceed 72 hours. Samples left out for longer than 3 hours must be covered with aluminum foil or any suitable cover and kept out of direct sunlight to avoid excessive oxidation.

Note 5: It is recommended that RMTOA specimens be placed in the oven on a schedule matched to the time needed to compact gyratory specimens.

E.5. HEATING TO COMPACTION TEMPERATURE

Preheat oven for a minimum of 2 hours prior to testing so that when the oven is fully loaded and the air is on, the oven will equilibrate at the mixture's compaction temperature ± 3°C (± 5°F).

1. Place the uncovered pan with the mixture from E.1, E.2, E.3, or E.4 in a pre-heated oven for 2 h ± 15 min.
2. Stir the mixture after 1 h ± 5 min to maintain uniform heating.
3. Proceed to compaction in accordance with AASHTO T 312.

Note 6: Any mixture that has been in the oven at compaction temperature for greater than 2 h + 15 min must be discarded.

F. REPORTING OF RESULTS

If required by the contract documents, submit test results electronically in accordance with the guidance documents found at the following link:

DIME Website

G. HEALTH AND SAFETY

It is the responsibility of the user of this test method to establish appropriate safety and health practices and determine the applicability of regulatory limitations prior to use. Prior to handling, testing or disposing of any materials, testers must be knowledgeable about safe laboratory practices, hazards and exposure, chemical procurement and storage, and personal protective apparel and equipment.

End of Text
(California Test 320 contains 5 pages)

APPENDIX B IDEAL-CT MEDIUM-TERM OVEN AGING BUCKET SAMPLE RESULTS

The appendix includes IDEAL-CT results for MTOA QA bucket samples.

Table B.1: IDEAL-CT Results for QA Sample 1 (SL1) Bucket MTOA Samples

Mix ID	Cracking Tolerance (CT #)	Std Dev Cracking Tolerance (CT #)	Strength (psi)	Std Dev Strength (psi)	Fracture Energy (Gf)	Std Dev Fracture Energy (Gf)	Post-Peak Slope	Std Dev Post-Peak Slope
Mix J (PG 64-28M, 0% RP, 0% RS, 0% RA) QA Sample 1 (SL1)	33.7	8.6	89	4	3807	335	2.84	0.50
Mix K (PG 58-34M, 25% RP, 0% RS, 1.0% RA) QA Sample 1 (SL1)	39.6	8.9	128	9	5915	100	4.05	0.72
Mix L (PG 58-34M, 30% RP, 0% RS, 1.0% RA) QA Sample 1 (SL1)	51.3	8.7	127	6	6467	536	3.58	0.22
Mix M (PG 58-34M, 35% RP, 0% RS, 1.5% RA) QA Sample 1 (SL1)	36.2	8.7	136	5	5965	438	4.34	0.68
Mix N (PG 58-34M, 40% RP, 0% RS, 1.5% RA) QA Sample 1 (SL1)	27.0	5.1	167	11	7026	352	6.34	1.23
Mix O (PG 58-34M, 25% RP, 3% RS, 1.5% RA) QA Sample 1 (SL1)	36.0	11.1	127	13	5793	389	4.32	1.07
Mix P (PG 64-28M, 15% RP, 0% RS, 0% RA) QA Sample 1 (SL1)	37.5	7.8	108	6	4733	288	3.26	0.58

Table B.2: IDEAL-CT Results for QA Sample 2 (SL2) Bucket MTOA Samples

Mix ID	Cracking Tolerance (CT #)	Std Dev Cracking Tolerance (CT #)	Strength (psi)	Std Dev Strength (psi)	Fracture Energy (Gf)	Std Dev Fracture Energy (Gf)	Post-Peak Slope	Std Dev Post-Peak Slope
Mix J (PG 64-28M, 0% RP, 0% RS, 0% RA) QA Sample 2 (SL2)	36.0	4.7	82	4	3712	253	2.52	0.28
Mix K (PG 58-34M, 25% RP, 0% RS, 1.0% RA) QA Sample 2 (SL2)	35.1	8.1	129	5	5807	421	4.29	0.55
Mix L (PG 58-34M, 30% RP, 0% RS, 1.0% RA) QA Sample 2 (SL2)	48.7	14.9	124	10	6030	434	3.57	0.61
Mix M (PG 58-34M, 35% RP, 0% RS, 1.5% RA) QA Sample 2 (SL2)	24.7	2.7	157	8	6348	512	5.78	0.44
Mix N (PG 58-34M, 40% RP, 0% RS, 1.5% RA) QA Sample 2 (SL2)	39.1	11.2	137	12	6549	773	4.46	1.00
Mix O (PG 58-34M, 25% RP, 3% RS, 1.5% RA) QA Sample 2 (SL2)	47.4	8.1	128	7	6311	337	3.63	0.39

Caltrans®

UCPRC
UNIVERSITY of CALIFORNIA PAVEMENT RESEARCH CENTER
Davis
Berkeley